AUGUST, 1951

Journal of METALS

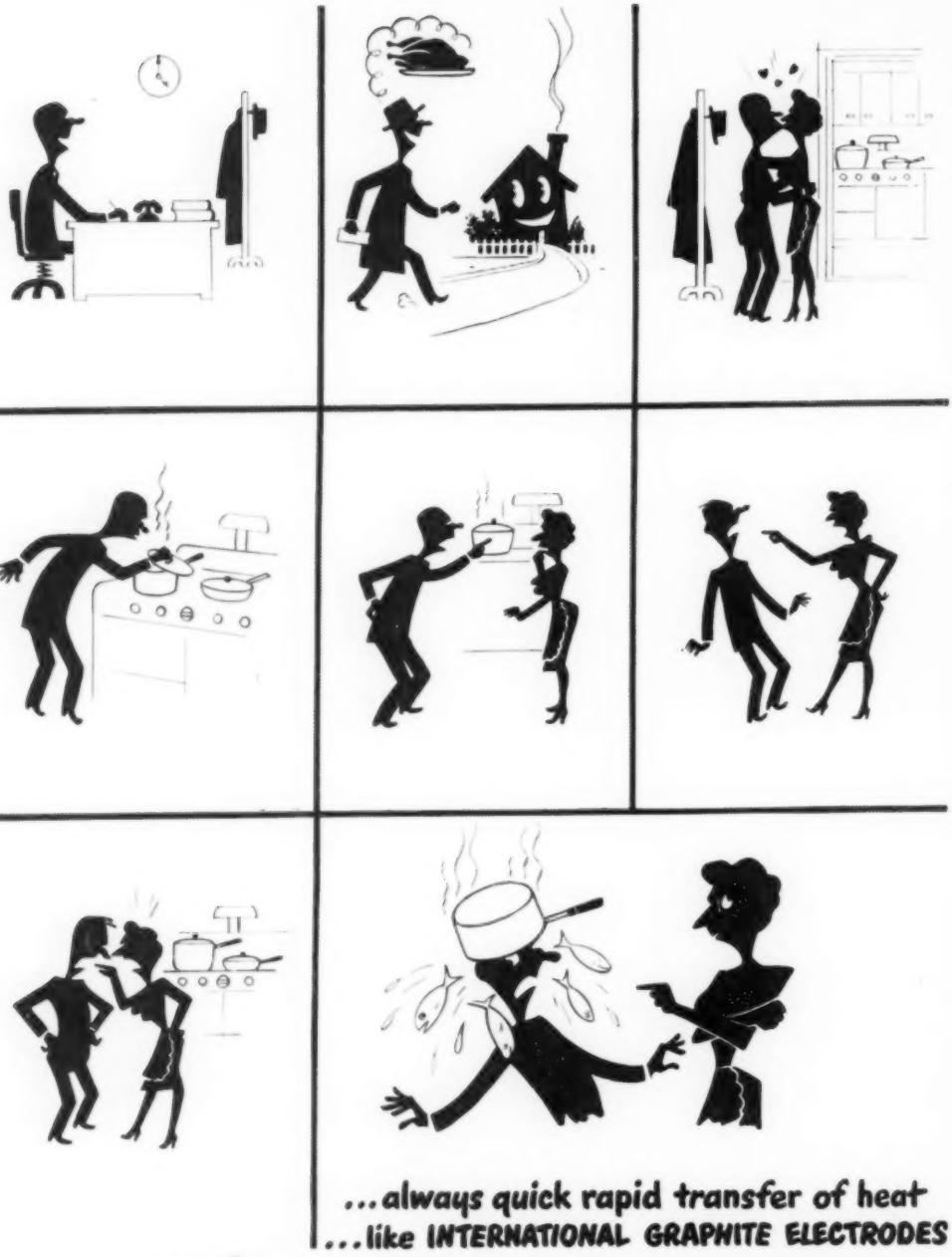

...always quick rapid transfer of heat
...like INTERNATIONAL GRAPHITE ELECTRODES

INTERNATIONAL *Graphite & Electrode* **CORP.**

A SPEER CARBON COMPANY SUBSIDIARY

ST. MARYS, PENNSYLVANIA

Journal of **METALS**

VOL. 3, NO. 8 AUGUST, 1951

COVER

Etched germanium single crystal produced at the Bell Telephone Metallurgical Laboratories.

FEATURES AND NEWS

Journal of Metals Reporter	591	AIME News	677
"Drift of Things"	589	Mexico City Meeting	679
Employment Service	586	Coming Events	579
Meet the Authors	581	Personals	683
New Products	584	New Members	685

TECHNICAL ARTICLES

Open Hearth Charge Ore—Key to Steel Capacity Expansion — L. B. Lindemuth — 592

Secondary Aluminum Recovery in the South Pacific — H. W. Franz — 597

Nylon, A Factor in Stress Corrosion of Aluminum Bronze — E. J. Silk — 600

Oxygen in Acid Electric Steel Production — J. H. Garrison — 601

Ore Practice in Acid Electrics — F. J. Stanley — 603

TRANSACTIONS

Twenty-Five More Years of Metallography — J. R. Vilella — 605

Arc Melting of Titanium Metal — S. F. Radtke, R. M. Scriver, J. A. Snyder — 620

Powder Metallurgy of Zirconium — H. H. Hausner, H. S. Kalish, R. P. Angier — 625

Production of Al from Kalunite Alumina — A. Fleischer, J. Glasser — 634

Intermetallic Compounds in the System Mo-Be — S. G. Gordon, J. A. McGurty, G. E. Klein, W. J. Koshuba — 637

Thermal Stability of the Cr, Fe, and W Borides in Streaming Ammonia and the Existence of a New W Nitride — R. Kiessling, Y. H. Liu — 639

Effect of Alloying Elements on the Elevated Temperature Plastic Properties of Alpha Solid Solutions of Al — O. D. Sherby, R. A. Anderson, J. E. Dorn — 643

Structural Studies of Plastic Deformation in Al Single Crystals — N. K. Chen, C. H. Mathewson — 653

Theory of Grain Boundary Migration Rates — D. Turnbull — 661

Effects of Mn and its Oxide on Desulphurization by Blast Furnace Type Slags — N. J. Grant, U. Kalling, J. Chipman — 666

Effect of Silica Reduction on the Desulphurizing Power of Blast Furnace Type Slags — N. J. Grant, O. Traili, J. Chipman — 672

Desulphurizing Action of Titanium in Steels — W. P. Fishel, W. P. Rae, J. F. Ellis — 674

Published to provide a continuing, authoritative, and up-to-date record of technological, engineering, and economic progress in all branches of the metals industry by the

Metals Branch

American Institute of Mining and Metallurgical Engineers, Inc.
29 West 39th Street, New York 18

• • •

THOMAS E. LLOYD
Manager of Publications
Editor, Journal of Metals

• • •

H. N. UNDERHILL A. S. COHAN
Associate Editors

D. G. GARRETT MARGARET BAGG
Assistant Editors

GRACE PUGSLEY Production Manager

W. J. SEWING Asst. Prod. Mgr.

• • •

METALS BRANCH COUNCIL

C. C. Long — Chairman
E. O. Kirkendall — Secretary
R. M. Brick — IMD Chairman
T. L. Joseph — ISD Chairman
O. C. Ralston — EMD Chairman
M. Gensamer, D. S. Eppelsheimer, H. K. Work, Evan Just

TECHNICAL PUBLICATIONS COMMITTEE

F. B. Foley — Chairman
E. J. Kennedy, Jr. — Secretary

AUXILIARY PUBLICATIONS COMMITTEE CHAIRMEN

F. N. Rhines — Institute of Metals Div.
F. M. Washburn — Iron & Steel Div.
Philip T. Stroup — Extract. Metal Div.

• • •

JAMES A. STANGARONE
Advertising Manager
New York

B. C. SNELL
Regional Manager, Pittsburgh
1110 McDonald Place, Sewickly, Pa.

• • •

The AIME Publishes:
Journal of Metals
Mining Engineering
Journal of Petroleum Technology

Published the first day of each month by the American Institute of Mining and Metallurgical Engineers, Inc., 29 West 39th Street, New York 18, N. Y. Telephone: PEnnsylvania 6-9220. Subscription $8 per year for non-AIME members in United States and North, South and Central America; $9, foreign; $6 for AIME members, or $4 additional in combination with a subscription to "Mining Engineering" or "Journal of Petroleum Technology". Single copies, 75 cents; special issues, $1.50 . . . The AIME is not responsible for any statement made or opinion expressed in its publications . . . Copyright 1951 by the American Institute of Mining and Metallurgical Engineers, Inc. . . . Registered cable address, AIME New York . . . Indexed in Engineering Index, Industrial Arts Index and Chemical Abstracts . . . Reentered as second-class matter Sept. 21, 1949, at the post office at New York, N. Y., under the Act of March 3, 1879. Additional entry established at Manchester, N. H.

Yes! AJAX Induction Melting Furnaces are Versatile!

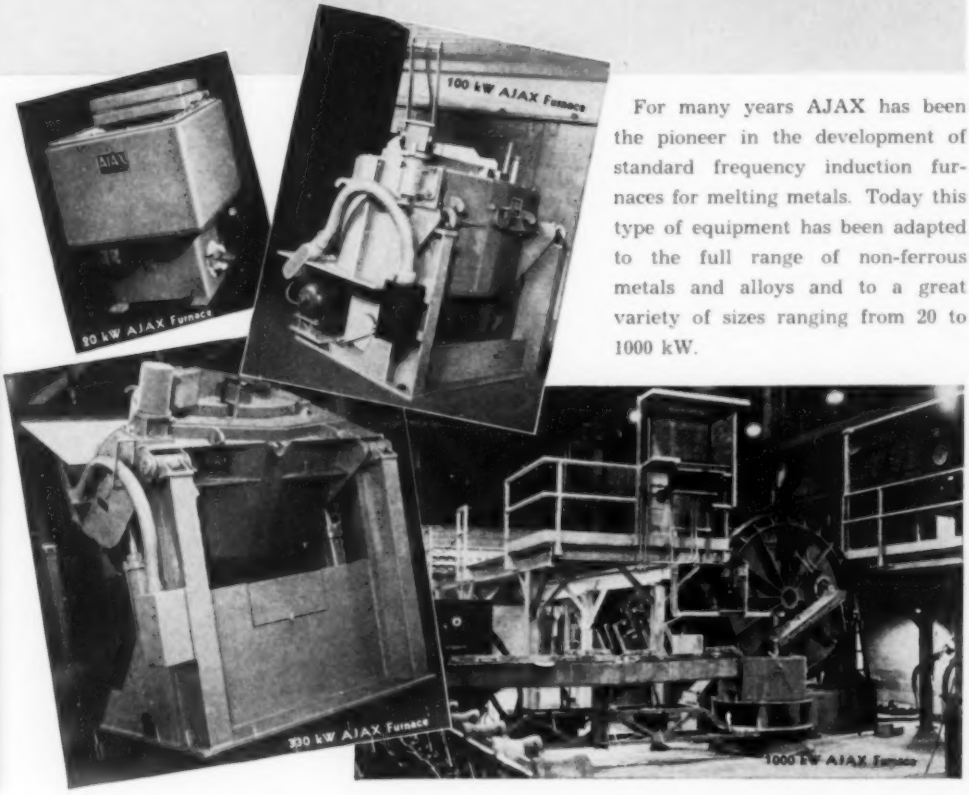

For many years AJAX has been the pioneer in the development of standard frequency induction furnaces for melting metals. Today this type of equipment has been adapted to the full range of non-ferrous metals and alloys and to a great variety of sizes ranging from 20 to 1000 kW.

AJAX Induction Melting Furnaces are now adapted for the following applications: Die Castings, Permanent Mold Castings, Sand Castings, Billets for Rolling and Extrusion, Recovery of Scrap, Galvanizing and Aluminizing of Steel and many others.

For special applications an Automatic Electromagnetic Pump allows continuous feeding of molten metal into the molds as they move past. Hand ladling is eliminated. Temperature of course, is also automatically regulated and there is no chance of overheating the bath at any time during the melting cycle.

AJAX ENGINEERING CORP., TRENTON 7, N. J.

AJAX TAMA-WYATT

INDUCTION MELTING FURNACE

AJAX ELECTRO METALLURGICAL CORP., and Associated Companies
AJAX ELECTROTHERMIC CORP., Ajax Northrup High Frequency Induction Furnaces
AJAX ELECTRIC CO., INC., The Ajax Hultgren Electric Salt Bath Furnace
AJAX ELECTRIC FURNACE CORP., Ajax Wyatt Induction Furnaces for Melting

Is YOUR laboratory a potential bottleneck?

HERE'S a complete line of Bausch & Lomb precision instruments to help you keep pace with capacity production . . . to give you increased speed, accuracy and simplicity in research and quality control.

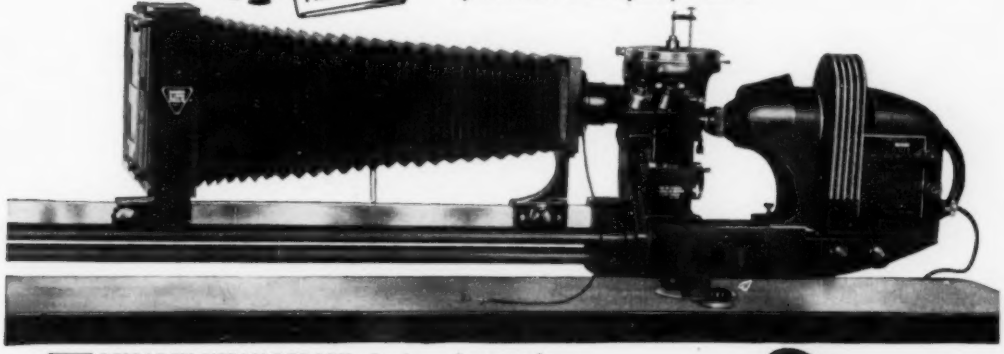

RESEARCH METALLOGRAPH—See it . . . photograph it . . . *four* ways! Four different accurate images of the same sample, for more complete identification. Exclusive, patented B&L features permit critical work with bright field, dark field or polarized light . . . with quick, easy change-over. For phase contrast work B&L accessories are simply, speedily attached. The "maximum use" instrument for visual observation and photomicrography. Catalog E-240.

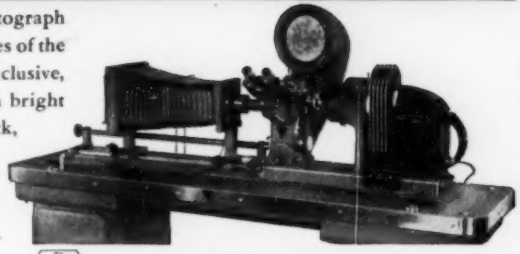

***NEW!* BALPHOT METALLOGRAPH**—*All new* design! The economy of limited capacity instruments, with bright field, dark field or polarized light and phase contrast . . . and many other performance advantages of the highest-priced metallographs. Quick-action stage elevating device eliminates coarse adjustment. New *Magna-Viewer* projects bright, magnified screen images . . . ideal for grain size determinations and group viewing. Catalog E-232.

PHOTOMICROGRAPHIC EQUIPMENT MODEL L—With proper accessories *this one unit* provides visual microscopy, high and low power photomicrography, as well as photocopying. Catalog E-210.

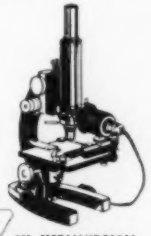

CM METALLURGICAL MICROSCOPE—For examination of opaque objects, polished metal specimens, similar materials. Catalog E-223. Tri-Vert Illuminator (optional) provides bright field, dark field, or polarized light. Catalog D-108.

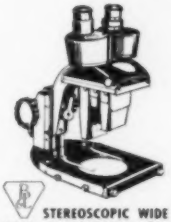

STEREOSCOPIC WIDE FIELD MICROSCOPES—Invaluable in preparation of polished metal specimens, study of fractures, porosity, macro-etched specimens and other low power metallurgical studies. Catalog D-15.

WRITE for complete information to Bausch & Lomb Optical Co., 787-8 St. Paul St., Rochester 2, N. Y.

Bausch & Lomb *Metallurgical* Equipment

STOKES HIGH VACUUM EQUIPMENT... *for every requirement of vacuum processing*

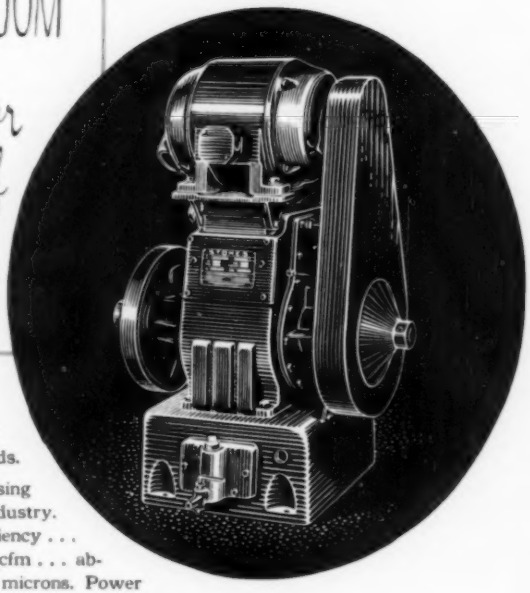

Modern design of Stokes vacuum equipment develops from the continuing contact of Stokes Engineers with processors in many fields.

Stokes Microvac Pumps — basic to vacuum processing —are designed for the broadest requirements of industry. They have high volumetric and mechanical efficiency . . . capacities of 15 to 500 cfm . . . absolute pressures to 10 microns. Power consumption is low. Compact design with top-mounted motor requires minimum floor space.

There are but four moving parts including the high speed, full-opening exhaust valve of corrosion-resistant Teflon. Lubrication is completely automatic, without packing, stuffing-boxes or grease fittings. Wear is kept to a minimum, and long trouble-free service assured. Parts are precision-finished, standard and interchangeable.

Stokes is the only manufacturer of equipment for complete vacuum systems, including Microvac mechanical pumps, oil diffusion pumps, McLeod Gages and Vacuum Valves.

Send for Catalog 700, "Stokes Microvac Pumps for High Vacuum", now a standard reference work on High Vacuum, containing charts, graphs, diagrams, schematics, typical problems, tables, formulas, constants, conversion factors.

Consult with Stokes on the application of vacuum to vacuum sintering, melting, de-gassing, heat treating, inert gas purging, vacuum metallizing, and to other applications in which vacuum deserves exploration.

STOKES MAKES

Plastics Molding Presses,
Industrial Tabletting
and Powder Metal Presses,
Pharmaceutical Equipment,
Vacuum Processing Equipment,
High Vacuum Pumps and Gages,
Special Machinery

STOKES

F. J. STOKES MACHINE COMPANY, 5916 TABOR ROAD, PHILADELPHIA 20, PA.

PROVE YOUR NEED FOR

X-ray Spectrometry in the *Norelco*® laboratory

★ on the *NEW* wide range High and Low Angle Goniometer

In our application laboratory, meticulous procedures are employed to determine the basic material composition of samples sent to us by producers of diversified basic compounds or manufactured products.

Here, analyses are made by X-ray diffraction, absorption and fluorescence—practical, nondestructive media for the identification, comparison and control of many materials, products and processes. Such analyses by other methods are difficult, time consuming, destructive and sometimes inaccurate.

This laboratory is maintained to demonstrate the value of the X-ray Spectrometer, Fluorescence Analysis and allied equipment in maintaining the quality of ingredients—in maintaining production control—and as a research facility which is a necessity in progressive manufacturing technology. As clearly as a fingerprint, the Spectrometer produces patterns on rectilinear charts which are directly comparable—one to the other. This is particularly important in process controls where duplication is imperative.

A diffraction school is held each spring and fall, at which lectures on the fundamental operation as well as advanced and new applications of X-ray in research and control are given by leading authorities.

NORTH AMERICAN PHILIPS COMPANY, INC. Norelco

Foremost in X-ray progress since 1896

NORTH AMERICAN PHILIPS COMPANY, INC.

RESEARCH and CONTROL INSTRUMENTS DIVISION ★ DEPT. IG-8, 750 S. FULTON AVENUE, MT. VERNON, N. Y.

IN CANADA: Philips Industries Ltd., 1203 Philips Square, Montreal ★ EXPORT REPRESENTATIVE: Philips Export Corporation, 750 South Fulton Avenue, Mt. Vernon, N. Y.

ZIRCONIUM METAL

in the form of

Sponge and Briquettes

with the following analysis

Zirconium	98.8 (by difference)	to 99.6%
Oxygen	0.1 (estimated)	to 0.2%
Nitrogen	.02	to .10%
Iron	.2	to .8%
Chromium	.02	to .10%
Nickel	.01	to .02%
Silicon	.02	to .10%

Write our New York Office for detailed information. 3½" diameter briquettes are furnished from ½" to 3" in height with bulk density of 160 to 190 lbs. per cu. ft. The sponge will be ¾" and down with a maximum of 15% through a 10 mesh screen.

TAM PRODUCTS
Registered U. S. Pat. Off.

TITANIUM ALLOY MFG. DIVISION
NATIONAL LEAD COMPANY
Executive and Sales Office: 111 BROADWAY, NEW YORK CITY · General Offices, Works, and Research Laboratories: NIAGARA FALLS, N. Y.

— Coming Events —

Aug. 7, AIME, Morenci Sub-section, Longfellow Inn, Morenci, Ariz.

Aug. 27-Sept. 6, Oak Ridge National Laboratory and Oak Ridge Institute of Nuclear Studies, annual summer symposium, Oak Ridge, Tenn.

Aug. 29-Sept. 1, Scientific Apparatus Makers Assn., summer meeting, laboratory equipment section, Northernaire Hotel, Three Lakes, Wis.

Sept. 13-14, Oak Ridge Institute of Nuclear Studies, symposium, Nuclear Physics in Europe, Oak Ridge.

Sept. 13-15, AIME, Industrial Minerals Div., fall meeting, University of West Virginia, Morgantown, W. Va.

Sept. 19, AIME, Carlsbad, Potash Section, Riverside Country Club, Carlsbad, N. Mex.

Sept. 20, AIME, Utah Section, Newhouse Hotel, Salt Lake City.

Sept. 25-28, ASME, fall meeting, Radisson Hotel, Minneapolis.

Oct. 1-4, Assn. of Iron & Steel Engineers, annual convention, Hotel Sherman, Chicago.

Oct. 3-5, AIME, petroleum branch, fall meeting, Oklahoma City.

Oct. 10-11, Joint Fuels Conference, AIME Coal Division, ASME Fuel Section, Roanoke Hotel, Roanoke, Va.

Oct. 10-11, AIME, Southwestern and Western Sections, Open Hearth Committee, joint meeting. Oct. 10, plant trip, Colorado Fuel & Iron Co., Pueblo. Oct. 11, Broadmoor Hotel, Colorado Springs.

Oct. 12, AIME, Eastern Section, Open Hearth Committee, Warwick Hotel, Philadelphia.

Oct. 12-14, Metal Treating Institute, annual meeting, Detroit.

Oct. 15-17, AIME, Institute of Metals Div., fall meeting, Detroit-Leland Hotel, Detroit

Oct. 15-19, National Metal Congress & Exposition, Detroit.

Oct. 18-19, Scientific Apparatus Makers Assn., midyear meeting, industrial instrument section, Seaview Country Club, Absecon, N. J.

Oct. 18-20, National Assn. of Corrosion Engineers, south central region, Corpus Christi, Texas.

Oct. 19-20, Engineers' Council for Professional Development, annual meeting, Hotel Statler, Boston.

Oct. 22, AIME, Chicago Section, Open Hearth Committee, Phil Schmidt's, Chicago.

Oct. 22-24, American Mining Congress, Metal and Nonmetallic Mining Convention, Biltmore Hotel, Los Angeles.

Oct. 25-26, AIME, Los Angeles Section, fall meeting, Los Angeles.

Oct. 26-27, AIME, National Openhearth Committee, Southern Ohio Section, Deshler-Wallick Hotel, Columbus, Ohio.

Oct. 29-Nov. 3, AIME, fall meeting, Mexico City.

Nov. 2, AIME, Pittsburgh Local Section and Open Hearth Local Section, annual off-the-record meeting, William Penn Hotel, Pittsburgh.

Nov. 25-30, ASME, annual meeting, Chalfonte-Haddon Hall, Atlantic City.

Nov. 28-30, Scientific Apparatus Makers Assn., midyear meeting, laboratory apparatus, optical, nautical, aeronautical, and military instrument sections, Hotel New Yorker, New York.

Nov. 29, AIME, Buffalo Section, Open Hearth Committee, Statler Hotel, Buffalo, N. Y.

Dec. 2-5, American Institute of Chemical Engineers, annual meeting, Chalfonte-Haddon Hall, Atlantic City.

Dec. 6-8, AIME, Electric Furnace Conference, William Penn Hotel, Pittsburgh.

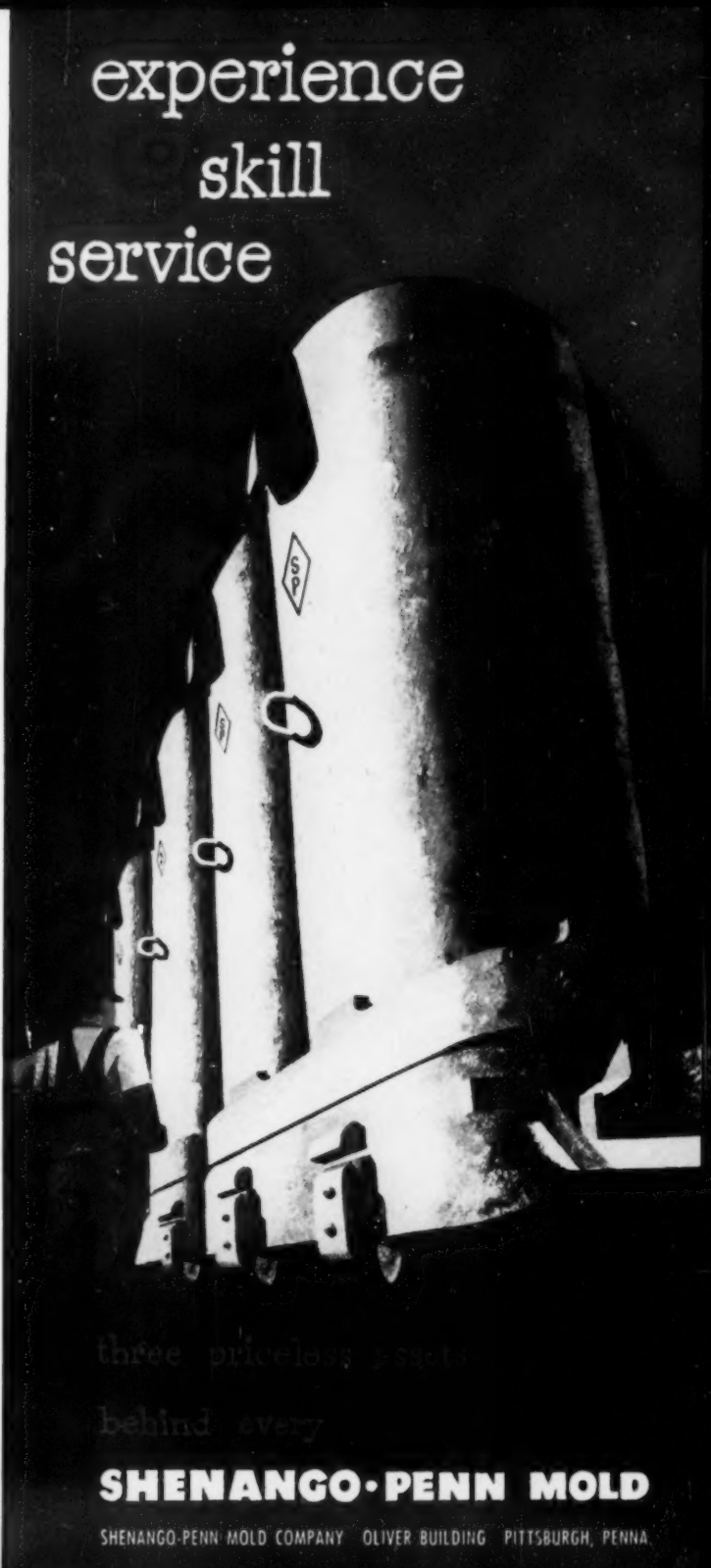

A MESSAGE TO AMERICAN INDUSTRY

"This is more than a shortage . . . this is an emergency.

Every pound of your scrap is needed, NOW !"

"THE STEEL INDUSTRY is currently operating at more than 100% of rated capacity—turning out well over 2 million tons of steel per week. This record high production—every ton of which is in urgent demand—cannot be kept up unless we get more scrap from every potential source. For without your scrap we cannot produce enough steel. Today, every ton of steel turned out requires a half a ton of scrap for its production. That's why scrap—more scrap—is so urgently needed, and needed right away.

"The fact we have to face today is that steel mills are operating on a hand-to-mouth basis as far as scrap is concerned. Some mills are working on only a two-day supply of scrap. We already have had to shut down steel-making furnaces for lack of scrap.

"That's why we are asking you to strain every effort to get more scrap out of your plants and yards and on its way to the mills . . . to search out the scrap that doesn't come to market in normal times. You'll find this "dormant" scrap in obsolete equipment, tools and machinery that you haven't used for years . . . overlooked in your storage sheds . . . or rusting away in a junk pile in some forgotten corner. It's there. Turn it in at once—*so we can turn out the steel you need.* We can't do it without your help."

President, United States Steel Corporation

USS

1-1182

UNITED STATES STEEL

Meet The Authors

J. R. VILELLA

J. R. Vilella (p. 605), with U. S. Steel's Kearney, N. J., Research Laboratory, presented the 1951 Howe Memorial Lecture, a paper entitled "Twenty-Five More Years of Metallography." Mr. Vilella, a graduate of Penn State, has been with U. S. Steel since 1934. Prior to that time he was with Union Carbide & Carbon's Research Laboratories and the Physiatric Institute. He lives in New York City, and his hobbies include photography and ornithology.

S. F. RADTKE

S. F. Radtke (p. 620) was born in Minneapolis, and studied at Massachusetts Institute of Technology, where he received his S.B. and Ph.D. While he has been a research fellow with the pigments dept. of du Pont since 1948, prior to that he was an instructor and did rubber research at MIT; spent several years in the Army, and worked for North Carolina Shipbuilding Co., at Wilmington, N. C. He is a Major in the U. S. Army Reserves, and his hobbies are flying, sailing, and photography.

G. E. KLEIN

Gilbert E. Klein (p. 637), a Hoosier from Indianapolis, received his B.S. from Case Institute of Technology and his M.S. (Physics) and S.M. (Geology, Crystallography) from Massachusetts Institute of Technology. He worked for National Smelting Co., as research physicist; was a research fellow in structural crystallography at M.I.T.; a research physicist for Burgess Battery Co., Freeport, Ill.; senior physical metallurgist for the NEPA Div., Fairchild Engine & Airplane Corp., Oak Ridge, Tenn., and presently is senior metallurgist at the Oak Ridge National Laboratory, Oak Ridge, Tenn. He likes golf and bridge.

S. G. GORDON

S. G. Gordon (p. 637) is a staff member of the Los Alamos Scientific Laboratory, at Los Alamos, N. M. Prior to joining the Los Alamos staff he was materials engineer for the NEPA project at Oak Ridge, Tenn. He also served as technologist in the office of the Chief Signal Officer, Pentagon, Washington, D. C., and was associate curator for the Academy of Natural Sciences of Philadelphia. He was one of the founders of the publication, *American Mineralogist* and an associate editor of the publication until 1949. Gordonite, the magnesium-aluminum-phosphate from Utah, was named in his honor. He co-authored "Crystallographic Tables for the Identification of Minerals," wrote "Mineralogy of Pennsylvania" and "Mineralogy of Tin Mines of Llallagua, Bolivia." His hobby? You guessed it—Collecting Rocks!

W. J. KOSHUBA

W. J. Koshuba (p. 637) born at St. Paul, Minn., received his B. Met. E. from Universtiy of Minnesota. He did development work in forging and casting high temperature alloys at Allis Chalmers Mfg. Co.'s supercharger works, and in 1946 joined Bergen Precision Castings Co., in Pleasantville, N. Y. as a consultant on precision casting. Later the same year he became general superintendent of Solar Aircraft Co.'s precision casting div. at Des Moines, Iowa. Then, in 1947 he joined the NEPA project at Oak Ridge, and became head of the materials section the same year. Now, his work concerns development of high temperature materials for nuclear applications. Color photography and coin collecting are his pastimes.

J. A. McGURTY

J. A. McGurty (p. 637), from Elizabeth, N. J., was graduated with a B.S. from M.I.T. He worked for Fairchild Engine & Airplane Corp. on the NEPA project and Callite Tungsten Corp.; and presently is employed by General Electric Co., AGTD, ANP project. A research metallurgist, his speciallized field is in metallurgy of high temperature materials. Flying, sailing, hiking, and target shooting take up his spare time.

R. KIESSLING

Roland Kiessling (p. 639), was born in Sweden and received his Ph.D. in Chemistry from the University of Uppsala, Sweden. He is assistant professor in general and inorganic chemistry at Uppsala, and has published about 20 papers, mainly on metal borides and high temperature equipment.

J. F. ELLIS

James F. Ellis (p. 674), born in Memphis, Tenn., was graduated from Memphis State College with a B.S., and Vanderbilt University with a B.S. in 1941 and an M.S. in 1948. In 1941 and 1942 he was a biochemist with the U. S. Veterans Hospital; from 1942 to 1946 was a Captain in the U. S. Army Medical Corps; and since 1948 has been in the melting dept. of American Cast Iron Pipe Co.

W. P. FISHEL

W. P. Fishel (p. 674) is professor of metallurgy at Vanderbilt University. Born in Pleasant City, Ohio, he received his degrees of A.B., M.S., and Ph.D. from Ohio University and Iowa State. He taught school and was superintendent of schools for six years prior to joining the teaching staff at Vanderbilt in 1923. "Distribution of Carbon Between Iron and Titanium in Steels" was a paper that he presented before AIME some time ago.

W. P. ROE

W. P. Roe (p. 674) is in the dept. of metallurgy at Vanderbilt University. Born in Cheswold, Dela., he received his B.A. and M.S. from Vanderbilt. In 1948 and 1949 he was a chemist with Carbide & Carbon Chemical Corp., but returned to Vanderbilt in 1949 to complete his Ph.D. When he gets his Ph.D. this year, he plans to join the Titanium Div., of National Lead Co., as a research metallurgist.

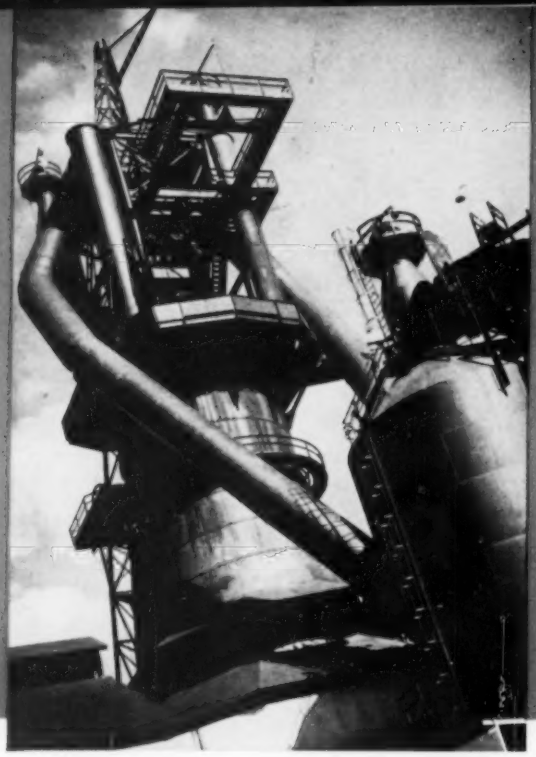

• • • • The world knows of America's fabulous steel production. It knows that our capacity to fashion the weapons of war is a fearsome thing.

And we know that steel has contributed more than any other industry to our daily lives. Everything we use . . . from toothbrushes to neckties . . . starts with steel.

The development of better refractories for every step in steel . . . and tremendous advances in production . . . have helped largely to make possible steel's progress. General Refractories is proud of its part.

Hot Air That Talks Sense

GENERAL REFRACTORIES

GENERAL REFRACTORIES COMPANY
PHILADELPHIA

General's OLIVE HILL fireclay brick lines this blast furnace. And elsewhere in the plant you'll find General Refractories silica brick, basic brick, plastics, castables and bulk products. There's scarcely a heat application for which General does not supply a refractory.

General's extensive research facilities and modern production methods . . . General's 43 mines, 29 plants, 18 sales offices and 200 distributing agencies . . . are at your service. If you have a refractory problem, depend on the company that offers a complete refractories service.

A Complete Refractories Service

●

New Products

New Products | New Literature | New Services

For Further Information or Literature on any Product, Fill in the Coupon and Send to JOURNAL OF METALS
Students are Requested to Apply Directly to Manufacturers for Bulletins and Information

1—ALUMINUM WELDING ALLOYS: High quality, flux-coated aluminum welding rods for oxyacetylene and oxyhydrogen welding have been released by *Eutectic Welding Alloys Corp.* The flux coating is low melting to provide for minimum heat application and once melted flows in a transparent pool. For structures and applications where an anodized silicon bearing rod has shown an objectionable dark weld, Eutec-Rod 22FC provides a base metal matching solution since corrosion resistance and color, as well as physical properties of the weld, closely match the aluminum.

2—ASH HANDLING SYSTEM: A vacuum system designed by *Beaumont Birch Co.* eliminates the need of manually handling ash. Ash, soot, etc., are conveyed dry by means of vacuum through pipes from the intakes to a receiver on top of an ash storage silo. The vacuum is created by a steam exhauster located beyond the ash receiver.

3—TESTING MACHINE: Universal testing machine, model 12-H of 12,000 lb capacity is announced by *Baldwin-Lima-Hamilton Corp.* The hydraulic loading unit is separate from the indicating and control unit, which isolates recoil from breaking test specimens and permits adjusting maximum hands with minimum drag. The 12,000 lb range is graduated in 20-lb units on a 16-in. diam indicator dial and a 3000 lb range is graduated in 5-lb units.

4—CONVEYOR SYSTEM: A new conveyor unit is battery powered, making it completely independent of any outside source of energy. Mono-Dyne system, developed by *Bloom System, Inc.*, eliminates need for overhead wiring. The unit is capable of multi-speeds, forward and reverse, and is operated by push button or remote control. It can operate outdoors, from plant to plant, indoors, and ascend grades.

5—TACHOMETER: Speeds of many machines are measured from one location with the *Metron Instrument Co.* tachometer, which employs a simple machine selector knob. Speed tests and comparisons are accomplished even when the indicator is located 1000 ft away from the machines. Over 50 standard full scale range markings are available. Direct reading in units such as rpm, fpm, in. per sec, etc. from speeds between 1/10 rpm and 100,000 rpm are possible.

6—CONVECTION FURNACES: Hevi Duty pit-type convection furnaces are used for heat treating operations that require temperatures from 250° to 1850°F. Available from *Hevi Duty Electric Co.*, these furnaces are suitable for tempering, drawing, annealing, and hardening steel, nonferrous annealing, and solution and aging treatments of aluminum. The centrifugal fan forces a stream of air or prepared atmosphere over the hot surfaces of the heating elements; the furnace charge is bombarded by this rapidly flowing stream.

7—CONTOUR MEASUREMENT: By utilizing a beam of light as a straight-line reference, deviations of supposedly flat surfaces as small as ±0.00005 in. may be measured. *F. T. Griswold Mfg. Co.* optical straightedge consists of a lens and prism housing and a feeler microscope with built-in illumination which rides along the surface under examination. It is made in standard lengths of approximately 3, 5, 10 and 13 ft; the housing rests on two blocks; and the feeler, which includes the optical system, slides on the work surfaces.

8—TUMBLING MACHINE: Large quantities of parts are precision finished at one time in the new model DW-60-36-2 automatic control machine recently developed by the *Roto-Finish Co.* Once the machine is started, automatic timer will stop its operation any time from 0 to 20 hr without further attention. It has a 5 hp variable speed power unit with a remote control handle for adjusting the speed of the cylinder from 10 to 30 rpm.

9—ANTIRUST PAINT: A penetrating and sealing paint which can be applied right over rusted surfaces without wire brushing, scraping or sand blasting, is announced by *Paint Corp. of America.* It penetrates through the rust layer into the base metal and seals the surface against further rusting. PCA-100 is furnished in black only and because of its penetrating characteristics should be used solely as a finish coat. It is suitable for either brush or spray application.

10—SCALE REMOVAL: A preheat chemical bath which completely removes furnace scale from steel forgings during quenching is being marketed by *Pennsylvania Salt Mfg. Co.* The bath is made of a new product, Pennsalt SR-4, dissolved in weak muriatic acid and water. Parts covered with forging scale are immersed in the bath for 5 min and then may be placed directly into heat treating furnaces or can be stored for later heat treating.

11—ION EXCHANGE UNIT: A new unit for the treatment of water in steam heating plants has been developed by *Permutit Co.* It eliminates the need for elaborate equipment and handling such dangerous chemicals as caustic soda sulphuric and hydrochloric acids during regeneration process. It employs new type resins that are regenerated with plain salt. In addition to softening water, the new resins remove alkalinity and sulphates.

12—SCREEN HEATER: For screening ores, lime, coal, chemicals and other materials containing moisture and which are neither readily inflammable nor explosive nor conductors, an electric screen heater is available. Applicable to woven wire screen No. 2 mesh or smaller, the heater is inexpensive to operate and will perform on new or old gravity or vibrating installations. It consists of a step-down transformer for low-voltage heating current, delivered through high amperage cables to special bus bars that extend the full length of the screen on each side. The screen acts as resistance to flow of current and is heated sufficiently to reduce the moisture content of materials on the screen.

Journal of Metals **August**
29 West 39th St.
New York 18, N. Y.

Please send me — More Information ☐ Free Literature ☐ Price Data ☐ — on items indicated

1	2	3	4	5	6	7	8	9	10
11	12	13	14	15	16	17	18	19	20
21	22	23	24	25	26	27	28	29	30
31	32	33	34	35	36	37	38	39	40

Name ..... Title .....
Company .....
Street .....
City and Zone ..... State .....

Screen capacity is increased and beating—to keep the screen open—is eliminated. *F. R. Hannon & Sons.*

13—SPRAYWELDER: A new model powder metallizing unit to execute the Colmonoy Sprayweld Process is announced by *Wall Colmonoy Corp.* The Model B spraywelder is light in weight, has an eye-level air gage, greater capacity air filter, convenient air regulator, more positive air and powder control valves, new trigger mechanism, increased cooling capacity in head for steadier operation and longer tip life, and locked feed mechanism on carburetor. The Spraywelder can be used to metallize base metals with copper, brass, stainless steel, zinc, and aluminum.

Free Literature

20—PYROMETERS: Two portable models suitable for plant and laboratory are described in bulletin PPY-1 released by *Wheelco Instruments Co.* Specifications on thermocouple holders and tips are also included. Price sheet provides a listing of standard scale ranges. Instruments are used where temperatures of molten aluminum, zinc, lead, tin, brass, and other nonferrous alloys must be measured before pouring.

21—SOAKING PIT: Technical bulletin on a soaking pit which reduces fuel consumption by 40 pct while almost doubling the amount of steel heated has been issued by *Loftus Engineering Corp.* Cycle time for accelerating initial temperature head, recirculation through normal combustion system, and fully automatic dual combustion system with dual outlets are just a few of the many features.

22—BARREL FINISHING: Booklet available from *Minnesota Mining & Mfg. Co.* describes this modern method of deburring and finishing a wide variety of metal parts by rotating them with abrasives and compounds in specially designed machinery. Abrasives and compounds used are illustrated and many advantages of using this method are fully described.

23—CONVEYOR MAINTENANCE: Installation, operation, and maintenance of chain drives and conveyors are fully detailed in brochure 51-7 issued by *Chain Belt Co.*

24—POWER SCREW DRIVER: Advantages and application of power screw drivers are contained in booklet obtainable from *Shakeproof, Inc.*, div. Illinois Tool Works. Detailed drawings illustrate application, installation, and mechanical features of the power screw driver, said to drive up to 60 or more screws per min. Typical industrial uses of the unit with specific data on production and time savings are included.

25—DRILLING MACHINES: Catalog DM published by *Wales-Strippit Corp.* illustrates machine for precision layout, drilling and reaming holes. Featured are the ¾ hp motor, precision-built drill head, two speed gearing, air clamp lever, and dial indicator calibrated in 0.0001 in. Specifications for model 3600 are also listed.

26—CORROSION NOTEBOOK: Sixteen-page booklet issued by *Carpenter Steel Co.* contains data on the corrosion resistance of various types of stainless tubing and pipe. Intergranular, galvanic, atmospheric, and pitt-type corrosive conditions are described.

27—METALLURGICAL GRINDING: Bulletin describes equipment available for fine grinding specimens with emery papers or wet type silicon carbide papers or cloths. Includes both hand and motor powered grinders. *Buehler Ltd.*

28—PRECISION TOOLS: The importance of heat processing machines as automatically controlled precision tools in production lines is stressed in booklet available from *Selas Corp. of America.* Descriptions and illustrations include metal brazing, selective hardening, heating-for-forging, tinplate fusion, melting, and normalizing.

29—CAST-WELD CONSTRUCTION: Valuable data on technical developments in the field of cast-weld construction are contained in brochure issued by *Steel Founders' Society of America.* Examples of metals conservation, production economies, improvements in functional design, and other engineering gains are cited. Booklet comprises a reprint outlining numerous practical examples of leading steel foundries' effective application of proven cast-weld techniques.

30—STAINLESS PIPE: Lightweight Schedule 5 is described in set of data sheets published by *Carpenter Steel Co.*, alloy tube div. Advantages of light walls that conserve critical alloys and reduce installation costs are outlined, and technical data on wall thickness, pressures, etc. are given.

31—METALLOGRAPH: Compact instrument complete for examining, studying and photographing metal samples and other materials is illustrated in bulletin from *F. T. Griswold Mfg. Co.* Typical microphotographs made by the instrument of hypereutectoid steel samples at magnifications of X400, X1200, X2000, and X3400 are shown.

32—MAGNETIC DRIVE: Complete information on magnetic drive and new magnetic amplifier regutron speed control are described in bulletin available from *Electric Machinery Mfg. Co.* Fully illustrated section is included that covers applications of drive and speed control.

33—METALLURGICAL POLISHING: Booklet issued by *Buehler, Ltd.* describes and includes sample of emery, aluminum oxide and silicon carbide papers and 12 polishing cloths. Trade names, particle size, etc. are given for many abrasives.

AIME Student Key

Now available, an attractive gold-plated sterling silver key for AIME Student Associates.

Blue enamel centerpiece with gold lettering, and the name of your school in blue enamel on a gold background.

ONLY $2.75, TAX INCLUDED

Name of school, 8c per letter extra

Actual Size

AIME
29 West 39th St.
New York 18, N. Y.

Please send me ____ Student Associate Keys, for which I enclose check ____ money order ____ for $ ____.

Name of School ____

Name ____

Address ____

City, Zone, State ____

(JM8)

Personnel Service

THE following employment items are made available to AIME members on a non-profit basis by the Engineering Societies Personnel Service, Inc., operating in cooperation with the Four Founder Societies. Local offices of the Personnel Service are at 8 W. 40th St., **New York 18**; 100 Farnsworth Ave., **Detroit**; 57 Post St., **San Francisco**; 84 E. Randolph St., **Chicago** 1. Applicants should address all mail to the proper key numbers in care of the New York office and include 6c in stamps for forwarding and returning application. The applicant agrees, if placed in a position by means of the Service, to pay the placement fee listed by the Service. AIME members may secure a weekly bulletin of positions available for $3.50 a quarter, $12 a year.

POSITIONS OPEN

Metallurgical or mechanical engineer with general background in light metals such as aluminum, magnesium or titanium, for statistical control and coordination to manufacturing divisions. Salary, $7600 a year. Location, Washington D. C. Y5699.

Metallurgical Engineer, 22 to 35, B.S. degree, for special investigation and development work in precision manufacturing operations. Previous experience in metallurgical processing or design of precision machinery helpful but not required. Location, suburban Philadelphia. Y5680.

Metallurgist, to develop welding procedures for improvement in quality and reduction in cost. Specify welding equipment and techniques for use in production products involving carbon and alloy steel in cast or rolled form. Advise product engineers as to materials for design of products for best application of welding. Supervise qualification testing of welding processes and welding operators. Supervise X-ray equipment and X-ray operators. Perform metallurgical tests as required, and interpret test results and reports and recommend any steps to be taken based on such tests. Location, New York State. Y5329(b).

Assistant Professor in metallurgy; young, preferably with Ph.D.; should have special interest in the field of ferrous metallurgy and an interest in research as well as teaching. Salary open. Position starts Sept. 1, location, Midwest. Y5564.

Engineers. (a) Copper smelter superintendent, familiar with reverberatory furnaces and converters. (b) Foremen and a mechanical engineer to take charge of maintenance and repairs at a copper refinery in northeastern Turkey. Y5433.

Metallurgical Engineer with several years' experience in ore concentration. Work to be mill operation and some development. Expanding organization. Salary, to $6000 a year. Location, Southeast. Y5405.

Assistant Chief Engineer in charge of metallurgical operations, 30 to 35, B.S. or M.A. in chemical engineering, experienced in the design of chemical and/or metallurgical processes equipment. Will work with process development engineer on design and development of new process equipment, especially rotary kilns and nickel-cobalt separation processes. Salary, $7200 to $8400 a year. Location, Cuba. Y5657.

Harper

DOUBLE DOOR *Electric* FURNACE
for BILLET and BAR HEATING

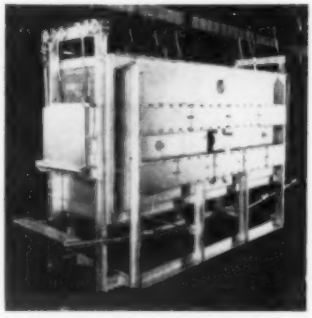

For speed in your general forging operations, specify Harper Electric Furnaces. Shown above is a versatile Harper Furnace designed for billet and bar heating of metals that require special atmospheres. This sturdy unit has a chamber size of 12" x 12" x 8' long with doors at each end.

Ninety kilowatts of power is supplied to the "Globar non-metallic heating elements to give rapid heating of heavy charges resulting in maximum production.

Accuracy of temperature control giving improved workability of billets and bars for rolling and drawing is provided through correct application of temperature control instruments.

Scale usually formed in heating is eliminated through accurate control of special atmospheres.

Double door forging furnaces of this general type are available in several sizes and we are equipped to build continuous furnaces with atmosphere controls for special operations. Write telling of your needs, stating type, size, weight of product and production required, firing cycle, available electric services and special characteristics, and Harper Engineers will be glad to recommend and quote on suitable equipment for you.

* Reg. T.M. Carborundum Company

HARPER ELECTRIC FURNACE CORPORATION
DEPT. No. 10, 38 RIVER STREET BUFFALO 2, N. Y.

TITANIUM RESEARCH & DEVELOPMENT

National Research Corp. and Monsanto Chemical Co. have united their research efforts on titanium and are planning a much expanded program. Additional technical manpower for all phases of the work will be required in the future. Specifically required immediately are one senior and two junior chemical engineers.

Write:
National Research Corp.
70 Memorial Drive
Cambridge 42, Mass.

RESEARCH METALLURGISTS

Excellent opportunity on enlarged research staff of nonferrous mill products mfgr. M.S. or Ph.D. Age 24 to 33. Applicants should be familiar with testing and instrumentation; have a good working knowledge of advanced mathematics and principles of theoretical metallurgy for alloy, diffusion and metal forming projects. Free medical and insurance coverage. Location Connecticut.
Box G-11 Journal of Metals

RESEARCH METALLURGIST—Thorough training in physical metallurgy and the structure of metals. Recent graduate acceptable. Advanced degree desirable. Field includes metallography, radiography, welding, elevated temperature evaluation, alloy development, foundry process studies, etc. Well established firm expanding under aggressive management.
Box G-9 JOURNAL OF METALS

FOUNDRY CONTROL METALLURGIST—Engineering education desirable. Assistant in staff group engaged in testing and control of foundry alloys, sands, etc., and "trouble shooting". Firm operates both ferrous and nonferrous foundries. Well recognized in its field, under progressive management. Offers opportunity for advancement for competent young man.
Box G-10 JOURNAL OF METALS

PROFESSIONAL SERVICES

Limited to AIME members, or to companies that have at least one AIME member on their staffs. Rates $40 per year per inch.

ENGINEERS
CONSULTANTS
METALLURGISTS

Small Jobs Welcomed

SAM TOUR & CO., INC.

Laboratories and offices
44 Trinity Place, New York 6, N. Y.

Testing—Certifying
American Standards
Testing Bureau, Inc.

MAX STERN
Consulting Engineer

Expert for Scrap Recovery and Shipwrecking — Modernization of Plants and Yards for Ferrous and Nonferrous Metal Scrap

150 Broadway New York 7, N. Y.

LEWIS B. LINDEMUTH
Consulting Engineer

140 CEDAR STREET, NEW YORK 6, N. Y.

STEEL PRODUCTION
DESIGN · OPERATION · CONSTRUCTION · METALLURGY

R. S. DEAN LABORATORIES, INC.

Consulting, Research Development Chemistry, Electrochemistry, & Metallurgy Laboratory Research on a Contract Basis

5810—47TH AVENUE AP-2821
RIVERDALE, MD.

COPPER SMELTER SUPERINTENDENT

For new copper smelter in Northeastern Turkey. Must be familiar with coal fired reverberatory furnaces and horizontal converters. Good living conditions and excellent climate.

Box F-6, JOURNAL OF METALS

Maintenance Engineer Copper Refinery

For new copper smelter in Northeastern Turkey. Must be familiar with coal fired reverberatory furnaces and horizontal converters. Good living conditions and excellent climate.

Box F-7, JOURNAL OF METALS

Versatility...without Costliness for

Photomicrography
Photomacrography

A highly versatile, yet inexpensive combination. Indispensable for routine photomicrography or photomacrography, with Micro-Summar lenses. For plates and cut films 3¼ x 4¼ inches, black and white or color. Accessories available for varied requirements.

Leitz MA IVb

Laboratory Camera

- Direct vision reflex housing for grain counting
- Vertical camera with bellows of 50 cm.
- Simplified time and instantaneous shutter
- Rack and pinion for lens panel
- Light-tight connecting sleeve for microscope

with

BMe

Metallurgical Microscope

- Built-in illumination
- Large, modern stand
- Rack and pinion coarse focusing
- Micrometer fine adjustment on double ball bearings
- Interchangeable large, square mechanical stage adjustable *vertically* by rack and pinion
- Dovetail slider for interchange of tubes
- Large vertical illuminator with compensating prism and plane glass

Write to Dept. Micro 1064 JM

E. LEITZ, Inc., 304 Hudson Street, New York 13, N. Y.

LEITZ MICROSCOPES • SCIENTIFIC INSTRUMENTS
BINOCULARS • LEICA CAMERAS AND ACCESSORIES

Basic values behind the trade mark

Service Division mixer feeds tempered Ramset onto conveyor for delivery OVER charging buggies to furnace.

For years Tom Pence, of the Basic Service Division, has spent most of his time in work clothes on customers' melt shop floors.

SPECIAL SERVICE EQUIPMENT

A FAMILIAR trade mark identifies a dependable product. But quality of product is only one of the values that stand back of the "man with the shovel."

You purchase valuable extras with any of our refractories. On Ramset hearth installations, for example, you benefit from the skilled supervision of the Basic Service Division, as well as from the availability of their special mixing, conveying and impacting equipment.

As a Basic customer, you pay no more for our products because of this service. It is just another plus for your money, another user benefit by which we seek to earn an increasing share of your granular basic refractories business.

Basic Refractories Incorporated 845 HANNA BUILDING, CLEVELAND 15, OHIO

Exclusive Agents in Canada: REFRACTORIES ENGINEERING AND SUPPLIES, LTD., Hamilton and Montreal

THE DRIFT OF THINGS

by Edward H. Robie

OWING to the fact that the usual Fall Meeting, or Mid-Year Meeting, or Regional Meeting, as it was variously called, was not held in 1950, many AIME members are wondering if any definite policy has been adopted as to its continuance. Although scheduling of the Fall Meeting is done on a year-to-year basis, there is no ground for the idea that such meetings will not be held at least fairly regularly in the future. Last year a combination of circumstances prevented holding such a meeting. The American Mining Congress held an important convention and exhibition at Salt Lake City late in August. The AIME was to hold its Annual Meeting in St. Louis in February 1951. To hold another national meeting in the Midwest or Far West in the interval between seemed, especially with a war going on, to be putting somewhat of a strain on the membership, both in preparing for and attending such a meeting.

This year the Fall Meeting is being resumed, of course, with the Mexico City meeting, Oct. 29 to Nov. 3. Next year, the Fall Meeting will be held in Chicago, sometime in the week beginning Sept. 8. This is the time of the Centennial of Engineering celebration, which the American Society of Civil Engineers is sponsoring in connection with its 100th anniversary. Many engineering societies will hold fall meetings in Chicago at that time, so that papers of general interest, or joint interest with other groups, will be especially appropriate. Several AIME Divisions are likely to participate in the program, though few have made any definite plans. No plans have yet been made for the Fall Meeting of 1953, so that invitations will be considered from any Local Section or city that wishes to sponsor a meeting at that time. A suggestion has been made that it be held in Montreal, with a field trip to some of the Canadian mining properties.

As to Annual Meetings, the present plan is to alternate them between New York and another city: New York 1948, San Francisco 1949, New York 1950, St. Louis 1951, New York 1952, Los Angeles, 1953, New York 1954, possibly Houston or some other petroleum center 1955, New York 1956, possibly Chicago 1957.

Chance to Clean House

Out in the country where we live the serenity recently has been punctured more often than formerly by the bells of the junkman's truck. It used to be that payment for scrap metal was little or nothing. The junkman charged as much for taking away the stuff that neither of us wanted as he was willing to give for the stuff that he could use. Anything of heavy metal now seems to be in demand, and the junkman's face lit up no end when we found an old cast iron stove for him. This led us to look into the situation a bit, and we find that steel producers are really threatened with a scrap shortage more serious than that which occurred about 10 years ago. Supplies of heavy industrial iron and steel scrap are dangerously low. Scrap inventories have dropped from two months' supply to stock sufficient only for a few days or weeks, according to the American Iron and Steel Institute.

Of the 1½ billion tons of steel now in use in the United States, millions of tons normally are discarded each year and eventually return to the mills as scrap. During World War II between 110 and 120 million tons were diverted overseas, and scarcely any came back to this country. Scrap has not been exported recently in any quantity, but the country's immense steel production, at the rate of 104 million tons a year, exceeding by 10 pct the World War peak, has absorbed an enormous amount of scrap. Producers would like to have about 60 pct scrap and 40 pct virgin metal to make steel to the best advantage; currently the proportions substantially are reversed.

The scrap cycle, steel from mill to product and back to mill, must be restored quickly to maintain current production, to say nothing of building up depleted inventories to carry mills through the winter months when collections fall off. Government, industry, and agriculture can aid in war preparedness and provide a public service by conducting an emergency inspection of their properties and sending obsolete machinery and equipment to the nearest scrap dealer. There will be no better time for housecleaning than now, in spite of the shortage of labor in many plants. All available heavy scrap is urgently needed.

Finding Summer Jobs

Though organized only three years ago, the Institute's Minerals Beneficiation Div. is one of its most active groups. Among its committees is the Education Committee, which one might perhaps be pardoned for thinking would have more or less prosaic activities. But under the chairmanship of Rush Spedden, at M.I.T., it is really doing a job that other committees might emulate. It has tackled the problem of summer jobs for students.

Its plan is designed: (1) To help students find suitable summer jobs so that they can get some valuable working experience while earning money to help meet the rapidly increasing cost of an education; and (2) To give the mining and metallurgical companies of this country a chance to have a wider choice of technical employes. Through a few months of summer work a company easily may appraise the capabilities of a man they may wish to employ later. The student himself may discover an interesting problem for a thesis or special project for his senior year.

Professor Spedden sent questionnaires to some 70 companies operating minerals beneficiation plants. He asked them how many students could be employed, the type of work available and the pay scale, living accommodations, special qualifications desired, preferences and restrictions, and the dead line for the receipt of applications. Upon receipt of the returned questionnaire, it was copied and sent to the Faculty Sponsors of interested Student Chapters. The students were invited to apply for the jobs on another prepared form, which gave the employer the information he would be likely to wish to know about the applicant.

More will be known about the success of the scheme by the end of the summer. An appreciable number of the employers approached replied with requests for several men, and presumably many students were thus placed in work in which they were especially interested.

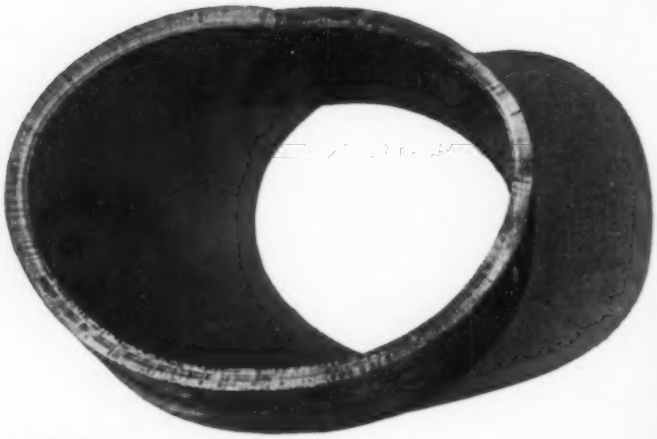

CRUSHING TEST: Ductile iron pipe sections, tested to fracture in compression, reveal the superior ductility of this new engineering material. Its strength and toughness make ductile iron an excellent material for tubular products. The average ring modulus of rupture on 8" diameter rings so tested by Underwriters Laboratories was 127,650 p.s.i. Photographs shown here were furnished by Lynchburg Foundry Company, Lynchburg, Va.

BURSTING TEST: This 8" diameter pipe was cast in ductile iron, welded with Ni-Rod 55® (nickel welding rod developed for cast iron) and then subjected to bursting tests. Average internal bursting pressure: 4,300 lbs. Average bursting tensile strength: 48,600 p.s.i. All cracks occurred outside of the weld, with no shattering.

DUCTILE IRON'S SUPERIOR PROPERTIES

revealed by crushing and bursting tests

DUCTILE IRON is a cast ferrous product that combines the *process advantages* of cast iron with many of the *product advantages* of cast steel.

In less than two years, ductile iron has attained wide acceptance because it offers excellent castability, high mechanical properties, and good machinability. Parts cast in ductile iron show superior pressure tightness, high modulus and resistance to shock.

Typical current applications include ball joints, brake drums, cover hangers for soaking pits, gears on agricultural machinery, large valves, pressure heads for pumps, snow guards and plow points.

AVAILABILITY: Send us details of your prospective uses, so that we may suggest a source of supply from some 100 authorized foundries now producing ductile iron under patent licenses.

Request a list of available publications on Ductile Iron... mail the coupon now.

The International Nickel Company, Inc.
Dept. J.M., 67 Wall Street, New York 5, N. Y.

Please send me a list of publications on: **DUCTILE IRON**

Name _____ Title _____

Company _____

Address _____

City _____ State _____

THE INTERNATIONAL NICKEL COMPANY, INC. 67 WALL STREET NEW YORK 5, N.Y.

A 100-kw, 3-phase, continuous, open top smelting furnace has been installed at the Bureau of Mines Lab, Albany, Ore., for research on direct smelting of nickel alloys from Riddle, Ore., iron-nickel ores; high-phos iron ores from Scappose, Ore., and chromite concentrates from Montana. A 500-kw unit is being completed for developing data upon which to base plans for industrial smelting procedure. Its capacity is 8 to 15 tons of ore in 24 hr, as compared to 1 to 2 tons for the 100-kw unit.

A new 16-in. high vacuum valve, largest of its type, was announced by F. J. Stokes Machine Co. The valve is designed for pressure differential in both directions and is offered in special metals for corrosive applications. Just a fraction of the size of corresponding rubber-diaphragm types, it has worm gear drive and features fast opening and closing.

Union Carbide & Carbon's Electro-Met Div. is planning an expansion at the Portland, Ore., plant including new buildings, facilities, and the addition of electric furnace units that should double calcium carbide and ferroalloy output.

Expansion of production of several mineral commodities important to metals refining is being encouraged by rapid tax amortization. Tax incentives have been issued or are being processed for production of metallurgical lime, dead-burned dolomite, sulphur, refractories, and magnesia.

Keokuk Electro-Metals Co., just completing a 50 pct capacity increase at its Wenatchee Div., Rock Island, Wash., is adding to its Keokuk facilities. An additional blast furnace will be built, graphite and slag control equipment will be added, and raw and finished material handling facilities will be modernized. The program will cost about $1.7 million.

Naval Ordnance Lab, White Oaks, Md., recently installed a new Sendzimir mill for producing thin steel stock needed for pulse transformers, magnetic amplifiers, guided missiles, and high frequency applications. The mill will roll strip up to 8.5 in. wide, reducing 1/16 in. stock to 0.0005 in.

While the Office of Naval Research announced the Horizons, Inc., new titanium process would reduce the price of titanium from $5 to about $1 a lb, the facts are that no one knows what it will cost. The process, an electrolytic technique, is a laboratory method, and has not been tested yet in the pilot plant stage.

Reynolds Metals, through an $85 million private loan, will build a new reduction plant and gas-diesel power plant at Corpus Christi, Texas, and add to facilities at Jones Mills, Ark., and Troutdale, Ore., plants. Another $12 million expansion at Longview, Wash., reduction plant will increase output by about 40 million lb per year. Capacity increase will be through melting pot enlargement.

Zirconium hydride powders are superior to straight zirconium powders for compacting and sintering. Compacting at 40 to 50 tons per sq in. at 1150° to 1260°C, and the use of graphite boats during sintering results in compacts of practically theoretical density and appreciable ductility.

Speer Carbon Co., in a $10.6 million expansion program, will build a new plant at Niagara Falls, N. Y., which should double the company's graphite electrode capacity. Also, expansion and improvement of facilities is underway at the company's plants in St. Marys and Bradford, Pa., and the present Niagara Falls unit.

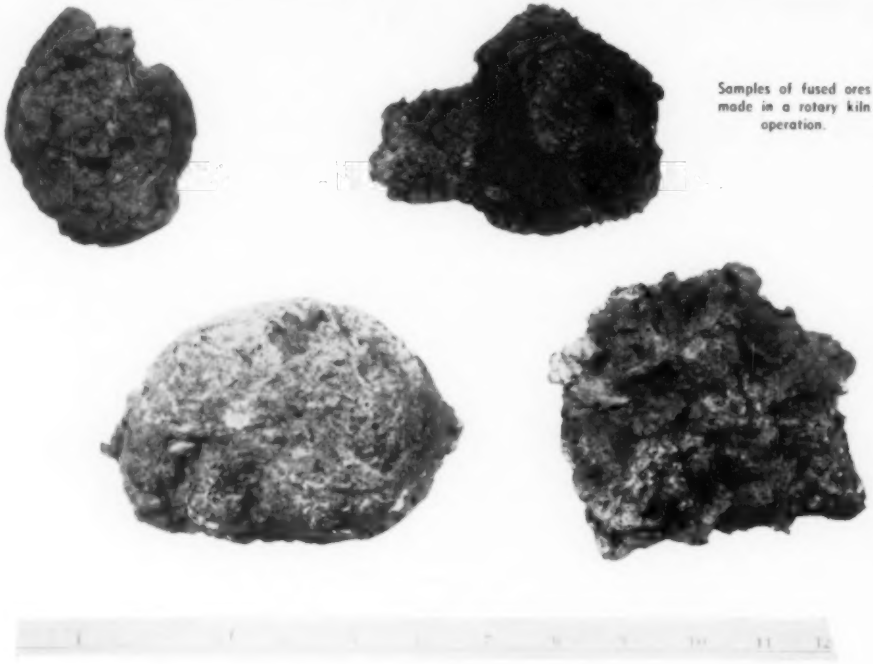

Samples of fused ores made in a rotary kiln operation.

Open Hearth Charge Ore . . .

Key To Steel Capacity Expansion

by LEWIS B. LINDEMUTH

WITH 117,000,000 tons of steel ingots projected for 1953,[1] 135,000,000 tons of metallic charge for the ingot producing furnaces will be required. This amounts to 23,000,000 tons more than was required in 1950. The difference between the scrap available and the necessary total metallic charge must come from blast furnace production and from ore charged into the open hearth furnaces to compensate for this extra proportion of blast furnace iron.

Steel scrap is from two sources—1—that produced within the plants or *home* scrap, 2—that supplied by manufacturers and dealers, *purchased* scrap. Purchased scrap in the early 1930's constituted about 31 pct of the open hearth charge,[2] but in 1950 was only 19.4 pct. It variously has been estimated that the amount of purchased scrap in 1953 will fall short of the 1950 tonnage by as much as 10 pct.[1] Home scrap is likely to be the same proportion of the metallic charge in 1953 as it was in 1950.

Ore substitution for scrap is important as the iron in the ore constitutes an appreciable and less expensive part of the metallic charge. Any circumstance that would permit a higher percentage of ore in the charge would aid in replacing the diminishing scrap supply. If an iron ore were in every way suitable for a charge ore and contained say half of the oxygen usually associated with a lump ore, twice as much charge ore could be used and the recovery of metallic iron from the ore would substitute for the equivalent tonnage of scrap.

For example, if a plant had 24 pct of home scrap for charging and no purchased scrap, but had a charge ore containing half the usual amount of oxygen that a good lump hematite has, the charge

LEWIS B. LINDEMUTH is Consultant in steel production, Lewis B. Lindemuth, Inc., New York.

would be made up approximately: *Home scrap*, 24.0 pct; *Hot metal*, 59.2 pct; and *Iron from ore*, 16.8 pct. This would result in 1.07 tons of ingots from each ton of iron and scrap and therefore it would be more than desirable to use as much charge ore as is metallurgically possible. If these same conditions were undertaken with a lump hematite of normal oxygen content (about 25 pct), the charge would be made up: *Home scrap*, 24.0 pct; *Hot metal*, 66.1 pct; and *Iron from ore*, 9.9 pct. In this case, 0.988 tons of ingots would be produced from one ton of iron and scrap.

A charge ore with half its oxygen content eliminated and with about 70 pct Fe has been produced and tests in open hearth furnaces, while not sufficiently extensive to be conclusive, have indicated that the results as outlined are highly probable.

Purchased scrap will, of course, be available in some percentage, which will reduce the requirement for hot metal and charge ore by a corresponding amount.

To further the use of a higher amount of charge ore, the silicon content of the hot metal is important. Higher silicon requires a higher percentage of ore.[3, 4] A convenient method of estimating the amount of charge ore is to determine the amount of scrap to be charged and then the amount of hot metal necessary to properly melt down this scrap if no ore was charged. On a rough average, with 1 pct silicon in the iron, the hot metal is 80 pct of the amount of scrap. It would be more with low silicon iron and less with higher silicon. It would be more with light scrap and less with heavy scrap. It varies with furnace design, size, fuel, etc. but for any given set of conditions is fairly constant.

If it is assumed that 35 pct of mixed scrap is to be used, iron of 1 pct silicon for melting this scrap amounts to 28 pct of the total charge. This leaves 37 pct of the weight of the charge to be made up from excess iron and from the iron content of the ore, which is charged to take care of this excess iron. In this case the ore requirement would be about 35 pct of the weight of the excess iron which, if the ore ran 60 pct iron, would introduce 21 pct of the weight of the excess iron as iron in the ore. The 37 pct of the charge—excess iron plus iron from the ore—would, therefore, be made up of 30.6 pct excess iron and 6.4 pct of iron from ore. The charge would then be: *Scrap*, 35.0 pct; *Iron*, 58.6 pct; and *Iron from ore*, 6.4 pct. The amount of ore necessary to charge would then be 10.7 pct. If the silicon were 0.50 pct, the charge would be: *Scrap*, 35.0 pct; *Iron*, 61.0 pct; and *Iron from ore*, 4.0 pct. This would amount to 6.7 pct iron ore. If the silicon were 1.25 pct, the charge would be: *Scrap*, 35.0 pct; *Iron*, 53.4 pct; and *Iron from ore*, 11.6 pct. The necessary iron ore would be 19.3 pct.

Storage pile of fused ore, ready for use as open hearth charge ore.

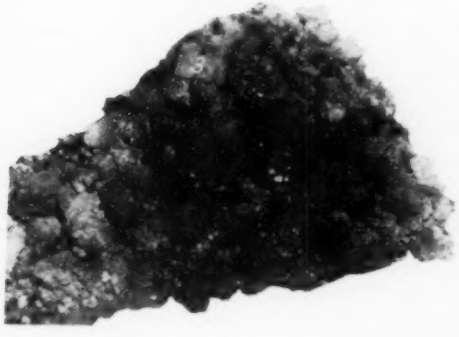

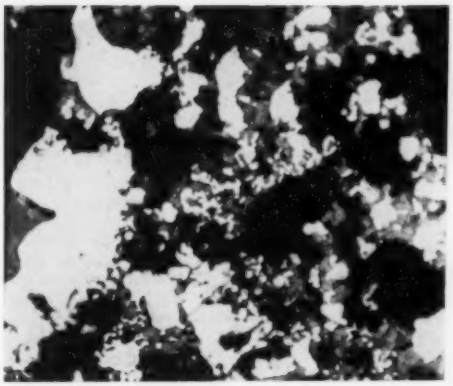

Structure of fused ore. Metallic iron appears white, iron oxide appears gray, and voids appear black.

Higher silicon in the hot metal, up to the limits where it would not interfere with blast furnace production or costs, would aid materially in supplying additional metallics from ore for the open hearth charge. The data from which these estimates were made, as well as previous estimates, were arrived at empirically. The furnaces at the plant where data were evolved are in excess of 200 tons capacity. While the data do not necessarily apply to other plants they are sufficiently close for guidance and estimation.

Open Hearth Charge Ore

Three important characteristics differentiate open hearth ore from blast furnace ore. They are: 1—The size of individual lumps should be in excess of 1 in. mesh. 2—The ore should be as free as possible from combined water. 3—The ore should have an apparent density of more than 3.5.

Ore meeting open hearth requirements is available in this country only in extremely limited quantities. If good ore was available, the furnace facilities for producing the 117,000,000 tons would be sufficient for 5 or 6 pct in excess of that figure. Ingot yield would be increased probably as much as 2 pct, requiring 2,000,000 tons less of metallic charge for the open hearth for the same ingot production. It has been demonstrated that variations of about 12 pct in production are attributable to charge ores.[5]

In 1950 ingot production was: Bessemer—4,534,558 tons; Electric Furnace—5,943,856 tons; and Open Hearth—86,200,000 tons. For the purpose of discussion it is assumed that the increased production will be provided for by the open hearth process, which would increase ingot production to 106,500,000 tons and require 122,500,000 tons metallic charge.

In 1950 the composite charge for the entire open hearth production was made up as shown in Table I. The iron ore was calculated on the basis of having

Table I. Composite Charge for Open Hearth Production

	1939 Tons	1939 Pct	1953 Tons	1953 Pct
Purchased Scrap	19,260,000	19.42	19,260,000	15.72
Home Scrap	24,340,000	24.50	29,962,000	24.50
Total Scrap	43,600,000	43.92	49,222,000	40.22
Iron		52.47		55.21
Iron from Ore		3.61		4.57
Total Charge	99,200,000		122,500,000	

available an ore as specified and this amounted to a requirement of 6,000,000 tons. It is probable that the actual tonnage of the poor grade open hearth ores charged amounted to 8,500,000 tons. The total open hearth metallic charge for an ingot yield of 86.9 pct was 99,200,000 tons. On the same basis, the composite charge for 1953 would be as shown in Table I.

The nonintegrated steel plants use 100 pct scrap, and the integrated plants use a lower percentage of steel scrap and a higher percentage of iron and ore than the industry average. For example, the average charge[1] for a number of integrated plants was: *Scrap*, 30.8 pct; *Iron*, 62.5 pct; *Iron from ore*, 6.7 pct.

Ingot Yield

Low ingot yield from using an unsuitable charge ore results mostly from the same causes that adversely affect other phases of the process under the same conditions. Wet ore, particularly that containing combined water, usually causes violent reactions after the hot metal addition. During these reactions metal frequently flows from the slag hole into the slag thimbles and may or may not be recovered. This can be considerable in extreme cases, but almost invariably a certain amount of metal is lost with a blow.

The same applies to fine ore, whether or not it contains combined water and particularly in wet weather when even the surface moisture may not be removed before the hot metal addition. It also can occur with fine ore where insufficient heating of the pile of ore has caused the hot metal addition to temporarily freeze over. It has been demonstrated that it requires about 4 hr to heat a pile of soft ore 8 in. thick to 212°F with a 3000°F surface exposure. Low apparent density contributes to a decrease in yield because a certain proportion of such ore floats out of the furnace with the flush slag. This is particularly true of down-draft sinter.

In heats that blow, the bath is chilled to varying degrees prolonging the time of heat. If the oxide charge was originally correct for a normal heat, the prolonged time brought about by the blow will cause the heat to melt soft and require further additions of metal to get it sufficiently hot for tapping. This will overcharge the furnace and, unless ladles with thin linings are available, metal will overflow the ladle into the slag thimble.

Accuracy in charging a heat requires that uniformity in reactions taking place in the furnace must be assured. Variations in the analysis and quantity of hot metal may be compensated for, but variations in the reactions of an unsatisfactory ore cannot. Unusual irregularities in timing the addition of hot metal can result in losses with any kind of ore, or with heats in which no ore has been charged, but such instances are exceptional.

Twenty-four plants using soft ore reported an ingot yield of 86.38 pct, while 20 plants using sinter or nodules reported a yield of 87.60 pct.[2] Soft ore is fine and contains high moisture and generally high combined water. Sinter is light in density, contains considerable fines, but is practically free from moisture and combined water.

A foreign plant for the year ended Nov. 30, 1939 averaged an ingot yield of 88.95 pct with a charge containing 72.42 pct iron. This is the usual yield under normal conditions at this plant. The plant is in the position, however, of being able to select open hearth charge ore to a size that has been found best for all percentages of iron in the charge and for all sizes of furnaces up to 250 gross tons. Only ore that passes over a 1 in. grizzly is used.

Open hearth metallic losses increase with an increase in the percentage of iron in the charge, because the normal loss with iron is approximately 10.5 pct while the loss on scrap and on the iron content of the ore is about 4.5 pct. Good open hearth practice will put scrap and butts at about 2 pct. Ingot yield in this country could be 89 pct or slightly higher. Steel plants using high iron charges (50 pct and over) reported an average ingot yield of 86.94 pct.[3]

Accuracy in charging a furnace so that it melts to the desired analysis each time cannot be obtained if the furnace blows, if the metal freezes, or if charged ore floats out of the furnace with the flush slag. Steel scrap requires a definite minimum amount of iron in the charge to have it melt as desired. There are variables affecting this minimum that can be controlled fairly accurately. When it is necessary to arbitrarily charge more iron than this minimum, there is a definite quantity of iron ore that must be charged to compensate for this excess iron. There variables are under control only as long as the ore being used does not cause serious interruptions to the metallurgical sequences. The fine ores and the wet ores, and the combinations of these, do not permit the accuracy necessary for high ingot yield and high production. Typical of the ores now being used are the screen tests on soft ores and sinter shown in Table II.[4]

The recognition of these conditions is further borne out in "Contributions to the Metallurgy of Steel—No. 36",[5] and the paper by Golden and Warren.[3] Under the conditions that will exist when the expansion program reaches the stage of 117,000,000 tons of ingots, the adverse effects of the present

Table II. Ores Used for Open Hearth Charges

Screen Size	Soft Ores, Pct Group 2	Soft Ores, Pct Group 6	Soft Ores, Pct Princeton	Sinter, Pct
+ 2 in.	—	—	—	8.90
+ 1 in.	—	—	13.51	11.19
+ ¾ in.	—	—	—	5.86
+ ½ in.	—	—	15.64	8.44
+ ¼ in.	—	—	17.55	19.16
+ ⅛ in.	—	—	8.21	16.54
+ 2 mesh	23.38	36.80	—	—
+ 8 mesh	19.38	19.49	—	—
+ 10 mesh	—	—	—	8.94
+ 20 mesh	7.81	13.29	14.10	7.37
+ 40 mesh	12.00	10.40	10.09	6.51
+ 60 mesh	10.25	6.82	4.05	2.12
+ 80 mesh	3.06	3.14	2.45	1.06
+ 80 mesh	—	—	—	3.91
+ 100 mesh	3.81	2.36	1.85	—
− 100 mesh	20.31	7.70	12.55	—
Combined water, pct	10.20	4.95	1.43	0.0

charge ores will be increased because there will be higher iron charges and larger furnaces.

While only size, density, and water in ore have been considered, there are also limitations on the usually found impurities and residual metallic contamination. These are, with the exception of acid content, more or less local considerations and do not affect the open hearth process using high iron charges.

It is believed that high acid content is beneficial in coarse sized, heavy oxide and assures a fast, fluid flush. When hot metal is added to a heat where iron ore has been charged, the furnace and the charge are at that moment comparatively cold. To form at this stage a free running slag for a quick flush, the additional acid in the ore materially assists at this temperature. Most of the silica of the ore passes out with the flush slag and does not subsequently interfere with the acid-basic relationships of the finishing slag; nor does it increase appreciably the volume of the finishing slag. In ores, 8 to 12 pct of acids ($Al_2O_3 + SiO_2 + TiO_2$) can be more desirable than an extremely low acid content.

To prepare a charge ore that will meet all of the physical and moisture requirements now recognized as essential for a satisfactory open hearth process, a pilot plant was built at The Hanna Furnace Corp. in Buffalo. As the process and product differ from down-draft sinter and nodules, the term *fused ore* was applied to differentiate from other processes and products. It was the intention to use existing fine or soft ores, or flue dust, or mixtures.

It was learned from this plant that such ore could be made readily, that the size and to some extent the density of the product could be controlled, and that the process was adaptable for preparing blast furnace ore from fines without regard to the degree of fineness. It was also learned that ore for either purpose could be half-reduced, giving a matrix of metallic iron and iron oxide. The pilot plant had a capacity of approximately 100 gross tons per day of ore feed. On the basis of the pilot plant, the estimated operating cost of a commercial plant would be about the same as that of a down-draft sintering plant, but would vary somewhat with location.

The Buffalo plant treated successfully all types of fine ores available at the time, including screened and unscreened Lake ores, fine magnetic concentrates, pyrite cinder, flue dust, sludge, and some waste materials, many of which were more than 65 pct −325 mesh. Taconite concentrates were not available at that time, but the treatment of materials physically and chemically approximating them indicates that the process will handle Taconite concentrates. It was also found that zinc could be removed.

The apparent density can be varied between 3.5 to 4.5, the larger sizes being in the higher density range. The appearance of the product is that of an irregularly rounded nodule, varying in size up to 8 to 10 in. diam. The ore also can be fused completely, in which event it flows as a liquid from the furnace and takes the shape of the molds on the conveyor onto which it is discharged.

The process was based upon a pilot operation in France previous to World War II, known as the "Follsain" process, but modified for higher unit production and greater flexibility of product. It is a rotary kiln operation, using a kiln of two diameters, each section being independently driven with variable speed drives. Fuel for the process, coke breeze or fine anthracite coal, is mixed with the ore and charged into the feed end of the rotary kiln. The fuel and the ore move down the kiln as it rotates and become preheated. At the end of the first section this preheat is below the temperature at which the ore would stick to the lining, but high enough that the fuel will ignite instantly in the second section.

The second section is larger in diameter. Near the discharge end is directed downward into the ore and fuel a blast of air preheated to 1200° to 1500°F, but at a constant temperature within this range. The air blast must have just sufficient pressure to agitate the ore through its entire depth to the lining of the kiln. The air blast and the preheated fuel supply the only heat for the process. Under the blast there is immediately an intense temperature that softens the ore sufficiently for it to agglomerate.

The size of the product is controlled by the rotat-

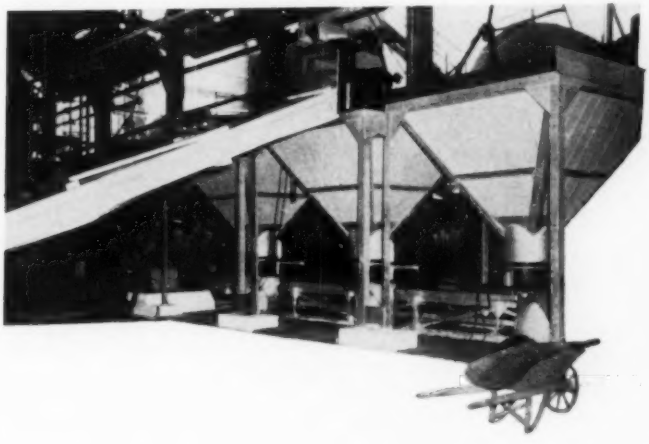

Ore fines, the raw material, and powdered coal are stored in hoppers above a belt that goes directly into the kiln. The operation is continuous.

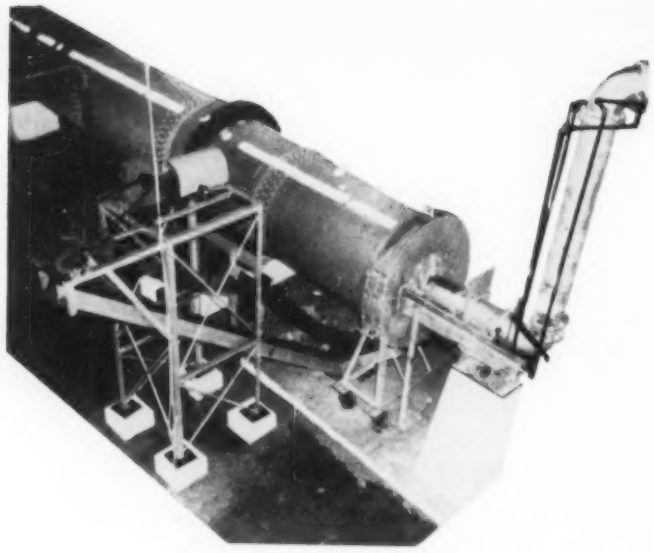

A blast of preheated air is directed downward into the ore and fuel near the discharge end of the kiln. This blast softens the ore sufficiently for it to agglomerate.

ing speed of the second kiln. High speeds, which take the material quickly through the zone under the blower and then quickly discharge it from the kiln, produce small sizes $\frac{1}{8}$ to 1 in. As the speed is decreased the sizes increase. Return fines under $\frac{1}{8}$ in. are less than 2 pct. The conditions for making large sizes are the same conditions which "ring" the lining of the nodulizing kiln. A knife-edge along the kiln wall cuts the soft ore from the lining. This, in turn, rolls back over the ascending sticky ore and coalesces with it, snowballing into the larger sizes.

No accurate mixing of the ore and fuel is required other than collecting them on a belt and discharging them into the kiln. The only moisture requirement is that it be low enough to permit the materials to pass through the bins and handling equipment. Moisture is taken care of, if necessary, by the speed of the preheat section.

The Buffalo plant had three bins, two for ore and one for fuel. These bins discharged through table feeders onto a belt. The belt discharged into a screw conveyor that was intended for mixing but found unnecessary, and then into a bucket elevator that carried the mixture up to the charge spout of the kiln. The agglomerated ore discharged from the kiln fell onto a conveyor similar to a pig casting machine but of sufficient length to cool the material to below a red heat without the use of water. Water, the same as in down-draft sintering, will make the product friable.

The amount of air required is about 100 cu ft per lb of carbon burned. The coal or coke breeze for mixing with the ore is from 4 to 6 pct, depending upon the refractoriness of the ore, and the fuel for preheating the air blast approximates 600,000 Btu per ton of product. An externally fired recuperator is necessary for the air as the temperature of the waste gases is only 400° to 600°F. A metallic recuperator is required because the blower is necessarily located on the cold side of the recuperator.

In treating −325-mesh materials, it was found necessary to keep the velocity of the products of combustion as they leave the kiln at not more than 300 ft per min. There will be a certain amount of material in suspension at the higher temperatures, but below this velocity the dust loss is very low with nothing more than a dust catcher at the end of the kiln.

Several modifications in the method of obtaining heat for special purposes have been considered and investigated. The most extreme case is that of agglomerating an oxide with a high fusing temperature, but which reduces readily in the presence of carbon or CO and which is + and − ten microns in size. For these conditions a flaming electric arc is proposed for replacing both the fuel and the preheated air. The absence of any volume of products of combustion is expected to minimize dust loss on this extremely fine material.

This agglomerating process for metallic oxides is continuous and simple. The plant for carrying it out was made up of units of standard equipment. Control of the preparation of the raw materials and of the operation of the process is not extremely critical at any stage. Its flexibility adapts it to many different materials and to the usually encountered variables when treating a given material, and also permits a variety of physical forms of any one material.

References

[1] *Wall Street Journal*, May 1, 1951.

[2] L. B. Lindemuth: "Steel Industry Faces Growing Scrap Scarcity." *Iron Age*, June 22, (1933).

[3] John J. Golden and Henry E. Warren, Jr.: "Open Hearth Charge Ores", AISI, May 1951.

[4] L. B. Lindemuth: "High-iron Charges in the Open Hearth Process", Proceedings of National Open Hearth Committee, AIME, 1942, Vol. 25, p. 143.

[5] AISI Contributions to the Metallurgy of Steel—No. 26, June 1949.

[6] AISI Contributions to the Metallurgy of Steel—No. 36, August 1950.

Secondary Aluminum Recovery

In the South Pacific

by H. W. Franz

Aluminum from scrapped aircraft around the island of Biak was recovered by means of rather crude but effective methods. This is the recovery plant.

AT the close of the last war some surplus war material used in the South Pacific Allied operations was brought together and placed in dumps for subsequent disposal, according to the then existing Allied policy. The larger dumps in the New Guinea area were located at Lae, Hollandia, Morotai, and Biak. The dump on Biak island consisted largely of surplus war planes, and this is a brief description of how the aluminum of these planes was recovered.

The island of Biak is located just north of the elbow formed by the western arm of Dutch New Guinea. The natives are unbelievably primitive, but rather intelligent and quick to learn. They readily adapted themselves to the work of the aluminum recovery program, and while extremely lazy, when given adequate instructions and supervision, the Papuas performed the work with surprisingly few accidents.

In order to conserve time, two tasks were undertaken simultaneously. The planes had to be broken up and prepared for the melting program, and the furnace plant had to be constructed. The surplus war planes on Biak had most of their instruments and radio equipment removed, so that only the air frames, wings, and motors remained. The motors were first removed from the plane bodies and placed in temporary open storage. The aluminum propellers were removed, cleaned of all foreign metals, and shipped as-is. After melting got under way, the motors were taken to *goedangs* for dismantling. These *goedangs* were large sheds entirely open at the sides, covered with corrugated sheet iron. As far as the aluminum program was concerned, only the aluminum pistons, cylinder heads, crankcases, and miscellaneous aluminum parts of the motors were of importance. As in the case of the propellers, the pistons were cleaned and shipped as-is while the cylinder heads, crankcases and smaller aluminum parts were stored for the melting program.

As the air frames and wings were rather bulky for shipping purposes, it was planned to melt them, and to cast the resulting metal into 1000 lb ingots. To control the quality of the ingots, a thorough preparation program was instituted. Before the planes were broken up, most of the foreign materials such as steel cables, copper wire, electrical equipment, plastics, zinc fittings, magnesium castings, and lead counterweights were removed. Rubber linings of the fuel tanks were removed and burned, but if this proved difficult, they were burned in place. The planes were cut by steel cables or by hand axes, and the bulky parts were flattened out by running a bulldozer over them. The cut parts were then transported to the furnace dump area. The dimensions of the furnaces limited the cut plane parts to about 16 ft.

Furnaces

Except for such items as certain instruments and oil burners and related equipment, most of the materials for the construction of the furnace plant came from either the dump areas of Biak or Hollandia. The furnaces were housed in what was part of a Butler hangar, arranged to act merely as protection from the heavy rains. There were three *sweating hearths* of 20 ft OD, the centers of which were on a semicircle of about 25 ft radius. The furnace hearths were made of fire brick laid over tamped coral sand. The top of the hearths were about 2 ft above the ground, and sloped in the direction of the center of the semicircle. Run-off troughs conducted the molten metal to a central holding or collector furnace, 14 ft diam. The hearths were covered by 6 ft high removable caps, lined with Sil-o-cel brick, having a

H. W. FRANZ is Metallurgical Engineer for Singmaster & Breyer, New York.

flat suspended Sil-o-cel roof. Openings were provided in the caps to permit combustion gases to escape. The outer steel plates for both the hearths and the caps were made of discarded corrugated 3/16 in. air raid shelter plates.

The furnace caps were removed by a 10-ton, pivoted bridge-type crane, with the pivot point located at the center of the semicircle and directly above the center of the holding furnace. The outer leg of the crane ran in a circular arc on guide rails and served the three furnaces. The lifting mechanism of the crane was powered by an electric motor, but the crane had to be moved or spotted over the furnaces by man power. Some 20 to 30 natives were required for this task.

The holding, or collector furnace, was about 12 ft ID, and about 7 ft high. The outer steel furnace shell was made of discarded air raid shelter plates, which were lined with firebrick. The roof was of the flat suspended type, while the hearth was made of firebrick laid on tamped coral sand. The hearth had a slight slope in the direction of the tap hole. The center of the tap hole was about 2 in. above the hearth. The original cast iron tap hole was replaced with firebricks having a tapered hole drilled in them. This tap hole gave very little trouble.

There was a short, brick-lined trough which led from the tap hole to the pour box. This pour box was lined with firebrick, and was of the usual tilting type which permitted intermittent pouring into the molds while metal flowed continuously from the holding furnace. The pour box was controlled through a manually operated worm gear, with an extended shaft which allowed the operator to be located about 20 ft from the tap hole.

The heat for the sweating furnaces was provided by three oil burners placed 180° apart on the circumference of the furnace walls. Two burners were located in the furnace cap, and the third burner was located to one side of the metal exit hole, and over the sloping section of the bottom hearth. There were two oil burners for the holding furnace, but it was found that when this furnace reached temperature only one burner was necessary to maintain temperature.

The casting ring was a circular affair constructed of odds and ends. The center post was taken from the main support of a Japanese anti-aircraft cannon. The casting ring was about 35 ft diam, and normally carried 13 molds. The molds were placed at the outer edge of the ring in a circular continuous pan type structure which was supported by a circular undercarriage made of discarded rails, which in turn carried small flanged wheels. The wheels ran on a double circular track laid on wooden ties. Three-eighth in. iron rods were used as bracing from the center post to the circular pan. Two turns of a steel cable were wound around two cable drums taken from a weapon carrier. By a crude arrangement of gears, levers, and clutches, a single electric motor wound, or unwound the cable from either drum which in turn actuated the casting ring. Because there was a definite length to this cable the casting ring was incapable of being operated continuously in any one direction. The installation was such that after about $1\frac{1}{2}$ turns of the casting ring, the mechanism had to be reversed. The same type arrangement served a small jib crane which was used to service the molds, and to remove the cast ingots. The casting area was roofed over by corrugated sheet iron laid on roof trusses made of scrap angle iron.

Electric power, 3-phase 220 v, was delivered to

Equipment was gathered by natives, stripped of foreign materials and metals, and then cut by steel cables or hand axes and flattened by a bulldozer. This scrap was then shipped to the furnace dump area.

Furnaces were housed in a Butler hangar. There were three sweating furnaces, such as this one, 20 ft diam. Hearths were made of fire brick laid over tamped coral sand. Runoff troughs conducted molten metal to a holding or collector furnace.

This sweating furnace is charged and ready for melting. The hearths were covered by 6 ft high removable caps, with openings to permit combustion gases to escape. The cap is shown removed from the furnace.

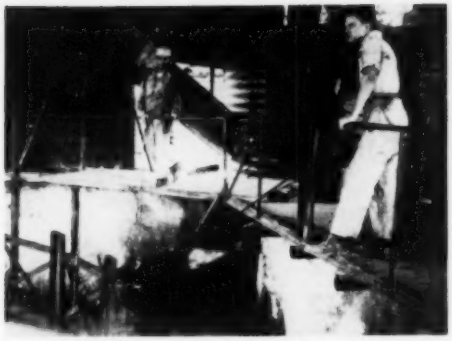

The collector furnace in the background is shown being tapped. In the foreground is the casting platform.

the plant through a transmission line about 300 ft long. The power plant consisted of a battery of four 25-kw reconditioned diesel driven portable units. Two oil pumps, as well as the 15 hp air blower, with respective motors were located in a small shed just outside the Butler hangar. Oil was piped from two 2000-gal storage tanks. The oil originally came from the former Navy dump at Hollandia. Stored rain water was used for ingot cooling.

The prepared scrap from the furnace dump area was transported to the furnace plant by means of small lorries pulled by small gasoline driven tractors. The scrap was hand charged onto the sweating hearth high enough to clear the inside of the furnace cap. After the hearth was charged with scrap aluminum, the cap was lowered in place and all three burners were turned on. Under the action of the heat, the aluminum (together with other low melting metals, if not previously removed) melted off dropwise and collected into small pools. These immediately flowed off to the collector furnace. Towards the end of the furnace cycle the two top burners were usually turned off, leaving only the hearth burner to complete the melting process. If the scrap was clean there was very little dross or foreign matter remaining, but usually the hearths had to be rabbled to break up the trapped aluminum pools. When the flow of aluminum from the sweating furnace ceased, the furnace cap was raised, foreign matter and dross were removed by hand, and the furnace was then ready for another charge.

Cast into iron molds, the metal was sprayed for rapid cooling. The plant, designed for 24 hr operation, had a capacity of 30 ton of finished ingots a day. This production, however, was never reached, and the melting program took longer than originally planned.

As the bridge crane served all three furnaces, the time cycle was generally worked so that as one furnace was charged, another would be ready for rabbling or was ready for charging. The furnace crews were given goggles, gloves, and shoes, as their normal mode of attire consisted simply of a short pair of trousers.

With this type of installation, it was imperative that all furnace scrap be previously cleaned and freed of low melting alloys as there was no provision for subsequent metal refining. However, in a few cases of high magnesium, rather vigorous rabbling of the metal in the collector furnace tended to oxidize the magnesium to acceptable limits (as well as oxidize some of the aluminum). The dross that accumulated on the surface of the metal within the collector furnace was removed as required as it contained a few metallic impurities which would slowly redissolve in the molten metal.

The molds were shaped to provide an ingot of roughly 2x5 ft, and about 10 in. thick. These ingots weighed about 1000 lb. On the inside, and about 4 in. from the bottom of the mold there was a shelf extending horizontally about 4 in. on each side which provided a convenient *set back* to the ingot so that the prongs of a fork-lift truck could be used in transporting the ingots. The molds were cast iron with about 1½ in. walls, and were made in a local foundry in Java. Considerable trouble was experienced with these molds as many cracks quickly appeared, due to thermal shock. This was caused by thin mold walls (2½ in. would have been better), and by the operators having the metal too hot for casting. An attempt to reinforce the molds by tie rods and channel iron was undertaken by the operating personnel, but the reinforcement was improperly applied with the result that almost all of the molds were shortly broken. As soon as the top surface of the ingot solidified in the mold, a water spray was directed on it to cause rapid cooling for the unloading operation.

At the mid-point of the casting operation, a ladle sample was taken out of the mold being filled. Part of this sample was cast into small disks for spectrographic analysis and the remaining sample metal was allowed to cool in the ladle. This last part was later drilled for chemical analysis. A visual long wave spectrometer was used as a quick rough check on ingot quality, while the wet chemical analysis permitted the ingots to be graded as to impurity content.

This aluminum recovery plant as constructed and operated was something unique in nonferrous metallurgy. It was designed for 24 hr operation, with a daily capacity of about 30 tons of finished ingots. Because of unforseen plant delays and local circumstances, this capacity was never attained, with the result that the melting program took just about twice as long as was originally planned.

The design was that of Dr. M. Asimow, who left before the plant was completed to resume his post at the University of California. Certain design details were altered, and the remaining construction was completed under the writer's supervision. Techniques of furnace operation, as well as chemical control, were established by the writer.

The contract to do the job was given by the Dutch Netherlands Government to S. Vles & Zonnen, of Rotterdam, and to the Richard Nathan Corp., New York, the latter firm supplying the technical skill, as well as the material and equipment not available locally.

NYLON

A Factor In STRESS CORROSION Of Aluminum Bronze

by E. J. Silk

STRESS corrosion cracking of aluminum bronze occasionally has been mentioned in technical literature. Plastics in contact with stressed aluminum bronze in tap water may cause stress corrosion cracking.

Stress corrosion cracking occurred in a clamp ring of aluminum bronze in contact with a nylon part in service in city water. The assembly consisted of a nylon part held to a stainless steel part by means of silicon-bronze screws through the clamp ring. The aluminum bronze clamp ring failed in a brittle manner at two points diametrically opposite and at right angles to the screw holes. The aluminum bronze was of the following composition: 94.5 pct Cu; 5.2 pct Al; 0.001 pct Pb; 0.04 pct Fe; and 0.20 pct As. This alloy had been chosen specifically because of its superior resistance to stress corrosion. The clamp rings tested prior to assembly showed that the material apparently was satisfactory in that it was ductile, and several broke at a reported stress of 105,000 psi.

One half of one of the aluminum bronze rings that had failed in service subsequently was tested in tension and shown to be quite ductile. A macroscopic examination indicated that the fracture was of the brittle type. No deformation was detected, whereas the samples that had been pulled in tension showed marked deformation.

On the other hand, the ring that failed in service showed distinct evidence of a stress corrosion failure. The major fracture was intergranular; and a second crack of the same nature was found immediately adjacent to the original fracture, apparently originating on the inside surface and extending approximately 1/3 across the section as shown in Fig. 1. A third intergranular crack was found approximately $^1/_8$ in. away from the original fracture and also originated at the inside surface of the ring, Fig. 2. Both photomicrographs indicate a uniformly satisfactory structure. Hardness tests gave uniform results; the total range was R_{15} 83 to 88.5, with an average of R_{15} 87, approximately equivalent to R_B 81. Evidence indicated that the cracks, and very probably the fracture, originated at the inside surface in contact or in relatively close proximity to the nylon gear. Fig. 3 is an end view of the assembly showing the relationship of the various components. The distortion of the aluminum bronze ring is evident and to be expected. The reported characteristics of all the failures encountered definitely placed the area of failure as being in contact with the nylon gear.

A number of the nylon parts were tested qualitatively for ammonia using the Nessler Reagent. All samples tested indicated the presence of trace amounts of ammonia, but it is questionable whether nylon in tap water will release ammonia. Nylons are complex polyamides, produced by the polymerization of dibasic acids and diamines. The resultant product is a complex linear polyamide. Amides as chemical compounds are hydrolyzed in the presence of mineral acid or alkali to form the corresponding organic acid and release ammonia. The reaction between nylon polyamide and the strong alkali present in the Nessler Reagent may have produced the ammonia, thereby giving a positive ammonia test. The hydrolysis reaction is more pronounced in acid than alkali solution and at elevated temperatures. As a possible source of amines from nylon, there may have been some residual diamines, which did not polymerize in the manufacture of the nylon.

In view of the definite evidence of a stress corrosion failure, and the fact that the aluminum bronze was metallurgically free of defects, it was only possible to conclude that the nylon gear was the contributing factor to the stress corrosion failure.

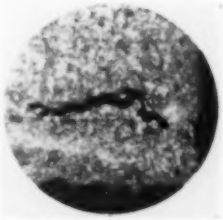

Fig. 1—Original intergranular fracture and second intergranular crack adjacent to it. X100.

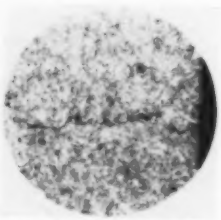

Fig. 2—Third intergranular crack that originated at inside surface of the ring. X100.

Fig. 3. End view of assembly showing the relationship of the various components.

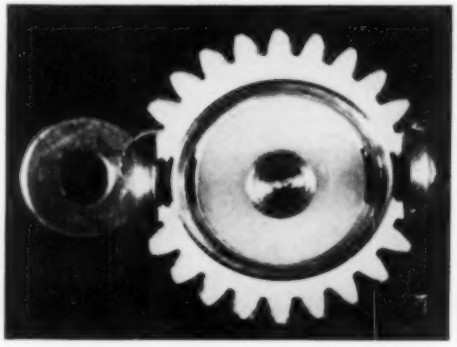

E. J. SILK is Senior Metallurgist at Sam Tour & Co., Inc., New York.

Oxygen in Acid Electric Steel Production

Tapping a 30-ton heat of alloy steel from a tilting furnace.

by J. H. Garrison

IN melting steel in an acid electric furnace, the various stages of the oxidizing and refining periods should follow in a definite sequence so that the reactions in the bath take place and are able to reach completion. Every steel melter probably has experienced having the furnace get ahead of him. By this is meant that he has erred in his judgment of when to go from high tap to a lower tap. This procedure upsets the usual reactions of oxidizing the silicon, carbon, and manganese in the bath. If allowed to go far enough much larger additions of iron ore or other oxidizing agent will be required to bring the carbon to the proper level and to produce the vigorous boil in the steel bath, which is necessary for successful casting of steel.

Another way this same condition can be brought about is to have a charge that contains a great amount of sand or slag, which covers the steel pool as it melts. This prevents the normal amount of oxidation to take place, and if extreme enough it may cause silicon to be reduced from the slag and enter the bath. This will prevent the usual oxidizing reactions.

The necessary steelmaking reactions take place most economically and quickly at certain times and temperatures in the melting cycle. To recognize the proper time to make furnace additions, and to regulate the current input to bring about these reactions is the big job of the melter and the test of his skill.

At Oklahoma Steel Castings Co., oxygen is used in the 2-ton acid electric furnace as the oxidizing agent. With the furnace charge made up of 55 pct plate and forging scrap and 45 pct shop scrap, the charge does not contain enough oxide to keep the bath sufficiently oxidizing for best operation. For this reason, an iron ore addition of 1.3 pct of the charge weight is placed in the cold charge along with approximately 15 points of carbon in the form of carbon electrode turnings. When no additional oxide was used in the charge, the furnace produced a reducing atmosphere that held the residual silicon

J. H. GARRISON is Chief Metallurgist of Oklahoma Steel Castings Co., Inc., Tulsa, Okla. This article was presented at the Electric Furnace Steel Conference, Pittsburgh, Dec. 7 to 9, 1950.

Table I—Typical slag and steel analyses

Time of Analysis	Steel Analysis, Pct			Viscosity, Herty, $\frac{1}{4}$-In.	Slag Analysis, Pct		
	C	Mn	Si		FeO	MnO	SiO_2
Before O_2 Injection	0.41	0.32	0.19	3.75 In.	25.5	8.15	51.9
After O_2 Injection	0.17	0.18	0.13	1.5 In.	20.6	9.5	55.5
At Tapping	0.23	0.74	0.46	1.25 In.	17.0	9.8	59.2

too high for the bath to respond quickly and vigorously in the oxygen boil.

Standard charge melts in with a carbon content of 0.40 pct and silicon 0.20 pct. The charge is melted down on high tap until it is almost completely melted. Practice has been to make a slag addition of sand and limestone as soon as the charge is sufficiently melted to get this material in the furnace door. It is believed that this slag with approximately 25 pct iron oxide from the charge and iron ore addition helps stabilize the arc and hasten the process of gaining the desired temperature to begin oxygen injection.

Control by Ammeter

A pyrometer is not used in maintaining furnace control. An Esterline Angus recording ammeter is used by the melters as a control instrument. The recorder is a 10-amp meter connected in the primary circuit of the melting furnace and located near the furnace switchboard. All melters know how important it is to watch the furnace, its flame and color, and the volume of the smoke; and to keep an ear tuned to its hum. This recording ammeter is successfully used by the melter as a guide in maintaining furnace control and aids in maintaining a standard practice from one shift to another. The chart paper of the recording ammeter moves at the rate of one division line every 7½ min. The current surges are shown as the lines swing to the left and are pronounced on high tap, as the charge is melting and the scrap slides in against the electrodes.

At No. 2 tap, the charge is all melted and the arc is stabilized as the metal quietly increases in temperature and the ammeter draws a straight line pattern until it abruptly reaches a boil. This point is shown by the ammeter as it causes a sudden surging in the flow of current into the bath. This is shown on the recording ammeter chart in the No. 2 tap period.

At this point, oxygen is injected. Carbon content is determined with a Carbanalyzer, the power is turned off at the furnace, electrodes are raised, the furnace door is opened, and oxygen is injected into the bath.

The oxygen is brought near to the furnace from a cascade system through a 1½ in. diam welded steel line. A 1-in. rubber hose fitted with a filter at either end makes the connection between the oxygen line and the lance. The lance is a 4 ft length of copper pipe and a 7 ft length of steel pipe, all 1 in. diam. The end of this lance is reduced to ⅜ in. pipe, 3 ft long and covered with a rammed refractory material, which is used green and is renewed for each oxygen injection.

This lance delivers a flow of oxygen of 100 cu ft per min at a pressure of 50 lb. Pressure is maintained by a globe valve pressure regulator. A portable shield placed in front of the furnace door protects the operator from the flames of the furnace. This shield is built with a service opening, through which the lance is injected into the furnace. As the oxygen is turned on, the lance is put into the bath to a depth of 6 in. at an angle of about 45°. A boil is quickly started and extends to all parts of the bath.

The length of time of oxygen injection is determined by calculating the time needed to reduce the carbon to the desired level at the rate of 4 points per min. The steel temperature increases considerably during the oxygen boil. When this period is finished, power is turned on, a carbon test is taken quickly and, if it is in the desired range, manganese and silicon additions are made. The heat is tapped 2 min later.

At the plant of Oklahoma Steel Casting Co., the recording ammeter is believed to be a convenient and dependable instrument, which helps the melter in maintaining furnace control in the practice of oxidizing steel with oxygen.

In the spring of 1948 when the use of oxygen in the steel furnace was started, data seemed to indicate that there were definite limits of total carbon drop and the rate of carbon drop necessary to prevent pin holes in the castings. Now, it is believed that maintaining the proper degree of oxidation during the meltdown period and bringing about the furnace reactions at the proper temperature and time are more important in producing quality steel than either the total carbon drop or the rate of carbon drop. By this, it is not meant to infer that a vigorous carbon boil is unnecessary to produce clean steel. However, the importance of the proper sequence of furnace conditions and reactions should be emphasized.

Averages of analyses of typical slag and steel tests were made: 1—before oxygen injection; 2—at the finish of oxygen injection; and 3—at tapping time. These analyses are shown in Table I.

From Aug. 15 to Sept. 15, a check made of 100 mild steel heats showed the following average values: Meltdown carbon, 38 pct; oxygen, 450 cu ft; carbon content after oxygen, 0.195 pct; and average rate of carbon drop, 4.17 points.

Table II shows some comparisons between present operations using oxygen and those of 1947 using iron ore. Monthly production was approximately the same for the two periods and therefore should give a true comparison of results. The periods compared are 2 month periods. The furnace roof and lining life in neither case are the highs or the lows, but are believed to be average.

This shows a substantial improvement over the record with iron ore oxidation in every respect except refractory life, which is more than offset by time saving, lower power cost, and a 30 pct improvement in manganese recovery.

Table II—Comparisons between operations using oxygen and those using ore

Furnace Data	Oxidation with Oxygen	Oxidation with Ore
Power consumption, Kwh per ton	457	518
Roof and lining life, No. heats	331	406
Electrode consumption, per ton of steel, Lb	6.99	7.61
Steel melted per min., Lb*	105.7	98.5

*—Time includes charging and delays.

Ore Practice

In Acid Electrics

by F. J. STANLEY

A MELTING practice in any foundry is designed to produce sound metal that possesses, after appropriate heat treatment, desired physical characteristics. Practices developed or adopted may differ, but objectives are the same. The practice in use in the operation of a 12-ton furnace at McConway & Torley Corp., Pittsburgh, achieves the objective outlined.

The data from which this article was prepared were taken during the production of a series of 17 heats. Averages are shown, and in no case were data deleted that were obtained from an unusual heat. Unusual conditions occur from time to time, when the boil and the slag development vary from the normal time requirements. To recount conditions arising in everyday practice, these conditions are included in the data shown.

These 17 heats were made in a 12-ton Moore Lectromelt furnace, powered by a 5000 kva transformer. Electrodes were 14-in. graphite, and were consumed at a rate of about 9 lb per ton of charge. Power consumption was between 460 and 470 kw per ton of charge. Roof life averaged about 300 heats and lining life about 325 heats. Shaped refractories were used to make up the roof.

In this article, the term *blow* designates the point at which the boil, usually vigorous, becomes violent and the period through which this violence continues. This is usually from 2 to 3 min. The rate of carbon reduction during the blow is slightly more than a point a minute, but diminishes during the milder but still active boil that follows. The blow doesn't always occur, but occasions when it does not are rare. On these occasions the heat is worked with no allowance for its failure to develop.

To avoid misunderstanding of the use of the term *the block*, it is used here to indicate the ferrosilicon and silicomanganese additions made to the bath. This is made as soon as the carbon and the slag adjustments are completed.

Original melting equipment at McConway & Torley Corp.'s plant consisted of three acid openhearth furnaces. These were replaced by two Moore Lectromelt top charge units of 6 tons and 12 tons capacity, respectively. The replacement of the open hearths took place from 1941 to 1945, the first unit installed being the 6 ton furnace in 1941. It was operated along with the two remaining open hearths. This circumstance influenced the practice that was established in operating the electric unit.

Experiments and tests were made in conjunction with the Acid Open Hearth Assn., resulting in an

FRANK J. STANLEY is Works Manager of McConway & Torley Corp., Pittsburgh. This paper was presented at the 8th Annual Electric Furnace Steel Conference.

Pouring a top charge 6-ton electric furnace.

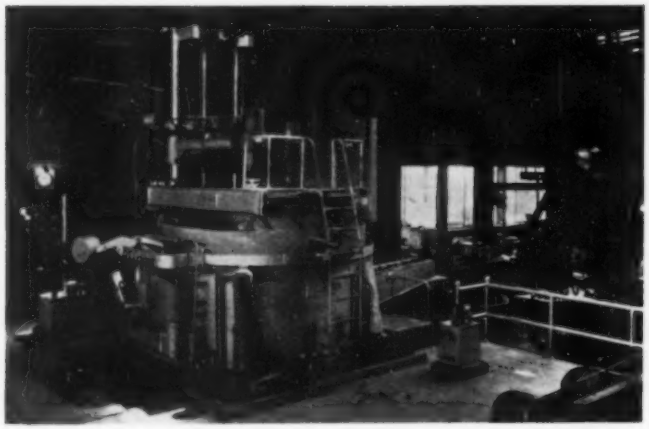

A 12-ton "OT" Lectromelt furnace similar to the one installed at McConway & Torley Corp.

ore practice in the open hearths that was predicated upon slag observation and manipulation. In establishing methods for the new unit, it was natural that much of the openhearth practice would carry over. This was the case, and by the time the 12-ton furnace was installed the practice was established. With but one exception, this practice has remained unchanged. This exception was the abandonment about two years ago of the practice of making all ore additions after the melt-down. It was found that the boil began earlier when an increment of ore was added with the charge, and the overall time required to process the heat was shortened. How much, however, is not a matter of record.

The present charge consists of 24,000 lb, consisting of 60 pct plate and structural scrap, 20 pct foundry returns, 14 pct steel car wheels, and 6 pct axle turnings. Because the furnace cannot hold the full charge, about 4000 lb is withheld until melting has progressed sufficiently to accomodate it, and with this final charge 300 lb of ore is added.

This charge gives a melt-down carbon between 0.28 and 0.36 pct, manganese between 0.11 to 0.20 pct, and silicon between 0.07 to 0.12 pct. The temperature at the melt-down is usually 2800° to 2830°F, with a slag that runs completely through the test mold. Incidentally, the test mold is the mold recommended by the Acid Open Hearth Assn., 18 in. long with a $\frac{3}{8}$ in. bore. Carbon determinations during the heat are made with the Carbometer, and temperature readings are taken with a Leeds and Northrup optical pyrometer.

Immediately after the melt-down, an addition of 300 lb of ore is made. The boil starts almost at once after this addition and continues with increasing vigor through the blow to the block. The time lapse from the beginning of the boil to the block is from 12 to 33 min, depending upon the carbon drop, the temperature rise, and the shaping up of the slag. The temperature at the beginning of the boil is about 2850°F. At the end of the blow, the temperature has risen to 2950° to 3000°F, with a slag test run of from 12 to 14 in. The slag at this point carries from 32.72 to 39.06 pct FeO, 8.52 to 9.92 pct MnO, and 39.22 to 47.13 SiO_2. The carbon drop during the boil and the blow is at a rate of 0.0036 to 0.0093 pct per min, with an average drop of 0.0064 pct per min, less than a point a minute.

The time from blow to block is devoted to carbon adjustment and development of the desired slag condition. Sand only is used in shaping the slag, and either ore for carbon reduction or pig iron for recarburization, as required, is used for carbon adjustment. During this period, the temperature rises to 3020° or 3050°F; and the slag test length decreases from 12 to 14 in. down to 5 to 7.25 in. The composition of the slag at this point, just before the block, is: 20.30 to 24.27 pct FeO; 13.60 to 16.95 pct MnO, and 50.70 to 55.20 pct SiO_2. With the slag and carbon satisfactorily adjusted, the block, consisting of silico-manganese and ferro-silicon, is made; and the heat is tapped as quickly as possible. To the ladle is added the balance of the additions, consisting of silico-manganese, aluminum at the rate of 3 lb per ton of charge, and calcium-silicon at the rate of 2 lb per ton of charge. The tapping temperature is 3025° to 3050°F.

These figures approximate those presented by Dr. G. R. Fitterer in his paper on Acid Electric Slags, presented at the fourth conference of the Electric Furnace Steel Conference, Dec. 6, 1946. Dr. Fitterer's observations were made on heats produced in the same furnace, and, with the exception of making all ore additions after the melt-down, were based on the same practice.

An attempt was made to determine whether slag depth on the bath changed materially from the time of its formation until the tap. No adequate method was devised to measure slag thickness. An estimate based only on observation is that slag is about $\frac{3}{8}$ in. thick after its formation and may reach a thickness of $\frac{1}{2}$ in. at the end of the heat, depending upon the weight of sand added.

In tests to determine the actual melting loss, three heats were studied. The method used was the weighing of the charge as usual, weighing a new ladle, and weighing the empty ladle plus the residual slag. The average of the three heats indicated a melting loss of 4.55 pct and a slag weight of 5.4 pct of the weight of the charges.

Twenty-Five More Years of Metallography

by J. R. Vilella

IN accordance with the custom of this society, we are gathered here, as we have every year since 1924, to honor the memory of the eminent American metallurgist and teacher, Professor Henry Marion Howe. Unlike many of the distinguished metallurgists who have preceded me as a Howe lecturer, I cannot bring to you reminiscences of his personality, for it was not my privilege to be associated with Professor Howe, or to be directly one of his students. Yet, Professor Howe and Professor Albert Sauveur, through the medium of their books, were my first teachers of metallography, as they have been of almost all American metallurgists of my generation. As a teacher, and for many years the acknowledged leader of American metallurgists, he exercised a profound influence in the growth of our science and was held in honor by the men of science of his time. I can speak no words of technical appreciation that will add luster to his fame, for by his prophetic vision, his teachings, and his researches he stands among the immortals in the memory of all metallurgists.

In 1926, the third Howe Memorial Lecture was presented by Professor William Campbell[1] of Columbia University, who entitled it "Twenty-Five Years of Metallography." He took as a starting date for his chronology the turn of the century, which coincided with his arrival from England to work in association with Howe at the Columbia School of Mines. In that informative lecture Professor Campbell enumerated the important advances in metallography achieved during the first quarter of the century, and, it now appears, may have established the custom of reviewing such progress every twenty-five years. The scope of Professor Campbell's lecture was as broad as his metallurgical knowledge, for it embraced a wide portion of the field of metallography, both ferrous and nonferrous.

Twenty-five years later, the Howe Memorial Lecture Committee saw fit to assign to me the honor of writing a lecture that would commemorate the work of Henry Marion Howe and would at the same time constitute the 25th anniversary of the lecture by Professor Campbell. The Committee suggested that this lecture might properly be called "Twenty-Five More Years of Metallography," a suggestion that I have adopted. I must confess, however, that I have not followed the precedent established by Campbell and have narrowed the scope of this lecture to an appraisal of those achievements which in my opinion have contributed most to the progress of microscopical metallography during the past twenty-five years.

J. R. VILELLA is with the Research Laboratory, U. S. Steel Co., Kearny, N. J.

TP 3117C. Manuscript, May 31, 1951. St. Louis Meeting, February 1951.

Progress in Metallography

The metallographic methods most widely used today, with the exception of the electron microscope, were firmly established more than twenty-five years ago. In general, our specimens were prepared for microscopic examination in those days in much the same manner as they are today. It is true that new details of technique have been introduced from time to time, and that superior equipment is available today, but on the whole, these improvements have been in the nature of refinements, often a matter of personal preference, and none can be considered essential to the attainment of the ultimate goal of the art and science of metallography, which is to reveal the structure of metallic specimens with unequivocal clarity so that they may be interpreted correctly.

Mechanical metallographic polishing, which was the only method available in 1926, is still universally practiced and still consists of abrading the metallic specimen with a series of abrasives of increasing fineness until a specular surface is attained. We have now the alternative method of electropolishing, but it is not widely used because, except in a few special cases, its results are inferior to those of competent mechanical polishing.

Likewise, most of the etching reagents preferred today were in common use more than twenty-five years ago and were applied in the same manner as they are today. Valuable improvements have been made in the optical and mechanical performance of metallurgical microscopes, but there was no dearth in those days of excellent instruments equipped with achromatic and apochromatic objectives capable of yielding micrographs comparable in quality with the best that we can make today. In fact, it would be a difficult task for any metallographer today to make optical micrographs at magnifications in excess of 3000 diameters that would surpass those made by Lucas more than twenty-five years ago. One of these is shown in Fig. 1. Yet, it is unquestionable that on the whole, the micrographs appearing in the metallurgical literature today are vastly superior to those

Fig. 1—Partly resolved nodule of fine pearlite. Made by F. F. Lucas prior to 1926. X3650.

of twenty-five years ago. Since progress in metallography is best reflected in the quality of the published micrographs, it suffices to compare those used as illustrations in the volume of the *Transactions* of this Institute which contains the Howe Memorial Lecture of Professor Campbell[1] with those illustrating any recent volume, to appreciate the magnitude of the progress accomplished during the past twenty-five years. But since this notable progress does not stem from new techniques or superior equipment, what brought it about? I believe it is the inevitable consequence of a better concept of what constitutes a properly prepared metallographic specimen. The aim of the metallographer some years ago was the attainment of a highly specular surface of adequate flatness, free from scratches. At the cost of many errors of interpretation and much confusion in our concept of some of the structures of steel, we have learned that these requisites are not enough; that in addition the nonmetallic inclusions have to be preserved intact so that the cleanliness of the steel may be judged correctly, and most important of all, that the polished surface has to be freed from all traces of flowed or disturbed metal before the true structure of the metal can be seen. Rapid progress began when the idea spread among metallographers that the structure observed in specimens which had been polished and etched just once, was seldom the true structure of the metal. The fact that a polished metallic surface owed its specular finish to a layer of flowed metal had long been known, but the effect of incomplete removal of this layer on the appearance of the structures of steel and other metals was not appreciated. In fact, it was generally assumed that this layer of flowed, or amorphous metal, as it used to be called, was removed completely during the first etching and therefore very few questioned the authenticity of a structure revealed in a sample polished by a competent operator and etched in one of the standard reagents. It is my belief that our failure to rid the surface of metallographic specimens of this insidious layer of disturbed metal was one of the most subtle but effective obstacles blocking progress in our knowledge of the structures of steel and that it entailed consequences from which metallography has but recently recovered.

We need only to recall our concepts of some of the structures of steel prevalent about 1926, and the nomenclature and phraseology that grew logically out of those concepts, to appreciate how greatly our ideas have changed since it became possible to see the true configuration of the structures of steel. It was then generally agreed that pearlite was the structure resulting from direct transformation of austenite and exhibiting alternate lamellae of ferrite and carbide, Fig. 2. Martensite was universally recognized as the slow-etching acicular structure of great hardness resulting from low temperature transformation of austenite and generally obtained by cooling steel rapidly from the austenitizing temperature, Fig. 3. Likewise, there was no hesitancy in identifying as troostite, the dark etching, nodular structure often found associated with martensite in rapidly cooled steels, Fig. 4. In the high carbon alloys there was no difficulty in identifying ledeburite or proeutectoid cementite occurring either as a massive network or as primary needles. These are illustrated in Figs. 5 and 6 respectively. Mixtures of martensite and retained austenite, such as illustrated in Fig. 7, were likewise readily recognized in very high carbon steels. However, if the structure observed under the microscope was a dark-

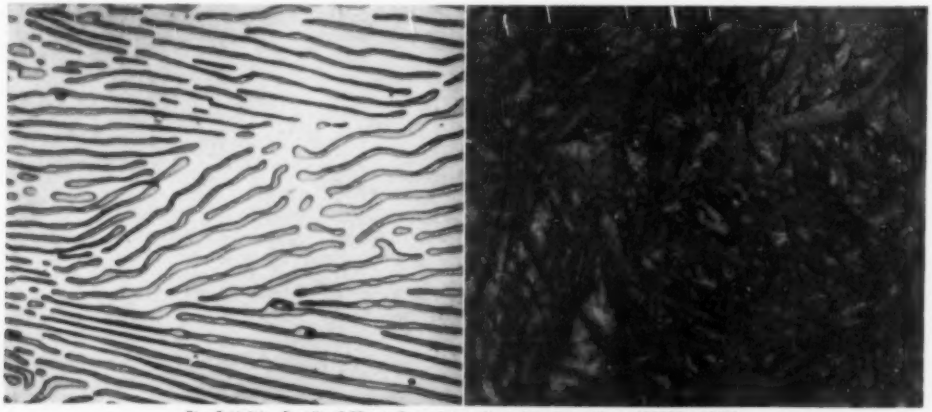

Fig. 2 (left)—Pearlite 0.89 pct C steel transformed isothermally at 1325°F. X2500.
Fig. 3 (right)—Martensite 0.87 pct C steel water quenched. X1000.

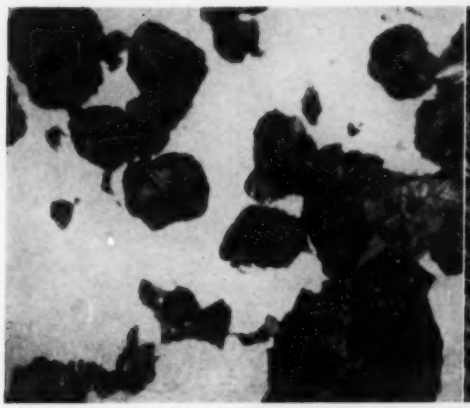

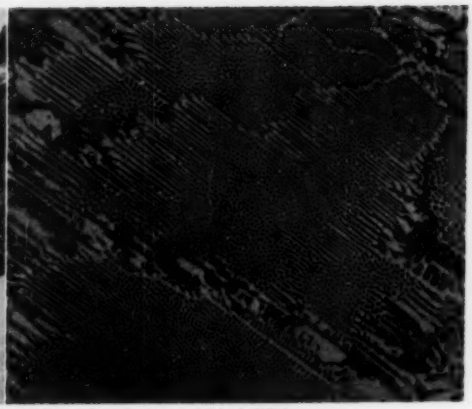

Fig. 4 (left)—Nodular fine pearlite (troostite) 0.89 pct C steel water quenched. X750.
Fig. 5 (right)—Ledeburite 3 pct Cr steel melted in a graphite crucible. X150.

etching conglomerate that could not be resolved into lamellae, then the metallurgist had to decide whether it was troostite or sorbite. Since these structures lacked characteristic patterns or configurations on which to base identification, the decision on what to call such a structure depended on the heat treatment that the steel had received. The structure was considered to be troostite if it had been obtained either by tempering martensite at slightly below 750°F or by cooling through the transformation range at a rate slower than that required to form martensite, as for example, by oil quenching, or in the middle of large pieces quenched in water. It was sorbite if produced by tempering martensite between 750° and 1300°F or by air cooling small pieces from the austenitizing temperature. In other words, it was generally accepted that essentially the same structure resulted from the decomposition of austenite on cooling and from the decomposition of martensite on tempering, although by 1926 there was an increasing number of metallurgists who questioned the correctness of that view. We find, for instance, that Professor Campbell in his Howe Memorial Lecture of that year asks, "But have we strong enough evidence to prove that it (troostite) is the same as the secondary troostite that occurs on cooling?" However, the fact is that the only reason this question had to be asked in 1926 was because, in spite of excellent microscopes and fine apochromatic objectives, we were unable to see that the structures resulting from the direct transformation of austenite were lamellar, whereas those derived from the tempering of martensite were granular. And the reason we could not see this fundamental difference, clearly shown in Figs. 8 and 9, was because our microscopes were focused on a false surface, just a few atomic layers in thickness, over the surface that would have given us a definitive answer. It was our inability to see beyond this false surface, more than any other cause, that gave permanence to the old concepts of sorbite and troostite.

After more than a quarter century of active participation in furthering the art and science of metallography, it is my considered opinion that recognition of the existence of a layer of disturbed metal formed during polishing and its elimination by the practice of alternate polishing and etching, Fig. 10, has been one of the observations that has contributed most to our knowledge of the structures of steel and to the progress of metallography in general. Yet, even after we were able to see clearly, our understanding and proper interpretation of these struc-

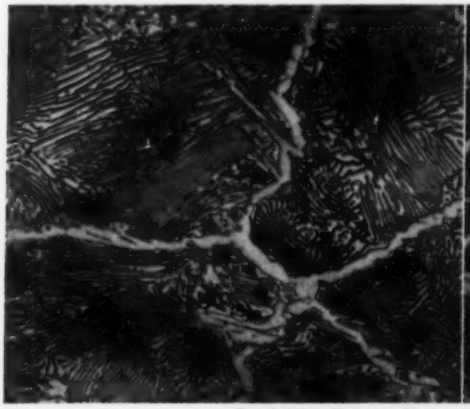

Fig. 6 (left)—Proeutectoid cementite case carburized steel. X2000.
Fig. 7 (right)—Austenite and martensite 1.6 pct C steel water quenched. X500.

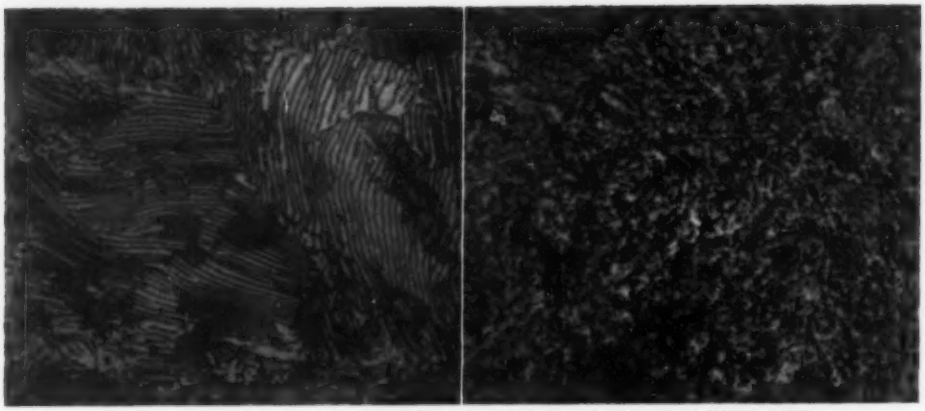

Fig. 8 (left)—Lamellar structure (pearlite) 0.89 pct C steel transformed isothermally at 1225°F. X2500.
Fig. 9 (right)—Granular structure (tempered martensite) 0.87 pct C steel, brine quenched and tempered 1 hr at 1100°F. X2500.

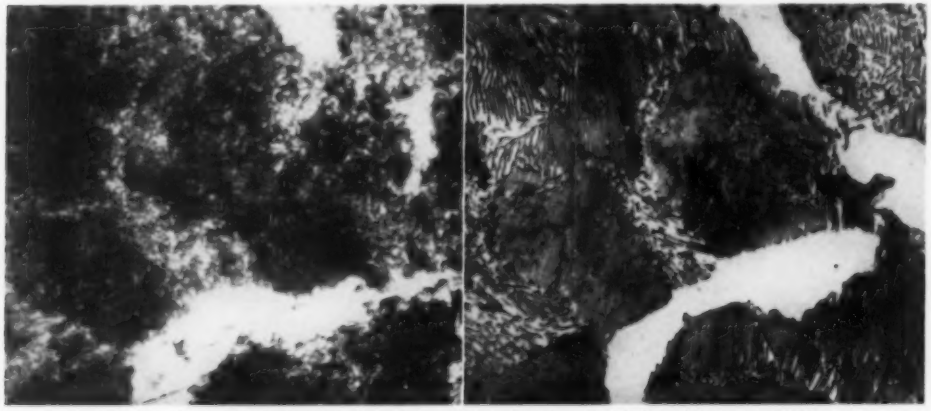

Fig. 10-a (left)—Disturbed metal produced during polishing. b (right)—Disturbed metal eliminated. X1000.

tures might have been delayed had it not been for a contribution from the field of physical metallurgy that I propose to discuss briefly.

This was the investigation by Bain and Davenport into the decomposition of austenite that led to the development of the isothermal transformation diagram. This method of investigation in a comparatively few years turned the emphasis in metallurgical thinking and research from the study of the constitution of alloys after attaining equilibrium at various temperatures to the study of the reactions in solid steel responsible for the aggregate structures, which in turn determine the properties of the alloy. Since the publication of their first paper[2] on the transformation of austenite at constant subcritical temperature in 1930, there have been few major contributions to our knowledge of steel metallography outside of the field of inquiry opened by this epochal work. Its contributions have been in many directions; it established the relation of transformation temperature to type of structure; it enabled us to measure rate of transformation in solid steel; it taught us how alloying elements and variations in austenite grain size exert their influence on hardenability; it disclosed the interrelation of the structures; it gave us a new family of structures, the bainites, Figs. 11 and 12, whose valuable properties are finding increasing application in diverse industries; it provided us with a scientific basis for revision of the obsolete nomenclature of the structures of steel; and most important of all, it transformed the heat treatment of steel from an art into a science.

In the struggle to rid the metallographic specimen of disturbed metal, the introduction of electropolishing was a welcome aid. For many years we realized that practically every metallographic specimen of austenitic, low carbon stainless steel exhibited striations and figures that were purely a surface condition produced during its preparation. The elimination of these false structures by the technique of alternately polishing and etching, employed with such success in carbon and low alloy steels as well as in nonferrous alloys, proved inadequate when applied to soft austenitic steels. Quite often we were forced to accept the presence of these defects in micrographs intended for publication because we were unable to eradicate them. With the advent of electrolytic polishing this vexatious condition disappeared. If we cannot by ordinary mechanical polishing, we can now by electropolishing, reveal the structure of the softest austenitic al-

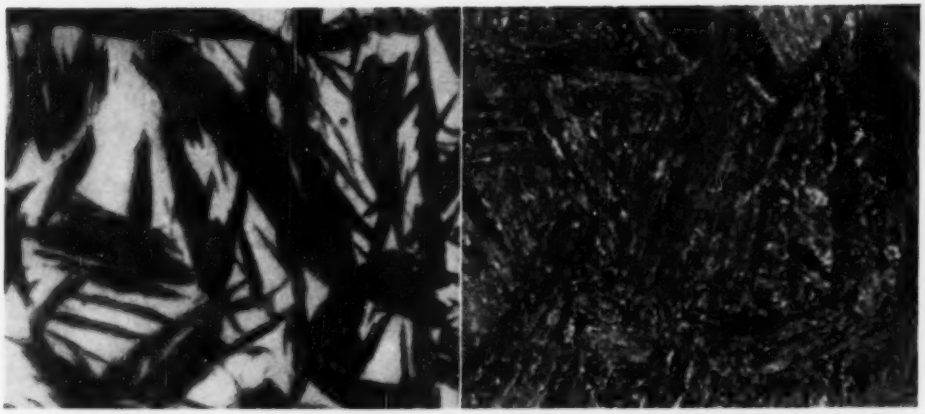

Fig. 11—Bainite 0.89 pct C steel transformed isothermally at 550°F. X2500. a (left)—Partial transformation. b (right)—Complete transformation.

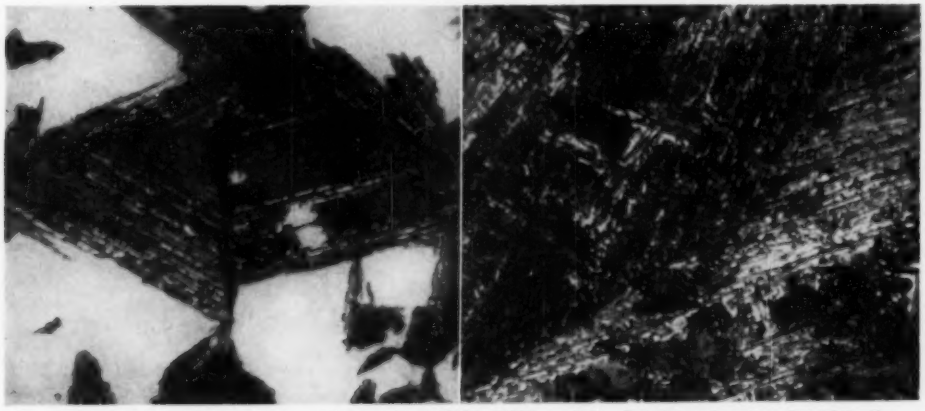

Fig. 12—Bainite 0.89 pct C steel transformed isothermally at 850°F. X2500. a (left)—Partial transformation. b (right)—Complete transformation.

loys free from confusing artifacts, as may be seen in Figs. 13 and 14. Unfortunately when electropolishing is applied to steels other than the stainless grades, it often results in excessive pitting of the nonmetallic inclusions and for this reason we do not often encounter in the literature micrographs made from electropolished surfaces. However, the method is finding increasing application in the preparation of specimens intended for routine examination at low power, and may lead, by simplifying their preparation, to more frequent use of the microscope as a tool of routine inspection.

Not many years ago a micrograph was considered satisfactory if the structure photographed was recognizable. Such defects as uneven illumination, pits resulting from dislodgement of nonmetallic inclusions, excessive or insufficient contrast, or incomplete removal of disturbed metal were all too common. Today any of these defects is deemed intolerable by an increasing number of metallographers. The excellence of the micrographs entered in competition every year at the American Society for Metals and other metallurgical conventions attest to the craftsmanship of many of our younger metallographers and to the pride they feel in achieving a beautiful photographic representation of a structure. Yet, careful examination of these selected micrographs often reveal deficiencies directly traceable to inability of the metallographers to make proper use of the adjustments and associated apparatus provided by the manufacturer of microscopes for improvement of the image. Such deficiencies, small as they are in contrast with the gross defects of years past, are nevertheless a glaring reflection of shortcomings in the training of metallographers. The microscope is their all-important tool, but because they are not always conversant with the principles of optics underlying the instrument, they often fail to utilize its full potentialities. They are expected to produce a faithful photographic reproduction of a microstructure, but they have not been trained in the art and science of photography sufficiently to use this very flexible process with skill and artistry. There is probably no greater contribution that our colleges can make toward future progress in the art of metallography than to stress the teaching of the fundamental principles of microscopy and of photography.

The Electron Microscope

Ever since the introduction of the electron microscope metallurgists have believed that the great

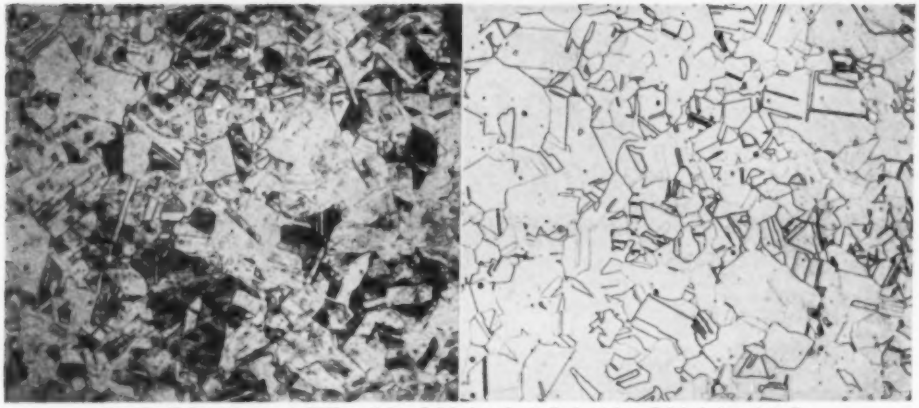

Fig. 13—18-8 stainless steel. X100. a (left)—Polished mechanically. b (right)—Polished electrolytically.

resolving and magnifying power of this instrument would be of inestimable value in exploring the fine microstructures of steel and in the study of metallurgical processes involving precipitation of constituents too fine for resolution with the optical microscope. The first attempt in this direction demonstrated the ability of the microscope to resolve significant details beyond the limits of the optical instrument, but it was immediately apparent from the markedly dissimilar results obtained by different investigators that before its inherent advantages could be realized the causes leading to such diversity of results had to be ascertained and eliminated.

It was the consensus of a group of electron microscopists and metallurgists that by concerted study of the various steps involved in the production of an electron micrograph it should be possible to arrive at a degree of standardization of procedure that would result in satisfactory agreement between different investigators as to the appearance of presumably similar structures. To accomplish this purpose the Joint Committee on Electron Microstructures of Steel was organized in 1948 and a program of investigation formulated, consisting of heat treating a series of pieces of eutectoid steel and dividing these pieces into specimens which were supplied, together with a high-power optical micrograph of each structure, to each of the cooperating laboratories for study with the electron microscope. In 1949 this group became affiliated with Committee E4 on Metallography of the American Society for Testing Materials and in 1950 the first progress report of this work was published. It is this report that I wish to review today because in my estimation it represents a contribution to our knowledge of the structures of steel.

Paraphrasing the conclusion and summary of this report, the work of this Committee demonstrates, first of all, that high fidelity electron micrographs of the structures of steel can be obtained by present-day replica techniques. This is evidenced particularly by the close similarity in appearance between light and electron micrographs of such structures as pearlite and spheroidized carbides which, because of their relative coarseness, can be well resolved with the optical microscope, see Fig. 15.

Inasmuch as these micrographs leave little doubt that faithful reproductions can be made by the replica technique of electron metallography, our confidence is greatly strengthened in the ability of the method to show us the true appearance of those structures that are too fine for adequate resolution with the optical microscope. Likewise, there should be little hesitancy in the use of electron micrographs for measurement of structural dimension, whenever such measurements are desired.

Considering some of the fine structures of steel, we see in Fig. 16 that the structure resulting from the transformation of austenite in the vicinity of the nose of the isothermal transformation diagram, which for years we had inferred was finely laminated pearlite, is actually just that.

It will not be possible to present all the micrographs contained in this report but it would be remiss to omit those that can teach us something. For example, the microstructure of bainite formed at 750°F, shown in Fig. 17, appears to have been completely resolved and found to consist of discreet, chunky cementite platelets, more or less randomly distributed and oriented in the ferrite matrix. The length of these platelets is estimated to vary between 600 and 1000A, with the larger size predominating.

Fig. 18 indicates that the structure of bainite obtained by isothermal transformation at 500°F consists of ferrite bands containing cementite platelets in parallel array.

No definite fine structure is identifiable in the needles of untempered martensite, as may be seen in Fig. 19, but the sharp definition of even very small areas of retained austenite suggests that the electron microscope would be of value in improving the accuracy of quantitative estimations of retained austenite.

While attention is focused on Fig. 19 exhibiting comparatively soft austenite in hard martensite, permit me a brief digression to point out that all these micrographs were obtained from surfaces polished as for optical metallography, yet, in spite of the high resolution and magnification of the electron microscope, no scratches or other imperfections attributable to mechanical polishing are detectable. This is significant because it attests to the adequacy of the technique of polishing on which optical metallography has always depended. Likewise, since our concept of the appearance of the structures of steel has been based on the use of

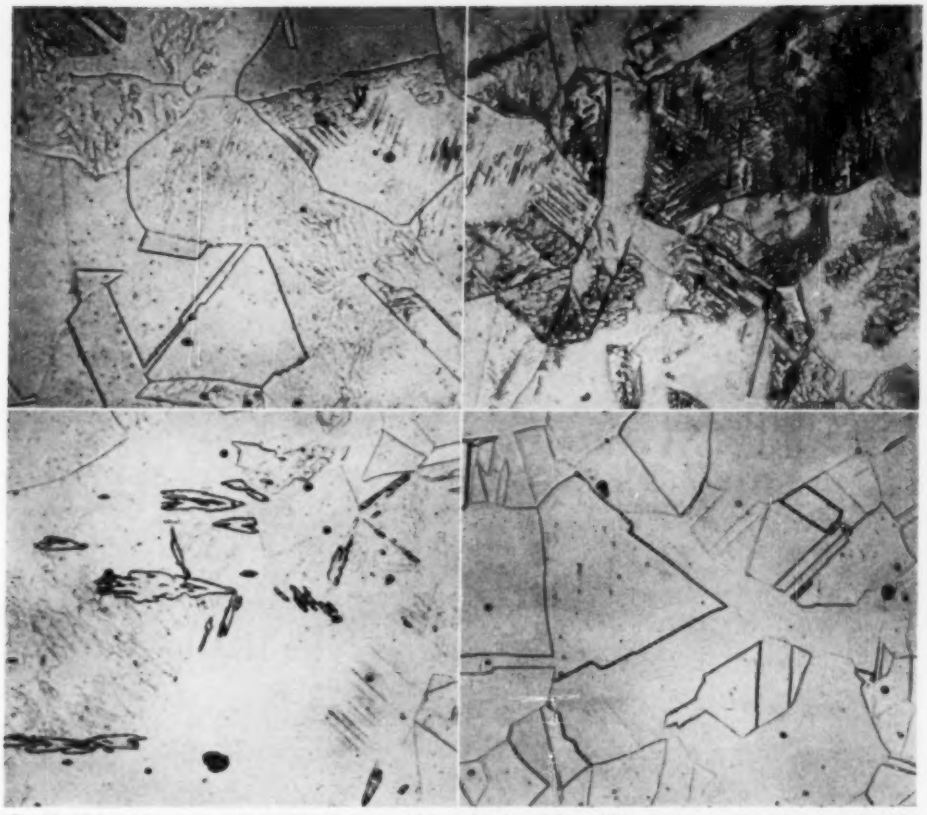

Fig. 14—18-8 stainless steel. a (upper left), b (upper right), and c (lower left) are false structures produced during mechanical polishing. d (lower right) is the true structure obtained by electrolytic polishing. X500.

picral and nital as etching reagents, it is indeed fortunate that these solutions have been found equally satisfactory for electron metallography.

The structure of martensite tempered at 400°F, illustrated in Fig. 20, is of particular interest for two reasons; first, because it shows that the precipitate responsible for the dark-etching characteristic of this structure is of such extreme fineness as to tax even the resolving power of the electron microscope, and second, because the areas of untransformed retained austenite so clearly shown in the optical micrographs are not identifiable in the electron picture.

Since, according to the isothermal transformation diagram for this steel, a considerable amount of the original retained austenite should remain untransformed after tempering 1 hr at 400°F, our inability to identify it in the electron micrograph can only be interpreted as a failure of the method to reveal clearly the true structure of the specimen. X-ray analysis shows that this specimen contains 9 pct of retained austenite.

Likewise, the optical micrograph and X-ray analysis of the specimen tempered 1 hr at 800°F, Fig. 21, indicates the disappearance of the last traces of retained austenite, which must have transformed isothermally to 800°F bainite during tempering, yet in the electron micrograph, martensite tempered at 800°F cannot be differentiated from bainite formed at the same temperature.

In calling attention to the apparent failures of the electron microscope to reveal subtle differences in the structure of steel my only purpose has been to emphasize my opinion that further refinements of technique are necessary before the full potentialities of this instrument are realized.

Microscopes

The first step in the development of the modern metallurgical microscope dates back to 1872 in Vienna, when V. von Lang[8] first fitted a microscope with a plain glass vertical illuminator in order to examine opaque objects. This was followed in 1897 by Le Chatelier's[9] design of an inverted instrument that made it possible, by merely placing the specimen on the stage, polished surface down, to attain the necessary perpendicularity to the optical axis. By 1926 this design had been adopted by the leading manufacturers of microscopes, and inverted instruments equipped with plain glass vertical illuminators had become standard equipment of the metallurgical laboratory. Numerous mechanical improvements and refinements, some of them marvelously ingenious, have been made in recent years and the versatility of the instrument has been increased many fold by the addition of several more or less

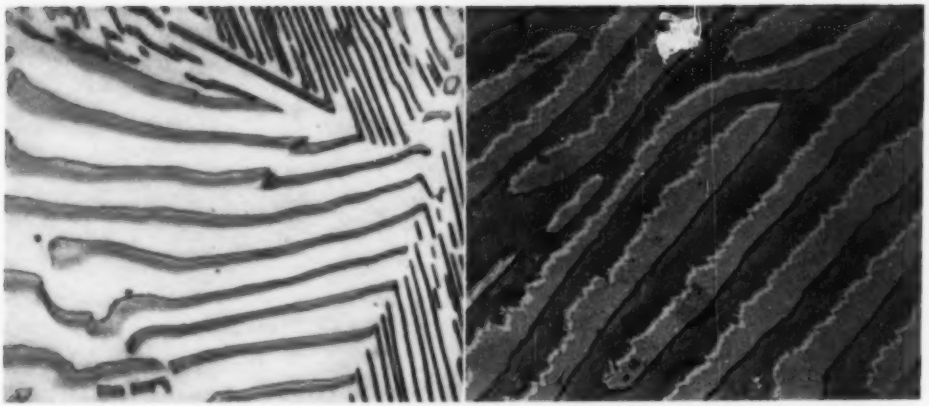

Fig. 15—Pearlite 0.87 pct C steel transformed isothermally at 1300°F. a (left)—Light micrograph X2500. b (right)—Electron micrograph X15,000.

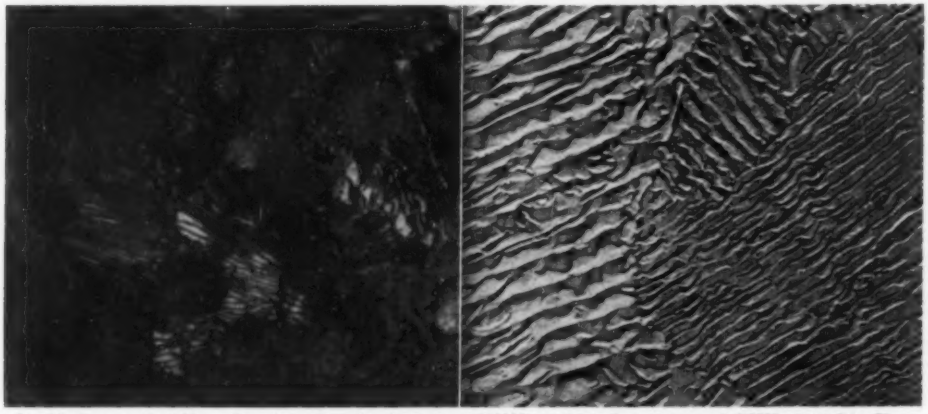

Fig. 16—Fine pearlite 0.87 pct C steel transformed isothermally at 1100°F. a (left)—Light micrograph X2500. b (right)—Electron micrograph X15,000.

useful attachments and accessories. It is the merits of these supplementary accessories that I propose to discuss now.

The first of these, and in my estimation the most valuable, was so-called conical illumination invented by Harry S. George,[5] then with the Union Carbide and Carbon Research Laboratories. The invention was made about 1922 but it was not incorporated into metallurgical microscopes until after 1926. With this simple but effective device it became possible to cut off from the illuminating pencil of light the central, more or less parallel rays, and by utilizing only inclined rays, to illuminate the specimen obliquely, thereby creating highlights and shadows that reveal with stereoscopic realism the three dimensions always present in polished and etched metallic surfaces.

While the geometric exactitude of a micrograph made with axial illumination may be unimpeachable, it is not a truly "natural" representation of the structure and sometimes it is not a satisfactory one. An image or a micrograph lacking such gradations of light and shadow as are encountered in objects illuminated by oblique light is little more than a drawing of a two dimensional pattern, or a map of the structure in which elevations and depressions are not dentifiable. Such representation of the structure is likely to be deficient technically as well as aesthetically, for in many structures significant detail is often not visible except when the highlights and shadows created by oblique lighting bring it out in relief. (See Figs. 22 and 23.)

Unfortunately, the very virtue of conical illumination by which it brings out hidden details and enables us to see the natural contours of a structure, discourages its use, for it also placed in bold relief polishing imperfections which the metallographer would rather not emphasize. But although micrographs made under conical illumination do not appear in the metallurgical literature as frequently as they deserve, conical illumination is nevertheless the most nearly indispensable of the supplementary accessories, for the need of knowing whether a constituent is in relief or in intaglio arises during a metallographic examination more often than the need to examine the structure under polarized light, dark field illumination, or phase contrast.

In addition to conical illumination, the modern, up-to-date, metallurgical microscope is equipped for viewing the specimen under polarized light,

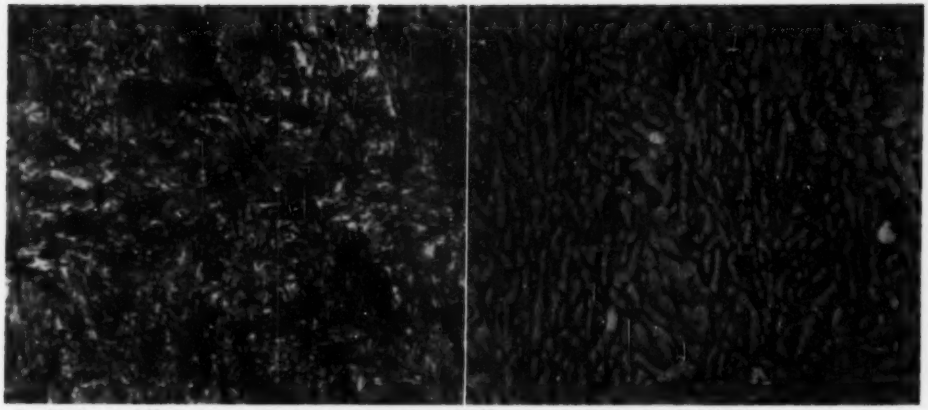

Fig. 17—Bainite 0.87 pct C steel transformed isothermally at 750°F. a (left)—Light micrograph X2500. b (right)—Electron micrograph X15,000.

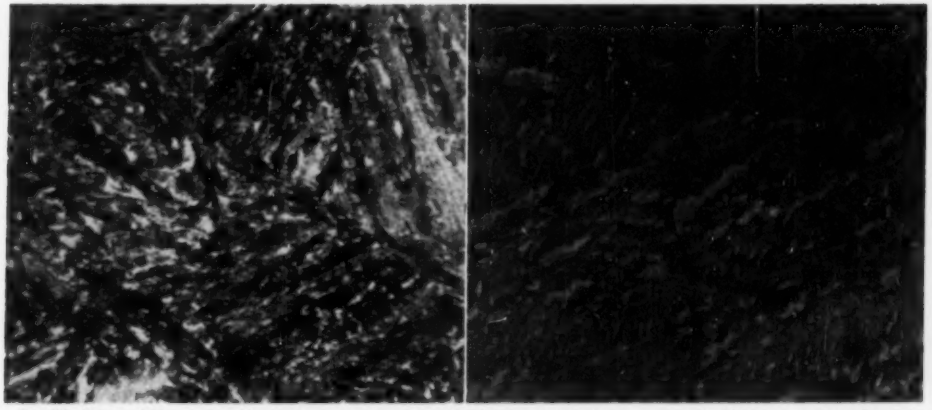

Fig. 18—Bainite 0.87 pct C steel transformed isothermally at 500°F. a (left)—Light micrograph X2500. b (right)—Electron micrograph, X15,000.

dark field and phase contrast illumination. Each of these systems of illumination contributes from time to time valuable items of information and their place in the metallurgical microscope is justified, but to date their contributions to our knowledge of the structure of steel have been decidedly minor.

Examination of unetched surfaces with reflected polarized light under crossed Nicols sometimes enables the metallographer to distinguish between inclusions having isotropic and anisotropic properties, and these characteristics together with the color reflected through transparent inclusions from the metal-inclusion interface, sometimes helps in identifying the inclusion. The vitreous character of some globular nonmetallic inclusions has been shown by the appearance of a dark optical cross when examined under crossed Nicols. Several investigators have made use of reflected polarized light in the identification of constituents, such as sigma phase in iron-chromium alloys; others to delineate grains in martensite, but these applications have been few and as yet the value of the method in the identification of constituents has not been proven.

The contribution of dark field illumination has been primarily to enhance contrast when such enhancement was deemed desirable. This enables one to see clearly grain boundaries and other details of structures not readily visible under bright field illumination because of insufficient contrast. Professor Desch[4] finds it particularly useful in the examination of deeply etched or pitted specimens, as when studying surface corrosion. He reports that, "pits which appear under vertical illumination merely as black spots may be examined in detail, the color or form of the corrosion product contained in them being clearly seen." At low power, when the depth of field is considerable, it is very useful in examining unpolished surfaces, for it reveals the colors of the specimen with greater brilliancy and fidelity than with any other form of illumination.

Phase Contrast

Another optical accessory recently made available for incorporation into the metallurgical microscope is an attachment for illuminating the specimen under the conditions known as phase-contrast. The theory and graphic representation of this system of illumination is too involved for presentation in a paper of this type, but the following may give an idea of its potential usefulness to metallography.

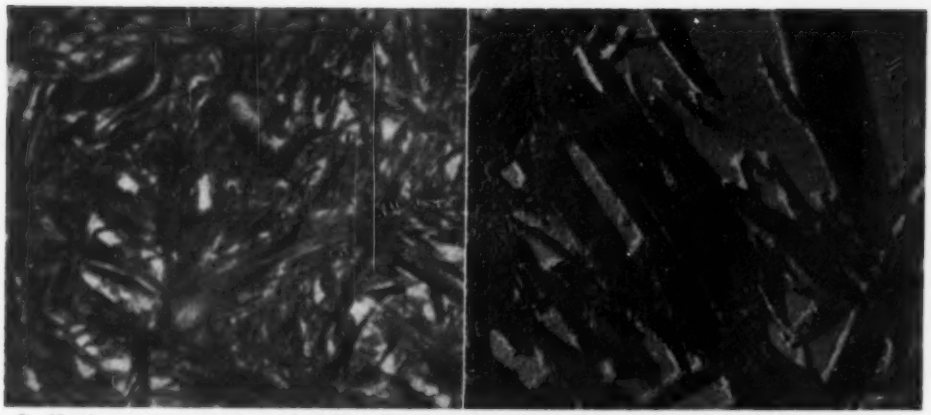

Fig. 19—Martensite and retained austenite 0.87 pct C steel water quenched. a (left)—Light micrograph X2500. b (right)—Electron micrograph X15,000.

The distribution of brightness throughout an image as we see it with an ordinary microscope depends on: 1—relative reflectivity of various parts of the structure, or 2—color differences, or 3—light scattered away from the objective by edges in the structure. It may be noted that it does not depend on differences in level at the surface of the specimen. In other words, two parts of the structure at different levels, their color and reflectivity being equal, will appear equally bright. However, by means of the phase-contrast system of illumination differences in level, which produce differences in the phase of the light reflected from them, are converted into differences in brightness, and hence the term phase-contrast.

It is claimed[7] that by this means it is possible to show differences in level of the order of 50Å (approximately 20 interatomic distances) and there is no question that for this purpose the method has great sensitivity, but as yet we do not know what use to make of the information supplied by this sensitive, ingenious method. It is also claimed that phase-contrast is sensitive to differences in surface material,[8] a claim that your speaker was unable to substantiate during his limited experience with this system of illumination. However, if this claim is found to be valid and incident phase-contrast can be employed to differentiate constituents which under ordinary illumination appear identical, then regardless of the usefulness of data pertaining to differences in level, the method will become a valued tool of metallography.

The contribution of phase-contrast illumination to our knowledge of the structure of steel to date has not been significant, but the tool has been available to metallographers for a short time and it would be premature to pass judgment on its eventual merit.

Coated Lenses

A development in the manufacture of photographic lenses which in recent years has aroused considerable interest and which, when extended to microscope objectives and eyepieces, led to a marked improvement of the image, is the anti-reflection coating applied to glass-air interfaces in order to decrease internal reflections, or flare.

In a metallurgical microscope the objective acts first as condenser to illuminate a portion of the polished surface and then as a lens to form an image of the illuminated field: Thus the opportunity for reflections are double those of a microscope used with transmitted light, and consequently, excessive

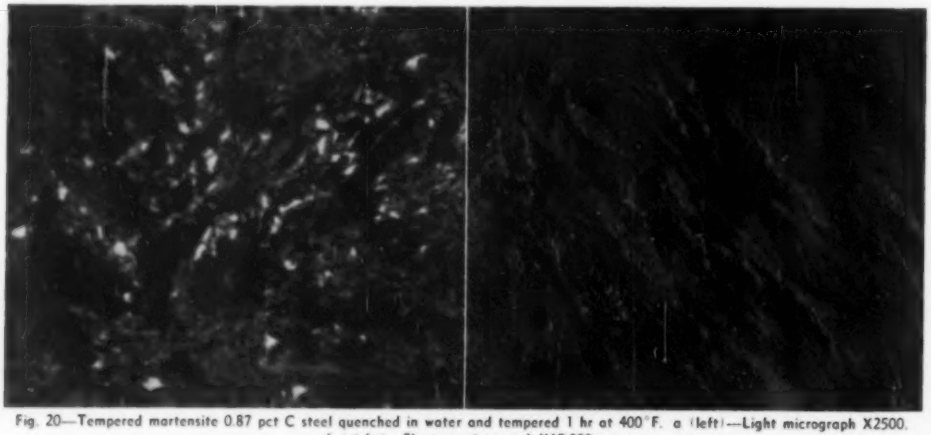

Fig. 20—Tempered martensite 0.87 pct C steel quenched in water and tempered 1 hr at 400°F. a (left)—Light micrograph X2500. b (right)—Electron micrograph X15,000.

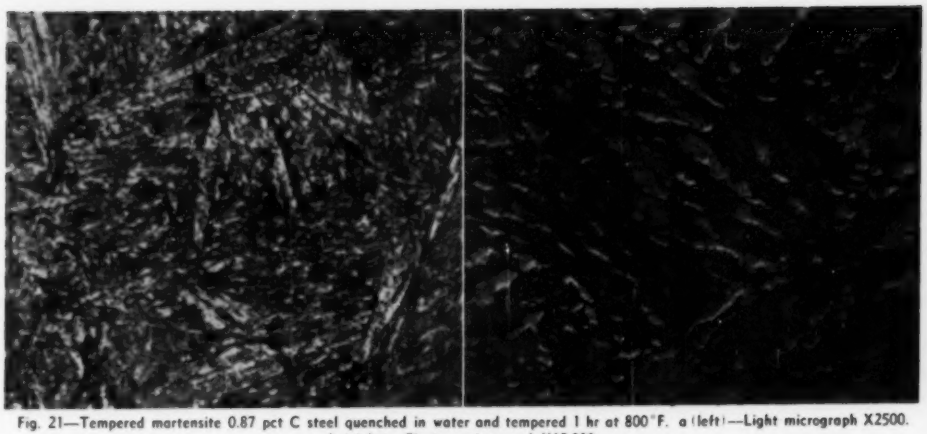

Fig. 21—Tempered martensite 0.87 pct C steel quenched in water and tempered 1 hr at 800°F. a (left)—Light micrograph X2500. b (right)—Electron micrograph X15,000.

internal reflections have been one of the most common and serious defects of objectives designed for metallography. When the illumination is by transmitted light the unwanted reflection is in the direction of the light source and can only reach the image after a second reflection, when its intensity is so low that its effect on the contrast of the image is negligible. On the other hand, when the illumination is by reflected light, the undesirable internal reflection is in the direction of the image and of sufficient intensity to produce a decided veiling effect that impairs seriously the contrast of the image, particularly when the reflectivity of the specimen is low.

To a very considerable extent this defect has been corrected by coating the objective and eyepiece with a transparent film whose thickness is approximately one fourth of the wavelength of the incident light. When the film material is of the correct index of refraction, the light reflected from the glass-film and from the film-air interfaces interfere destructively and only an inconsequential amount of light is then reflected from the surface.

There is another aspect to the application of anti-reflection coating to objectives and eyepieces of great interest to those of us who enjoy making the best possible micrographs. Since in order to disclose the finest and most delicate details it is necessary to etch lightly, the resulting contrast between the various constituents of the structure is so slight that we are forced to compensate by using photographic plates or films of very high contrast. But since high contrast emulsions are necessarily of slow speed, we have to resort to a strong source of illumination, such as the carbon arc. This is undesirable, for the carbon arc at its best is an unreliable source of the steady, even illumination needed for micrography. The tungsten ribbon filament is definitely preferable, for it gives a steadier and more uniform illumination and is also more convenient to operate, but it cannot always be used, particularly at high magnification, because of insufficient intensity for micrography on slow, high contrast emulsions. But the improvement in contrast brought about by coated optics is sufficiently great to permit the use of faster, lower contrast emulsions and this in turn allows the use of incandescent bulbs. Since the tone range of slow, high contrast emulsions is short, an improvement in tone gradations generally accompanies the use of faster, lower contrast emulsions.

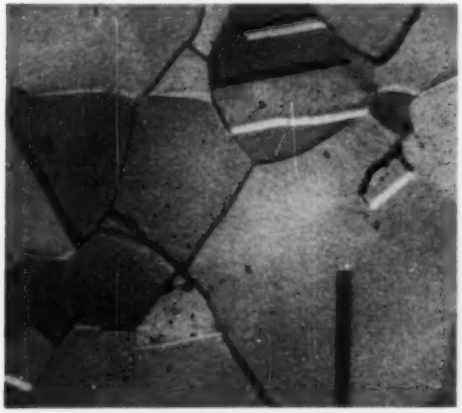

Fig. 22—Conical illumination. Austenite 1.2 pct C, 6.0 pct Mn steel quenched in brine from 2000°F. X500.

Interference Filters

Since not even the finest apochromatic objectives are fully corrected for all colors of the spectrum, it is necessary, if we are to avoid images blurred by residual aberrations, to suppress those wavelengths for which the objective is not corrected completely. For this purpose we employ light filters, mostly in the form of colored glass or gelatin sheets dyed and cemented between glass plates of adequate flatness. The yellow-green filter ordinarily used with achromatic objectives, or the blue-violet often employed to increase the resolving power of apochromats are, in a general way, satisfactory for all but the most exacting metallographic work, but they fall short of performing their intended function ideally since the portion of the spectrum which they transmit is sufficiently wide to include wavelengths for which the objective is not corrected adequately. The ideal filter would be monochromatic, that is, one transmitting only a narrow range of wavelengths in the immediate vicinity of the dominant color. Close approximations to such ideal filters are now available in the form of interference filters.

An interference filter of the transmission type

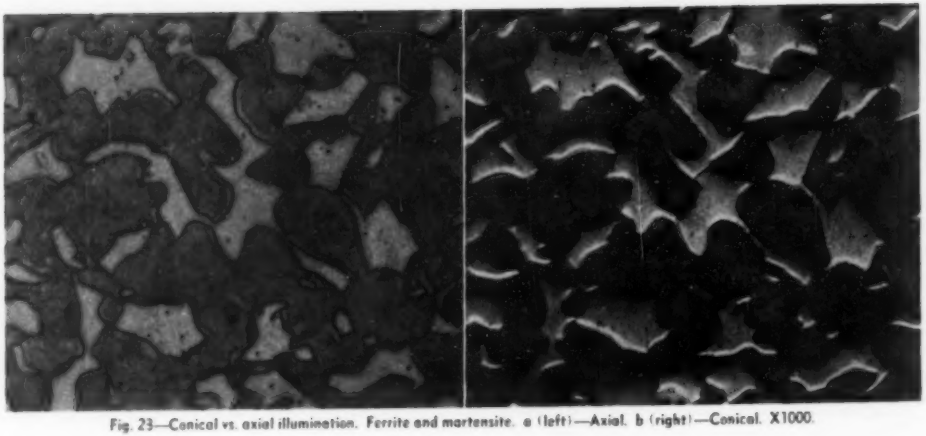

Fig. 23—Conical vs. axial illumination. Ferrite and martensite. a (left)—Axial. b (right)—Conical. X1000.

consists of two semitransparent films of silver separated by one of magnesium fluoride, these three films being deposited on a glass plate with a cemented cover glass for protection. The glass plate and cover glass are not shown in Fig. 24 which is a rather oversimplified schematic representation of the path of a light ray through the filter. The

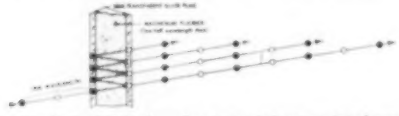

Fig. 24—Path of light through a transmission-type interference filter.

diagram as well as the following description are taken from a Bausch and Lomb publication:*

"When the light ray strikes the first silver film part of it is transmitted and passes through the magnesium fluoride coating to the second silver film. Here it is partly reflected and partly transmitted. This process is repeated and this gives rise to multiple reflections between the silver films, and produces a great number of emergent beams. Since the layer of magnesium fluoride is half a wavelength thick and since each doubling back of the light ray forces it to travel twice this distance, the successive emergent rays are precisely one wavelength apart. When this condition is fulfilled, maximum transmission of light of a particular wavelength occurs and light of other wavelengths is blocked. Consequently the color of the light produced will be determined by the thickness of the coating of magnesium fluoride. In short, the wavelength and, therefore, the color of the emergent light may be precisely controlled; the production of any desired color thus becomes a matter merely of the choice of film thicknesses."

An example of the quality obtained with an interference filter is shown in Fig. 25.

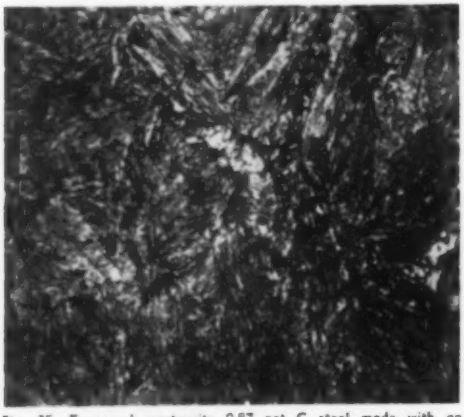

Fig. 25—Tempered martensite 0.87 pct C steel made with an interference filter transmitting λ4200A.

Color Metallography

Micrography in color is not a development of recent years but dates back probably to 1907 when the Lumiere Autochrome process was introduced commercially. Your speaker made micrographs in color of certain structures in aluminum alloys more than twenty-five years ago. Neither the exposure using a carbon arc nor the development of the plates presented any particular difficulty, and the resulting transparencies were pleasing to look at and accurate as to color rendition. Their main limitation was that when viewed magnified by projection, as in a lantern slide, the colored starch platelets which constituted the color filters of the process, could be seen simultaneously with the image. This granularity reduced somewhat the definition of the finest details of the structure.

With the introduction in more recent years of color films having a high order of resolving power and comparative ease of development in the laboratory, such as Eastman Kodak Ektachrome, or Ansco Color Film, there has been a rebirth of interest in color metallography and some interesting micrographs appear in the literature from time to time. There is no doubt that brilliantly colored subjects are reproduced more faithfully in color transparencies or prints than in black and white and in certain cases the added cost and difficulties inherent in color micrography are fully justified, but one must guard against the temptation of photographing in color for no reason other than making colorful pictures.

In the photographic reproduction of biological subjects where differential staining for purposes of identification is essential, and in metallography when color differences are significant, micrography in color

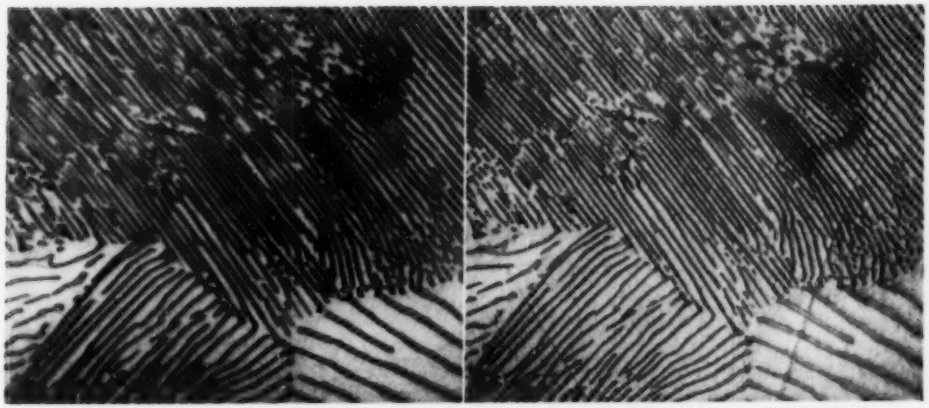

Fig. 26—Ultraviolet microscopy. Pearlite, 1300°F, 0.87 pct C steel. a (left)—λ5460Å. b (right)—λ3650Å. X2000.

is of unquestionable value. However, in many applications of ferrous metallography, where color differences other than variations in shades of gray are rare, its extended use can hardly be justified. If someday, paralleling the technique of the biologist, we learn to identify constituents or structures in steel by differential staining, then color metallography may become an indispensable tool of steel metallography.

Photographic Materials

The metallographer has always been fortunate in having at his command a wealth of photographic emulsions from which to choose one well suited to the contrast of his subject. Yet, from the beginning the tendency has been to use exclusively glass plates coated with emulsions of high contrast. For a high percentage of micrographs emulsions of high contrast are the correct choice, although their exclusive use often results in unpleasant black and white reproductions devoid of half tones. But regardless of the type employed there is no valid reason why an emulsion intended for metallography should be coated on glass rather than on film. We are told that the superior flatness of plate glass is desirable for micrography at high power, but actually, except in rare instances when it is desirable to make precise measurements on the photographic negative, the flatness of films inserted in well-made sheaths is perfectly satisfactory at all magnifications.

There are two distinct disadvantages to glass plates; they are liable to breakage and, because of their bulk and weight they require specially strong cabinets for filing and storage and much floor space. One would gladly overlook these disadvantages if in some small measure they were compensated by some advantage in favor of glass plates, but in truth, glass as a supporting medium for emulsions specially compounded for metallography has no merit to justify its continued use. The manufacturers of photographic materials would render a distinct service to metallography if they would coat on film an orthochromatic emulsion of medium speed which could be developed to a wide range of contrast. Such film would not need to be extremely fine grained, since in optical metallography contact printing is the usual practice.

Ultraviolet Microscopy

The metallographer has long been interested in ultraviolet microscopy for two reasons; as a means of increasing resolving power and as a possible means of structural differentiation by differential

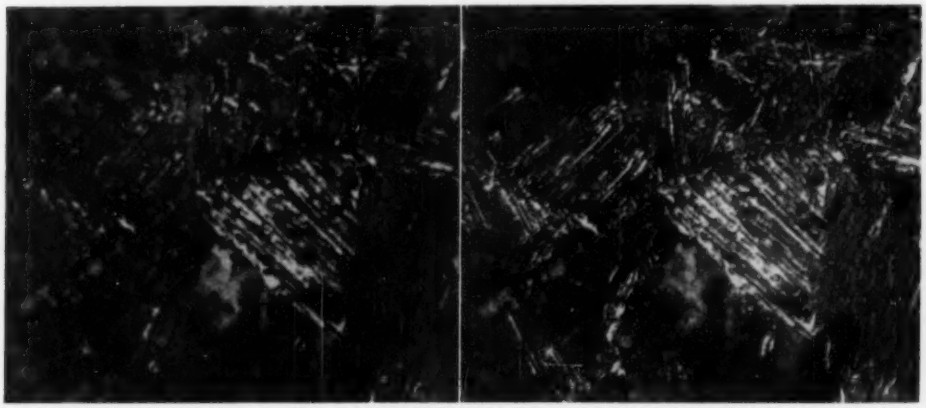

Fig. 27—Ultraviolet microscopy. Fine pearlite and bainite, 950°F, 0.87 pct C steel. a (left)—λ5460Å. b (right)—λ3650Å. X2000.

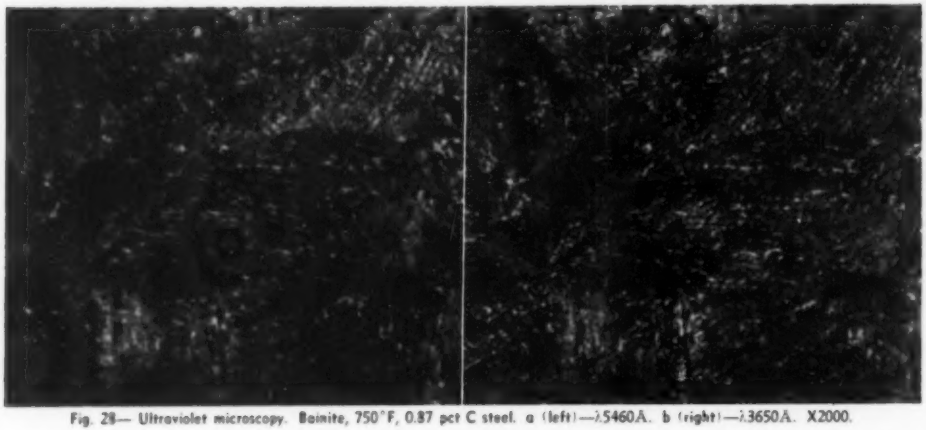

Fig. 28— Ultraviolet microscopy. Bainite, 750°F, 0.87 pct C steel. a (left)—λ5460Å. b (right)—λ3650Å. X2000.

absorption. The first of these reasons is a reality, the second, a possibility not yet sufficiently explored.

According to Abbe's well-known formula, the resolving power of an objective is proportional to twice the numerical aperture (N.A.) and inversely proportional to the wavelength of the light used. This means that resolution can be improved either by increasing the numerical aperture of the objective or by decreasing the wavelength of the light used. The question of greatest interest to the metallographer is, which of these alternatives is preferable? In answering this question let us consider the extreme differences in numerical aperture existing between electron and light microscopes. The numerical aperture of the magnetic lens of an electron microscope is of the order of 0.001, that is, about 1600 times smaller than that of a 1.6 N.A. monobromonapthalene immersion objective, which has the greatest aperture of all the objectives available for metallography. On the other hand, the wavelength of the green light generally used in metallography is about 5500Å as compared with 0.05Å for the electron radiation, that is, the electron microscope employs wavelengths more than 100,000 times finer than those used in the light instrument.

In consequence of these great differences, micrographs made with the extremely small aperture of a magnetic lens are critically sharp and possess remarkable depth and flatness of field even at the highest magnification of the electron instrument, while those made with a light microscope, because of the relatively wider aperture of glass objectives, are of shallow depth of field and except at low magnification, seldom in optimum focus outside of a small area in the center of the field. Sharp focusing with an electron microscope at any magnification within its range is no problem at all, but making a micrograph in good focus with a 1.6 N.A. objective using blue light at a magnification of 2500 diameters is an achievement, and in all candor, more a matter of good luck than of skill.

The preceding comparison indicates the advantages of increasing resolution by employing illuminants of short wavelength rather than by resorting to objectives of higher numerical aperture. This question was raised because the need for choosing between objectives of high numerical aperture using visible light and objectives of lower aperture using ultraviolet is a distinct possibility in the not too distant future. Even today the metallographer who

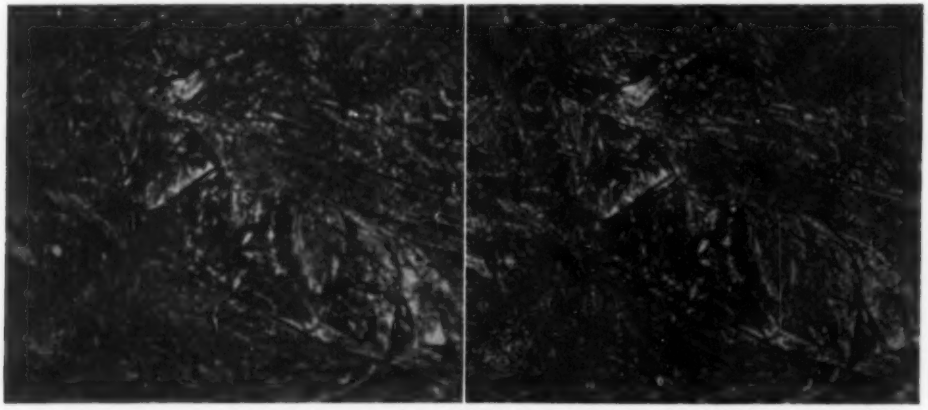

Fig. 29—Ultraviolet microscopy. Tempered martensite, 1 hr at 800°F, 0.87 pct C steel. a (left)—λ5460Å. b (right)—λ3650Å. X2000.

wishes to resolve the finest detail possible with an ordinary metallurgical microscope has a choice of two objectives of approximately equal resolving power, one of numerical aperture 1.6 corrected for blue light of wavelength in the vicinity of 4500A and one of numerical aperture 1.3 corrected for ultraviolet light of 3650A. The theoretical limit of resolving power of both objectives is about 0.14 microns.

The ultraviolet objective referred to is not a recent development;[10] it was manufactured commercially by Bausch and Lomb Optical Co. about 1930, but for some unknown reason it was never used extensively in metallography. It was designed so that the green mercury line with wavelength 5460A and the ultraviolet of 3650A are simultaneously in focus. This makes it possible to focus with a green filter, substitute a filter with maximum transmission at 3650A and make the exposure. Since the absorption of ultraviolet light of 3650A wavelength by glass is slight, no change from glass to quartz of any part of the optical system is necessary. However, oil of sandalwood is preferable to cedar oil for the immersion medium because it absorbs less of this wavelength.

The process is simple and the results are gratifying, as may be judged from Figs. 26 to 29 inclusive. I am unable to present to you a direct comparison of the same structures photographed with a 1.6 N.A. objective using visible light and with the 1.3 N.A. ultraviolet light of 3650A wavelength, but there is no doubt in my mind that the image of the ultraviolet objective is superior in resolution, flatness, depth of field and in freedom from flare.

A convenient source of ultraviolet light is the high intensity mercury lamp, type H4, obtainable from General Electric Co. or in a housing for micrography from Bausch and Lomb Optical Co. The exposure for micrographs at 2000 diameters using Corning filter No. 5680, 5 mm thick, varies between 5 and 15 min, depending on the speed of the photographic emulsion and the reflectivity of the structure. Since ultraviolet images tend to be low in contrast, high contrast emulsions such as Kodak Process Ortho, or the equivalent product of other manufacturers, are preferable. The resulting negatives possess sufficient contrast to print well on No. 1 contact printing paper.

Another possibility of a practical system of ultraviolet metallography exists in the application in this field of the reflecting objectives recently introduced for ultraviolet microscopy by transmitted light. These lenses have the very attractive property of being achromatic over a wide range of wavelengths, including both visible and ultraviolet portions of the spectrum. They offer the possibility of attaining a resolving power equivalent to that of a refracting objective of numerical aperture 2.0 without the very serious limitations that such an objective would have if it existed. Since they are achromatic for visible and invisible light, focusing for micrography with the shortest wavelengths in the ultraviolet would be no problem. Fig. 30 was made with a water immersion reflecting objective of numerical aperture 1.1, adapted experimentally for use by reflected incident light and loaned to your speaker by Bausch and Lomb Optical Co. This is possibly one of the first micrographs of a metallic specimen made with a reflecting objective.

Since with these objectives it would be possible to photograph a structure with ultraviolet light of different wavelengths, they offer a means of investigating the possibility of identification of structures and constituents by selective absorption.

Fig. 30—Ultraviolet microscopy. Bainite. Micrograph made with a reflecting objective using ultraviolet light of 3650A. X2000.

However, these objectives are not yet available for use in metallography and therefore an appraisal of their contribution to the advancement of our science may have to wait until a future Howe lecturer reviews the achievement of the next twenty-five years.

Summary

It may be said by way of recapitulation, that the progress achieved in the preceding quarter century in our understanding of the structures of steel was brought about by the following accomplishments:

1—Elimination of disturbed metal from the surface of metallographic specimens. This enabled us to see the true configuration of the structures of steel.

2—Development of the isothermal transformation diagram. This helped us to understand the structures unveiled by the elimination of disturbed metal.

3—Application of the electron microscope to the study of the structures of steel. This enabled us to see finer details than we have seen before and brought us closer to definitive resolution of the structures.

References

[1] William Campbell: Twenty-five Years of Metallography. *Trans.* AIME (1926) **73**, p. 1135.

[2] E. S. Davenport and E. C. Bain: Transformation of Austenite at Constant Subcritical Temperatures. *Trans.* AIME (1930) **90**, pp. 117-154.

[3] V. von Lang: Auz. Kais. Akad. Wiss. Wien (1872) p. 175.

[4] H. Le Chatelier: Etude de Alliages. (1901) p. 421.

[5] Harry S. George: *Trans.* Amer. Soc. for Steel Treating (1923) **4**, p. 140.

[6] Cecil H. Desch. *Metallography.* 5th Ed. p. 129, (1942) London. Longmans-Green.

[7] D. McLean: Phase-contrast Metallography. In *The Examination of Metals by Optical Methods*, a restricted publication of the British Iron and Steel Research Association, p. 13.

[8] K. J. Habell: *Ibid.* p. 7.

[9] *The Educational Focus.* Fall issue (1950) pp. 10-14.

[10] A. P. H. Trivelli and L. V. Foster: Photomicrography with the 365-millimicrone Mercury Arc Line. *Journal* Optical Soc. of Amer. (February 1931) **21**, pp. 124-131.

Arc Melting of Titanium Metal

by S. F. Radtke, R. M. Scriver, and J. A. Snyder

An automatic, continuous casting arc furnace employing a nonconsumable electrode and a direct current arc has been constructed and operated successfully for titanium. A comparison of the properties of arc and induction-melted titanium indicates that where high ductility, formability, and toughness are required, arc-melted metal is preferable.

BECAUSE of the reactivity of titanium metal with all known refractories and the common atmospheric gases, melting of the metal presents numerous problems. It is necessary to provide an inert atmosphere in the furnace as well as a crucible material that will not react with the molten metal, if a ductile ingot is to be produced. Two special furnaces have been developed that meet the requirements and one, the induction heated graphite furnace, has been described in some detail.[1] Little information is available for sizable units wherein power is applied to the melt through an arc, and the dearth of technical information on such a furnace prompted this report. It has been demonstrated clearly that arc melting produces titanium metal with superior toughness, ductility, and formability. To produce titanium ingots with these properties, an automatic, continuous casting arc furnace has been developed and is described herein.

S. F. RADTKE, Associate Member AIME, and R. M. SCRIVER are with the Pigments Department, E. I. du Pont de Nemours & Co., Inc., Newport, Del. J. A. SNYDER, Member AIME, is with the Engineering Department, E. I. du Pont de Nemours & Co., Inc., Wilmington, Del.

Discussion on this paper, TP 3087D, may be sent, 2 copies, to AIME by Oct. 1, 1951. Manuscript, Feb. 7, 1951. St. Louis Meeting, February 1951.

The history of arc melting may be traced to 1800, when Sir Humphrey Davy[2] first experimented with Volta's electric battery and found that light could be produced and an arc formed between two carbon points attached to the cell. The discovery of the arc was followed by the design and construction of an arc furnace by Napier,[3] in 1845, for the reduction of metal oxides. In 1853, Pichou[4] described a similar furnace, although it was not until the discovery of the dynamo in 1867 that the arc furnace could achieve commercial significance. In 1878, Siemens[5] designed the first arc furnace intended for the melting of metals and by 1882 had melted steel and platinum successfully.

This was followed by Moissan's[6] classical work with the arc furnace in 1892. W. von Bolton,[7] in 1905, found that the arc furnace was suited admirably for melting refractory metals. In his work with tantalum, no suitable refractories for retaining the molten metal were found to exist. Together with Otto Simpson, he developed an arc furnace with a water-cooled copper crucible in which tantalum could be melted without contamination. This technique proved eminently successful.

In his paper on the preparation of ductile titanium, Kroll[8] first described an application of the von Bolton furnace to the melting of this metal. The

Kroll furnace utilized an electric arc, a tungsten electrode, a water-cooled copper crucible, and an argon atmosphere to prevent melt contamination.

The basic principles developed by von Bolton have been applied with increasing frequency in recent years for melting refractory and highly reactive metals on a laboratory and commercial scale. Parke and Ham[9] described a very interesting furnace for arc melting molybdenum, and Eastwood, Simmons, et al.[10] employed the arc furnace in their preparation and study of titanium alloys.

Furnace Development

In the development of an arc furnace for melting titanium, a manually operated pilot model was constructed first. From this unit, techniques for feeding titanium sponge, characteristics of inert atmospheres, and the consumption rates of various types of electrode materials were determined. It was found that crushed titanium sponge could be fed at a controllable rate to the furnace chamber by means of a vibratory feeder either continuously or at desired intervals. An atmosphere of argon or helium proved to be satisfactory for manual as well as automatic melting procedures.

The choice of electrode materials narrowed rapidly to tungsten and graphite. Electrode consumption was held at a minimum by making the electrode the cathode of a direct current arc. Other effects such as spatter from the melt played an important part in electrode consumption. Tungsten was eroded severely by titanium, which attacked the electrode material intergranularly. One or more grains of tungsten would drop from the electrode into the melt, settling to the bottom of the molten pool without alloying completely with the melt. This observation had been noted previously by workers at Battelle Memorial Institute.[11] The basic physical properties of the matrix metal were not affected seriously by the presence of these tungsten particles, although surface blemishes appeared when the material was rolled. Graphite proved to be a very satisfactory electrode material, and by the use of very dense grades, carbon contamination was held to about 0.2 pct.

During initial runs of the manually operated furnace, it was found that the ingot could be removed continuously at the same rate as sponge was melted in the furnace. Operating at a slight positive internal pressure, it was possible to maintain an effective seal between the ingot and the crucible wall. If a leak occurred, the inert atmosphere bleeding outward prevented the ingress of air.

Construction

With the above data available, the furnace illustrated in Fig. 1 was designed and constructed. The furnace proper is entirely water-jacketed, including the crucible, furnace neck, furnace head, and electrode assembly. An auxiliary pump circulates water through the system, the major portion of which is recycled. The ingot, $5\frac{3}{4}$ in. in diam, may be cast continuously by retracting it at a uniform rate by means of a hydraulic ram. Because of the desirability of having a rugged crucible that could stand constant use without frequent replacement, thin-walled copper crucible sleeves were replaced with extra heavy sleeves of copper pipe. This latter type of crucible has proved very satisfactory.

The electrode mechanism of the furnace is composed of a long copper shaft that projects from the top of the furnace through the head to the ingot surface. This shaft, rotated by a motor mounted on the electrode support, revolves an offset electrode holder and permits the electrode to cover the surface of the molten pool. Any variation in the potential across the arc actuates the racking motor which automatically raises or lowers the electrode to regain the desired operating voltage. By such a technique, constant power input to the melt is maintained.

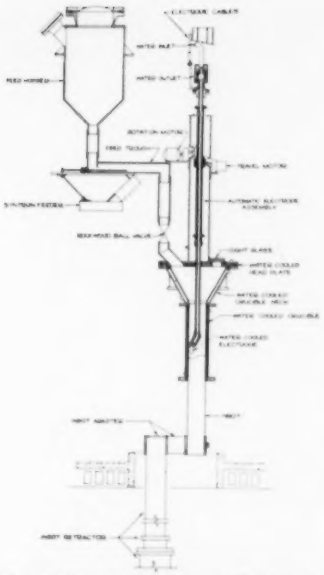

Fig. 1—This schematic diagram of the automatic arc melting, continuous casting furnace shows essential furnace and control details and the manner in which the ingot is withdrawn from the unit.

A cam is mounted on the rotating electrode shaft and actuates the vibratory feeder. It has been found advisable to feed in short bursts rather than continuously at a low feed rate, since the rate of sponge addition can be controlled more accurately at higher feed rates. This type of operation permits automatic and uniform additions of melt metal and eliminates variations inherent with manual feeding. This particular furnace can feed crushed sponge varying in size from an average diameter of $\frac{3}{4}$ in. to 12 mesh. The size of feed is limited only by the electrode offset and the feeder trough. Sponge of larger size undoubtedly could be handled in a modified furnace, although the limiting size at the present power level has not been fully determined.

Operation and Scope

The typical melting cycle is carried out in the following manner. A stub ingot is secured into the ingot retractor and raised into the crucible cavity, and a charge of sponge is loaded into the feed hopper. Mastic material is employed to seal the space between the ingot and the crucible, thus permitting evacuation of the system. After several flushings with an inert gas, the atmosphere finally is admitted until a slight positive pressure is obtained. At this point, the generators are started, and the melt switch

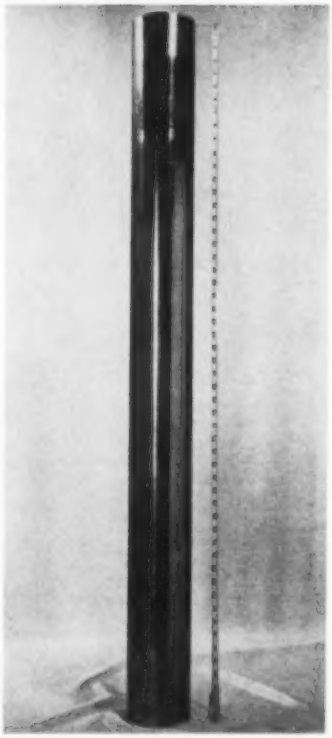

Fig. 2—Titanium ingots up to about 60 in. are continuously cast from the furnace.

thrown in. The electrode, based upon a pre-set voltage, is lowered automatically to strike an arc. After the arc is struck, the electrode rises until the desired potential is attained. The electrode, driven by the rotor motor, begins to rotate and move the arc over the ingot surface.

When the surface of the stub ingot becomes molten, the feeder switch is turned on and in each rotation of the electrode, sponge is fed into the crucible.

As soon as the feed is started, the ingot retractor is set in motion, and the speed of ingot withdrawal is adjusted to conform to the rate of sponge feed. After these manipulations are carried out by the furnace operator, no further work is required of him, except to check the furnace controls. Should the arc be broken for any reason, the control mechanism automatically restrikes the arc. Thus after the furnace is started, the melt is carried out completely automatically.

Commercially pure sponge can be melted at a rate of 0.6 to 1.0 lb per min with a power input of 64 to 100 kw. Alloys can be melted at an even higher rate, provided that they have a lower melting point than pure titanium.

The furnace operation is believed safe. Should the crucible be burned through for any reason, the pressure developed by the steam generated would break either the large rupture disk in the feed hopper or in the furnace head. At the same time, the vapor formed would extinguish the arc and open the electrical circuit.

Two furnaces of this type are now in operation. They have demonstrated the feasibility of this basic design and are paving the way for large-scale automatic, continuous casting furnaces. In addition to casting titanium, this type of furnace could be employed for other metals whose reactivity requires the use of an inert atmosphere and a chemically inert crucible.

Alloys of titanium as well as pure titanium can be melted in this furnace. Sponge of relatively uniform particle size usually is tumbled with the powdered alloying elements in an inert atmosphere. After blending, the alloying powders fill the interstices of the sponge and leave little if any residual powder in the blender. If metal powders are not used, the alloying metals should be screened to a relatively uniform size before blending with the sponge. This method has been used successfully for a variety of alloys. A continuously cast ingot 4 ft 5 in. in length and scalped to a depth of $\frac{1}{4}$ in. on the diameter is shown in Fig. 2.

Although this discussion has been limited primarily to an arc furnace of the nonconsumable electrode type, it has been shown to be feasible to melt titanium as a consumable electrode. The basic furnace described herein need be modified only slightly to accomplish this end.

Characteristics of Ingots

If arc-melted ingots are allowed to cool to room temperature before being removed from the furnace,

Fig. 3—This shows the top of a typical ingot produced by arc melting. It is in the as-cast condition, enlarged 2X. This ingot is actually $5\frac{3}{4}$ in. diam, but a reduction in size was necessary to reproduce the photograph.

the top of the ingot appears as a bright, shiny surface with the grain boundaries clearly delineated. The top of a typical ingot is shown in Fig. 3. When a hot ingot is removed from the furnace, a thin oxide film is formed on the entire ingot surface. The oxide film formed on continuously cast ingots is very thin and is not considered objectionable. For this reason, and the fact that all subsequent hot-working of the ingot is done in air, no effort has been made to prevent oxide film formation during the continuous casting operation. The side of the ingot presents a slightly rippled surface, Fig. 4. This ingot was furnace-cooled and presents a bright metallic surface. To produce a void-free surface, it usually is necessary to remove from $\frac{1}{8}$ to $\frac{1}{4}$ in. on the diameter. Any minor voids which then appear at the surface can be removed readily by surface grinding. After the above operations, the ingot is ready for forging.

Although Fig. 3 indicates that the grains might possibly be equiaxed and of relatively uniform size, such is not the case. Several ingots have been cross-sectioned to determine the longitudinal grain configuration. These ingots, as typified by the ingot shown in Fig. 5, have long grains growing from the bottom of the ingot toward the top. Grains up to 10 in. long have been noted. Small, preferentially oriented grains are found at the mold surfaces. In general, the structure of arc-melted material is typical of that obtained in chill-case ingots. The ingots as-cast are usually sound and free from extensive porosity. It has been found that internal pores which may occur in arc-melted ingots seal up readily when the ingot is forged, while external defects usually result in cracking.

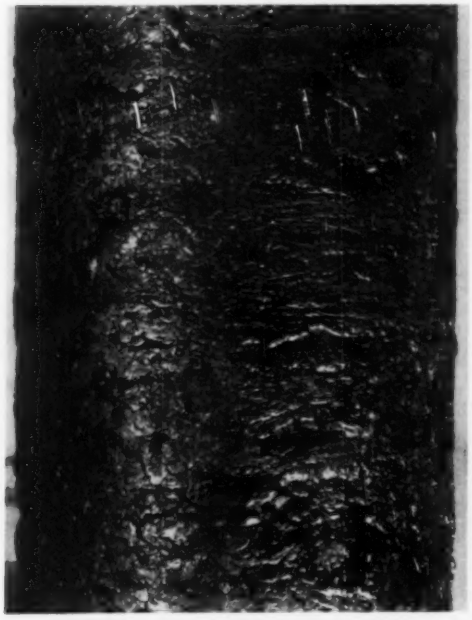

Fig. 4—The surface of an as-cast ingot is relatively in good condition, as shown in this $1\frac{1}{2}$ diam enlargement.

Fig. 5—An as-cast arc-melted ingot etched with HF-HNO_3 shows columnar grain structure. X3.

Despite the fact that the feed metal is contaminated to the extent of about 0.2 pct by the graphite electrode employed during melting, this is virtually the only contaminant added to the melt. In batch melting, a static sealed inert atmosphere is employed which, if gettered by passing over hot titanium sponge, will reduce the contamination by oxygen and nitrogen to trace amounts. In continuous casting, nitrogen contamination can be held at virtually the same level if gettered gas is employed, since the rate of flow of helium required to maintain a slight positive pressure in the furnace is only of the order of 0.5 cfm. With the exception of an arc furnace em-

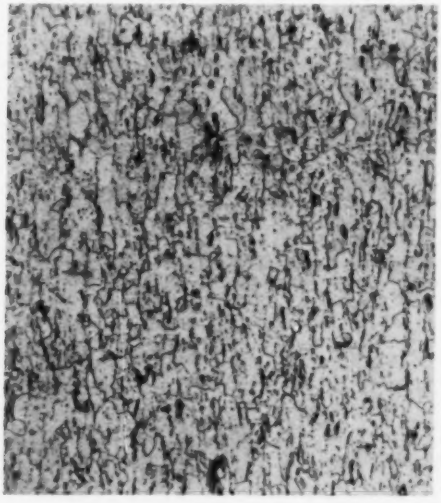

Fig. 6—This section of arc-melted titanium sheet, etched with HF-HNO_3 and enlarged 250X, shows grain structure of rolled material.

Table I—Typical Physical Properties of Arc Melted, Induction Melted, and Iodide Titanium

	0.2 Pct Offset Yield Strength, psi	Ultimate Strength, psi	Elongation in 2 In., Pct	Reduction of Area, Pct	Minimum Bend Radius 75° (Times Thickness of Metal)	Vickers Hardness Number
Arc-melted titanium						
Forged bar[10]	80,000-85,000	90,000-95,000	15-25	30		200-250
Regular annealed sheet[14]	70,000-80,000	80,000-90,000	15-20	55	2-2.5	200-250
High purity annealed sheet[15]	55,000	65,000	25	60	1.5-2.0	170-200
Induction-melted titanium						
Forged bar[12]	80,000-85,000	90,000-100,000	10-15	20		225-275
Annealed sheet[12]	80,000-85,000	90,000-95,000	10-20	10	3-4	235-275
Arc-melted iodide titanium						
Annealed sheet[16]	22,000	46,000	50	60	0	90-110
Charpy V-notch impact strengths						
Testing temperature		Room temperature		500°F		
Arc-melted titanium[13]		18 ft-lb.		60 ft-lb.		
Induction-melted titanium[12]		9 ft-lb.		35 ft-lb.		

ploying a consumable titanium electrode, the nonconsumable electrode technique produces titanium ingots of the highest purity.

Properties of Arc-Melted Titanium

The physical properties of arc-melted titanium of commercial purity are intermediate between those of high purity titanium made by the iodide process and induction-melted metal. Arc-melted titanium shows much higher strength than iodide titanium and can be rolled readily to thin sheets that can be fabricated by standard techniques. While induction-melted titanium containing 0.4 pct C and above has slightly higher strength, sheet rolled from this material shows lower formability and requires larger bend radii. In addition, the toughness of induction-melted material, as indicated by Charpy V-notch impact tests, is only half that of arc-melted titanium. A tabulation of typical physical properties of arc-melted, induction-melted, and iodide titanium is presented in Table I. The microstructure of sheet rolled from arc-melted titanium is typified by that shown in Fig. 6.

The microstructure of annealed, arc-melted titanium sheet shows a matrix of irregularly shaped grains of α titanium. Carbides usually are present in relief because of their high hardness. There are also a number of small dark etching particles which seem quite numerous for a metal with less than 1 pct of impurities. The exact nature of these dark etching particles has not been determined.

Arc-melted titanium is preferred for the production of sheet metal as the higher purity results in material with greater ductility and formability. Annealed sheet with an 0.2 pct offset yield strength of 80,000 psi can be bent around a mandrel with a radius that is only double the sheet thickness. The ductility of titanium is restricted by its hexagonal structure, and at room temperature titanium deforms by slip along the basal planes of the crystals. The additional work performed during rolling, as compared to a bar that is only forged, seems to improve the ductility of the finished sheet.

Impact tests of arc-melted titanium show breaking strengths almost double those for induction-melted metal. Values listed in Table I were for small ingots forged to $\frac{1}{2}$ in. square bars.

From the data presented in Table I, it may be seen clearly that arc-melted titanium has higher formability and toughness than induction-melted metal containing carbon above 0.4 pct. For end uses where these properties are required, it will be necessary to melt sponge titanium by arc melting or similar techniques, hence, the need for developing arc-melting know-how.

Summary

An automatic, continuous casting arc furnace employing a direct current arc has been constructed and operated successfully. While designed specifically for melting and casting titanium it can be employed for melting other reactive metals. Comparative properties of arc and induction-melted titanium indicate that where high ductility and formability and toughness are required, arc-melted material is preferable.

Acknowledgment

The electrode mechanism and electrode control circuit of the arc furnace described herein were designed in conjunction with Mark F. Gouran, Philadelphia.

References

[1] E. A. Gee, W. H. VanDerhoef, and C. H. Winter, Jr.: *Journal* Electrochem. Soc. (1950) **97**, pp. 49-53.
[2] H. Davy: *Phil. Trans.* Roy. Soc. (1809) **97**, p. 71; and (1821) **111**, p. 427.
[3] A. Stansfield: *The Electric Furnace*. P. 3 (1914) New York. McGraw-Hill Book Co.
[4] P. 4 of ref. 3.
[5] W. Siemens: English Patents. 4,208 (1878), and 2,110 (1879).
[6] H. Moissan: *Comptes Rendus* (1892) **115**, p. 1031.
[7] W. von Bolton: *Ztsch. Elektrochemie* (1905) **11**, pp. 45-50.
[8] W. Kroll: *Trans.* Electrochem. Soc. (1941) **78**, pp. 35-47.
[9] R. M. Parke and J. L. Ham: *Trans.* AIME (1947) **171**, pp. 416-427; METALS TECHNOLOGY (September 1946).
[10] L. W. Eastwood, et al.: Summary Report on Preparation and Evaluation of Titanium Alloys. Part III, May 18, 1948 to July 30, 1949. Report to Air Material Command, Wright-Patterson Air Force Base, Dayton, Ohio, by Battelle Memorial Institute, Columbus, Ohio, pp. 21-31 (1949).
[11] Pp. 47-49 of ref. 10.
[12] Averages of samples tested in the authors' laboratory.
[13] Technical Information on Titanium Metal. Pp. 5-10 (1950). Rem-Cru Titanium, Inc., Bridgeport, Conn.
[14] W. L. Finlay and J. A. Snyder: *Trans.* AIME (1950) **188**, pp. 277-286; JOURNAL OF METALS (February 1950).

Powder Metallurgy of Zirconium

by Henry H. Hausner, Herbert S. Kalish, and Roswell P. Angier

POWDER metallurgical methods as applied to zirconium are of great interest because they permit not only the fabrication of parts directly to shape with a minimum loss of material but also the utilization of scrap, and the metal may be processed at temperatures well below the melting point. There are two difficulties involved in the melting of zirconium: 1—High vacuum is necessary for melting, and 2—zirconium reduces nearly all oxides so that it is difficult to find a suitable crucible material. The purest material, zirconium crystal bar, is expensive, and the methods of subsequent fabrication are limited. Cold rolling or extrusion of zirconium crystal bar is suitable for making certain shaped parts, but where melting is involved, the purity of the metal is invariably decreased, and a method of casting to a definite shape does not seem to be feasible.

Where it is necessary to hot roll, zirconium must be covered with a steel or copper jacket to protect it from the air. This is necessarily a costly operation. Where annealing of zirconium is necessary it must be conducted in a high vacuum.

H. H. HAUSNER, and H. S. KALISH, Members AIME, are Section Head and Senior Engineer, respectively, Metallurgical Laboratories, Sylvania Electric Products Inc., Bayside, L. I., N. Y. R. P. ANGIER, Member AIME, formerly with Sylvania Electric Products Inc., is now with North American Philips Co., Lewiston, Maine.

Discussion on this paper, TP 3101E, may be sent, 2 copies, to AIME by Oct. 1, 1951. Manuscript, Feb. 16, 1951. St. Louis Meeting, February 1951.

This work was done for the Atomic Energy Commission at the Metallurgical Laboratories, Sylvania Electric Products Inc.

In an investigation of powder metallurgical methods for zirconium, the zirconium powder used should be characterized by the following properties: 1—Highest degree of purity, 2—uniformity in particle shape and particle size distribution, 3—low compression ratio, and 4—satisfactory strength of the compacted powder (green strength). Zirconium powders have been made by two methods: By the reduction of zirconium tetrachloride ($ZrCl_4$) with sodium,[2, 4, 5] and by the reduction of zirconium oxide with calcium and calcium chloride.[5] The first method represents one of the earliest attempts to make pure zirconium metal, and the sintered product from this powder is extremely brittle. The second method of making zirconium powder is far more successful, but the powder made in this way has an extremely low apparent density and, therefore, a high compression ratio which makes it difficult to use it for powder metallurgical purposes. For these reasons the above-mentioned zirconium powders were not used in this investigation. To obtain sintered zirconium compacts of highest purity and good ductility, it was first necessary to produce a suitable powder.

Pure zirconium has been made chiefly by two methods. The iodide method, from which the product is "crystal bar" zirconium, was developed first.[1-3] By this purification process very soft, pure, and ductile zirconium metal can be produced. The second method, developed by the U. S. Bureau of Mines, is the reduction of zirconium chloride with magnesium.[5] The sponge zirconium thus produced is also soft, pure, and ductile.

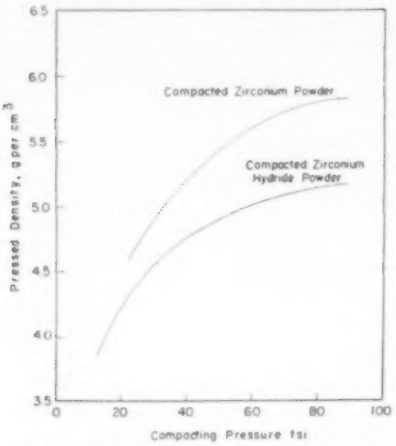

Fig. 1—Effect of compacting pressure on the pressed density of compacted zirconium and zirconium hydride powders.

There are, however, several distinct differences between zirconium produced by these two methods. The sponge metal must be melted and cast to make it suitable for subsequent fabrication, while the crystal bar can be directly rolled or extruded to the desired shape. Both methods yield metal with about 0.5 to 3.0 wt pct hafnium. The melted and cast sponge contains appreciable carbon, about 0.1 wt pct, and perhaps more oxygen and nitrogen than the crystal bar, but it is equally as pure in respect to other elements. Zirconium made from Bureau of Mines sponge is harder, somewhat lower in ductility, and higher in tensile strength than the crystal bar product. These differences may be attributed chiefly to the higher oxygen and carbon content of the zirconium sponge product, although it is not clear what role the carbon plays in affecting physical properties. In order to investigate the powder metallurgy of zirconium, powders made from zirconium crystal bar were used.

Powder Preparation

Processing: Zirconium crystal bar is too ductile at room temperature and even at very low temperatures, such as that of liquid nitrogen, to be comminuted by mechanical methods. Zirconium, however, forms a hydride that is brittle enough to be comminuted mechanically, and the hydride powder then can be readily decomposed in vacuum. Therefore, the hydride method was chosen for the preparation of the powder.

Zirconium hydride forms in the temperature range from about 235° to 800°C.[6] The absorption of hydrogen, whether it goes into solid solution or forms the hydride or both, is most rapid at about 400°C. At this temperature, face-centered tetragonal ZrH_2 forms. Above this temperature ZrH_2 is no longer stable, and hydrogen will be given off, if the sample has been previously heated at 400°C until it has taken up enough hydrogen to form ZrH_2. At about 800°C the face-centered cubic ZrH forms and can be retained if quenched to room temperature or cooled from this temperature in an inert gas or vacuum. If the ZrH is cooled slowly in hydrogen the formation of ZrH_2 will again occur in the vicinity of 400°C. Above 800°C hydrogen is given off until, at the transformation temperature of 862°C, there is a sudden absorption of hydrogen. Above this temperature hydrogen would again be given off. The mechanism of the formation of ZrH_2, ZrH, and the solid solution of hydrogen in α and β Zr is described in the literature.[6-9]

Zirconium hydride was made at 400° and 800°C for subsequent processing. The zirconium hydride made at 400°C was primarily ZrH_2. At 800°C, ZrH formed, but furnace cooling in hydrogen permitted the formation of ZrH_2 to occur. X-ray analysis revealed that the product of the 800°C treatment was a mixture of ZrH and ZrH_2, but contained a larger proportion of ZrH_2. Subsequent to the hydriding process, the friable hydride pieces are ground by hand in a steel mortar with a steel pestle or in a hammer mill to the desired size. Both hydrides are so friable that they can be ground easily to pass a 400 mesh screen (0.037 mm) if that is desired. The product of the 400°C treatment appeared to be more friable, but it took somewhat more grinding to make it fine enough to pass through a 325 mesh screen.

The zirconium metal powder can be prepared by vacuum decomposition of a powdered charge of either of the hydrides, ZrH_2 or ZrH. The decomposition occurs by heating the hydride up to a temperature of 800°C or above in a vacuum of 0.05 micron or better. During the heating operation of the cycle, the pressure of hydrogen in the vacuum system rises to more than 25 microns and then diminishes rapidly to its initial value after being heated for a certain time (depending upon the amount of the charge) at 800°C or above. The slow rate of heating, the fast pumping speed, and the temperature of approximately 800°C are considered critical to the removal of hydrogen to a few hundredths of a percent and the obtaining of a loosely sintered cake of zirconium that can be easily ground to a powder.

The particle size distribution, densities, and apparent densities of the powders obtained by these methods are shown in Table I. Zirconium hydride pulverizes more easily than the zirconium obtained by the decomposition of the hydride and, therefore, contains a larger amount of fine particles. Both powders, zirconium hydride as well as zirconium, contain traces of Al, Ca, Cu, Fe, Mg, Mn, and Si of

Table I. Particle Size Distribution, Density, and Apparent Density of Zirconium Hydride and Zirconium Powder

Particle Size Microns	ZrH_2 Powder, Run No. 33	Zr Powder Made from ZrH_2, Run No. 33
0-1	10.2	1.5
1-2	10.3	2.8
2-3	13.3	2.0
3-4	19.0	4.3
4-5	8.3	3.8
5-6	5.0	5.4
6-8	5.4	6.6
8-10	1.8	5.5
10-12	1.1	5.3
12-14	1.3	5.6
14-16	1.5	5.5
16-20	1.8	8.0
20-30	7.7	15.4
30-44	10.5	19.4
44	2.3	8.9
Photolometric average size, microns	10.3	20.0
Particle density, g per cc	5.72	6.59
Apparent density, g per cc	2.2	2.0

practically the same amount as found in the zirconium crystal bar from which the hydride was made. Chemical analysis revealed the presence of gaseous impurities, i. e. 0.2 to 0.4 pct O and 0.01 to 0.015 pct N. There was very little difference in the particle shape of the three kinds of powders, ZrH, ZrH_2, and Zr. All particles were of angular shape, similar to most particles obtained by crushing.

Equipment: The equipment for the preparation of the hydride comprises a quartz tube electric furnace and a hydrogen purification train. Formation of zirconium hydride requires the use of highly purified hydrogen, if the purity of the powder is to be maintained. Tank hydrogen which is reported to contain 0.2 pct O and no other appreciable impurities, was passed over copper turnings at 600°C to catalyze the reaction between hydrogen and oxygen to form water. The water was removed by activated alumina (Lectrodryer). A furnace, containing calcium turnings at 700°C, was used to remove the last traces of oxygen, nitrogen, and water. This purified hydrogen was permitted to flow over the zirconium crystal bar during the entire processing of the zirconium hydride, including the heating and cooling cycles. The charge was maintained at a temperature of 400° or 800°C for 1 to 20 hr, depending on the amount of zirconium, and the furnace was cooled in the hydrogen flow.

The vacuum furnace (globar type) used for the decomposition of the hydride powder to zirconium powder contains a sillimanite furnace tube and comprises a compound model CVD Kinney pump and a Distillation Products MC-500 metal diffusion pump.

Processing Methods

Compacting of Zirconium and Zirconium Hydride Powders: Both zirconium powder and zirconium hydride powder can be compacted without the use of a binder. The powders flow easily and the filling of the compacting die can be done without any difficulties. The powder within the die cavity is levelled as easily as any conventional commercial metal powder.

The compression ratio is defined as the ratio of the volume of a loose powder to the volume of the compact after application of a specified pressure.

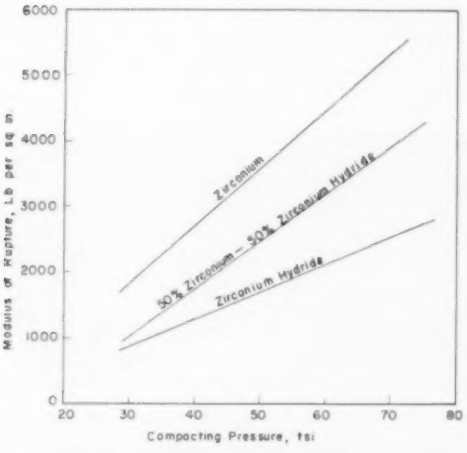

Fig. 2—Green strength of compacted —200 mesh zirconium and zirconium hydride powders.

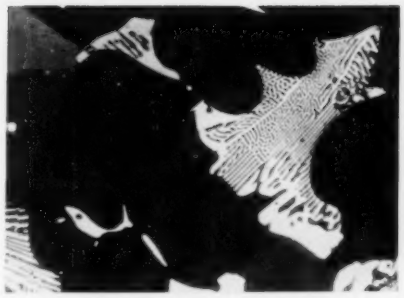

Fig. 3—Effect of BeO on zirconium at sintering temperatures. Microstructure of the interior of a zirconium bar packed in BeO powder and heated 4 hr at 1250°C in high vacuum. Polarized light. X250. Area reduced approximately 50 pct for reproduction.

This ratio is low for both powders, as mentioned above. When conventional pressures of 40 to 50 tons per sq in. (tsi) are applied, the compression ratio ranges between 2:1 to 2.5:1. Inasmuch as the compression ratio determines the height of the compacting die, the low compression ratio of zirconium and zirconium hydride powders is very favorable for the die design.

Fig. 1 shows the effect of the compacting pressure on the density of the compacts made from zirconium hydride and zirconium powder. The powders were pressed in a single-action die of $\frac{3}{8}$x2 in. die cavity at pressures varying from 20 to 90 tsi. Higher densities of the compacts may be obtained by using double-action dies or by pressing samples with a more favorable ratio between pressing area and die-wall area. The application of 100 tsi compacting pressure resulted in slightly higher density, but some of the compacts, pressed at 100 tsi, showed indications of lamination.

To determine the relative green strength of this compacted material, zirconium powder, zirconium hydride powder, and a mixture of 50 pct zirconium and 50 pct zirconium hydride powders were pressed at 30 and 70 tsi. Three samples of each type of approximately $\frac{1}{8}$x$\frac{3}{8}$x2 in. were compacted at each pressure in the above described rectangular, single-action die. The compacts were placed on semi-knife edge supports which were 1 in. apart and loaded transversely with a dead load suspended from a semi-knife edge. The load was increased constantly until the sample broke. The differences in modulus of rupture between samples of the same material compacted at the same pressure correlated the slight differences in density that occurred from sample to sample. The data are presented in Fig. 2. There is probably some deviation from a straight line particularly at higher pressures, but for the present correlation it seems adequate to present the data as shown. The green strength of compacted zirconium is approximately twice as high as the green strength of zirconium hydride compacts. The addition of zirconium powder to zirconium hydride powder increases the green strength of compacts made therefrom.

If the pressed compact were the ultimate product, zirconium powder would be clearly a more suitable material than zirconium hydride. It will be shown later, however, that to produce a sintered material of good density, zirconium hydride can be compacted

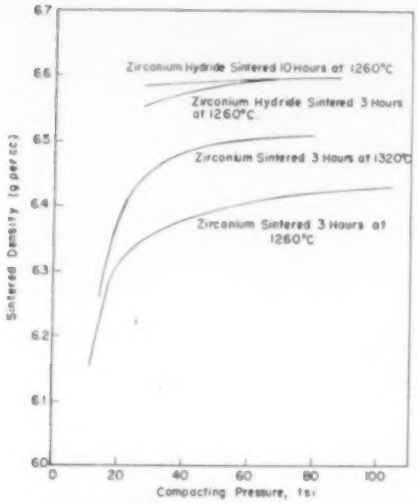

Fig. 4—Effect of compacting pressure on the sintered density of pressed and sintered zirconium and zirconium hydride powders, sintered in high vacuo.

at even lower pressures than zirconium powder. In addition, many large thin briquettes, approximately $\frac{1}{8}$x2x13 in., of zirconium hydride have been pressed at pressures as low as 15 tsi without a single loss by breakage.

Sintering of Zirconium and Zirconium Hydride: The extreme affinity of zirconium for oxygen and nitrogen[6, 10] makes it necessary to sinter in either a very pure inert gas or in a high vacuum. Compacted zirconium powder was sintered in purified argon. Even though the tank argon was purified by hot copper turnings, a Lectrodryer, drying towers of phosphorous pentoxide and magnesium perchlorate, and hot uranium turnings, it was not pure enough for the sintering of zirconium. The last traces of nitrogen could not be removed completely from the argon by the hot uranium turnings, and the zirconium invariably picked up excessive nitrogen. Sintering in vacuum of the order of 5×10^{-5} mm Hg or better was carried out successfully at temperatures of 1300°C or less without any noticeable increase in oxygen or nitrogen content. Vacuum sintering was also advantageous because compacted zirconium hydride powder could be sintered directly, decomposition occurring concurrently with sintering, thereby eliminating a step in the process. When compacted zirconium hydride powder was sintered in purified argon, the residual hydrogen content was always high, but vacuum sintering reduced the hydrogen content to that of the original crystal bar.

When a compact of zirconium hydride powder is heated in vacuum above 400°C, an appreciable decomposition of the hydride occurs that is closely related with a considerable increase of the mobility of the metallic atoms. The degree of mobility of the metallic atoms at the temperature of the decomposition corresponds to far higher temperatures than those at which the decomposition actually takes place. When the hydride is destroyed, the metallic atoms are at a certain state of unstability that leads to their increased mobility. Because of the high degree of mobility, the metal atoms will migrate until they have found positions corresponding to a minimum of free energy. This process causes a faster rate in sintering of the compacts made from zirconium hydride powder compared to the sintering rate of compacts made from metal powder.

In sintering it is frequently desirable to pack the compacts in a refractory powder in order to have samples of all shapes readily supported and separated during sintering. To investigate the possible use of a packing material, pieces of zirconium crystal bar were packed in different refractory oxides and heated to the sintering temperature of 1250°C in vacuum for 2 hr. X-ray analysis revealed that during sintering the zirconium reduced BeO, SiO_2, and ZrO_2 and became contaminated with oxygen and Be or Si. Fig. 3 shows the extent to which zirconium reacted with BeO. The interior of the crystal bar after being heated in BeO powder revealed the typical Zr-Be eutectic structure, as described previously,[11] characteristic of about 2 to 5 wt pct Be. Melting was, of course, evident in this sample by the appearance after the 1250°C treatment. The use of a packing medium of refractory was abandoned because it was expected that even if no reaction occurred the out-gassing of the refractory powder surrounding the zirconium would increase the gas content during sintering.

Stabilized zirconium oxide boats and slabs were used with some success for sintering since the contact with the refractory was not so intimate that much reduction of the ZrO_2 could occur. Even so, the

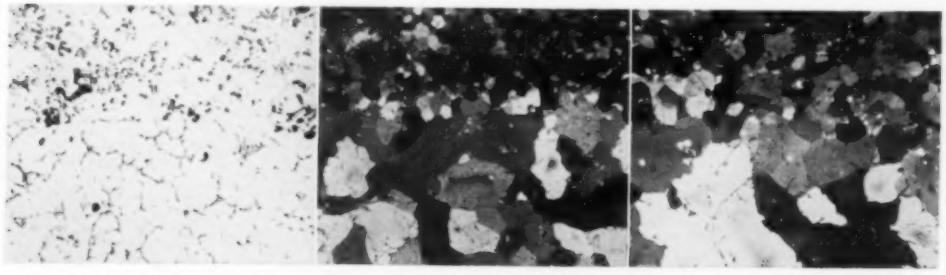

Fig. 5—Interface between zirconium and zirconium hydride. Zirconium hydride powder (shown after sintering on the bottom) placed in the die and pressed at 7 tsi. Zirconium powder (shown on top) added and the entire compact was pressed at 50 tsi. Sintered as indicated in high vacuum. a (left)—Sintered 2 hr at 1190°C. Bright field. b (center)—Sintered 2 hr at 1190°C. Polarized light. c (right)—Same sample as b. Resintered 2 hr at 1300°C. Polarized light. X100. Area reduced approximately 50 pct for reproduction.

reduction of the ZrO_2 was a possible source of oxygen pickup, and the difficulty in obtaining large boats of stabilized zirconium oxide prompted a search for a better container for sintering.

It was found that samples in intimate contact with graphite did not pick up carbon. Graphite adhered to small areas of the resting surface of the sample, but the carbon penetration was never more than a few mils even after sintering at 1390°C. Samples sintered in a covered graphite boat and separated by graphite slabs had bright, shiny surfaces. Pieces of zirconium crystal bar revealed no oxygen or nitrogen pickup after being heated in these graphite boats for as long as 10 hr at 1260°C in a vacuum of about 2×10^{-5} mm. The excellent surface appearance, freedom from contamination, and ease of preparation of graphite boats and slabs of any size made the use of covered graphite boats the most desirable container for sintering zirconium.

In the discussion of the properties of sintered zirconium and other information on the powder metallurgy of zirconium, the powder used for compacting and sintering is zirconium hydride. It is essential, then, that the relative merits of pressed and sintered zirconium powder and zirconium hydride powder be discussed before eliminating the former in the general discussion.

Earlier unpublished work by Angier and Hausner clearly indicated that the sintered product of compacted zirconium hydride powder is superior in most respects to that of zirconium powder, i.e., the ductility, corrosion resistance, and gas content was more favorable in the former. Obviously these superior properties are a function of the lower oxygen and nitrogen content, the source of this added gas being in the extra pulverization step necessary to produce zirconium powder. Fig. 4 shows that compacted zirconium hydride sinters readily to the full density of zirconium and that it is comparatively insensitive to differences in compacting pressure in the range shown. In reality, then, if the full density of zirconium is to be obtained, zirconium hydride powder can be compacted at lower pressures than zirconium powder. The inferior green strength of compacted zirconium hydride powder is a small sacrifice for the other benefits obtained, especially since the green strength of these compacts pressed at practicable pressures is sufficient to make them easy to handle.

A test was made to determine if compacted zirconium powder could be pressed together with compacted zirconium hydride powder to give a good final bond during sintering. Such a process might have an application in making specialized shapes where the large shrinkage differential between the two types of compacted powders during sintering could be utilized. The process is indeed favorable. As shown in Fig. 5 an excellent bond was developed. This investigation proved, however, to be a more decisive indication of the superiority of zirconium hydride powder than could be determined by other tests. In Fig. 5a, b, and c, the sintered product of compacted zirconium powder is shown on the top and that of compacted zirconium hydride powder on the bottom of the micrographs. The zirconium hydride powder was pressed in a die at 7 tsi and zirconium powder was added, levelled, and the two layer compact pressed together at 50 tsi. The sample was then sintered in high vacuum for 2 hr at 1190°C. It is evident from Fig. 5a that the zirconium hydride powder yielded a much less porous sintered zirconium

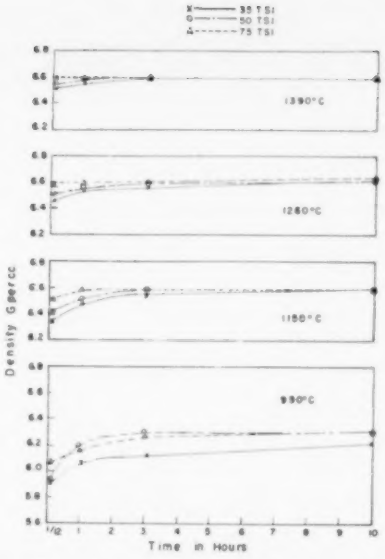

Fig. 6—Effect of sintering time and compacting pressure on the sintered density of zirconium. Samples compacted from zirconium hydride powder and sintered in vacua at various temperatures.

than did the zirconium powder. Fig. 5b shows how the grain growth of the zirconium progressed.

Even though the original particle size of the zirconium hydride powder was much less than that of the zirconium powder, the sintered product of the former has a much coarser grain size. The sintered zirconium powder shows very little if any grain growth at this stage (2 hr at 1190°C). However, as would be expected, the sintered zirconium of compacted zirconium hydride shows marked grain growth. In Fig. 5c the resintered sample shows the further progress of grain growth and densification. Evidently the decomposition of zirconium hydride during sintering yields a compact composed of particles that have extremely clean active surfaces ideal for bonding. Whatever the fundamental sintering mechanism may be these highly activated surfaces, then, are ideal for the sintering phenomenon to occur. It is interesting to note that many of the large pores which remain (Fig. 5a and b are identical fields) are within the grains and do not seem to act as barriers to grain growth. This test may be used as another proof that the sintering of compacted zirconium hydride powder may be carried out at lower sintering temperatures and shorter sintering times. There are, then, at least six factors which point to the direct use of zirconium hydride powder for pressing and sintering. These are: 1—Reduction in processing cost of the powder. 2—Reduction in time for processing the powder. 3—Better physical properties of the sintered compact because of lower gas content. 4—Less opportunity for the pickup of impurities during the various processing steps. 5—Permits the use of lower compacting pressure to attain ideal or any arbitrary density. 6—Permits the use of lower sintering temperature and shorter sintering time to attain the ideal or any arbitrary density.

Hot Pressing of Zirconium Powder: Tests were

made with pressing of zirconium powder at elevated temperatures. The pressing was done in a graphite-lined steel die at 650°C for 15 min in vacuum at a pressure of 25 tsi. Under these conditions the powder compacted to a solid mass to a density of 6.53 g per cc. The hot-pressed specimens showed uniform fine grain size slightly less than that of cold-pressed and subsequently sintered specimens of similar density. The hardness of the hot-pressed specimen was slightly higher than that of the corresponding cold-compacted and sintered sample.

Properties of Sintered Zirconium

Experimental Procedure: The best processing methods as derived from information incorporated in the preceding sections were utilized to make a comprehensive study of the powder metallurgy of zirconium as processed under a set of standard conditions.

The zirconium hydride was formed at 800°C and ground in a steel mortar and pestle to pass through a 325 mesh screen. One batch of thoroughly blended powder was used for all the tests to be described subsequently thereby eliminating possible variables that may be introduced by variations in the powder.

The samples were compacted in a rectangular steel die 3x$\frac{1}{4}$ in. to a thickness of about $\frac{1}{8}$ in., each sample containing a uniform charge of 7 g of zirconium hydride powder. The compacts were pressed at 35, 50, and 75 tsi, placed in a covered graphite boat, and separated by graphite slabs. The boat was placed in a vacuum furnace, evacuated for at least 16 hr and sintered at 990°, 1150°, 1260°, and 1390°C for 5 min, 1, 3, and 10 hr. During the heating of the specimens the pressure in the furnace tube increased at about 800°C due to decomposition of the zirconium hydride and did not begin to decrease until the temperature was about 950°C. The samples were furnace-cooled in vacuum.

The sintering was done in a globar furnace containing a sillimanite tube. This tube was sealed to glass and the entire pumping system up to the mechanical pump was glass. The vacuum was generally about 2×10^{-5} mm at temperature. The as-sintered samples had bright, clean, shiny surfaces.

Densification of the Sintered Compact: The ultimate density of compacted and sintered zirconium was investigated as a function of the compacting pressure and sintering variables such as time and temperature. The powder was not varied as pointed out earlier. It is worthy of mention, however, that experiments with zirconium hydride powder ground to a particle size less fine than the —325 mesh did not densify during sintering as readily as the compacted —325 mesh powder at the same time and temperature.

In Fig. 6 the effect of compacting pressure, sintering time, and sintering temperature on the density of zirconium is shown. The role of compacting pressure becomes insignificant at the higher sintering temperatures and longer times. When a minimum of sintering time and the lowest possible temperature is desired, the use of higher pressure becomes important. Ideal density can be attained, for instance, by sintering 1 hr at 1150°C provided a compacting pressure of 75 tsi has been used.

Fig. 7 shows a plot of isodense lines after sintering at any time and temperature in the range shown for compacts pressed at 50 tsi. From this the density obtainable for any given sintering temperature and time can be predicted. The densities would vary, of course, to perhaps ±0.03 g per cu cm because of deviation in both measurement and sample. Compacts pressed at 50 tsi, however, can be sintered to full density as shown by the line for completion of densification. In order to better show the effect of compacting pressure on completion of densification, Fig. 8 is presented. If a sample is to be sintered to ideal density for 8 hr at 1250°C, compacting pressures as low as 35 tsi can be used. If the sintering temperature must be low, however, higher compacting pressures become necessary. At 1100°C, for instance, a sample which has been compacted at 75 tsi can be sintered for as little as 3 hr to attain ideal density.

Grain Growth: The grain growth of zirconium during sintering is very rapid provided the material charged to the sintering furnace was compacted zirconium hydride powder. In Fig. 9 the grain size of zirconium, sintered at various times and temperatures, is shown. The actual grain size is shown in microns and in grains per sq mm in Table II.

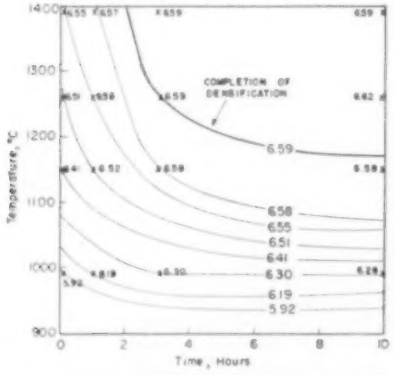

Fig. 7—Constant density lines as a function of sintering time and temperature for zirconium. Vacuum sintered from —325 mesh zirconium hydride powder compacted at 50 tsi.

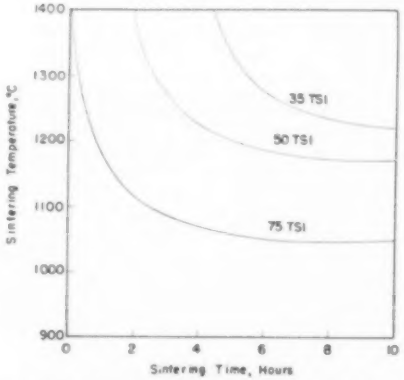

Fig. 8—Isodense lines representing 6.59 g per cu cm (complete densification) for three compacting pressures. Data for —325 mesh zirconium hydride compacted as indicated and vacuum sintered.

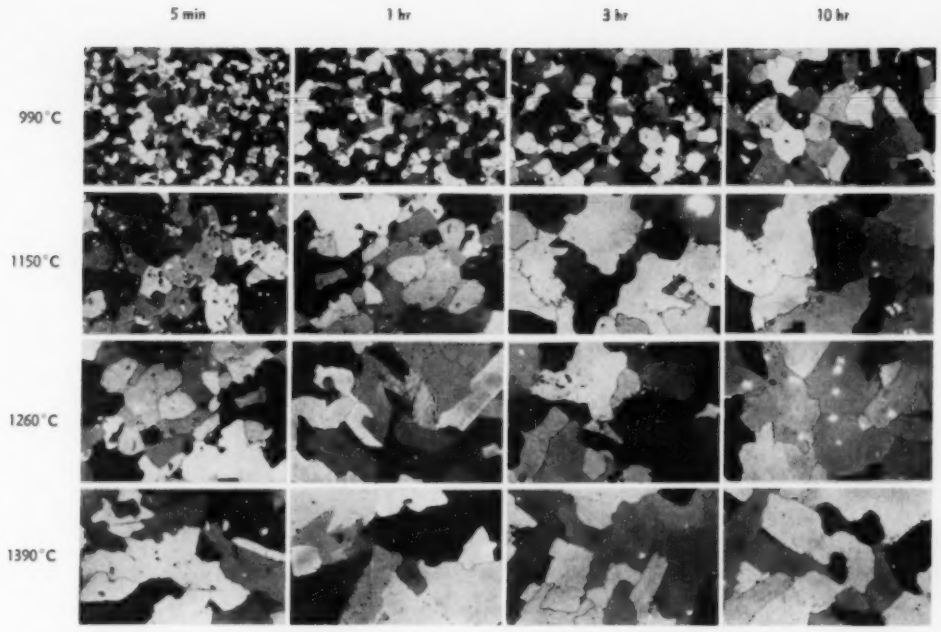

Fig. 9—Effect of sintering time and temperature on the grain growth of zirconium. Compacts pressed at 50 tsi from —325 mesh zirconium hydride powder and sintered in vacuum. X250. Area reduced approximately 80 pct for reproduction.

It appears that grain growth is most rapid in the vicinity of 1100° to 1200°C. At 990°C the growth was quite slow compared to the rapid growth which occurred on sintering at more elevated temperatures. Densification, on the other hand, is relatively rapid at lower temperatures. The relationship between density and grain size is shown in Fig. 10. Initially in the sintering process considerable densification occurs with little grain growth. Toward the end of the sintering process the density becomes asymptotic to ideal and little densification occurs, but grain growth is quite rapid. The relationship between the sintering mechanism and grain boundary movement, if one exists, should have some interesting theoretical ramifications.

Table II. Grain Size of Zirconium after Sintering

Sintering Time	Grain Size, Microns				Grains per Sq Mm			
	990°C	1150°C	1260°C	1390°C	990°C	1150°C	1260°C	1390°C
5 min	21.8	49.7	69.4	117	2670	515	265	93
1 hr	28.4	68.4	108	131	1590	208	109	75
3 hr	31.2	107	128	119	1309	112	79	90
10 hr	51.6	139	143	152	480	66	63	55

Hardness: The hardness of sintered zirconium may be influenced among other things by oxygen content, grain size, and density. The first two factors affect the intrinsic properties of the metal, but the hardness when affected by density is merely another indication of the amount of porosity.

In Fig. 11 the hardness is shown as a function of sintering time and compacting pressure for samples sintered at 990°C. It is clear that the only difference in the sintered product affected by compacting pressure is porosity. The differences in hardness, then, shown in Fig. 11, are representative of the trend in density. After sintering at higher temperatures, the effect of compacting pressure on the hardness becomes negligible. In fact, after a density of about 6.3 g per cu cm is reached, the hardness seems to become insensitive to the slight differences in density.

The hardness of dense sintered zirconium made by these methods is about Rockwell B 92. Variations in hardness may occur so that values from 90 to 94 Rockwell B are obtained. This deviation may be

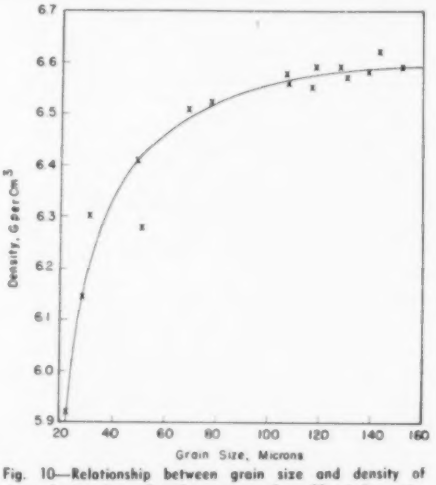

Fig. 10—Relationship between grain size and density of sintered zirconium. Samples compacted at 50 tsi from zirconium hydride powder and sintered in high vacuum at various times and temperatures.

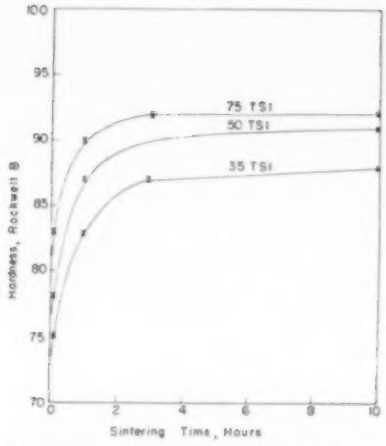

Fig. 11—Effect of compacting pressure and sintering time on the hardness of zirconium sintered in vacuum at 990°C from compacted —325 mesh zirconium hydride powder.

attributed to the variation in grain size and oxygen content, the former influencing lower hardness with more sintering because of grain growth and the latter influencing higher hardness with sintering at higher temperatures or for longer times. It is difficult to isolate the effect of these two variables on the hardness except at 1390°C where the increase in oxygen content noticeably increases the hardness, as shown in Table III. This effect is also clearly illustrated in both the experimental data on electrical resistivity shown in Fig. 12 and the schematic representation, Fig. 13.

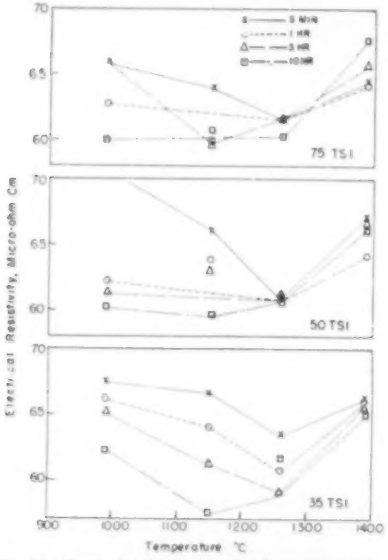

Fig. 12—Electrical resistivity of sintered zirconium compacts pressed as indicated from zirconium hydride powder and sintered in vacuum at the times and temperatures shown.

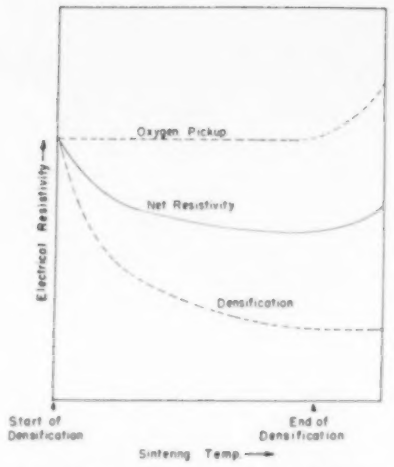

Fig. 13—Idealized curves showing the probable effect of densification and of oxygen pickup during sintering on the electrical resistivity of sintered zirconium.

Electrical Resistivity: The electrical resistivity may reflect many variables operating in the processing of sintered zirconium. As explained in the sections on experimental procedure, the control of these experiments was such, however, that many variables can be eliminated from the discussion, and it is indicated that there are only three fundamental differences in the sintered compacts. These are: 1—Grain size, 2—oxygen content, and 3—density. It is probable that grain size would have little if any measurable effect on the resistivity. The two variables which need to be considered, then, are oxygen content and density. The pressed compacts to begin with have an oxygen content of about 0.2 wt pct, the main source of this oxygen being in pulverizing as has been described earlier. Little oxygen is picked up during sintering at temperatures up to 1260°C, but

Table III. Rockwell B Hardness of Sintered Zirconium. Samples Sintered in Vacuum from —325 Mesh Zirconium Hydride Powder Compacted at 50 tsi

Sintering Time	Sintering Temperature, °C			
	990	1150	1260	1390
5 min	78	88	90	95
1 hr	87	90	91	95
3 hr	92	93	92	97
10 hr	91	91	95	98

there is some increase at the higher sintering temperatures and very long sintering times. This oxygen which is undoubtedly in solid solution after sintering would have a marked influence on the resistivity.

The electrical resistivity was measured for all sintered samples and these data are shown in Fig. 12. It is immediately apparent that the resistivity first decreases with sintering temperature and then increases. The decrease is definitely due to densification and the increase probably to oxygen pickup. This is shown in the schematic representation in Fig. 13. The resistivity, then, is a splendid guide to optimum sintering conditions, a minimum resistivity

Fig. 14—Microstructure of cold worked and annealed zirconium. Compacted from —325 mesh zirconium hydride powder and sintered 3 hr at 1260°C in high vacuum. a (left)—As sintered. b (center)—Cold rolled 75 pct reduction in thickness, longitudinal section. c (right)—Same as b but annealed 1 hr at 900°C. Polarized light. X200. Area reduced approximately 50 pct for reproduction.

indicating the optimum. From Fig. 12 it appears that the best sintering temperature is in the range 1150° to 1260°C. The data are insufficient to pick a value and establish this as the exact sintering cycle, but a useful sintering range can be ascertained. Compacting pressure plays a role, but the limits on compacting pressure are wide if the selected sintering range is 3 to 10 hr at 1150°C and 1 to 10 hr at 1260°C. This is in agreement with data on the other properties investigated. Samples sintered in these ranges had good density, relatively low hardness, and relatively low oxygen content.

The electrical resistivity of pure zirconium is reported[12, 13] to be from 39 to 41 microhm-cm at 0°C, which corresponds to about 40 to 42 microhm-cm at room temperature. The lowest resistivity found in this investigation for sintered zirconium was 58 to 60 microhm-cm at room temperature. The difference between this and the reported electrical resistivity can probably be attributed to the higher oxygen content in the sintered product, which oxygen pickup has occurred during powdering of the zirconium hydride.

Ductility: Although tensile tests were not made, cold rolling permitted an evaluation of the ductility of the sintered zirconium. The sintered samples were cold rolled about 5 pct per pass, examined carefully for edge cracking after each pass, and rolling continued until the first sign of edge cracking. Treatment, i.e., compacting pressure, sintering time, and temperature, seemed to have no significant effect on the ductility, practically regardless of the density. In 50 samples of various densities that were cold rolled, the range in reduction of thickness to the first sign of edge cracking was 53 to 72 pct. The average reduction in thickness was 62 pct. The sintered zirconium, then, is quite ductile.

Fig. 14 shows the microstructure of zirconium. These rolling studies proved the existence of a high degree of ductility in sintered zirconium, which makes the powder metallurgy method of manufacturing zirconium parts most valuable.

Conclusions

Zirconium of high purity can be fabricated by powder metallurgy methods. The use of zirconium hydride powder for compacting and sintering leads to a more superior product than does the use of zirconium powder.

The pressing and sintering conditions that permit the powder metallurgical fabrication of sintered zirconium are established. Compacting at conventional pressure of 40 to 50 tsi, sintering in vacuum within the temperature range 1150° to 1260°C, and the use of covered graphite boats, during sintering, results in sintered zirconium compacts of practically theoretical density and appreciable ductility.

The superiority of zirconium hydride powder over zirconium powder is shown clearly. It should be useful to determine how well other metal compound powders, such as hydrides, oxides, and others, can be decomposed during sintering and whether this decomposition facilitates the sintering process. Further studies in these directions are under consideration.

Acknowledgments

We wish to thank H. W. Woods and Eleanor Polukis for their preparation of metallographic specimens, N. P. Pinto for hot pressing studies, H. Mansfield for physical properties testing, and H. B. Michaelson for editorial work. We are particularly indebted to W. E. Kingston for numerous valuable discussions and suggestions regarding this work.

References

[1] J. H. deBoer and J. D. Fast: On the Production of Pure Metals of the Titanium Group by Thermal Decomposition of the Iodides, Part I—Zirconium. *Ztsch. Anorg. Allgem. Chem.* **153**, p. 1.

[2] J. D. Fast: Zirconium and Its Compounds with a High Melting Point. *Philips Technical Review* (December 1938) **3**, No. 12.

[3] T. E. Hayes, E. D. Dilling, and A. H. Roberson: Fabrication and Mechanical Properties of Ductile Zirconium. *Trans.* ASM (1950) **42**, p. 619.

[4] D. Lely and L. Hamburger: The Production of the Elements Thorium, Uranium, Zirconium, and Titanium. *Ztsch. Anorg. Allgem. Chem.* (1914) **87**, p. 209.

[5] W. C. Lilliendahl and H. C. Rentschler: Recent Developments on the Preparation of Zirconium. *Trans.* Electrochemical Soc. (1947) **91**, p. 286.

[6] E. A. Gulbransen and K. E. Andrew: Kinetics of the Reactions of Zirconium with O_2, N_2, and H_2. *Trans.* AIME (1949) **185**, p. 515; JOURNAL OF METALS (August 1949).

[7] J. H. deBoer and J. D. Fast: The α-β Transition in Zirconium in the Presence of Hydrogen. *Rec. Trav. Chim* (1936) **55**, p. 350.

[8] A. Sieverts, A. Gotta, S. Halberstadt: *Ztsch. Anorg. Allgem. Chem.* (1930) **187**, p. 155.

[9] G. Hagg: *Ztsch. Physik. Chem.* (1931) **11B**, p. 433.

[10] J. D. Fast: *Metallwirtschaft* (1938) **17**, p. 641.

[11] H. H. Hausner and H. S. Kalish: A Preliminary Investigation of the Zirconium-Beryllium System by Powder Metallurgy Methods. *Trans.* AIME (1950) **188**, p. 59; JOURNAL OF METALS (January 1950).

[12] J. D. Fast: Zirconium As A Getter. *Foote Prints* (1940) **13**, No. 1.

[13] *Metals Handbook*, ASM (1948).

Production of Aluminum from Kalunite Alumina

by Arthur Fleischer and Julian Glasser

THIS country was faced with the possible necessity of utilizing nonbauxitic ores for producing aluminum during World War II. Construction of four experimental plants to treat such ores by four different processes was authorized[1-4] including one at Salt Lake City, for the conversion of Marysvale alunite to metal-grade alumina and potassium sulphate by the Kalunite process.[4] An aluminum reduction plant in Tacoma, Wash., with a capacity of 50 tons of aluminum per day, was constructed to handle the Kalunite alumina produced at the Salt Lake City plant. The alumina and aluminum plants were Defense Plant Corp. projects operated by Kalunite, Inc. and Olin Industries, Inc., respectively.

Kalunite alumina differs from Bayer alumina in several respects, particularly in that the former contains potash instead of soda. The presence of potassium in the alumina feed to the cryolite bath was stated by aluminum technologists to be undesirable under the usual operating conditions of aluminum furnaces. In 1940, about 20 tons of Kalunite alumina produced in the Kalunite pilot plant, were reduced electrolytically in a 10,000 amp furnace at Battelle Memorial Institute and at the aluminum reduction plant at Neuhausen, Switzerland. These relatively small scale tests indicated that satisfactory commercial aluminum could be produced in a practical manner.

The Tacoma plant reduced about 2,500,000 lb of Kalunite alumina to produce more than 1,200,000 lb of aluminum, in accordance with the accepted practice for reducing Bayer alumina. It was desired to determine whether commercial aluminum could be produced on a large scale and to establish the technological differences in commercial reduction practice between Kalunite and Bayer alumina. In the course of collecting data, the effects of the abnormal chemical composition and physical properties of Kalunite alumina were observed wherever possible.

Tacoma Reduction Plant

The reduction plant had two pot lines, each with 120 cells in series, operated at approximately 32,000 amp. Each cell was provided with a single rectangular Soederberg continuous anode, with side-pin electrical contacts. Each cell was hooded and ventilated through a stack connected to 14 other cells, with 25,000 cfm blower. When the plant started operation in 1942, all of the cathode linings were of block construction. Rebuilt cells were of rammed paste construction.

A. FLEISCHER, Member AIME, formerly Technical Director, Kalunite, Inc., Salt Lake City, is now with Nickel Cadmium Battery Corp., Easthampton, Mass. J. GLASSER, Member AIME, formerly Chief Chemist, Aluminum Division, Olin Industries, Inc., Tacoma, Wash., is now with Armour Research Foundation of Illinois Institute of Technology, Chicago.

Discussion on this paper, TP 3088D, may be sent, 2 copies, to AIME by Oct. 1, 1951. Manuscript, Feb. 17, 1950; revision, March 28, 1951. New York Meeting, February 1950.

Paper published by permission of Olin Industries, Inc. and Kalunite, Inc., East Alton, Ill.

A total of 12 cells in pot room No. 1 were operated on Kalunite alumina over a period of 17 months. The remainder of the plant operated on Bayer alumina. Shutdowns immediately after the war brought an abrupt halt to operations.

Operating Conditions

The average charge of alumina was 240 lb to a 9000-lb bath with an average of 3.5 to 3.8 anode effects per day. Normal operating voltage was maintained at 4.9 v and each anode effect (30 to 40 v) averaged 6 min. The crust on alternate sides and both ends of a pot was broken through at anode effects. Before placing a new charge of alumina on the exposed electrolyte, the space between anode and cathode was raked thoroughly. During normal operations, four gas holes, about 6 in. from the anode, were maintained in the crust. Surface temperature of the electrolyte was about 950°C. The ratio of NaF to AlF_3 in the bath was maintained between 1.45 and 1.50. The alumina content in the bath varied between 2 and 7 pct. Anode paste, prepared on the side, was loaded at the rate of about 5000 lb every 15 days. Each pot was tapped every third day, leaving 2 in. of metal pad after each tap.

Since only a small part of the reduction plant was operated on Kalunite alumina, special procedures were required in order to obtain accurate data. Ordinarily, raw material consumption, production, and power data are obtained from overall plant inventories and meter readings from the rectifier station. However, information on a small number of pots cannot be obtained in this manner. Therefore, it was necessary to record weights of all raw materials charged, weight of metal tapped, and voltages for each individual pot operating on Kalunite alumina. To compare the operation with Bayer alumina on the same basis, a section of eight pots was started approximately at the same time and operated for several months, with four each on Bayer and on Kalunite alumina, following identical processing and control procedures.

Each pot was tapped singly with return of all scrap metal to the pot. Total production was obtained from the weight of the as-cast metal. Metal was sampled prior to pouring and analyzed by wet and spectrographic methods. Alumina for each charge was weighed in 60 to 80-lb lots. Each carload of alumina was sampled and analyzed by wet methods. Cryolite and aluminum fluoride were measured from 100-lb sacks. The quantity of anode paste consumed was determined by weights of coke and pitch mixed in the paste plant. Ampere-hours, used for calculating current efficiency and power input, were very accurately measured by the line ampere hour meter. Voltages at each pot were recorded hourly, and voltage and time were recorded for anode effects. A time-weighted average of voltage was used for power input.

Raw Materials

Natural Greenland cryolite, aluminum fluoride, fluorspar, Bayer alumina, calcined petroleum coke for anodes, soft anode pitch, and cathode paste or blocks were purchased on specifications generally acceptable for aluminum reduction. Typical chemical composition and physical properties of Kalunite and Bayer aluminas are summarized in Table I.

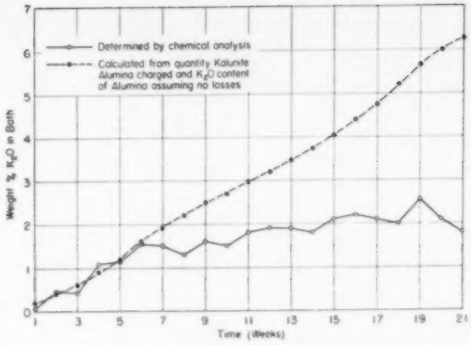

Fig. 1—Potash buildup in electrolyte, pot 95, starting Aug. 13, 1944.

The average chemical composition of the Kalunite alumina showed higher silica, iron oxide, titania, and lead than Bayer alumina. Phosphorous pentoxide, potash and sulphur trioxide were also present in Kalunite alumina in appreciable quantities; but calcium oxide and soda, present in Bayer alumina, were not found in Kalunite alumina. Ignition loss and water absorption were comparable for the two aluminas.

Particle size distribution* was not nearly so uniform for Kalunite alumina as it was for Bayer alumina. Excessive quantities of both coarse and fine sizing were present.

The uniformity in composition of the Kalunite alumina was poor. For 17 carloads of alumina, sulphur trioxide (SO_3) varied from 0.40 to 2.30 pct, potash (K_2O) from 0.25 to 0.78 pct, phosphorus pentoxide (P_2O_5) from 0.01 to 0.08 pct, iron oxide (Fe_2O_3) from 0.08 to 0.14 pct, and silica (SiO_2) from 0.03 to 0.24 pct. This variability in the impurities

Table I. Chemical Composition and Physical Properties of Kalunite and Bayer Aluminas

	Kalunite		
	Typical*	For Comparative Data**	Bayer (Typical)*
Chemical composition			
Silica (SiO_2)	0.06	0.07	0.02
Iron oxide (Fe_2O_3)	0.12	0.12	0.02
Titanium dioxide (TiO_2)	0.005	0.006	0.003
Phosphorus pentoxide (P_2O_5)	0.06	0.09	Nil
Potash (K_2O)	0.35	0.38	Nil
Sulphur trioxide (SO_3)	0.91	1.24	Nil
Soda (Na_2O)	Nil	Nil	0.45
Calcium oxide (CaO)	Nil	Nil	0.02
Lead (Pb)	0.01	0.01	Nil
Ignition loss and water absorption			
L.O.I. (1000°C)	2.09	2.37	2.67
Water absorption (bone dry basis)	1.59	1.58	3.16
Screen analysis (Tyler mesh)			
+ 48	9.1	0.6	Nil
−48 + 100	14.1	5.3	0.5
−100 + 200	22.6	29.6	53.5
−200	65.4	64.5	46.0
−325 (wet on original sample)	52.0	n.d.†	12.0

* Average for first half of 1945.
** Alumina used for data shown in Table II.
† n.d. not determined, but same order as "Typical."

* The particle size refers here to the aggregates that persist on handling the alumina on the screens. Comparative X-ray diffraction patterns of Kalunite and Bayer aluminas made in 1940 showed that the primary crystallite sizes are the same; diffraction line breadths and intensities agreed very closely. The difference in particle (grain) sizes is to be attributed to the types of aggregation encountered in the two aluminas.

Table II. Summary of Operational Data, Bayer Alumina vs. Kalunite Alumina

	Kalunite	Bayer
Number of pots	4	4
Average age per pot, days	173	200
Production		
Lb per pot per day	405	464
Composition, pct		
Al	99.54	99.79
Si	0.18	0.07
Fe	0.25	0.14
Ti	0.01	Trace
Pb	0.02	Nil
Raw materials consumption, lb per 100 lb production		
Alumina	215	189
Cryolite	15.1	9.7
Aluminum fluoride	0	1.8
Anode paste	72	64
Skimmings removed	2.2	0.6
Current efficiency, pct	71.7	82.1
DC kw-hr per lb of metal	9.9	8.7

was due mainly to unsatisfactory operating conditions and difficulties encountered in the operation of the Salt Lake alumina plant, inflicting the penalties of low capacity operation. The quality of the alumina was lower than that of alumina produced experimentally from alunite ores in laboratory and pilot plant studies.

Results of Reduction

Quality of Metal: Acceptable commercial grades of pig aluminum were produced. In the first half of 1945, 50 pct of the metal produced from Kalunite alumina was 99.60 pct metal (grade B) or better; 4 pct was 2A grade, 99.70 pct metal. To obtain higher grade metal it would be necessary to reduce the impurities in the alumina.

Operating Record: The overall operating record for all pots operating on Kalunite alumina showed that commercial alumina could be produced on a large scale without very serious handicaps in production, raw material consumption, and power input. No obnoxious fumes were emitted from the pots, either during normal operation or while breaking in the crust. However, difficulty was experienced in handling the Kalunite alumina, because it was not so free-flowing.

Effect of Particle Size: The coarse grain size contained in Kalunite alumina was undoubtedly the most serious factor in disturbing smooth pot operation.** This also masked effects of other abnormal properties of Kalunite alumina. The excessive fine particles caused dust losses. Both the coarse and fine particles were probably responsible for adverse temperature distribution in the pots. The coarse, settling to the cathode bottom, and the fines, acting as a poorer insulator over the crust, would tend to make the bottom hotter. For efficient operation, the cathode should be considerably colder than the anode.

Potash in Electrolyte: Of the abnormal impurities in Kalunite alumina, potash appeared to be the only one that was retained in the electrolyte to any appreciable extent. Usually, the potash reached a maximum concentration between 1 and 3 pct in about six weeks. Apparently a steady state condition was reached whereby the charging and volatilization losses were essentially equal. Fig. 1 illustrates typical data obtained during the operation of one of the cells. The upper limit of potash content of the bath is of the same order of magnitude as previously found in the operation of the 10,000 amp cell at Battelle Memorial Institute during 1940.

Cathode Lining: No particular adverse effects were noted on cathode linings. The absorption of potash in the lining was about the same as found for the absorption of soda from Bayer alumina.

Comparative Reduction Data: The data have been summarized in Table II. The Kalunite alumina used for comparative reduction data was screened to eliminate most of the excess coarse sizing. As compared to equivalent operation on Bayer alumina, the metal produced contained somewhat higher quantities of silicon, iron, titanium, and lead. Alumina consumed was about 13 pct higher than for Bayer alumina, mostly because of dust losses. No aluminum fluoride was required for the Kalunite alumina operation, because the potash did not continually build up in the bath. The higher rate of carbon dusting from the anodes is reflected in anode paste consumptions and skimmings removed. The current efficiency for pots operating on Kalunite alumina was about 10 pct lower than for those on Bayer alumina.† This caused higher energy input per pound of metal for pots operating on Kalunite alumina. Miscellaneous differences in operating characteristics for pots operating on Kalunite alumina as compared to those on Bayer alumina included lower anode effect voltages, lower bath surface temperatures, less potent anode gas flames, less serious anode corrosion, and less movement of the electrolyte.

Pot Life: The life of pots charged with Kalunite alumina appeared comparable to those charged with Bayer alumina. As an example, four pots were started on Kalunite alumina and at approximately the same time ten pots were started on Bayer alumina in pot room No. 1. They averaged 238 and 233 days of operation, respectively.

Summary and Conclusions

The reduction of Kalunite alumina has produced commercially acceptable metal on a fairly large scale. While the operating record was not as favorable as for Bayer alumina, particularly with respect to current efficiency, it would appear that the operation will be controlled by economic conditions rather than technological consideration. Adverse effects of particle size were definitely confirmed. Improvement of the quality of Kalunite alumina with respect to chemical and physical properties, and/or modifying the electrolytic treatment will undoubtedly improve the reduction operation.

References

[1] F. R. Archibald and C. F. Jackson: Alumina from Clay by the Lime-sinter Method. *Trans.* AIME (1944) **159**, pp. 227-238; *C.A.* **38**, p. 6057.

[2] George C. Heikes: Aluminum and Magnesium. MINING AND METALLURGY (1945) **26**, pp. 70-74; *C.A.* **39**, p. 1378.

[3] C. K. White: Alumina from Clay Plant at Salem, Oregon. *Mining Congress Journal* (1945) **31**, No. 4, pp. 32-34; *C.A.* **39**, p. 3127.

[4] A. Fleischer: The Kalunite Process. *Trans.* AIME (1944) **159**, pp. 267-279; *C.A.* **38**, p. 6057.

** Operation of the 10,000 amp furnace at Battelle Memorial Institute during 1940 was unsuccessful until coarse fractions were removed from the alumina feed by screening.

† The 10,000 amp cell operated at Battelle Memorial Institute showed a current efficiency of 85 pct.

Intermetallic Compounds in the System Molybdenum-Beryllium

by Samuel G. Gordon, James A. McGurty, Gilbert E. Klein, and Walter J. Koshuba

ONE of the problems encountered in working with metals at elevated temperatures is the instability resulting from solid-solid diffusion at a common interface. A determination of the nature and magnitude of this phenomenon is important as related to structural properties of materials potentially useful in high temperature applications. This paper is concerned with the solid state reaction between metallic molybdenum and beryllium at elevated temperatures.

In the older literature,[1] there were no known intermetallic compounds in the system Be-Mo, and the list of beryllium intermetallics was rather small. New compilations have been made by Smithells[2] and by Taylor,[3] listing all the then known beryllium binary intermetallic compounds. In addition to these, some new phases have just been reported[4] in the system Zr-Be and some further compounds of the type MBe_{13} have been currently described.[5] The new compound $MoBe_{12}$ which is reported upon in this paper differs considerably from the above mentioned MBe_{13} group, and will be discussed in detail.

Diffusion Study

The nature of the solid diffusion at a Mo-Be interface was determined by sealing a beryllium rod inside a molybdenum capsule and heating at a temperature of 2000°F (1100°C) for 100 hr. The molybdenum capsule was fabricated from ⅝ in. swaged molybdenum rod obtained from the Fansteel Metallurgical Corp. The beryllium metal was obtained from Brush Beryllium Corp. as ¼ in. cold-drawn rod. This material assayed 99.05 pct Be and contained as impurities 0.84 pct BeO and 0.19 pct Be_2C.

The molybdenum capsule was ⅝ in. in OD x 2 in. long. To prepare it, a concentric hole 0.250 in. + 0.001 in. — 0.000 in. in diam was drilled and reamed in one end of a rod to a depth of 1½ in. A 1 in. long beryllium rod 0.250 in. + 0.000 in. — 0.001 in. in diam was pressed into the molybdenum capsule. A molybdenum plug 0.250 in. ± 0.001 in. in diam x 9/16 in. long was then used to seal the beryllium in place. The capsules were placed in a molybdenum

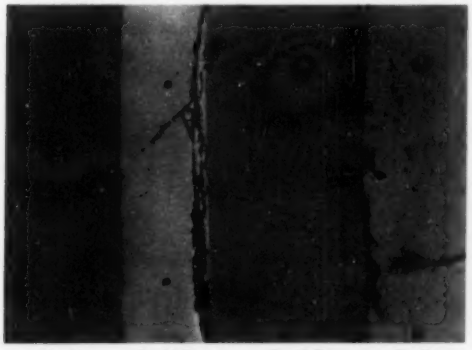

A—Mo B—$MoBe_2$ C—$MoBe_{12}$ D—Be

Fig. 1—$MoBe_2$ and $MoBe_{12}$ formed by solid-solid reaction between Mo and Be at 1100°C (2012°F), polished section at X250, unetched.

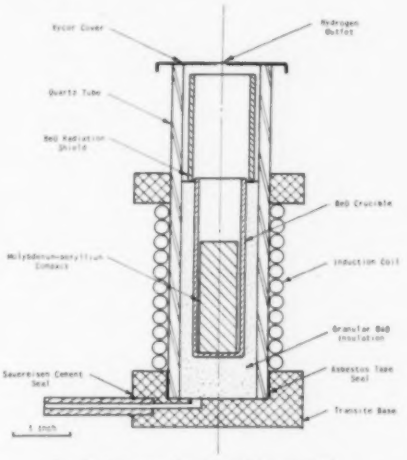

Fig. 2—Induction-heating melting assembly.

resistance furnace and heated at 2000°F (1100°C) for 100 hr. On cooling, the specimens were cut and examined metallographically. Fig. 1 is a micrograph at X250 of a portion of the interface from a transverse section. Four phases are clearly visible, with sharp boundaries between them. Phase A is a section of the molybdenum capsule; phase B is the molybdenum-rich intermetallic composition $MoBe_2$; phase C is the beryllium-rich compound $MoBe_{12}$; phase D is a section of the beryllium rod. All phases were readily polished to a high metallic luster.

The molybdenum-rich phase has a pronounced purple tinge. The beryllium-rich phase (C) is only slightly darker than the pure beryllium. In polarized reflected light, however, it shows striking birefringence between crossed Nicols. The black areas represent flaws or pores in the material. A small representative amount of powdered material from each of the phases was carefully removed under the microscope with a diamond tool. With this material, powder X-ray diffraction patterns were made for the identification of each phase. Table I lists the X-ray diffraction spacings and corresponding indexes characteristic of these intermetallic compounds.

Synthesis

To establish the formula of the new intermetallic compound, X-ray diffraction patterns were made from powders obtained from solidified melts of known composition. The syntheses were made by

S. G. GORDON and G. E. KLEIN, formerly with Nepa Project, Fairchild Engine and Airplane Corp., are now with Los Alamos Scientific Laboratory, Los Alamos, N. M., and Oak Ridge National Laboratory, Oak Ridge, Tenn., respectively. J. A. McGURTY and W. J. KOSHUBA, Member AIME, are with the Nepa Project, Fairchild Engine and Airplane Corp., Oak Ridge, Tenn.

Discussion on this paper, TP 3089E, may be sent, 2 copies, to AIME by Dec. 1, 1951. Manuscript, March 2, 1951; revision, June 4, 1951. Detroit Meeting, October 1951.

Table I. Interplanar Spacings of Powdered Crystals

Ni-filtered Cu radiation ($K\alpha$ = 1.5418A)

$MoBe_2$				$MoBe_{12}$			
hk.l	Calculated	Observed	I*	hkl	Calculated	Observed	I*
10.0	3.83	3.83		200	5.12	5.12	0.7
10.1	3.37	3.37		111	4.02	4.02	
10.2	2.62	2.62		220	3.62	3.63	1.0
00.3	2.52	2.54		300	3.37	3.37	0.1
11.0	2.21	2.21	0.8	311	2.64	2.64	
10.3	2.06	2.05	1.0	400	2.56	2.56	0.9
20.0	1.916	1.914	0.6	330	2.38	2.38	
11.2	1.885	1.884		401	2.21	2.21	0.2
00.4	1.843	1.848		102	2.10	2.10	0.5
20.2	1.695	1.692		500	2.05	2.05	0.3
20.3	1.504	1.500	0.4	510	2.01	2.00	
21.0	1.450	1.450		212	1.952	1.954	0.2
21.1	1.424	1.420		501	1.886	1.890	0.2
21.2	1.356	1.360	0.5	222	1.840	1.840	
20.4	1.342	1.345		440	1.816	1.814	0.9
30.0	1.280	1.279	0.3	600	1.700	1.701	0.1
21.3	1.249	1.246	0.6	412	1.624	1.621	0.3
30.2	1.206	1.206	0.3	601	1.555	1.552	0.3
20.5	1.160	1.159	0.5	502	1.506	1.509	0.2
22.0	1.107	1.109	0.3	700	1.460	1.453	0.1
31.0	1.065	1.063	0.4	003	1.420	1.420	0.1
21.5	1.030	1.028	0.5	213	1.365	1.368	0.4
31.3	0.974	0.976	0.4	602	1.346	1.349	
40.1	0.951	0.952		313	1.322	1.326	0.1
40.2	0.935	0.931		800	1.282	1.282	0.6
20.7	0.906	0.906		403	1.250	1.247	0.3
40.3	0.895	0.894		660	1.214	1.215	0.1
30.6	0.888	0.887		702	1.210	1.209	
23.0	0.880	0.882		552	1.194	1.192	
31.5	0.859	0.861		503	1.176	1.179	
21.7	0.848	0.847		661	1.160	1.162	0.3
41.0	0.838	0.840		513	1.150	1.153	0.3
41.1	0.831	0.830		900	1.144	1.144	
20.8	0.825	0.824	0.6	443	1.110	1.109	0.2
22.6	0.821	0.820		004	1.070	1.071	
41.2	0.818	0.818	0.6	204	1.050	1.048	0.2
31.6	0.803	0.803	0.8	770	1.032	1.031	0.1
23.4	0.795	0.793		1000	1.025	1.025	
50.0	0.772	0.773		304	1.010	1.010	0.2
				771	1.007	1.006	
				005	0.978	0.977	0.2
				703	0.950	0.953	
				1100	0.935	0.933	
				444	0.925	0.923	
				880	0.914	0.914	0.4
				604	0.910	0.908	
				581	0.885	0.887	

* Relative intensities are given where they are 0.1 or greater.

melting Mo-Be mixtures in various stoichiometric proportions.

A high purity molybdenum powder averaging 2 to 5 microns in particle size was obtained from the Fansteel Metallurgical Corp. A beryllium metal 200 mesh powder was obtained from the Brush Beryllium Corp. The material assayed 99.5 pct Be and contained as impurities 0.63 pct BeO, 0.12 pct Al, 0.12 pct Fe, and 0.04 pct Be_2C. Powder mixtures of the two elements were ball milled in a rubber-lined mill using rubber-covered steel balls; the mixtures were then mechanically compressed at 100,000 psi into compacts which were approximately 2 in. long x $\frac{5}{8}$ in. diam. These compacts were melted directly by induction. Fig. 2 is a schematic drawing of the melting assembly. A 20 kw Ajax induction unit permitted rapid heating to 3092° to 3272°F (1700° to 1800°C) in which temperature range all the compositions investigated were liquid.

On heating the unsintered compacts, an exothermic reaction was noted in the range 1472° to 1832°F (800° to 1000°C), due perhaps to a solid-solid reaction between the molybdenum and beryllium. The liquid melt was held at a temperature of 3092° to 3272°F (1700° to 1800°C) for 10 min and then was allowed to cool in the crucible. The solid button readily separated from the crucible with little surface adherence. X-ray powder patterns were made of representative specimens from each melt. Comparison of these patterns with the standards for the two phases B and C showed that the composition corresponding to $MoBe_2$ was identifiable as the molybdenum-rich phase (B). The beryllium-rich phase was found to be $MoBe_{12}$.

Table II. Unit Cell Constants ($MoBe_x$)

	NEPA	Taylor
a_o	4.433A	4.434A
$a_o\sqrt{2}$	3.838	
c_o	7.341A	7.275A
Z	4	4
ρ	6.08	6.13
Density	5.92 g per cc	

Space group D^5_{4h}—C6 mmc.

Crystallographic Investigation

Well developed single crystals of the intermetallic compounds up to one millimeter in size were recovered from aggregates found in the ingots prepared for X-ray identification work. By careful mounting of these single crystals on a two-circle goniometer, oriented specimens were prepared suitable for use with a Weissenberg camera, using Ni-filtered Cu radiation (K_α = 1.5418A) and with a precession X-ray camera. Measurements of the resulting X-ray diffraction patterns made possible the determination of unit cell constants of both intermetallic compounds. The density of single crystals of the relatively heavy $MoBe_2$ was measured by pycnometric methods using toluene. The density of $MoBe_{12}$ was measured using the float or sink method with Clerici solution and subsequently determining pycnometrically the density of the solution in which the crystal neither sinks nor floats.

$MoBe_2$, the molybdenum-rich phase, occurred as parallel growths of tabular hexagonal crystals which showed the purple tinge characteristic of this phase. The unit cell constants determined from the diffraction pattern measurements are compared with values reported by Taylor[3, 4] in Table II.

$MoBe_{12}$, the new beryllium-rich phase occurred as aggregates of prismatic tetragonal crystals. Single crystal measurements yielded the following constants: a_o, 10.27A; $a_o\sqrt{2}$, 14.52; c_o, 4.29A; Z, 4; ρ, 3.13; and density, 3.13 g per cc. Since there were no systematic extinctions, the following space groups were possible: P42m, P4/m, or P42. Considerations of placing the 56 atoms (4 Mo and 52 Be) and of evidence obtained by Laue techniques indicate the space group P42 as being the most probable. The formula ($MoBe_{13}$), was calculated from the unit cell dimensions and the measured density.

Conclusions

1—The existence of the intermetallic compound $MoBe_2$ has been verified. A table of the interplanar spacings of this compound is given.

2—A new intermetallic compound, $MoBe_{12}$, is reported. This differs from other intermetallic compounds of the type MBe_{13} in being tetragonal instead of cubic. A table of the interplanar spacings of this compound is also included.

References

[1] J. W. Mellor: *Comprehensive Treatise on Inorganic and Theoretical Chemistry.* (1931) **11**, p. 522; (1923) **4**, pp. 666, 668. London, Longmans Green & Co.

[2] C. J. Smithells: *Metals Reference Book.* pp. 181 et seq. (1949) New York. Interscience Publishers, Inc.

[3] A. Taylor: *An Introduction to X-ray Metallography.* pp. 375. (1949) New York. John Wiley & Sons.

[4] H. H. Hausner and H. S. Kalish: *Trans.* AIME (1950) **188**, p. 59; JOURNAL OF METALS (January 1950).

[5] N. C. Baenziger and R. E. Rundle: *Acta Cryst.* (1949) **2**, p. 258.

[6] L. Misch: *Metallwirtschaft* (1936) **15**, p. 163.

Thermal Stability of The Chromium, Iron, and Tungsten Borides In Streaming Ammonia And The Existence of a New Tungsten Nitride

by R. Kiessling and Y. H. Liu

The chromium, iron, and tungsten borides have been treated with ammonia at different temperatures. They are attacked, forming metal nitride and boron nitride, and the results are summarized in the tables. In the tungsten-nitrogen system a new phase has been observed, closely related to the known β phase.

THE present investigations were begun to determine whether any ternary phases exist in the transition metal-boron-nitrogen systems for the metals chromium, iron, and tungsten. Attempts to prepare such phases were made by using the borides of the metals as starting materials and ammonia as the nitriding agent. Although no new ternary phases have been found to exist, the results may be of some interest with regard to the technical use of the borides.

General Procedure

A steady stream[9] of dry ammonia was passed through a silica reaction tube, the central part of which was kept at the reaction temperature while its ends were water-cooled. Weighed amounts of the borides were placed in a silica or porcelain boat and heated at different temperatures for a period of 10 to 24 hr. The boat was then rapidly removed from the reaction zone to the quenching zone, the water-cooled end of the tube, by means of a simple magnetic device. The nitrogen content of the products was determined by the increase in weight of the specimens, and the phase analysis was carried out by X-ray methods. For this analysis a Guinier-type camera, constructed at this Institute, was used with a bent, ground quartz crystal monochromator.

The general reaction, which occurred in all the experiments, may be summarized as:

$$\text{metal boride} + \text{nitrogen} \rightarrow \text{boron nitride} + \text{metal nitride}$$

For the higher temperatures pure metal was formed instead of metal nitride. It is sometimes difficult to detect boron nitride among the reaction products by X-ray methods. Prolonged exposures of some specimens showed, however, that the strongest reflections of boron nitride were present. Additional evidence for its presence was given by the increase in weight of the specimens after nitriding. This increase was always greater than that corresponding to nitride formation only and was often in close agreement with the formula given above. Finally, a white powder, which was shown by X-ray methods to be boron nitride, was left if the reaction products after nitriding Fe_2B at 448°C and FeB at 768°C were dissolved in diluted sulphuric acid.

Chromium-Boron-Nitrogen

Five phases have been found to exist in the Cr-B system,[1, 2] and all were used as starting materials. Investigations on the Cr-N system have shown the existence of two nitrides with ideal composition Cr_2N and CrN.[3, 4] The results are summarized in Table I. All the borides are attacked and decomposed into chromium nitride and boron nitride, and the kind of nitride formed depends only on the temperature and not on the boride used as starting material. The lowest reaction temperature, however, is different for the different borides. Thus the δ phase begins to react at about 735°C, the ϵ phase at about 800°, the ζ phase at about 900°, the η phase

R. KIESSLING and Y. H. LIU are associated with the Institute of Chemistry, University of Uppsala, Uppsala, Sweden.

Discussion on this paper, TP 3105E, may be sent, 2 copies, to AIME by Dec. 1, 1951. Manuscript, March 26, 1951. Detroit Meeting, October 1951.

Table I. Phases Present After Nitriding of the Chromium Borides in a Dry Ammonia Stream for 10 Hr. All Specimens Quenched from the Reaction Temperature. The Phases Present after Nitriding Have Been Placed in Order of Decreasing Amount in This and the Following Tables Except for Boron Nitride, which Always Has Been Placed Last.

Temperature, °C	Initial Chromium Boride				
	δ ($\sim Cr_2B$)	ϵ (Cr_2B_2)	ζ (CrB)	η (Cr_3B_4)	θ (CrB_2)
553	Cr_2B	Cr_2B_2	CrB	Cr_3B_4	CrB_2
735	$Cr_2B + CrN + BN$	Cr_2B_2	CrB	Cr_3B_4	
800	$CrN + Cr_2N + BN$	$Cr_2B_2 + (CrN)$	CrB	Cr_3B_4	CrB_2
900		$CrN + Cr_2N + BN$	$CrB + (CrN)$	Cr_3B_4	
954	$CrN + Cr_2N + BN$				CrB_2
1000		$CrN + Cr_2N + BN$	$CrB + CrN + BN$		CrB_2
1050	$CrN + Cr_2N + BN$				
1100			$CrN + Cr_2N + BN$	$CrN + Cr_2B_4 +$ (Cr_2N) + BN	$CrB_2 + CrN$
1180	$Cr_2N + BN$	$Cr_2N + BN$	$Cr_2N + BN$	$Cr_2N + BN$	$Cr_2N + BN$

The lattice parameters found for the nitrides were:
CrN: $a = 4.150$ to 4.145A° (Blix: $a = 4.148$A)
Cr_2N: $a = 4.805$ to 4.786, $c = 4.480$ to 4.463A° (Eriksson: $a = 4.806$ to 4.760A, $c = 4.479$ to 4.438A)

No change in lattice parameters was observed for the borides.

* Depending on temperature.

between 900° and 1000°, and the θ phase at about 1000°C. It is of interest to note that this increase in stability bears a relationship to the crystal structures of the borides. The boron atoms in the δ phase are only in contact with metal atoms, but not with any other boron atoms.* The structure of the ϵ phase is not known; but in the ζ phase the boron atoms form chains; in the η phase, double chains; and in the θ phase, hexagonal nets. The boron atoms thus form an increasing number of boron-boron bonds with increasing boron content of the phases, and the lower temperature limit where reaction occurs also seems to increase with the number of bonds. The dimensions of the chromium nitrides formed during the reactions are very similar to those reported in the literature, Table I. As the radius of boron is considerably greater than that of nitrogen this indicates that the nitrides formed do not contain any boron.

Iron-Boron-Nitrogen

Both the Fe-B[5, 6] and the Fe-N[7, 8] systems have been investigated. The two iron borides, Fe_2B and FeB, were used as starting materials, and the results are summarized in Table II. The lowest temperature at which reaction occurs seems to be lower for Fe_2B (isolated boron atoms) than for FeB (boron chains). The products of the reaction are boron nitride and those iron nitrides which are stable in streaming ammonia at the reaction temperature. Thus the same tendency is shown by the iron borides as by the chromium borides. The borides seem to be more stable if the boron atoms are forming boron-boron bonds than if they are isolated, but the difference is not so marked in this system. The dimensions of the unit cells of the iron nitrides and iron formed in the reactions are in close agreement with those reported in the literature, Table II. Therefore the nitrides formed in this system do not seem to contain any boron either.

Table II. Phases Present after Nitriding of the Iron Borides in a Dry Ammonia Stream for 24 hr. All Specimens Were Quenched from the Reaction Temperature

Temperature, °C	Initial Iron Boride	
	Fe_2B	FeB
352	Fe_2B	FeB
400	$\zeta + BN$	$FeB + \zeta + BN(?)$
448	$\epsilon + BN$	
505	$\epsilon + \gamma' + BN$	
550	$\gamma' + \epsilon + BN$	$\gamma' + \epsilon + BN$
602	$\alpha Fe + \gamma' + \epsilon + BN$	$\gamma' + \epsilon + \alpha Fe + BN$
702	$\alpha Fe + BN$	
768	$\alpha Fe + BN$	$\alpha Fe + BN$

The Greek letters denote the nitrides of iron according to Hägg's notation. The lattice parameters found for the different nitrides were:

ζ: $a = 2.758$, $b = 4.777$, $c = 4.416$ (Jack: $a = 2.763 - 2.761$, $b = 4.828 - 4.830$, $c = 4.425$A)

ϵ: $a = 2.714$ to 2.748, $b = 4.701$ to 4.760, $c = 4.381$ to 4.409* (Jack: $a = 2.764$, $b = 4.787$, $c = 4.420$A)

γ': $a = 3.789$ to 3.795A* (Jack: $a = 3.794$A)

αFe: $a = 2.867$A

No change in lattice parameters was observed for the borides.

* Depending on temperature.

Tungsten-Boron-Nitrogen

The three known tungsten borides[9] were used as starting materials. Investigations on the W-N system[10] have shown the existence of one nitride of probable composition W_2N, called the β phase. The results of nitriding are summarized in Table III. In specimens nitrided between 825° and 875°C, lines of a new phase appeared, which has not been described before. This phase was also found when pure tungsten was nitrided. It was called the γ phase in the W-N system and will be discussed below.

The marked increase in stability of the borides with increasing number of boron-boron bonds, which was noted for the chromium and the iron borides, is not found in this system. All of them begin to be attacked at temperatures between 800° and 900°C. The parameter of the cubic β-tungsten nitride was found to agree with that reported in the literature, indicating that the nitride is free from interstitial boron in the lattice.

γ Phase, Tungsten-Nitrogen

Earlier investigations on the W-N system have shown the existence of one tungsten nitride, slowly formed by nitriding tungsten with ammonia between 700° and 800°C.[10] It has not been possible to obtain this phase, called the β phase and assumed to have the composition W_2N, in a pure state. It

* As a result of a renewed study of the δ phase in the Cr-B system there is reason to suppose that it has the same structure as the δ phase in the Mn-B system, where boron-boron contacts do not appear. In an earlier study,[2] one of the present authors (R. Kiessling) suggested that there is a slight difference between the structures of these two phases. This assumption was based on differences between rotation and Weissenberg photographs which seem to have been caused by twinning of the crystals of the Cr-B phase.

Table III. Phases Present After Nitriding of Tungsten and the Tungsten Borides in a Dry Ammonia Stream for 10 Hr. All Specimens Were Quenched from the Reaction Temperature.

Temperature, °C	Initial Tungsten Boride			
	W	W_2B	"WB"	WB_2
700	$\alpha W + (\beta)$	W_2B	WB	WB_2
750	$\alpha W + \beta$	W_2B	WB	WB_2
800	$\alpha W + \beta$	W_2B	$WB + (W + \beta + BN)$	
825	$\alpha W + \gamma$			
850	$\alpha W + \gamma$	$W_2B + \alpha W + (\gamma + BN)$	$\alpha W + WB + (\gamma + BN)$	$\alpha W + WB_2 + (\gamma + BN)$
875	$\alpha W + \gamma$			
900	αW	$\alpha W + W_2B + BN$	$\alpha W + (WB) + BN$	$\alpha W + (WB_2) + BN$
1000	αW	$\alpha W + (W_2B) + BN$	$\alpha W + BN$	
1100		$\alpha W + BN$	$\alpha W + BN$	$\alpha W + BN$

β and γ denote the known nitride "W_2N" and the new nitride, respectively.
The lattice parameters were found to be:
β : a = 4.128Å (Hägg : a = 4.126Å)
γ : a = 4.130 to 4.122Å*
αW : a = 3.164Å
No change in lattice parameters was observed for the borides.

*Depending on nitriding temperature.

always appears mixed with tungsten. The crystal structure is that of a face-centered cubic metal lattice with four atoms in the unit cell and a parameter of a = 4.126Å. On nitriding tungsten with ammonia at temperatures between 825° and 875°C, the quenched specimens showed lines of a new phase, called the γ phase by the present authors, Tables III and IV. Its lattice is probably closely related to that of the β phase, see below. The γ phase always appeared mixed with tungsten, and it was thus not possible to determine its nitrogen content. It probably has a composition close to that of the β phase (ideal composition W_2N), as the increase in weight of tungsten was about the same when the β phase was formed as when the γ phase was formed (1.6 pct). Some heat treatments were carried out in order to study the thermal stability of the γ phase and the relationship between the β and γ phases. The β phase, formed at 750°C, was transformed to the γ phase on heating in a stream of ammonia at 850°C for 10 hr. The γ phase formed at 850°C was decomposed into tungsten and nitrogen on heating at 900°C in ammonia or in evacuated silica tubes. All attempts to transform the γ to the β phase, however, were unsuccessful. The γ phase was, for instance, heated at 700°, 760°, and 800°C for times up to 36 hr in streaming ammonia or at the same temperatures in evacuated silica tubes for times up to 24 hr, but no change was observed. It is thus impossible to decide from these experiments, whether the γ phase is a high temperature phase which transforms only very slowly to the β phase at lower temperatures, or a stable phase formed with the maximum velocity in streaming ammonia between 825° and 875°C, but the former possibility is the most probable.

X-ray investigations show that the γ phase gives reflections attributable to a simple cubic lattice. The length of the unit cell axis varies between the limits a = 4.130Å at 825°C and a = 4.122Å at 875°C, indicating an extended homogeneity range. All the reflections from a simple cubic lattice were present, but those with unmixed indexes were appreciably stronger than those with mixed indexes. This indicates a close relationship between the face-centered β phase, which only gives reflections with unmixed indexes and an axis of a = 4.126Å, and this new γ phase.

The authors have assumed that the products after nitriding at 825° to 875°C consist of two phases, tungsten and the new γ nitride. There is also a possibility that a mixture of three phases exists, namely tungsten, γ nitride, and β nitride, and that some of the reflections from the β and γ phases coincide. This assumption is not very probable, however, as all the reflections fit exactly into the same quadratic form. In addition, there is no indication of any extended homogeneity range of the β phase which would have to exist if some of the reflections of the β and γ phases were always to coincide. All the reflections from the nitride formed between 825° and 875°C therefore have been assumed to belong to one phase alone, the new γ phase.

The new reflections are much too strong to be considered as due only to an ordered distribution of the nitrogen atoms of the β phase. Consequently, the metal lattice must be deformed so that the face-centering disappears. Such a deformation may be caused by an ordering of the nitrogen atoms or by a change in the nitrogen content. The γ phase thus might be regarded as analogous to the β phase in the Mo-N[10] and the δ phase in the Mn-N[11] systems. They are both high temperature phases, closely related to the face-centered cubic phases in the Mo-N (γ) and Mn-N (ϵ) systems, respectively, and are formed by a tetragonal deformation of the face-centered metal lattices.

An attempt to determine the crystal structure of

Table IV. Tungsten-Nitrogen System. Powder Diffraction Lines of the γ Phase Quenched from 875°C. Cu-K_α Radiation.

I	$\sin^2\theta$	a = 4.122 hkl	a = 16.488 hkl	I	$\sin^2\theta$	a = 4.122 hkl	a = 16.488 hkl
w	0350	100	200	w	4540	320	640
w	0706	110	220	m	4736	αW	
s	1050	111	222	w–	4898	321	642
s	1190	αW		w	5579	400	800
s	1395	200	400	s*	5922	αW	
w	1750	210	420	w–	6291	330	822 660
w	2097	211	422	m	6624	331	662
s	2374	αW		m	6973	420	840
m	2783	220	440	m	7114	αW	
w	3134	300	600 442	s	8295	αW	
				w–	8347	422	844
w	3489	310	620	w	8720	500	1000 860
s	3552	αW					
m	3825	311	622	w–	9078	510	1020 862
w	4186	222	444	w	9417	333	1022 666

w, weak; s, strong; m, medium.
* 410 (resp. 820 + 644) coincide with 310 from α-tungsten.

Table V. γ Phase, Quenched from 875°C.

Structure factor values for the limits of the parameter (x) in 4: (e), space group $P23$ or $P\bar{4}3m$ for some reflections.

hkl	A^2 for x =			I, Obs.
	0.23	0.25	0.27	
100	0.24	0	0.24	50
110	0.004	0	0.004	50
200	15.3	16	15.3	250

the new phase was not successful. If it is assumed to have four tungsten atoms per unit cell, which is very probable because of the close correspondence in dimensions between the β and γ phase, and a simple cubic lattice, only the space groups $Pm3$, $P23$, $Pm3m$, $P43$, and $P\bar{4}3m$ are possible. Four metal atoms forming a noncentered lattice can only be placed in these space groups in the fourfold positions 4: (e) in $P23$ and $P\bar{4}3m$. They both give the same arrangement with the coordinates xxx; $\bar{x}\bar{x}x$; $\bar{x}x\bar{x}$; $x\bar{x}\bar{x}$. For $x = \frac{1}{4}$ a face-centered lattice is obtained, and from space considerations ($r_a > 1.34$) it is easily seen that the limits for the parameter are $0.23 < x < 0.27$. A study of the structure factors shows that this arrangement is not in agreement with the observed intensities, Table V. The possibility of a cubic unit cell with an axis of $a_1 = 2a$ or $a_1 = 3a$ must be excluded as some observed lines then correspond to numbers in the quadratic form which are not sums of squares of integers (28 in the former case, 15, 39, and 60 in the latter). A unit cell with an axis of $a_1 = 4a$ is again possible, however, and the indexes of this bigger cell are also given in Table IV. The probable space groups for this cell are $Fm3c$, $F\bar{4}3c$, $Fm3$, and $F23$. The structure of the metal lattice must be closely related to that formed by 64 face-centered cubic cells, each with $a = 4.130$ to 4.122Å and four metal atoms per unit cell. It is possible to place 256 atoms in positions corresponding to such a structure in the space groups mentioned, but the task of varying the parameters in a systematic way to obtain a deformed structure giving the observed intensities is too difficult when only powder data are available.

The symmetry might also be tetragonal or still lower. No indication of splitting up the reflections was observed, however, and thus the ratio c/a must be equal or nearly equal to an integer. This case, although possible, is not very plausible.

The possibilities of a defect lattice with missing tungsten atoms or a lattice where tungsten atoms are replaced by nitrogen atoms are not conceivable.

Summing up the different possibilities discussed, the most probable, in the opinion of the authors, is a cubic cell containing 256 tungsten atoms with positions nearly corresponding to a cubic close-packing.

Discussion

The present results indicate that the formation of boron nitride is a deceivable factor in the reaction:

$$\text{metal boride} + \text{nitrogen} \rightarrow \text{metal nitride} + \text{boron nitride}$$

Boron nitride is a very stable compound with a high melting point. Its lattice is similar to that of graphite, consisting of hexagonal nets where each boron atom within a net is in contact with three nitrogen atoms and each nitrogen atom with three boron atoms. A B-N pair has the same number of electrons as two carbon atoms and the nets are probably formed by strong resonating B-N bonds. The fact that the stability of the chromium and iron borides in ammonia increases with increasing number of boron-boron contacts is of interest and supports the assumption that strong boron-boron bonds exist in the higher borides.

It is also of interest to note that the δ phase in the Cr-B system is attacked at a considerably higher temperature than Fe_2B, and that the ζ phase in the Cr-B system is more stable against attack than FeB. Although δ Cr-B and Fe_2B, as well as ζ Cr-B and FeB, are not isomorphous, their structures are closely related and the results consequently support the view that the strength of the metal-boron bond decreases with increasing atomic number of the transition element in the same period. This decrease has also been noted for the metal-hydrogen, metal-carbon, and metal-nitrogen bonds. The stability of hydrides, carbides, and nitrides decreases with increasing atomic number of the transition element in a period.

Summary

The borides of chromium, iron, and tungsten have been treated with ammonia at different temperatures. They are all attacked and form metal nitride and boron nitride. For the chromium and iron borides, the stability in ammonia increases with increasing boron content, which supports the view that strong boron-boron bonds exist in the higher borides.

In the W-N system a new phase (γ) has been observed. It is formed at nitriding temperatures between 825° and 875°C and is probably closely related to the already known β phase. All the reflections observed may be interpreted assuming a cubic cell with $a = 4.130$ to 4.122Å (depending on nitriding temperature) and containing 4 tungsten atoms. There are reasons to assume that the real unit cell of this phase is cubic and contains 256 tungsten atoms (cube edge = $4a$) in positions nearly corresponding to a cubic close-packing.

The investigations also support the view that the strength of the metal-boron bond decreases with increasing atomic number of the transition metal in the same period.

Acknowledgment

The authors wish to thank Professor G. Hägg for valuable discussions. They also wish to thank S. Wahlgren for technical assistance. The investigation has been supported by a grant from the Swedish State Council of Technical Research, which is gratefully acknowledged.

References

[1] R. Kiessling: *Acta Chem. Scand.* (1949) **3**, p. 595.
[2] L. H. Andersson and R. Kiessling: *Ibid.* (1950) **4**, p. 160.
[3] R. Blix: *Ztsch. Physik. Chem.* (1929) **3B**, p. 229.
[4] S. Eriksson: *Jernkontorets Ann.* (1934) p. 530.
[5] T. Bjurström: *Arkiv Kemi, Mineral. Geol.* (1933) **11A**, nr. 5.
[6] G. Hägg: *Ztsch. Physik. Chem.* (1930) **11B**, p. 152.
[7] G. Hägg: *Nova Acta Regiae Soc. Sci. Upsaliensis* (1929) [4] **7** (1).
[8] K. H. Jack: *Proc.* Royal Soc. (London) (1948) **195A**, p. 34.
[9] R. Kiessling: *Acta Chem. Scand.* (1947) **1**, p. 893.
[10] G. Hägg: *Ztsch. Physik. Chem.* (1930) **7B**, p. 339.
[11] G. Hägg: *Ibid.* (1929) **4B**, p. 346.

Effect of Alloying Elements on the Elevated Temperature Plastic Properties of Alpha Solid Solutions of Aluminum

by O. D. Sherby, R. A. Anderson, and J. E. Dorn

Solid solution alloying increases the plastic properties of aluminum at elevated temperatures by solid solution strengthening, by restraining recovery and recrystallization, and by a Cottrell effect. When binary aluminum alloys are strained and aged at 194° to 300°K they develop a yield point. This is attributed to a migration of dislocations to solute atoms during aging.

IN view of the ever expanding interest in applications of metals and alloys to high temperature service conditions, it becomes increasingly important to be cognizant of the effect of various metallurgical factors on the strength of alloys at elevated temperatures. One problem of wide interest, not only because of its engineering significance but also due to its fundamental scientific importance, is the elucidation of the effect of alloying elements on the plastic properties of homogeneous α solid solutions at elevated temperatures. It is indeed astonishing to note that in spite of its importance, and in spite of extensive random testing of alloys at elevated temperatures, no systematic investigation has been reported yet on the effect of alloying additions on the plastic properties of α solid solutions at elevated temperatures. This deficiency in our knowledge prompted the investigation described in this report.

Rather extensive data are currently available on the effect of alloying elements on the plastic properties of α solid solutions at atmospheric and subatmospheric temperatures. Such data might be extrapolated to higher temperatures and reasonable guesses might be made regarding the influence of such factors as recovery and recrystallization in order to hazard a qualitative estimate of the effect of alloying elements on the plastic properties of α solid solutions at elevated temperatures. Such

O. D. SHERBY, Junior Member AIME, and R. A. ANDERSON are Research Engineers, and J. E. DORN, Member AIME, is Professor of Physical Metallurgy, University of California, Berkeley.

Discussion on this paper, TP 3102E, may be sent, 2 copies, to AIME by Dec. 1, 1951. Manuscript, March 7, 1951. Detroit Meeting, October 1951.

Table I. Chemical Analyses and Grain Size of Alloys

Alloying Element	Atomic Pct	Grain Size Diam. mm	Chemical Analyses (Wt Pct Impurities) Si	Fe	Cu	Mg	Mn
Al	0	0.21	0.003	0.003	0.006	0.001	
Mg	0.554	0.25	0.003	0.003	0.007		
	1.097	0.28	0.004	0.004	0.007		
	1.617	0.26	0.003	0.004	0.008		
	3.228	0.27	0.003	0.004	0.007		
Cu	0.029	0.29	0.003	0.004		0.0006	0.001
	0.054	0.29	0.003	0.004		0.0007	0.001
	0.101	0.29	0.003	0.003		0.0006	0.001
	0.233	0.30	0.003	0.004		0.0006	0.001
Zn	0.211	0.36	0.004	0.004	0.006	0.001	
	0.402	0.27	0.004	0.005	0.006	0.001	
	0.755	0.26	0.004	0.005	0.006	0.001	
	1.616	0.26	0.003	0.005	0.007	0.001	
Ge	0.015	0.27	0.004	0.004	0.006	0.001	
	0.033	0.26	0.004	0.004	0.006	0.001	
	0.082	0.27	0.003	0.005	0.007	0.001	
	0.145	0.26	0.003	0.006	0.007	0.001	
Ag	0.025	0.31	0.003	0.005	0.006	0.001	
	0.053	0.29	0.003	0.005	0.006	0.001	

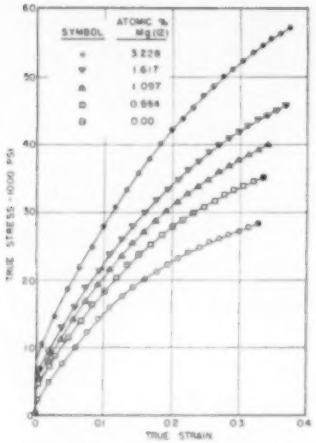

Fig. 1—Effect of magnesium on the work hardening of aluminum at 78°K.

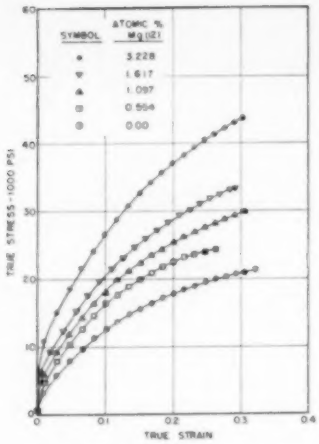

Fig. 2—Effect of magnesium on the work hardening of aluminum at 116°K.

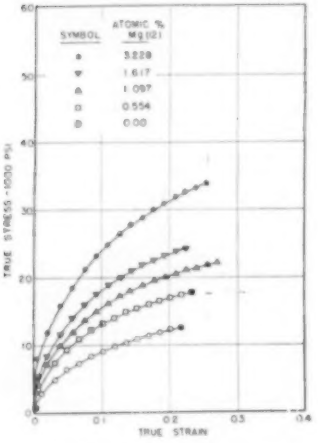

Fig. 3—Effect of magnesium on the work hardening of aluminum at 194°K.

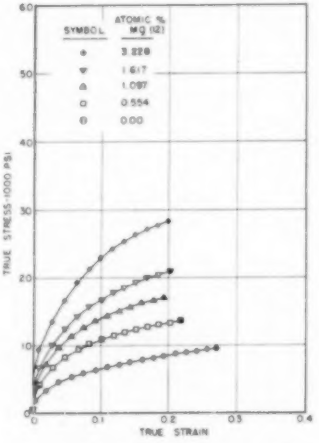

Fig. 4—Effect of magnesium on the work hardening of aluminum at 293°K.

guesses would indicate the recognized factors of importance in the plastic properties of homogeneous alloys at elevated temperatures and would prescribe the interesting variables to be considered in studying the problem more thoroughly. If such guesses prove to be fairly accurate the need for detailed research on the elevated temperature plastic properties will be much reduced.

It is quite possible, however, that other factors, not so widely recognized, may also prove to be important in affecting the elevated temperature plastic properties of alloys. The following investigation was therefore undertaken in order to evaluate more completely the effect of various factors on the solid solution strengthening of alloys at elevated temperatures. Aluminum was selected as the solvent in view of the extensive correlatable data now available on its plastic properties at low temperatures.[1] The general principles uncovered in this investigation, however, are probably applicable to other systems using higher melting solvents.

Materials and Method

The compositions and grain sizes of the alloys used in this investigation are given in Table I. Each alloy was homogenized, cold rolled, and then recrystallized to give about the same grain size. The details of these treatments are recorded in a previous publication.[1]

The tensile stress-strain curves for the alloys at elevated temperatures were obtained by means of equipment that has been described in the literature.[1] Strains were determined to a precision of better than ±0.001 and the stresses were measured to an accuracy of about ±25 psi. All tests, except where otherwise specified, were conducted at an average strain rate of about 0.118 per min.

Elevated temperatures were obtained by placing

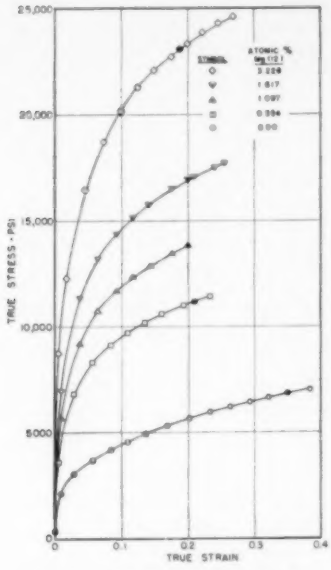

Fig. 5—Effect of magnesium on the work hardening of aluminum at 422°K.

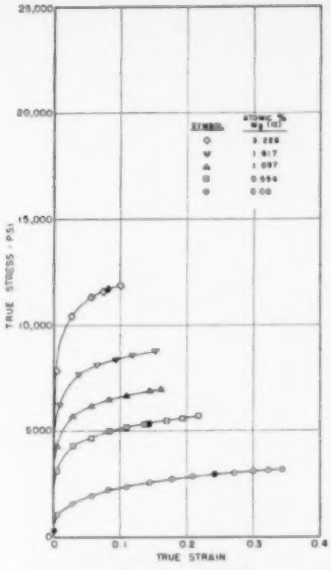

Fig. 6—Effect of magnesium on the work hardening of aluminum at 550°K.

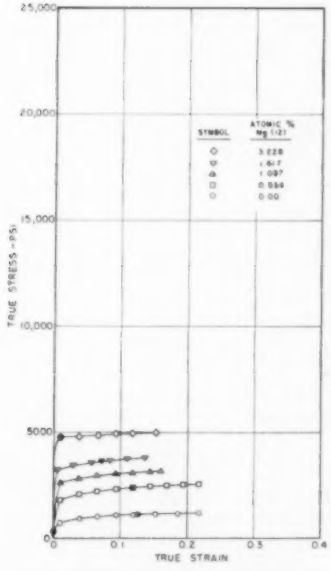

Fig. 7—Effect of magnesium on the work hardening of aluminum at 650°K.

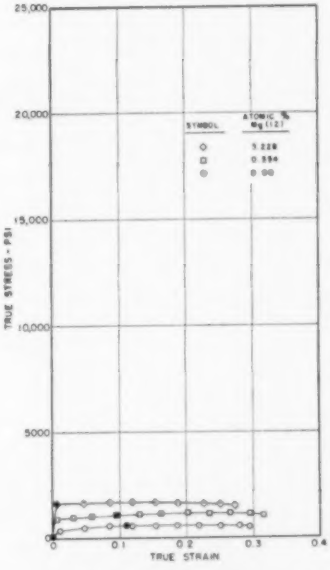

Fig. 8—Effect of magnesium on the work hardening of aluminum at 750°K.

a three element electric resistance furnace about the specimen. The upper, central, and lower zones of the furnace were each controlled independently by means of three commercial indicating controllers. A stainless steel liner 2½ in. in diam and 15 in. long was inserted in the center of the furnace in order to further assure rather uniform temperature over the length of the specimen. Temperatures at three points along the 2-in. gage section of the specimen were measured during the test with iron constantan thermocouples bound to the specimen by means of flexible glass cord. Variations of temperature along

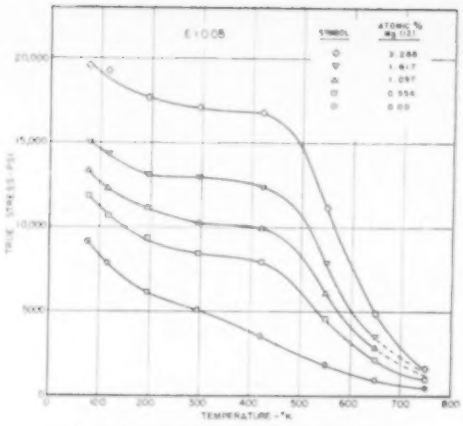

Fig. 9—Effect of test temperature on the flow stress of Al-Mg alloys for a true strain of 0.05.

the length of the specimen were held to less than ±1°C during any one test.

Experimental Results

The most pronounced effects of alloying additions on the elevated temperature tensile properties of α solid solutions in aluminum were exhibited by the Al-Mg series of alloys. The true stress-true strain curves for these alloys over the range from 78° to 750°K are given in Figs. 1 to 8.

The point at which the maximum load was observed is shown by the solid symbol on each curve. At the lower temperatures of 78° to 298°K, specimens of all of the alloys began to develop a neck at this point. At the higher temperatures of 422°K and above, however, necking did not occur when the maximum load was reached. Consequently, the true stress-true strain curves at 422°K and above were obtainable beyond the point of maximum load.

The stress-strain curves given in Figs. 1 to 8 reveal that the effect of alloying additions on the plastic properties of α solid solutions is dependent on the temperature of testing. At temperatures of about 298°K and below, magnesium additions result in appreciably higher stress-strain curves than those obtained for the pure aluminum. At the highest test temperature of 750°K, the alloying additions of magnesium had only a minor effect on the plastic properties of aluminum. The greatest effect of alloying is clearly seen to occur in the intermediate ranges of temperature from about 298° to about 422°K for the Al-Mg series of alloys. Similar trends also were observed for the remainder of the alloys that were investigated.

The temperature dependence of alloy strengthening upon additions of magnesium to aluminum is revealed more effectively in Fig. 9. In this diagram the flow stress at a fixed strain of $\epsilon = 0.05$ is plotted as a function of the temperature for each magnesium alloy of the series, including pure aluminum. The strengthening of aluminum due to additions of magnesium is quite substantial over the range from 78° to 298°K. At 700°K, however, the strengthening due to magnesium additions is small and becomes negligible at about 750°K. The maximum effect of alloying additions on the strengthening of aluminum, however, occurs over an intermediate range of temperatures from about 300°K to about 425°K.

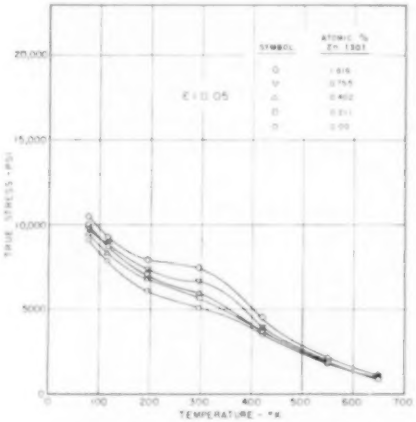

Fig. 11—Effect of test temperature on the flow stress of Al-Zn alloys for a true strain of 0.05.

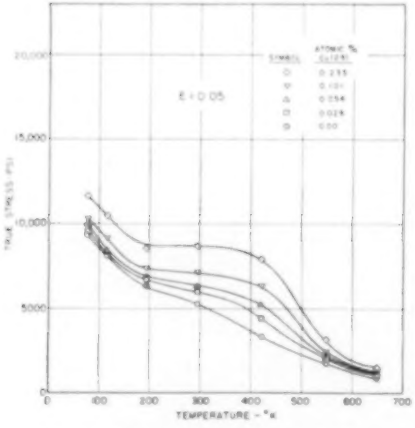

Fig. 10—Effect of test temperature on the flow stress of Al-Cu alloys for a true strain of 0.05.

Similar data for the remainder of the alloys are given in Figs. 10 to 13. Although all of the alloys showed similar trends, the effects were much less pronounced than those of the magnesium series.

Discussion of Results

The data reported under Experimental Results reveal that the strengthening of aluminum due to alloying additions is dependent on the test temperature. Apparently many factors contribute to this dependency and it will prove interesting to attempt to identify the most important ones.

Consider first the range of temperatures from that of liquid nitrogen (78°K) to that at which recovery first appears to have a significant effect on the tensile stress-strain curve (about 300°K for

pure aluminum.) In this range of temperatures the plastic properties of alloys are probably ascribable to two factors. The first consists of the increase in the initial flow stress due to alloying. This will be represented by $\Delta\sigma_s$, the solid solution strengthening, which is equal to $(\sigma_{alloy} - \sigma_{Al})_{\epsilon=0}$, the flow stress of the alloy minus that for pure aluminum, where both are measured at the same temperature and at infinitesimally small plastic strains. At greater strains, however, a second factor, namely the difference in strain hardening of the alloy and pure aluminum, enters the analysis. As shown in Figs. 1 to 4, alloying elements not only increase the initial flow stress but they also induce greater rates of strengthening with strain resulting in higher slopes of the stress-strain curves of the alloys than of pure aluminum when the curves are compared at the same temperature and strain. Thus at some given plastic strain larger than zero, the improvement in the plastic flow stress upon alloying $(\sigma_{alloy} - \sigma_{Al})_\epsilon$ is due to the increase in the initial flow stress resulting from

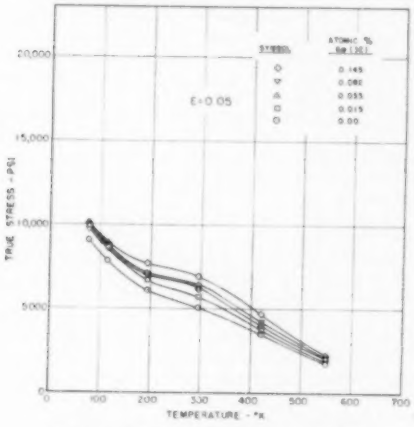

Fig. 12—Effect of test temperature on the flow stress of Al-Ge alloys for a true strain of 0.05.

solution strengthening $\Delta\sigma_s$, plus the increase in the flow stress of the alloy over and above the increase in the flow stress of pure aluminum upon strain hardening, namely $\Delta\sigma_\epsilon$.

A preliminary guess based on the hypothesis of dislocations can be made as to how $\Delta\sigma_s$ varies with temperature. Solid solution strengthening is visualized as arising from the interaction forces between a dislocation and the solute atoms in the alloy. A major part of the interaction force is attributable to the internal stress fields surrounding the dislocation and the solute atoms. It also appears that part of the interaction force might have an electronic origin as revealed by the fact that solid solution hardening is dependent not only on the local lattice strains induced by the solute atoms but also on the difference in valence of the solute and solvent atoms.[1] Cottrell[2,3] has shown that the interaction force arising from the elastic strain energy interaction of a dislocation and a solute atom is proportional to the shear modulus of elasticity according to the relationship:

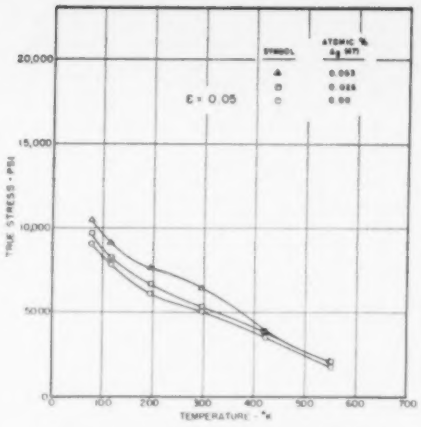

Fig. 13—Effect of test temperature on the flow stress of Al-Ag alloys for a true strain of 0.05.

$$F = \frac{4}{3}\,\frac{(1+\nu)}{(1-\nu)}\,\frac{G\epsilon r^3\lambda}{R^2} \qquad [1]$$

where, G is the shear modulus of elasticity; ν, Poisson's ratio; r, the atomic radius of the solvent; ϵ the local lattice strain due to the introduction of the solute atom; R, the distance between a solute atom and a dislocation; and λ, the strength of the dislocation (shear displacement when a unit dislocation traverses the crystal).

Cottrell's equation is admittedly an approximation to the facts, insofar as it is invalid for values of R approaching atomic dimensions and also because it is based on the interaction between a single solute atom and a single dislocation, whereas it is widely applied to solid solutions containing many atoms and dislocations. On the other hand, it probably gives a satisfactory qualitative, though distorted, picture of the facts.

In a pure metal R is infinite and F is zero. As alloying elements are added, however, the average value of R between the solute atoms and the dislocations decreases giving significant interaction forces F. If the alloy and the pure metal contain

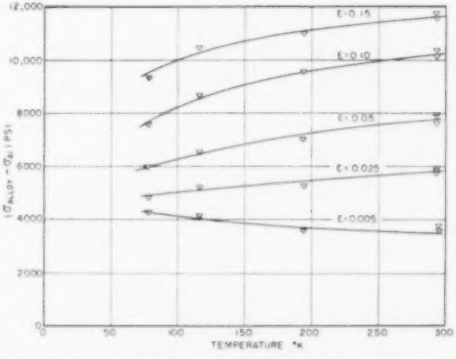

Fig. 14—Effect of strain and temperature on the increase in flow stress upon alloying aluminum with 1.618 atomic pct Mg.

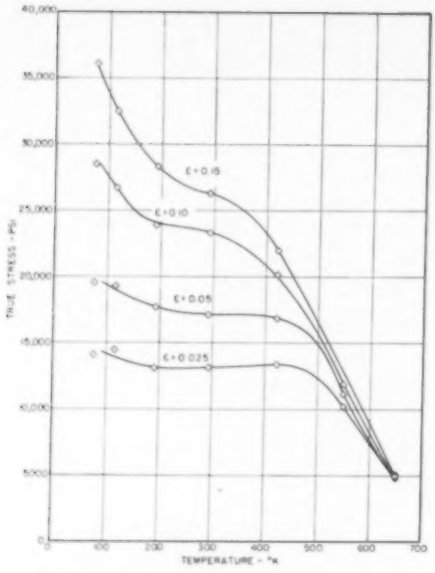

Fig. 15—Effect of test temperature on the flow stress of 3.2 pct Mg in aluminum alloy for various strains.

about the same density and distribution of dislocations, the increase in the initial flow stress upon alloying, $\Delta\sigma_i$, is primarily ascribable to the increase in F upon alloying. At higher test temperatures, however, F decreases because the shear modulus G decreases with increase in temperature. Consequently, $\Delta\sigma_i$ should decrease with increasing temperature. This deduction is in part confirmed by the data shown in Fig. 14 for $(\sigma_{\text{alloy}} - \sigma_{Al})_\epsilon$ at $\epsilon = 0.005$. At such small strains $\Delta\sigma_i$ is small and, therefore, $\Delta\sigma_i \cong (\sigma_{\text{alloy}} - \sigma_{Al})$. The decrease in $(\sigma_{\text{alloy}} - \sigma_{Al})_\epsilon$ for $\epsilon = 0.005$ with increasing temperatures therefore suggests that $\Delta\sigma_i$ decreases with increasing temperatures. Confirmation that $\Delta\sigma_i$ is small at elevated temperatures is shown in Figs. 9 to 13. At the highest test temperatures where the alloys and pure aluminum recover extremely rapidly during the test, the flow strength of the alloys is not significantly greater than that for pure aluminum. These data strongly suggest that a solid solution alloying is not particularly effective in improving the strength characteristics of a metal for application at temperatures well above the recovery temperature of the alloy. Other methods of strengthening, such as the introduction of intermediate phases, may prove more useful for strengthening in this range of temperatures.

The strain hardening of metals is commonly ascribed to the interaction forces between dislocations. Since alloying additions promote greater rates of strain hardening, it is consistent to assume that this is due to the more rapid accumulation of dislocations in the alloy than in the pure metal. The data of Figs. 1 to 8 reveal that the rate of strain hardening of aluminum and its α solid solutions decreases with increasing temperatures, suggesting that the rate of accumulation of dislocations is less at the higher temperatures. The data of Fig. 14 show that $(\sigma_{\text{alloy}} - \sigma_{Al}) = \Delta\sigma_i + \Delta\sigma_s$ increases for strains above 0.025 with increasing temperatures. Since $\Delta\sigma_i$ decreases with increasing temperatures, $\Delta\sigma_s$ must, therefore, increase with increasing temperatures. This suggests that the accumulation of dislocations upon straining decreases less rapidly with increase in temperature in the alloys than in pure aluminum. The detailed explanation of these observations is not yet clear to the authors. The practical significance of the observations, however, is obvious. Alloying additions primarily influence $\Delta\sigma_i$ at low temperatures, whereas they primarily influence $\Delta\sigma_s$ at high temperatures within the range where recovery is negligible. In fact, if an extrapolation of the data of Fig. 14 to 0°K be attempted, it appears as if the curves for various strains will coincide at about 4800 psi, suggesting that alloys of aluminum will strain harden no more rapidly than pure aluminum at the absolute zero temperature. At this temperature the flow stress of 1.62 atomic pct Mg alloy will exceed that for pure aluminum by about 4800 psi for all strains, whereas, at 300°K and a strain of 0.15, the flow stress for the same alloy will exceed that for pure aluminum by about 11,700 psi. Since the flow stress for aluminum decreases rapidly with an increase in temperature, these differences become yet more pronounced when they are based on a percentage basis.

Previous investigations have shown that pure aluminum begins to exhibit rapid recovery at just about 300°K.[4] The data shown in Figs. 9 to 13 reveal that the stress-temperature curves of aluminum for a strain of 0.05 drops slightly in this range, indicative that recovery is occurring during the test. Presumably the rapid decrease in the flow stress with increasing temperature shown for the Al-Mg alloys in Fig. 9 at about 425°K is also indicative of rapid recovery during the test. Further evidence of this contention is revealed by the data recorded in Fig. 15, where it is noted that the temperature at which the flow stress first begins to decrease with increasing temperature is displaced to lower temperatures for the higher strains. Obviously for the strain rate employed in these tests, the 3.2 pct Mg alloy had recovered to the same flow stress for all recorded strains at about 650°K.

The remainder of the alloys also exhibit the same general trends of a rapid decrease in the flow stress

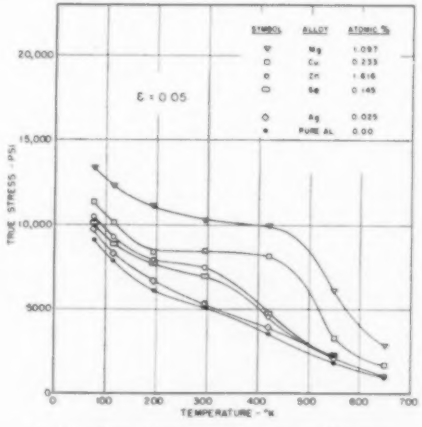

Fig. 16—Effect of test temperature on the flow stress of various aluminum alloys for a true strain of 0.05.

with increasing temperature in the recovery range of temperatures. The temperature at which the rapid decrease in flow stress first occurs appears to be practically independent of the concentration of the alloying elements in any one series of alloys as revealed in Figs. 9 to 13. On the other hand, as shown in Fig. 16, the temperature at which a rapid decrease in flow stress occurs with increasing temperature is sensitive to the particular alloying element that is present. In this respect the various alloying elements appear to have a unique effect on the plastic properties at elevated temperatures.

The effect of alloying elements on the plastic properties of aluminum alloys is particularly interesting over the intermediate range of temperatures from about 300° to 425°K. In this range the stress-temperature curves exhibit a plateau and, as shown in Fig. 15 for a strain of 0.025, in some instances actually reveal a hump. These data appear to suggest that the alloys are undergoing precipitation hardening over this intermediate range of temperatures in spite of the precautions exercised in selecting the compositions to be below the solubility limit at about 100°C as given by the best data currently available. Errors in extrapolation of the solubility data to atmospheric temperature could have been made, so that the highest composition of each alloy series might have exceeded the solubility limit. But it is quite inconceivable that the lowest compositions, which revealed identical trends, were also supersaturated. Nevertheless tests were made to ascertain whether precipitation had occurred. In view of the possible insensitivity of lattice parameter data and microscopic methods of detection, mechanical tests were considered to be more sensitive indexes of precipitation.

The planned test consisted of prestraining an alloy about 0.05 at 194°K, unloading, and then aging for 5 min at successively higher temperatures, following which the specimen was again to be mechanically tested at 194°K. It was anticipated that if precipitation were responsible for the observed plateaus in the stress-temperature diagrams of the alloys, the stress-strain curve at 194°K, following a prestrain and an aging treatment at some appropriate temperature, would lie above the stress-strain curve for the same alloy when the test had not been interrupted for aging.

The various stress-strain curves that were obtained on the 3.2 pct Mg alloy are recorded in Fig. 17. Curve *A* reveals that 5 min of aging at 194°K, following a prestrain at 194°K, had practically no effect on the stress-strain curve at 194°K. After aging for 5 min at 250°K, however, a distinct yield point was observed. This yield point became very pronounced following aging at about 295°K. But the yield-point effect was transient since after the yield phenomenon, the stress-strain curve of the aged material again coincided with that for unaged specimens at the same total strain. Thus, it was assumed that no real precipitation had occurred. After aging for 5 min at 371°K, however, the yield-point effect was reduced and the stress-strain curve after yielding fell below that for the unaged alloy, indicating that recovery had occurred during aging at this elevated temperature.

The absence of evidence for real precipitation and the introduction of a yield point upon appropriate aging suggested a strong parallelism between these data and that obtained upon the strain aging of steels.[2,3,5] It was, therefore, considered possible that during aging the solute atoms might have migrated toward the dislocations under the interaction forces described by Cottrell, solutes larger than the solvent diffusing toward the expanded half of the dislocations and solutes smaller than the solvent diffusing toward the contracted regions of the dislocations. The interaction forces between the dislocations and the atmosphere of solute atoms which concentrated in its environs during aging would then be higher than in the homogeneous α solid solution. Consequently, a higher than normal stress would be required to cause the dislocations to move after appropriate aging treatments. But once the dislocations have been displaced from their atmospheres, they again move in a more or less homogeneous dispersion of solute atoms and the flow stress again reduces to the usual value obtained for the unaged material at the same total strain.

One major difficulty with the above explanation of the strain-aging phenomenon centers about the small rates of diffusion of the solute atoms at the aging temperature. This will be discussed later. On the other hand, a Cottrell effect of this type could serve to explain the observed plateau in the stress-temperature diagrams even in the absence of precipitation. For example, at low temperatures the solute atoms cannot diffuse sufficiently rapidly to migrate with the dislocations. The increase in the flow stress of the alloy over that for the pure aluminum is then attributable primarily to the solution strengthening, $\Delta\sigma_s$, resulting from the interaction forces between the dislocations and the randomly dispersed solute atoms plus the effect of the increased rate of strain hardening $\Delta\sigma_s$, that occurs in the alloy. Although the second factor increases with

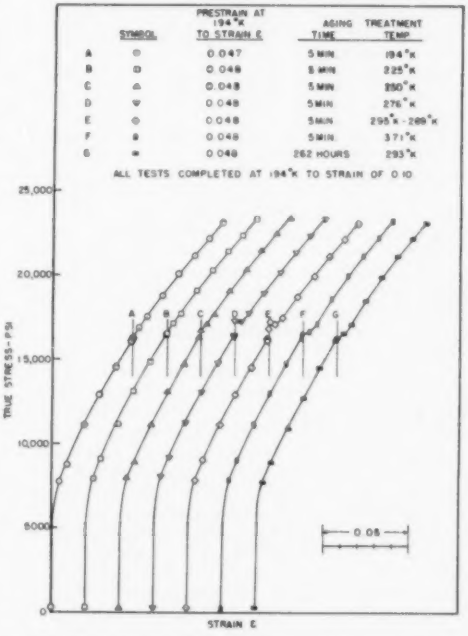

Fig. 17—Effect of strain-aging treatments on the true stress-true strain curve of 3.2 atomic pct Mg in aluminum alloy at 194°K.

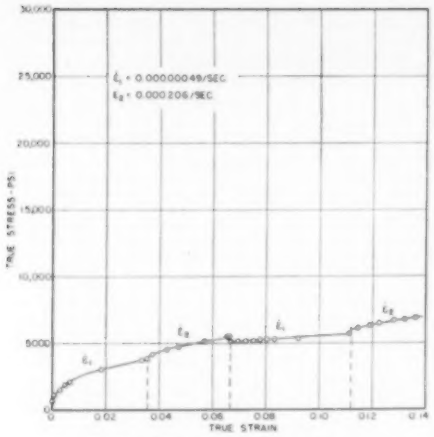

Fig. 18—Effect of strain rate on work hardening of pure aluminum at 295°K.

increasing temperatures, the first factor decreases with increasing temperatures. As higher test temperatures are used, the diffusivity of the solute atoms increases and finally reaches a value which permits their migration with the dislocation under the interaction forces that exist. When this occurs, the flow stress must be sufficiently great to continuously exceed the additional interaction forces between the dislocations and their atmospheres. Consequently, over some range of temperatures, the flow stress will decrease less rapidly than normal, leading to a plateau in the stress-temperature diagram which will be terminated at higher temperatures where rapid recovery occurs. Thus, the increase in the flow stress at high temperatures upon alloying is the increase in the flow stress due not only to the dislocations moving through a solid solution, $\Delta\sigma_s + \Delta\sigma_i$, but also to the increase in flow stress $\Delta\sigma_s$ due to the fact that the solute atoms can migrate with the dislocation.

A critical experimental check on the above-outlined proposal for the cause of the plateau in the stress-temperature diagram is easily obtained. In general, an increase in strain rate causes an increase in the flow stress as shown in Fig. 18 for pure aluminum at 295°K. If the plateau that is obtained in the stress-temperature diagram is ascribable to a Cottrell effect, it follows that over the lower temperature range of the plateau, the atoms have just sufficient diffusivity to migrate with the dislocations. If either the temperature were reduced or the strain rate were increased, the solute atoms could no longer keep up with the moving dislocations. At a low strain rate at this critical temperature, for example, the solute atoms would migrate with the dislocations causing the increase in flow stress due to alloying to be $\Delta\sigma_s + \Delta\sigma_i + \Delta\sigma_s$, whereas at the higher strain rates the solute atoms could no longer diffuse with the dislocations, and, consequently, the increase in flow stress due to alloying would be only $\Delta\sigma_s + \Delta\sigma_i + \Delta\sigma_i'$, where $\Delta\sigma_i'$ is the increase in the flow stress due to an increase in strain rate. Thus, an increase in strain rate, at some appropriate temperature, might result in a decrease in the flow stress, if $\Delta\sigma_s$ is greater than the strain rate effect $\Delta\sigma_i'$. Since this is contrary to the usual effect of strain rate on the flow stress, it serves as a critical evaluation of the hypothesis. As shown in Fig. 19 the 3.2 atomic pct Mg alloy experiences a decrease in flow stress at 295°K with an increase in strain rate as predicted by a Cottrell effect. The large number of overlapping points on the fast strain rate curve are due to the fact that the load increased in a step-like manner for the given constant strain rate employed. Maximum and minimum load readings were observed and plotted in the figure. This occurrence is very similar to the process of deformation observed in aluminum alloys by McReynolds[6] and also Lubahn.[7]

Additional evidence that favors the hypothesis that the observed plateaus in the stress-temperature diagrams of the various aluminum alloys is attributable to a Cottrell effect might be obtained by calculating the density of the edge dislocations per square centimeter of the face of a unit cube of the alloy. If ρ is the density of the active edge-type dislocations per square centimeter of a unit cube of the alloy, the shear strain rate is:

$$\frac{\dot{\epsilon}}{2} = \lambda v \rho \qquad [2]$$

where, $\dot{\epsilon}$ is the tensile strain rate; v, the average velocity of the dislocations; and λ, the shear displacement per dislocation.

When the solute atoms diffuse just fast enough to keep up with the moving dislocations, the stream velocity of diffusion is just equal to the velocity v of the dislocations. It is possible, of course, that a Cottrell effect might also be noted when the velocity of streaming of the atoms is yet slightly below the mean velocity of the moving dislocations. This would give a slightly higher flow stress than in the complete absence of streaming, because many dislocations would carry the solute atoms with them over short distances. Thus, the critical velocity v of the motion of the dislocations for a Cottrell effect might be slightly larger than the streaming velocity of the solute atoms v' under the interaction energy between the solute atoms and the dislocations. Cottrell assumed that the streaming velocity v' is given by the Einstein equation:

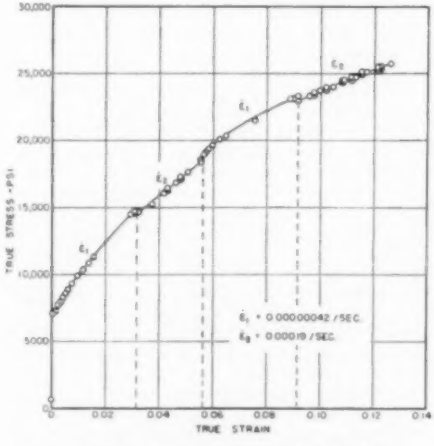

Fig. 19—Effect of strain rate on work hardening of 3.2 atomic pct Mg in aluminum alloy at 295°K.

$$v' = \frac{D}{kT} F \qquad [3]$$

where, D is the diffusivity of the solute atoms; k, Boltzmann's constant; T, the absolute temperature; and F, the interaction energy between an atom and a dislocation (eq 1).

If v' approaches the order of magnitude of v, a Cottrell effect will be observed, and under these conditions:

$$\rho = \frac{\dot{\epsilon}}{2\lambda v'} = \frac{\dot{\epsilon} kT}{2\lambda DF} \qquad [4]$$

The following data might be taken to estimate the value of F given in eq 1:

$G = 2.65 \times 10^{11}$ dynes per sq cm
$\nu = 0.33$
$r = 1.43 \times 10^{-8}$ cm
$\lambda = 2.86 \times 10^{-8}$ cm
$\epsilon = 0.09$
$R = 5 \times 10^{-8}$ cm.

The value of ϵ was estimated from the change in lattice parameter from 4.0413A to 4.0449A upon the addition of 1 atomic pct Mg to aluminum. Then $\epsilon = \frac{100\,\Delta a}{a} = \frac{0.0036 \times 100}{4.04} = 0.09$. The value of R was estimated by assuming a random distribution of the magnesium atoms in the 3.2 atomic pct Mg alloy. Since there are 4 atoms per unit cell in aluminum the volume surrounding a magnesium atom would be $\left(\frac{100}{p}\right)\frac{a^3}{4}$ where p is the atomic percentage of magnesium. The mean distance, R, between any dislocation and an atom is then given by:

$$4/3\,\pi R^3 = \frac{100}{p}\,\frac{a^3}{4}$$

Introduction of 3.2 for p and 4.04×10^{-8} cm for a gives $R = 5.0 \times 10^{-8}$ cm. Of course, the data reveal that the initiation of the plateau in the stress-temperature diagrams occurs at approximately the same temperature for all compositions, suggesting that this estimate is not critical. Introducing these values into eq 1 reveals that $F \cong 10^{-4}$ dynes.

In order to estimate ρ from eq 4 the following data were assumed:

$\dot{\epsilon}$ = between 0.4×10^{-4} to 190×10^{-4} per sec (from Fig. 19)
$T = 295$°K
$k = 1.38 \times 10^{-16}$ dyne-cm per degree
$\lambda = 2.86 \times 10^{-8}$ cm
$F \cong 10^{-4}$ dynes
$D = 5 \times 10^{-20}$ to 5×10^{-26} sq cm per sec.

The values of D for magnesium were obtained by extrapolating from ordinary diffusivity data at elevated temperatures to atmospheric temperature. The wide range of values quoted above for D results from differences in the activation energies of magnesium in aluminum reported by various investigators.[9,10] It is conceivable that the correct value of D to be applied to the cold-worked Al-Mg alloy is several orders of magnitude greater than the extrapolated values. When the above values are introduced into eq 4 the values of ρ range from $\rho_{min} = 5 \times 10^{15}$ per sq cm to $\rho_{max} = 3 \times 10^{20}$ per sq cm. Obviously ρ_{max} is much too large. On the other hand, ρ_{min} begins to approach the value of ρ of 10^{12} quoted by Seitz and Read[11] for severely cold-worked metal. If the actual diffusivities in the cold-worked metal could be about 5000 times those for the annealed state, ρ_{min} would reduce to about 10^{12} in fair agreement with the estimate made by Seitz and Read. It appears, however, that several improvements in analysis and data will have to be made before quantitative agreement between theory and experiment can be achieved in this field.

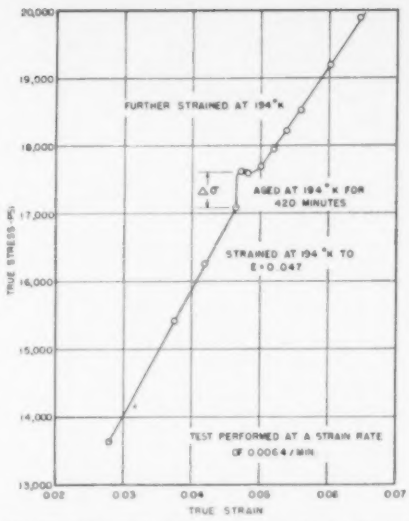

Fig. 20—Effect of a strain-aging treatment on the true stress-true strain curve of 3.2 atomic pct Mg in aluminum alloy at 194°K.

Although the decrease in flow stress resulting from an increase in strain rate is probably ascribable to the fact that the solute atoms cannot diffuse sufficiently rapidly to migrate with the dislocations, it is by no means certain that the yield-point phenomenon upon aging is also attributable to the diffusion of the solute atoms to the dislocations. It is quite possible that the dislocations might migrate with greater ease toward the solute atoms during aging than the solute atoms can migrate toward the dislocations. If the solute atoms were diffusing toward the dislocations, the activation energy for the yield-point phenomenon would be that for the diffusion of the atoms, but if the dislocations were more mobile than the solute atoms the activation energy for the strain-aging process should be that for the activation of dislocations. Inasmuch as dislocations are activated during recovery at 298°K in pure aluminum, whereas the rate of migration of solute atoms is quite low at this temperature, preference must be expressed for the process involving the migration of dislocations to account for the observed yield-point phenomenon. This preference is emphasized by the data shown in Fig. 20. Careful prestraining at 194°K at a slow strain rate of $\dot{\epsilon} = 0.0064$ per min, unloading, aging at 194°K for 420 min, and then continuing the straining at 194°K gives a well-defined yield point. At this temperature the diffusivity of magnesium in aluminum is about 10^{-26} sq cm per sec, strongly suggesting that the yield point induced by strain aging cannot be ascribed to the migration of the solute atoms. The values of the yield-point hump $\Delta\sigma$, which is defined in Fig. 20,

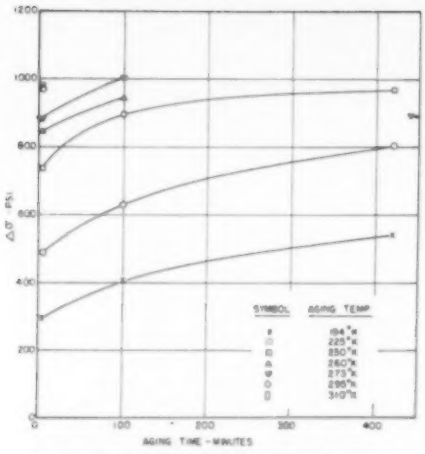

Fig. 21—Effect of strain-aging treatments at various times and temperatures on the increase in flow stress $\Delta\sigma$. 3.2 atomic pct Mg in aluminum alloy.

were obtained at 194°K after aging for various times and temperatures as shown in Fig. 21. Calculations based on these data suggest that the activation energy for the aging process is indeed low. No single activation energy, however, could be found. For small values of $\Delta\sigma$ a low average activation energy of about 8000 cal per mol was obtained. The average activation energies for higher values of $\Delta\sigma$ were estimated to be about 10,000 cal per mol, and yet higher values of $\Delta\sigma$ suggested average activation energies of about 15,000 cal per mol. Since these values of the activation energy are less than half of the accepted values of activation energy for diffusion of magnesium in aluminum, the aging process cannot be attributed to diffusion of magnesium. These trends of increasing activation energies for increasing values of $\Delta\sigma$ are highly reminiscent of the variation in activation energies for recovery which were previously reported.[12,13] It appears as if the smaller loops of the dislocations which have lower activation energies migrate rapidly and subsequently the more difficultly activated dislocation loops are induced to migrate to the solute atoms. Thus, the mean activation energy for the process steadily increases as the process proceeds.

Conclusions

1—The effect of various alloying elements on the plastic properties of α solid solutions of aluminum at elevated temperatures was studied.

2—The solid solution strengthening of the annealed metals decreases with increasing temperature as predicted by the dislocation theory.

3—On the other hand, the alloys exhibited greater relative rates of strain hardening than aluminum as the test temperature was increased.

4—Solid solution alloying is not very effective in improving the flow strength of aluminum at high temperatures where both the pure aluminum and the alloy recover rapidly.

5—In an intermediate range of temperatures from 300° to 425°K, the alloys showed the most pronounced improvement in flow stress over that for pure aluminum.

6—Some of this improvement was attributed to the restraint offered by the alloying elements to recovery.

7—The major factor causing solid solution hardening in the intermediate range of temperatures, however, was shown to arise from the migration of the solute atoms with the dislocations as postulated by Cottrell.

8—When aluminum alloys are aged after straining, they develop a yield point. This occurs even when the straining and aging is done at 194°K and is probably attributable to the migration of dislocations to the solute atoms.

Acknowledgments

This investigation is part of a more extensive program of research on the effect of alloying elements on the plastic properties of aluminum alloys sponsored by the Office of Naval Research. The authors wish to express their appreciation to the O.N.R. for its continued interest throughout the course of these studies. They are especially grateful to the Aluminum Research Laboratories and their staff for furnishing the alloys that were investigated and their chemical analyses.

In addition, the authors wish to thank T. E. Tietz and C. D. Starr for their helpful criticisms and numerous suggestions made during the conduct of this study. To Mrs. G. Pelatowski they extend their sincere appreciation for her careful preparation of the many figures in this report.

References

[1] J. E. Dorn, P. Pietrokowsky and T. E. Tietz: The Effect of Alloying Elements on the Plastic Properties of Aluminum Alloys. *Trans.* AIME (1950) **188**, pp. 933-943; JOURNAL OF METALS (July 1950).

[2] A. H. Cottrell: Effect of Solute Atoms on the Behavior of Dislocations. Report of A Conference on Strength of Solids, The Physical Society (1947) pp. 30-38.

[3] A. H. Cottrell and M. A. Jawson: Distribution of Solute Atoms Round a Slow Dislocation. *Proc.* The Royal Society (October-December 1949) **199A**.

[4] T. E. Tietz and J. E. Dorn: The Effect of Strain Histories on the Work-Hardening of Metals. *Trans.* ASM (1949) **41A**.

[5] F. R. N. Nabarro: Mechanical Effects of Carbon in Iron. Report of a Conference on Strength of Solids, The Physical Society (1947) pp. 38-45.

[6] A. W. McReynolds: Plastic Deformation Waves in Aluminum. *Trans.* AIME (1949) **185**, pp. 32-45; JOURNAL OF METALS (January 1949).

[7] J. D. Lubahn: Simultaneous Aging and Deformation in Metals. *Trans.* AIME (1949) **185**, pp. 702-708; JOURNAL OF METALS (October 1949).

[8] Von A. Beerwald: Diffusion Verschiedener Metalle in Aluminium. *Ztsch. für Elektrochemie und Angewandte Physikalische Chemie* (1939) **45**, p. 792.

[9] Von W. Bungardt and Franz Bollenrath: Uber die Diffusion von Magnesium in Aluminum. *Ztsch. für Metallkunde* (1938) **30**, p. 382.

[10] R. M. Brick and Arthur Phillips: Diffusion of Copper and Magnesium into Aluminum. *Trans.* AIME (1937) **124**, p. 337.

[11] F. Seitz and T. A. Read: Theory of Plastic Properties of Solids. II. *Journal of Applied Physics* (1941) **12**, pp. 170-186.

[12] T. E. Tietz, R. A. Anderson and J. E. Dorn: Effect of Prestraining Temperatures on the Recovery of Cold Worked Aluminum. *Trans.* AIME (1949) **185**, pp. 921-926; JOURNAL OF METALS (December 1949).

[13] T. E. Tietz, R. A. Anderson, A. Goldberg, and J. E. Dorn: Investigations on the Strain-Hardening of 2S-O Alloy. University of California Institute of Engineering Research Report, Berkeley, Series No. 22, Issue No. 9, (April 1950).

Structural Studies of Plastic Deformation

In Aluminum Single Crystals

by N. K. Chen and C. H. Mathewson

Single crystals of high purity aluminum of various orientations were carefully documented after plastic extension. Special attention was given to the formation of slip lines, deformation bands, and asterism. An explanation for the geometry and mechanism of formation of deformation bands is considered.

WHILE the general process of plastic extension of face-centered cubic metals is well understood,[1] the accompanying structural changes due to slip and rotation are far more complex than ordinarily assumed.[2-5] In the case of stretched single crystals of aluminum, the complicated behavior is especially marked by the formation of deformation bands, as first indicated by Collins and Mathewson.[5] Such bands were believed by them and also by others,[6, 7] who have discussed banded structure in general, to represent one of the important modes of lattice reorientation and to be intimately connected with the recrystallization process. Yet, despite their fundamental importance to the understanding of the mechanism of both plastic deformation and recrystallization, practically no study of the crystallographic features of these bands in their relationship to the conventional slip process has been attempted.

This paper describes part of an extensive investigation on the structural behavior during plastic deformation of aluminum single crystals and is especially concerned with the characteristics of deformation bands. The investigation of the subsequent recrystallization of deformed aluminum single crystals will be discussed in a later publication.

Experimental Procedure

Single crystal specimens of 99.996+ pct pure aluminum, ½ in. in diam and 5 to 6 in. in length were made both by the Bridgman method[8] and by a modified temperature gradient method.[9,*]

N. K. CHEN, Junior Member AIME, formerly a Graduate Student, Department of Metallurgy, Yale University, is now Research Associate, The Johns Hopkins University, Baltimore. C. H. MATHEWSON, Member AIME, is Professor Emeritus of Metallurgy and Metallography, Yale University, New Haven, Conn.

Discussion on this paper, TP 3100E, may be sent, 2 copies, to AIME by Dec. 1, 1951. Manuscript, March 6, 1951. Detroit Meeting, October 1951.

This paper represents part of a thesis by N. K. Chen submitted in partial fulfillment of requirements for the degree of Doctor of Engineering to the Graduate School of Engineering, Yale University.

Crystals were selected in which the lineage deviation did not exceed 2°; i.e., as determined from the back-reflection Laue X-ray photograms. These crystals were radiographed to insure that no internal porosity was present. The orientations showed good coverage of the whole area of the Taylor and Elam triangle.[1] Orientations of the crystals were obtained by the back-reflection Laue technique described by Greninger.[10]

Crystals so selected were tapered very carefully in a lathe to obtain a linear decrease in diameter from 0.500 to 0.350 in. along a gage length of 3 in. This is considered desirable because it permits a strain gradient to be introduced in a single specimen at one initial orientation. The advantages of tapered crystals for studying the development of slip lines and recrystallized grains have been pointed out by previous investigators.[11] The cold-worked layer resulting from the machining operation was removed by alternate etching in aqua regia and careful polishing with 2/0 emery paper until undistorted Laue back-reflection spots were obtained. A homogenization treatment at 600°C for 24 hr was then introduced to insure the removal of residual stress. Two of the crystals so prepared were also checked by use of a glancing angle technique. Using a copper target, at 30 kv and 10 microamperes, a monochromatic beam was positioned at right angles to the axis of the crystal about which it rotated. The time of exposure was 24 hr. From these X-ray photograms, it was concluded that the present method of preparation of single crystals is satisfactory.

Following this procedure, the crystals were electrolytically polished in a 2:1 solution of methyl alcohol and concentrated nitric acid. Intermittent

* A third method, a particular type of strain-anneal technique, developed in the present investigation, was also used for specimen preparation. It differs in a striking way from the ordinary strain-anneal procedure in that a tapered single crystal of one orientation can be transformed to another single crystal of a different orientation by first stretching it (not a critical amount) and then annealing it isothermally at a high temperature. The details will be discussed in a separate publication.

polishing periods of from 10 to 12 min at a current density of 10 amp per sq dm resulted in a high polish and smooth metallographic surface. Fine black lines then were painted on each specimen at ¼-in. intervals. These intervals were carefully measured in a Zeiss metallograph at a magnification of X77, yielding an accuracy of ±0.05 mm.

The straining of the specimens was carried out for the most part on a Southwark Emery 20,000-lb hydraulic testing machine equipped with self-aligning grips and gimbals. The rate of loading was approximately 100 lb per min, and the load values could be estimated to 5 lb. In two cases (first extension of crystals A-2 and A-4) the loading equipment devised by Miller[12] and modified by Rosi[13] was used. In their equipment, uniform flow of sand produced loading at approximately 3 lb per min. The average of repeated measurements of the gage intervals painted on each crystal before and after extension gave a mean value of elongation for each gage section after extension as measured by an optical micrometer. A series of back-reflection Laue photograms per gage interval gave reorientation values in terms of λ and χ, where λ is the angle between the specimen axis and the primary slip direction and χ is the angle between the specimen axis and the primary slip plane. These values were used to calculate the elongation, resolved shear stress and shear, according to classical crystal mechanics.

The gross orientation changes of each tapered crystal are plotted in Fig. 1. During extension the stress axes of the crystal rotated, generally, toward the slip direction in the usual manner. In some cases when a symmetry position was reached, the lattice rotation did not obey the classical behavior; i.e., towards an equilibrium position at <112>. In these cases, the stress axes continued to rotate toward the slip direction. This behavior has been generally observed in cylindrical and tapered α brass single crystals.[13, 14] It should be noted, however, that both the measured and the observed values of reorientation of any tapered section of the crystal constituted an average representation of the lattice changes during deformation. It became clear that after asterism had developed, orientation determined by X-rays actually should be plotted as a range of orientation rather than a single axial position. The stress-strain curves indicated differences in the strain-hardening characteristics of the different specimens, but the nature and cause of these variations has not been established.

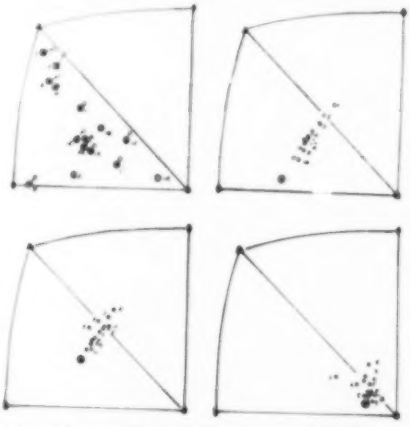

Fig. 1—Stereographic projection showing orientation of various aluminum crystals in relation to the axis of tension.
○ — Original orientation (position of axis).
◌ — Predicted orientation after deformation.
● — Measured orientation after deformation.
a (upper left)—12 crystals with comparatively small deformation. b (upper right)—Crystal A-2. c (lower left)—Crystal A-6. d (lower right)—Crystal A-18.

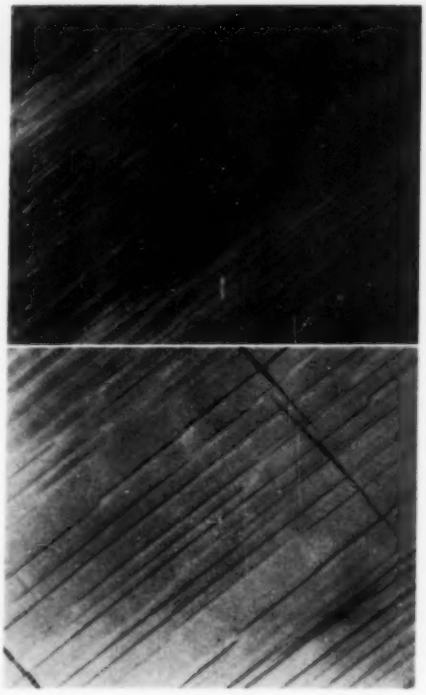

Fig. 2—Crystal A-18.
a (upper)—Pronounced cross slip at a position perpendicular to the plane containing the reference mark along the crystal and the stress axis. Shear is 0.16. Stress axis, horizontal; position No. 6 in Fig. 1d. Electrolytic polish. X150. b (lower)—Primary, conjugate, and cross-slip lines at a position perpendicular to the plane containing the reference mark along the crystal and the stress axis. The stress axis is horizontal. Shear is 0.24. X400.

Slip Lines and Deformation Bands

In all crystals, primary slip lines occurred in close association with cross-slip lines during the early stages of deformation. Early slip on the conjugate plane[15] was observed in crystals of certain orientations such as, A-7, A-5, A-16, and A-18. These lines were irregularly spaced (Fig. 2a) and, generally, discontinuous over primary slip clusters (Fig. 2b). It is clearly seen from Fig. 2b that the conjugate slip segments are displaced by primary slip lines formed subsequent to this slip on the conjugate plane.

Generally it is assumed that the slip bands in aluminum single crystals are quite regularly spaced. Nevertheless, in the present investigation, an orientational effect was found to exist. All crystals having their stress axes located near <111> showed slip clusters during extension (Fig. 3a and b), whereas crystals oriented well away from <111> exhibited dispersed slip lines (Fig. 3c, d, and e), or barely developed clusters; which were also observed in crystal A-18 having its axis near <100> (see Fig. 2a). Since deformation bands were not found in crystals con-

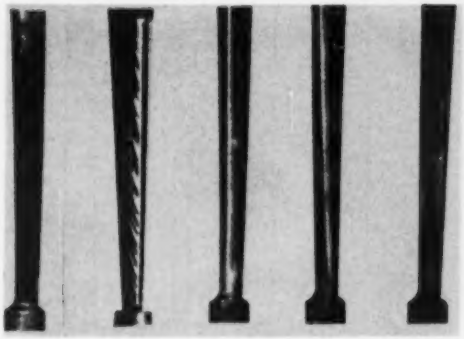

a b c d e

Fig. 3—Orientation effect on dispersion of slip lines.

a—Crystal A-7 showing slip clusters along the crystal; shear at small end of taper, 0.20, and at larger end, 0.09. b—Crystal A-3 showing same as a; shear is from 0.33 to 0.14. c—Crystal A-15, second extension; dispersed slip lines; shear is from 0.65 to 0.10. d—Crystal A-12', second extension; dispersed slip lines; shear is from 0.70 to 0.15. e—Crystal A-6, dispersed slip lines; shear is from 0.98 to 0.20. All photographs X1.

taining slip clusters, a close correlation seems to exist between the orientations concerned in the slip process and the generation of deformation bands. Furthermore, a similarity exists with brass crystals which always exhibit clustered slip lines, but no deformation bands as far as we can learn.

On an electrolytically polished surface, the deformation bands in an early stage of formation (shear about 0.05) can best be described as striations which reflect under very low magnifications or even to the naked eye. They would seem to disappear on observation under high magnification, as the observed slip lines give no indication of a banded arrangement. Thus, there is the likelihood of overlooking them in ordinary metallographic examination.

Deformation bands could be revealed by etching as shown in Fig. 4, with properly controlled conditions. A modified aqua regia solution (three parts HCl, one part HNO_3, one part H_2O) as an etchant after the crystal was polished with 2/0 emery paper was found to give very satisfactory and reproducible results. At the early stages of deformation (shear about 0.04 to 0.08), the boundaries of the bands could be easily identified as plane surfaces with elliptical peripheries on the cylindrical specimen. The distance between any two bands was not quite uniform, for at the large end of the tapered crystal they were more widely spaced than at the small end. Nevertheless, in the early stages of deformation, the average distance between bands was of the order of 1 mm.

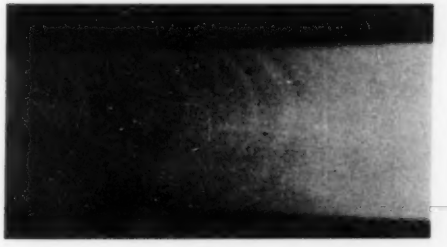

Fig. 4—Deformation bands in crystal A-1'.
Shear is 0.11 to 0.08. Average distance between bands appearing on the surface is 1.2 mm. Etched in modified aqua regia solution. X4.

As the deformation increased, the bands also increased in intensity (but not in width) and became wavy. New bands of lesser intensity and more imperfect development were also generated between the older ones as shown in Fig. 5 representing crystal A-2. These pictures confirm the observation previously made by Collins and Mathewson[2] that the ". . . bands varied in thickness and character. When viewed from one point, they appeared straight and regular while from another, they appeared forked and wavy. When held in a certain position they reflected light strongly, as a twin would, while the remaining part of the crystal was dark."

On the unetched surface, the bands, after considerable extension seemed to show ridges and valleys as may be seen in Fig. 6a and b. With one of the crystals in which the strained surface was first etched and later repolished electrolytically, the bands appearing after the second extension could be resolved in some locations, indicating their narrow width, as shown in Figs. 7 and 8a. This width is about 0.038 mm and the average spacing about 0.3 mm. The slip lines crossing the band change their direction as would be the case if the material in the band lagged behind the material in the matrix during the process of lattice reorientation. This was found to be true by subsequent X-ray examination. In other cases revealing slip lines across a band of no clearly resolvable width, Fig. 8b, the directional changes of the slip lines were in agreement with the above statement.

Crystallographic Location of Deformation Bands

Two methods were used in determining the crystallographic location of deformation bands at the early stages of formation (shear below 0.10). One method consisted of measuring the azimuth angle of the band (the horizontal angle around the circumference of the crystal from the reference mark to the element containing the minimum or maximum point of the band) and the angle which the band made with the stress axis. The crystal was centered end for end on a one-circle goniometer, with the reference mark coinciding with the vertical cross-hair of a comparator which was also vertically located for the purpose of measuring the vertical difference from an arbitrary horizontal plane at various locations around the conical surface. With the diameter of the crystal corresponding to the maximum and minimum point of the band known, the required results could be obtained either graphically or by calculation. The other method was to determine the trace of the band on two known reference planes under the micro-

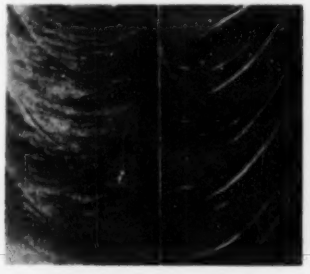

Fig. 5—Deformation bands of crystal A-2. a (left), b (right)—Second extension to a shear 1.03 at the small end and 0.20 at the large end. The wider bands make a smaller angle with the stress axis than the finer bands. Etched in modified aqua regia. X7.

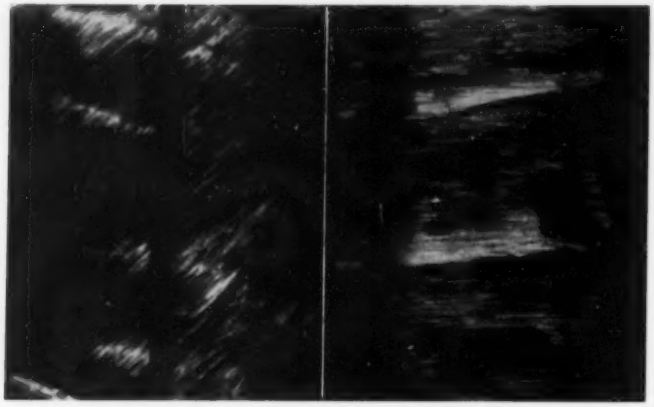

Fig. 6—Deformation bands in crystal A-12'. Second extension.

a (left)—Position shown is around the conical section between the major and minor axes of the glide ellipses. The stress axis is vertical as represented by the central scratch line. Shear, 0.3. Electrolytic polish. X60. b (right)—Position shown is perpendicular to the plane containing the major axis of the glide ellipse and the stress axis. Stress axis is vertical. Shear, 0.3. Electrolytic polish. X60.

scope. In all the cases the pole of the band was found to coincide with the slip direction within experimental error.

The resulting data are summarized in the stereographic plot, Fig. 9. It is seen that more than half of the crystals have produced bands but that an area of orientation spreading out from the octahedral pole is exempt from band formation. These crystals, without band formation, were characterized by irregularly spaced slip lines of a strongly clustered appearance. In the subsequent recrystallization studies, it was found that in the absence of band formation, the inner face of crystal growth lies parallel to the old glide plane, whereas with band formation, the growing face is decisively affected by the band.

Mechanism of Band Formation—X-ray Results

The fundamental process which causes the formation of deformation bands is believed to be due to the necessity for inhomogeneous rotations (within and adjacent to a band) in a forced pattern of flexual gliding wherein the slip direction conventionally approaches the axis. This recalls the action of bend planes in zinc crystals, as described in 1934 by Miller.[10] However, in the present case, there are paired bend planes defining an intermediate band in which the process of reorientation is restrained.

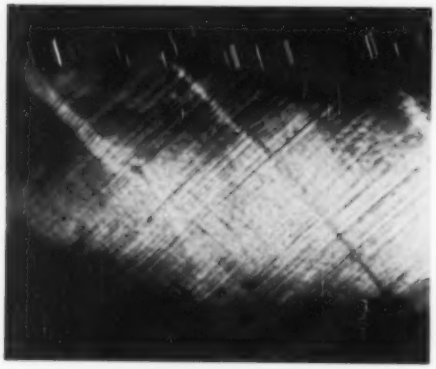

Fig. 7—Slip lines crossing deformation bands in crystal A-1'. Deformation bands were first generated after a shear of 0.05 corresponding to a reorientation of about 1°. Repolished electrolytically and again extended to a shear of about 0.20 corresponding to a reorientation of 8°. Taken at a position perpendicular to the plane containing the reference mark along the crystal and the stress axis. The stress is horizontal. X118.

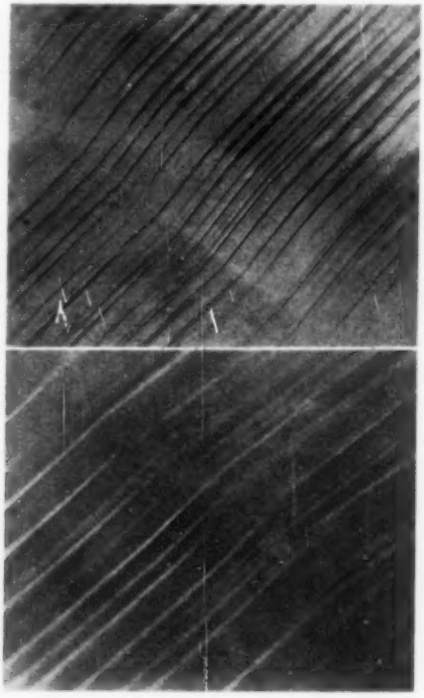

Fig. 8—Slip lines crossing deformation bands in crystal A-1'.
a (upper)—Enlarged section of a deformation band shown in Fig. 7. X472.
b (lower)—Same location as in Fig. 7. X1000.

or held to a minimum. This corresponds to that part of the Miller crystal which is prevented from slip and reorientation by an anchorage to polycrystalline material intentionally introduced for this purpose. X-ray studies of the bands in the very early stages of deformation (shear below 0.1) have indicated that both the axis of rotation and the sense of rotation corresponding to extension of the crystal could be properly correlated with the formation, structure, and location of the bands. An analysis of the situation follows:

As a rule, it was found that in the very earliest stage of deformation, when the bands are far apart (approximately 1 mm), the X-ray photogram taken on a band would give clear indication of distortion with a range of orientation of about 2°, whereas a photogram from the region between the two bands would show little or no asterism. This can be illustrated in Fig. 10a and b. In this case the width of the band was believed to be of the order of a few hundredths of a millimeter, and the spacing between bands along the crystal surface was about 1.7 mm. The X-ray beam was collimated by means of a pinhole 0.5 mm in diam x 2.5 in. long. Therefore, when the X-ray beam was carefully adjusted to the band, it also covered some material outside of the band (Fig. 10a). But it impinged only on the slipped matrix when adjusted to the material between bands. After stereographically plotting the streaks seen in Fig. 10a, an axis of rotation could be located as clearly indicated in Fig. 11. This is the <112> direction in the slip plane, normal to the slip direction. This axis of rotation could also be derived from plot of other X-ray photograms taken on the same band but with the beam located at a point around the conical surface 90° from the first position. It should be noted here that this axis of rotation is also the line of intersection of the primary slip plane and the plane of the deformation band.

In order to study the sense of the rotation, Fig. 10a and b and the film representing the original orientation of the crystal before extension were carefully superimposed. It was found, as indicated in Fig. 11, that the orientation of the slipped matrix corresponds to the left-hand part of each elongated streak, whereas the original orientation before extension coincides with the right-hand edge of the streak. This implies that while maxima in the Laue streaks represent the slipped matrix, the continuous background arises from the structure of the deformation bands. Examination of this situation shows that the sense of rotation about <112> is counterclockwise, which is in agreement with the rotational requirements of a slip process in which the slip direction, IV, approaches the stress axis, *T*, during extension. It should be noted, therefore, that the material in the band has lagged about 2° behind the matrix in this process of lattice reorientation. A standard projection summarizing these facts is shown in Fig. 12.

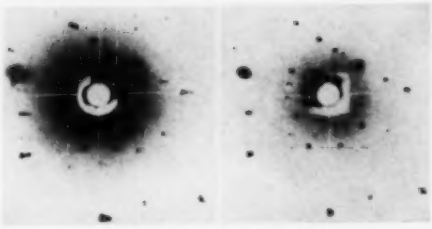

Fig. 10—Back-reflection Laue photograms taken on crystal A-12′ after the first extension.
Shear 0.08. X-ray beam was carefully located: a (left) on a deformation band, and b (right) between deformation bands immediately adjacent to position a.

Similar analyses were carried out for rotations associated with deformation bands in other crystals. In all cases examined, excellent agreement with the above conclusions was obtained.

In crystals without band formation, no measurable amount of asterism could be noted in the Laue spots up to a shear of about 0.15. In such cases, X-ray photograms taken on and between areas with clustered slip bands represent the same orientation. This, again, brings out the similarity to brass crystals in which asterism is absent up to a shear of about 0.46.[10]

Micrographic Analysis

The microstructure shown in Figs. 7 and 8a give good visual information concerning the formation and rotation of the bands. A stereographic projection referring to this particular region, representing the orientation changes of crystal A-1′ after the second extension, is shown in Fig. 13. The axis of

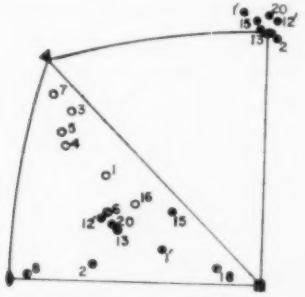

Fig. 9—Dependence of banding on initial orientation.
● — Initial orientations of crystals that subsequently formed deformation bands (the poles of the bands are shown clustering around the slip direction).
○ — Initial orientations of crystals that did not form deformation bands.
ϕ — Initial orientations of crystals that formed bands whose locations were not accurately determined.

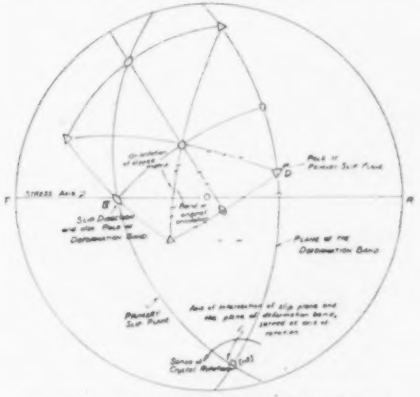

Fig. 11—Stereographic representation of the asterism of Fig. 10a.

Fig. 12—Standard projection showing lattice rotation in a deformation band. Crystal A-12′ after first extension. p_o, original position of the stress axis; p_m, position of the stress axis of the slipped material between bands ($p_o - p_m = 2°$); p_s, position of the stress axis corresponding to the orientation of the band ($p_o - p_s$) not measurable with X-ray.

rotation after the first extension; i. e., when the band was formed, was not measurable by means of X-rays (calculated shear, below 0.05), but the amount of axis rotation for the second extension was found to be 8°. Since the projection plane here coincides with the plane of observation, traces on the micrographs can easily be compared with the orientation plot. Thus, Fig. 14a and b were drawn from these indications. It is seen that the prediction embodied in Fig. 14b is in good agreement with the angular measurements actually made on the crystal, Fig. 14a, except that the axis of the band is not strictly parallel to *S-S* or *Q-Q*, following the analysis of Fig. 13, but lies in the direction *R-R* making a somewhat smaller angle with the stress axis. This probably indicates that the band was actually formed along the line *S-S*, as would be determined after the first extension, and has rotated toward the stress axis, but in the opposite direction to the rotation of the slip planes.

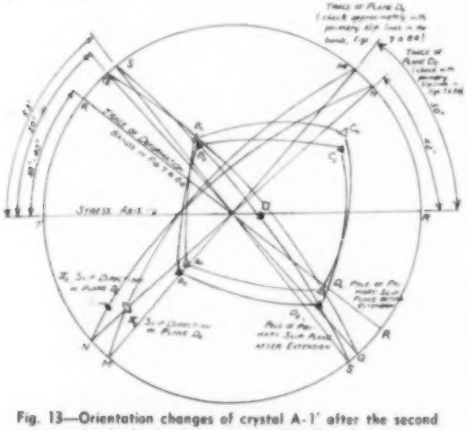

Fig. 13—Orientation changes of crystal A-1′ after the second extension in the position represented by Figs. 7 and 8a. The projection is perpendicular to the plane containing the stress axis and the reference mark. Stress axis, horizontal; X-ray beam at the center of the projection.

Complex behaviors were noticed in crystal A-18, Fig. 15a and b. At the large end, where the shear was about 0.11, no indication of the formation of bands was obtained. At the small end of the taper, however, where the shear was 1.04, much distortion in the form of irregular bands was noticed. The appearance of the slip lines across a band gives evidence indicating a change of elevation at the "bend site" in some cases, while in other, the change of direction of slip lines confirms the observation that the material in the band lags behind the matrix in the process of the lattice reorientation. At the large end, where bands were absent, clustered slip lines and early conjugate slip were observed (cf. Fig. 2).

Rotation of Deformation Bands

The question arises as to whether, after initial formation of a band, the two "bend planes" would move away from the stress axis during further rotation of the slip planes or would move toward the stress axis, but in the opposite direction to the rotation of the slip planes. Experiments seem to furnish many illustrations confirming this latter condition. It was more difficult to obtain clear evidence of the former condition, but it is believed that this also may have occurred.

For example, deformation bands developed in the first extension of crystal A-12′ were carefully traced with a sharp pencil. The crystal was then subjected to a second extension causing both the bands and the markings to rotate. The bands, behaving quite similarly to the mechanical marks, rotated toward the stress axis as the crystal elongated. The coincidence of the marks and the boundaries was not quite perfect because the bands became wavy during the large amount of rotation. New bands formed between the earlier bands, with an even more wavy and irregular appearance, and a larger inclined angle to the stress axis than in the case of the initial bands. This implies that these new bands may have formed as a result of flexual gliding of the slip planes at their progressively reoriented positions.

Another example of the rotations of the bands themselves was encountered in the second extension of crystal A-2 plotted stereographically in Fig. 16 (cf. also Fig. 5). In the subsequent recrystallization process, new grains formed in this crystal along the boundaries of the initial bands but in their rotated positions.

No detailed study has been attempted with respect to the crystallite rotations within a narrow band,

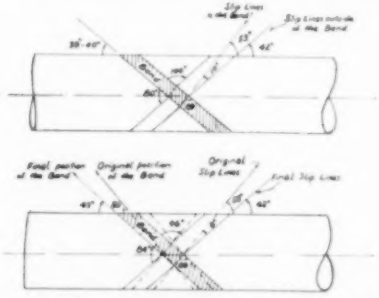

Fig. 14—Crystal rotation of a deformation band of crystal A-1′.
a (upper)—Observed positions of slip lines and band traced from Fig. 8a. b (lower)—Predicted positions of slip lines and band assuming a rotation according to orientation changes analyzed in Fig. 13.

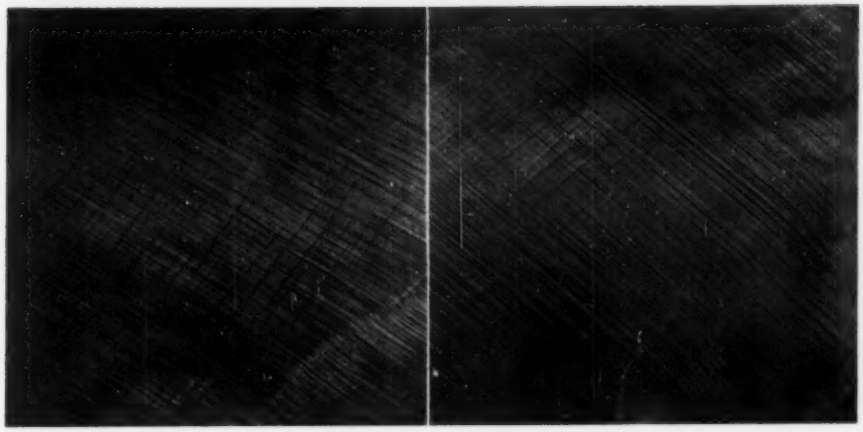

Fig. 15—Irregular deformation bands in crystal A-18.
a (left)—Position shown is No. 1 of Fig. 1d in the plane containing the reference mark along the crystal and the stress axis. Shear is 1.04. Stress axis is horizontal. Electrolytic polish. X150. b (right)—Position shown is No. 4 of Fig. 1d in the plane containing the reference mark along the crystal and the stress axis. Shear is 0.30. Stress axis is horizontal. Electrolytic polish. X150.

which must accompany the progressive rotations of the matrix during deformation. X-ray photograms have indicated, however, that the range of orientation increased as deformation proceeded, confirming this type of rotation. The number of intensity maxima also increased. This may be due to the development of new bands.

Discussion of Results

Deformation bands produced in the extension of aluminum single crystals possess, in general, the same characteristics as the banded structures found in other metals, after different types of deformation,[6,7] such as a gradual development of orientation differences between bands and matrix, and an unchanging width of the bands during progressive deformation. However, in the early stages of band formation, there is clear evidence of a process of crystal slip and abrupt flexual gliding at band boundaries, similar to the action of the "bend plane" which Miller observed in zinc.[10] A "bend plane" is the locus of the axes around which the slip planes bend in this modification of simple flexual gliding. Thus, a pair of bend planes defines a band in which the reorientation lags behind that of the matrix material in the process of axial extension. A diagrammatic illustration is given in Fig. 17, embracing the following experimental facts:

1—The slip direction constitutes the pole of the band.

2—The reoriented material in the band lags behind that of the slipped matrix about 2° at an early stage of observation.

3—The axis of rotation in the process of band formation is <112> which is also the intersection of the slip plane with the parallel planar boundaries of the band.

4—The slip lines change directions in crossing a band.

Recent studies by Hess and Barrett on the kink bands in zinc[7] also revealed an axis of rotation of the same general character. Thus, it would be profitable to examine other metals with respect to band formation and the details of reorientation during plastic deformation.

The tendency towards formation of deformation bands is orientationally dependent in the present case of axial extension of aluminum single crystals. Generally it has been assumed[8] that this tendency depends upon the orientation of the crystal or grain with respect to the direction of flow. Thus an iron

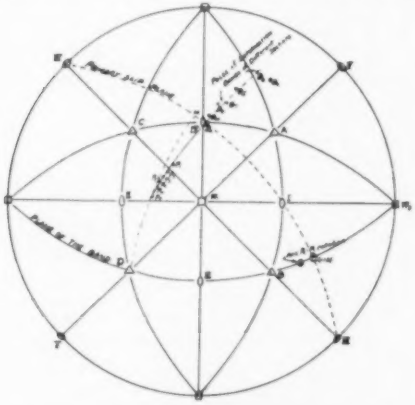

Fig. 16—Stereographic projection showing rotation of deformation bands in crystal A-2', second extension.

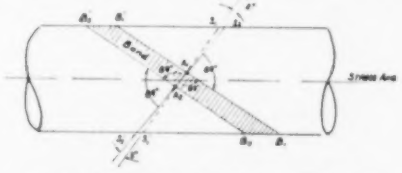

Fig. 17—Hypothetical mechanism of formation of deformation bands. Plane of sketch contains stress axis and slip direction.
$S_1A_1A_2S_2$ — Original position of slip plane.
S_1A_1; S_2A_2 — Final position of slip plane.
$B_1A_1B_1$ — "Bend plane" 1.
$B_2A_2B_2$ — "Bend plane" 2.

crystal having a <100> or <111> axis parallel to the axis of compression will form no bands, but crystal of all other orientations become banded.[6]

Homogeneous rotation of the lattice during extension is prohibited because of constraints imposed by grips and by unslipped matrix material. The methods hitherto assumed by which a lattice could rotate and still satisfy the boundary conditions in aluminum have been flexual gliding[17] and crystal fragmentation.[18] The presence of asterism in the Laue X-ray photograms has been interpreted by various investigators as evidence in support of both mechanisms. In brass, collateral slip on cross and conjugate slip planes is assumed to contribute to lattice reorientation and thus modifies the pattern of asterism.[4, 18] It is shown here, however, that asterism in extended aluminum single crystals may arise entirely from the presence of deformation bands. In crystals which do not produce bands, no asterism was found up to a shear of 0.15, similar to the earlier observations on brass. Thus, it is believed that the absence of asterism in aluminum crystals indicates a modified condition of inhomogeneity due to cross-slip and early conjugate slip. Similar correlations between asterism and deformation bands in stretched aluminum crystals have recently been obtained by Cahn and Honeycombe.[19, 20]

There is a further similarity between aluminum single crystals oriented near <111> and brass in that slip bands are much more irregularly spaced in such orientations, assuming a strongly clustered appearance. Thus the density of slip bands in such orientations should be expected to be much less than for crystals of other orientations. Actual measurement of slip bands in aluminum in the early stages of extension confirms this general orientational relationship.[21]

Strain hardening characteristics could not be correlated with differences in the appearance of slip lines. Since deformation bands were not found after extension in crystals of aluminum containing slip clusters nor in brass, it seems that dispersed slip lines indicate the probable generation of deformation bands. According to the mechanism previously described a band must traverse a slipped matrix throughout its entire course, and it is clear that prominent slip clusters are not conducive to band formation in the present sense.

Conclusions

1—The tendency towards the formation of deformation bands in the plastic extension of aluminum single crystals is orientationally dependent. Axes oriented near <111> in the standard projection do not lead to band formation.

2—The slip direction constitutes the pole of the band and the axis around which the slip direction changes its orientation is the intersection of the glide ellipse with the band ellipse, namely <112>.

3—A mechanism is considered whereby a pair of bend planes defines a band in which the reorientation lags behind that of the matrix material in the process of axial extension.

4—Asterism found in the early stages of extension of aluminum is due to deformation bands, while the absence of asterism in crystals with no band formation in an early stage of deformation indicates that the inhomogeneities of deformation have been modified by cross-slip and early conjugate slip.

5—Crystals which develop bands reveal more regularly dispersed slip lines than crystals which do not produce bands. In the latter case, a distinct clustering of the slip lines is invariably observed. This correlates properly with the plastic behavior of brass crystals, which develop slip clusters, but no deformation bands.

6—The band structure here observed possesses certain general features previously observed in deformation bands. A rotation of the bands after their initial stage of formation is confirmed and various possibilities in this direction are critically examined.

Acknowledgments

The authors wish to extend their gratitude to W. R. Hibbard, Jr., of the Yale Metallurgical faculty, for his constructive criticism throughout the course of this investigation and to M. L. Kronberg and R. Maddin for their helpful discussions. Thanks are also due to the Aluminum Company of America for supplying the high purity aluminum used.

References

[1] Boas and Schmid: *Kristallplastizitat.* Berlin (1935).

[2] C. H. Mathewson: Structural Premises of Strain Hardening and Recrystallization. *Trans.* ASM (1944) **32**, p. 38.

[3] J. A. Collins and C. H. Mathewson: Plastic Deformation and Recrystallization of Aluminum Single Crystals. *Trans.* AIME (1940) **137**, p. 150.

[4] R. Maddin, C. H. Mathewson, and W. R. Hibbard, Jr.: Unpredicted Cross-Slip in Single Crystals of Alpha Brass. *Trans.* AIME (1948) **175**, p. 86; METALS TECHNOLOGY (February 1948).

[5] R. D. Heidenreich: Structure of Slip Bands and Cold-worked Metal. Symposium, Cold Working of Metals. ASM (1949).

[6] C. S. Barrett: *Structure of Metals.* (1943) New York. McGraw-Hill Book Co.

[7] J. B. Hess and C. S. Barrett: Structure and Nature of Kink Bands in Zinc. *Trans.* AIME (1949) **185**, p. 599; JOURNAL OF METALS (September 1949).

[8] P. W. Bridgman: Certain Physical Properties of Single Crystals of Tungsten, Antimony, Bismuth, Cadmium, Zinc and Tin. *Proc.* Amer. Academy of Arts and Sciences (1923) **58**, p. 165.

[9] D. C. Jillson: Production and Examination of Zinc Single Crystals. *Trans.* AIME (1950) **188**, p. 1005; JOURNAL OF METALS (August 1950).

[10] A. B. Greninger: Determination of Orientation of Metallic Crystals by Means of Back-reflection Laue Photograms. *Trans.* AIME (1935) **117**, p. 6.

[11] R. Maddin, C. H. Mathewson, and W. R. Hibbard, Jr.: The Origin of Annealing Twins in Brass. *Trans.* AIME (1949) **185**, p. 655; JOURNAL OF METALS (September 1949).

[12] R. F. Miller: Creep and Twinning in Zinc Single Crystals. *Trans.* AIME (1936) **122**, p. 176.

[13] F. D. Rosi and C. H. Mathewson: A Study of the Plastic Behavior of High-Purity Aluminum Single Crystals at Various Temperatures. *Trans.* AIME (1950) **188**, p. 1159; JOURNAL OF METALS (September 1950).

[14] V. Goler and G. Sachs: *Ztsch. Physik* (1929) **55**, p. 581.

[15] R. Maddin, C. H. Mathewson, and W. R. Hibbard, Jr.: The Active Slip Systems in the Simple Axial Extension of Single Crystalline Alpha Brass. *Trans.* AIME (1949) **185**, p. 529; JOURNAL OF METALS (August 1949).

[16] R. F. Miller: Influence of a Grain Boundary on the Deformation of a Single Crystal of Zinc. *Trans.* AIME (1934) **111**, p. 135.

[17] M. Polanyi: Deformation, Rupture and Hardening of Crystals. *Trans.* Faraday Soc. (1928) **24**, p. 72.

[18] W. G. Burgers and P. C. Louwerse: Zusammenhang Zwischen Deformationvorgang und Rekrystallisationtexture bei Aluminum. *Ztsch. Physik* (1931) **67**, p. 605.

[19] R. W. Cahn: *Proc.* Phys. Society (1950) **63A**, p. 323.

[20] R. W. K. Honeycombe: *Proc.* Phys. Society (1950) **63A**, p. 673.

[21] N. K. Chen and R. Maddin: Discussion of ref. 13. JOURNAL OF METALS (July 1951), *Trans.* AIME p. 545.

Theory of Grain Boundary Migration Rates

by David Turnbull

IN isothermal recrystallization processes, new crystals generally grow into the matrix until they impinge upon other new crystals or an external surface, at constant linear rates G. Before impingement the perceptible course of growth can be described by the equation:

$$l = G(t - \tau) \qquad [1]$$

where, $G = dl/dt$,

l is a crystal dimension measured in a constant direction, t is the time, and τ, the nucleation period, is a positive intercept on the time axis. Fig. 1 is a schematic representation of l as a function of time for a recrystallizing grain. G is dependent upon temperature, driving energy (strain or surface energy), relative grain and boundary orientations, but is generally independent of time. The frequency of nucleation, $\dot{N}$, (time^{-1} volume^{-1}) can be defined by the equation:

$$\dot{N} = 1/\bar{\tau}V \qquad [2]$$

where $\bar{\tau}$ is the mean nucleation period and V is the volume of the specimen that has not recrystallized. The kinetics of primary and secondary recrystallization generally can be described satisfactorily in terms of the parameters $\dot{N}$ and G only.[1-3]

After recrystallization is complete the average grain size $\bar{l}$ increases with time by "normal grain growth;" $d\bar{l}/dt$, the average rate of grain growth, is strongly time dependent and has not yet been precisely related to G for the motion of the individual grain boundaries constituting the system.

It has been suggested[4, 5] that the elementary act in grain boundary migration is closely related to the elementary act in grain boundary self-diffusion. Although the distance of atom movement in the two processes may be somewhat different, there is reason to expect that the activated states may be very similar, so that the free energy of activation for grain boundary migration should be of the same order of magnitude as for grain boundary self-diffusion. Therefore, it is desirable to develop a satisfactory basis for comparing data on self-diffusion and grain boundary migration and to make such comparisons where possible.

Theory

The formal theory of grain boundary migration rates is analogous to the theory for the rate of growth of crystals into supercooled liquids reviewed elsewhere.[6-8] Borelius[6] has shown that the latter theory describes, within the theoretical uncertainty, the growth of selenium crystals into supercooled liquid selenium. Mott[7] and more recently Smoluchowski[10] have derived expressions for the rate of boundary migration in recrystallization. The treatment to be presented is similar to Mott's excepting that the formalism of the absolute reaction rate theory will be used.

The atomic mobility, M, in grain boundary migration is defined by:

$$G = -M\delta\mu/\delta x \qquad [3]$$

where μ is the chemical potential per atom and x is the coordinate measured in the direction of grain boundary movement. Let ΔF be the free energy difference per gram atom on the two sides of the boundary and λ the thickness of the boundary. For $RT >> \Delta F$ the potential gradient across the boundary $(\delta\mu/\delta x)$ is essentially linear and it follows that:

$$\delta\mu/\delta x = -\Delta F/N\lambda \qquad [4]$$

where N is Avogadro's number. According to the Nernst-Einstein equation, M is related to a diffusion coefficient, D_G, for matter transport in grain boundary migration by the equation:

$$M = D_G/kT \qquad [5]$$

Substituting eqs 4 and 5 into eq 3 gives the basic relation between D_G and G:

$$G = D_G\Delta F/\lambda RT \qquad [6]$$

D_G values may be calculated from experimental values of G from eq 6 and directly compared with the coefficient of self-diffusion within the crystal, D_L, or the grain boundary self-diffusion coefficient D_s. However, a more convenient, though equivalent, basis for comparing atomic mobility in grain boundary migration and self-diffusion is through the constants of the absolute reaction rate theory. According to this theory diffusion coefficients may be written:[11]

$$D = \lambda^2(kT/h)\exp[-\Delta F_A/RT] \qquad [7]$$

ΔF_A, the free energy of activation, is related to the measured energy of activation, Q, by the equation:

$$\Delta F_A = Q - T\Delta S_A - RT \qquad [8]$$

where ΔS_A is the entropy of activation. Substituting eqs 8 and 7 into eq 6 gives:

$$G = e\lambda(kT/h)(\Delta F/RT)\exp[(\Delta S_A)_G/R]\exp[-Q_G/RT] \qquad [9]$$

where the subscript G refers to boundary migration. The relationship between the driving free energy and the free energy of activation in boundary migration is indicated schematically in Fig. 2.

Experience indicates that the variation of G with temperature can be described by:

$$G = G_o\exp[-Q_G/RT] \qquad [10]$$

where G_o and Q_G are generally temperature independent over wide ranges of temperature. Comparison of eq 9 with eq 10 gives:

$$G_o = e\lambda(kT/h)(\Delta F/RT)\exp[(\Delta S_A)_G/R] \qquad [11]$$

D. TURNBULL, Associate Member AIME, is Research Associate, Research Laboratory, General Electric Co., Schenectady.

Discussion on this paper, TP 3103E, may be sent, 2 copies, to AIME by Dec. 1, 1951. Manuscript, March 1, 1951. Detroit Meeting, October 1951.

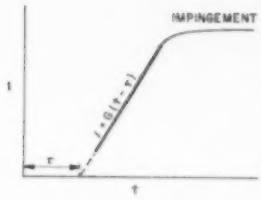

Fig. 1—Size of a growing grain as a function of time in primary or secondary recrystallization processes.

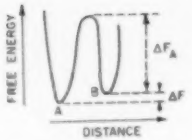

Fig. 2—Representation of free energy relationships between atoms on lattice sites A and B on opposite sides of a grain boundary.

Also it is found experimentally that:

$$D = D_o \exp [-Q/RT] \quad [12]$$

By comparing eqs 7 and 12:

$$D_o = e\lambda^2 (kT/h) \exp [\Delta S_i/R] \quad [13]$$

The relation between atomic mobility and free energy of activation is from eqs 5 and 7:

$$M = \lambda^2 (1/h) \exp [-\Delta F_i/RT] \quad [14]$$

From eq 14 it follows that the ratio of the atomic mobility in grain boundary migration to that in self-diffusion is, to within an order of magnitude, the same as the ratio of the corresponding factors $\exp [-\Delta F_i/RT]$.

Comparison of Free Energies of Activation for Self-Diffusion and Grain Boundary Migration

Primary Recrystallization: The free energy and entropy of activation in self-diffusion processes were calculated from the experimentally determined constants D_o, Q_L, and Q_B (where L refers to lattice self-diffusion and B to grain boundary self-diffusion) using eqs 13 and 8. However, in order to calculate the free energy $(\Delta F_a)_G$ and entropy $(\Delta S_a)_G$ of activation for boundry migration from the experimental constants G_o and Q_G, a value must be assigned to the "free energy" ΔF driving primary recrystallization. It has been pointed out[12] that ΔF cannot be evaluated by the methods of classical thermodynamics. However, it seems reasonable to assume that the driving energy for recrystallization is of the same order of magnitude as the energy stored in cold working, Z. According to the measurements of Taylor and Quinney[12] the maximum stored energy for metals Z_m is of the order of 25 to 50 cal per g atom and is usually reached at strains of 0.7 or more. For strains, ϵ, of the order of magnitude ($\sim$0.10) of those for which G values in recrystallization are known, it may be assumed that $Z = Z_m \epsilon/0.7$ and for most experimental conditions that are encountered in primary recrystallization:

$$Z_m\epsilon/0.7RT \sim \Delta F/RT \sim \epsilon \times 10^{\pm 1}$$

It seems probable that ΔF must be less than Z because of recovery prior to boundary migration. Due to the uncertainty in $\Delta F/RT$ the calculated $(\Delta F_a)_G$ may be in error by as much as $\pm$ 2 kcal per g atom.

In developing the theory it is assumed that the driving energy is uniformly distributed in the cold-worked matrix. More information about the state of the cold-worked matrix is needed to test this assumption. Bragg[11] and Heidenreich[13] have suggested that the cold-worked state of a crystal may consist of an aggregation of small misoriented blocks demarcated by intersecting slip planes. If it is further supposed that the strain energy is proportional to the surface area of these blocks, the theory of boundary migration driven by strain

Table I. Comparison of Energy, Entropy, and Free Energy of Activation in Self-Diffusion and Grain Boundary Migration

Substance	Strain	Grain Size, Cm	Temperature Range, °C	G_o Cm per Sec	ΔS_a (Cal per Degree, Gram Atom)			Q (Kcal per Gram Atom)			ΔF_a (Kcal per Gram Atom)		
					$(\Delta S_a)_L$	$(\Delta S_a)_G$	$(\Delta S_a)_B$	Q_L	Q_G	Q_B	$(\Delta F_a)_L$	$(\Delta F_a)_G$	$(\Delta F_a)_B$
a—Primary Recrystallization													
Aluminum[17]	0.04		425-540	4.5×10^7	9.2	22.2		37.5	34.0		30.5	17.2	
Aluminum[1]	0.051		310-370	1.5×10^{16}		60.7			59.0		32.0	21.8	
Rock salt[19]	~0.1*		650-770	9×10^{11}	18.4[21]	40		51.4[21]	59.0		33.0	19.8	
	~0.3*		400-520	4.2×10^8		23			32.0		38.0	15.0	
Copper[16]	0.10		300-320	10^{15}	14.[22]	45		57.2[22]	50.0		49.0	23.8	
			340-360	10^7		17.4			33.0		48.8	21.1	
Silicon ferrite[19]	0.07		740-800	1.7×10^{11}	13.**	37.5		59.7**	73.0		46.2	33.8	
b—Secondary Recrystallization													
Copper[7]			900-1000	10^{15}	14.	47		57.2	73.0		40.1	15.5	
Silver[6]			433-533	2×10^8	9.[24]	11.8	2[25]	46.0	28.0	20.2	39.2	19.1	18.7
c—Normal Grain Growth													
Aluminum[26]		0.03	400-500	10^{23}	9.2	93		37.5	87.0		30.8	19.7	
α brass[27] (comm. purity)		0.03	450-700	10^9		38			60.0			27.8	
α brass[27] (high purity)		0.03	450-850	10^4		15			40.0			26.0	

Superscripts except exponents of ten refer to references.
* Given data on synthetic crystal expressed as stress. Strains estimated from stress-strain curve on natural crystals.
** From data on self-diffusion on pure iron.[23]

energy is analogous to that driven by surface energy, where it is correct to suppose that ΔF is uniformly distributed.

Data are available giving G as a function of temperature and strain in the primary recrystallization of some lightly deformed polycrystalline metals[10-10, 1] and more heavily deformed single crystals of rock salt.[20] The entropy $(\Delta S_A)_G$ and free energy $(\Delta F_A)_G$ of activation for grain boundary migration have been calculated from these data and are compared with the entropy $(\Delta S_A)_L$ and free energy $(\Delta F_A)_L$ of activation for lattice self-diffusion in Table Ia. In all cases ΔF_A was calculated at the average temperature in the range of measurements.

Since no self-diffusion data for aluminum are available, Q_L was calculated from the empirical relation[24] discovered by Steigman, Shockley, and Nix[25] that $Q_L \sim 0.7$ times the heat of sublimation. D_o was estimated from this value of Q_L using the Dushman-Langmuir equation. D_L for rock salt was calculated from the anion (slowest moving ion) conductivity data[23] using eq 5. The grain boundary thickness and diffusion distance λ were assumed to be 2×10^{-8} cm in all cases.

Secondary Recrystallization: Suppose that a large grain of dimension l grows into a recrystallized matrix having a small grain size l_o. Let the grain boundary free energy between matrix grains be σ and that between the large grain and the matrix be σ'. Then if the grain growth is driven by surface tension forces only ΔF between the large grain and the matrix grains is given by:

$$\Delta F = KV\ (\sigma/l_o - \sigma'/l) \qquad [14]$$

where K is a geometric factor of the order of unity and V is the gram-atomic volume of the material. When secondary recrystallization becomes perceptible $l >> l_o$, $\sigma/l_o >> \sigma'/l$ and eq 14 becomes:

$$\Delta F = KV\sigma/l_o \qquad [15]$$

G has been measured in the secondary recrystallization of copper[2] and silver.[3] The absolute grain boundary free energy in copper has been measured absolutely in several investigations.[26-27] The results have been summarized by Fisher and Dunn[27] who suggest 600 ergs per sq cm at 800°C as the best value for grains of large orientation difference. Assuming typical experimental conditions in the secondary recrystallization of copper to be $l_o = 0.01$ cm and $T = 1000$°K it follows: *

$\Delta F/RT = K\sigma V/l_o RT \sim 10^{-3 \pm 1}$. It can be assumed that $\Delta F/RT$ in the secondary recrystallization of silver is also $\sim 10^{-3 \pm 1}$. $(\Delta S_A)_G$ and $(\Delta F_A)_G$ for secondary recrystallization calculated on the basis of these assumptions are compared with the corresponding constants for lattice and grain boundary self-diffusion in Table Ib.

Normal Grain Growth: Experimental data on normal grain growth are available from which $d\bar{l}/dt$ may be calculated as a function of temperature and grain size. Thus far it has not been possible to deduce from this data the velocity of migration of particular boundaries driven by a known free energy. For the purposes of the present calculation it will be assumed that: 1—$d\bar{l}/dt = G$; and 2—

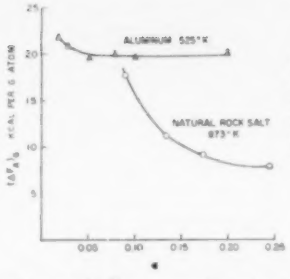

Fig. 3—Free energy of activation as a function of strain, ϵ, in the primary recrystallization of polycrystalline aluminum[1] and rock salt single crystals.[20]

$\Delta F = K\sigma V/\bar{l}$ in normal grain growth. $(\Delta F_A)_G$ calculated with these assumptions will be too large, possibly by 2 to 4 kcal per g atom. However, it will be seen that this uncertainty in $(\Delta F_A)_G$ does not affect the validity of the general conclusion drawn from the calculations. The values of the entropy and free energy of activation in normal grain growth are summarized in Table Ic.

Interpretation of the Results: The most important conclusion that follows from the comparisons made in Table I is that the free energy of activation for self-diffusion within a crystal exceeds the free energy of activation in boundary migration by a large amount (10 to 25 kcal per g atom) that is much greater than the uncertainties in the calculation in all cases.† From this result it follows that the atomic mobility in grain boundary migration, M_G, is always larger by many orders of magnitude than the atomic mobility in lattice self-diffusion M_L; e.g., in the secondary recrystallization of OFHC copper at 950°C, $M_G = 10^{8}$ compared to $M_L = 10^{2.6}$.

There is good reason to expect that the grain boundary regions in metals are highly disordered relative to regions within the body of the crystal. Since it is further supposed that diffusion is promoted by crystal imperfections, it is not surprising that $M_G >> M_L$. However, this result is not obvious from comparing Q_L with Q_G for Q_L is sometimes smaller, about the same, or larger than Q_G.

Data on the rate of self-diffusion at grain boundaries are available only for silver,[28] and it may be very significant that the free energy of activation $(\Delta F_A)_S$ agrees closely with the free energy of activation $(\Delta F_A)_G$ in the secondary recrystallization of silver. This fact suggests the possibility that the generalization $(\Delta F_A)_S = (\Delta F_A)_G$ holds for grain boundary migration processes driven by interfacial tension. The results also suggest that the generalization $(\Delta F_A)_S \cong (\Delta F_A)_G$ holds for primary recrystallization.

$(\Delta F_A)_G$ at 625°K as a function of strain has been calculated for Anderson and Mehl's[1] data on the primary recrystallization of aluminum and plotted in Fig. 3. For $0.2 > \epsilon > 0.05$, $(\Delta F_A)_G$ is independent of ϵ. However, between $\epsilon = 0.02$ and 0.05 $(\Delta F_A)_G$ decreases about 2 kcal per g atom, a number that is about 1000 times larger than the stored energy of cold working, Z. Also shown in Fig. 3 is $(\Delta F_A)_G$ vs. ϵ calculated from Muller's data[20] on the primary recrystallization of rock salt crystals at 600°C. It is evident that $(\Delta F_A)_G$ is much more strain-sensitive for rock salt single crystals than for polycrystalline aluminum.

It might be inferred from inspection of the constants Q_G and $(\Delta S_A)_G$ that the G values in the three investigations on aluminum are in wide disagreement. Actually $(\Delta F_A)_G$ values for the temperatures

* Because of the small orientation differences of neighboring grains $\sigma < 600$ for cube texture copper. However, in view of the sharp increase in σ with increasing misorientation, θ,[29] an uncertainty no greater than a factor of 2 results from assuming $\sigma \sim 600$.

† The comparisons were not made for α brass because of the uncertainty in the interpretation of the diffusion data.

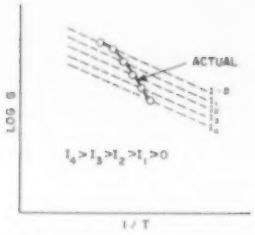

Fig. 4 — Representation of log G vs. 1/T for various degrees of dispersion (I) of inclusions at grain boundaries.

at which the measurements nearly overlap approximately agree. At 400°C for $\epsilon = 0.05$, Anderson-Mehl's[1] results give $(\Delta F_s)_a = 18.0$ compared to 19.0 kcal per g atom obtained by Kornfeld-Pavlov[17] for $\epsilon = 0.04$. These values are in reasonable agreement with $(\Delta F_s)_a = 24.5$ kcal per g atom for normal grain growth in aluminum at 400°C[36] in view of the fact that the theory as now formulated gives too large a value to $(\Delta F_s)_a$ in normal grain growth.

Though the atomic mobility in grain boundary migration is many times larger than in lattice self-diffusion, the activation energy for the former process is often as great and sometimes even greater than for the latter process. These relations are consistent with the fact that the entropy of activation in boundary migration is generally 10 to 30 entropy units larger than in lattice self-diffusion. On the basis of the arguments used to account for $(\Delta F_s)_L > (\Delta F_s)_a$, it would be expected that $Q_L > Q_a$. Also there is no obvious reason for the entropies of activation for the two processes to be very different.

In order to account for these seeming anomalies Mott[7] has proposed the hypothesis that activation for grain boundary migration consists in melting several (n) atoms at the boundary. According to this view the energy of activation for boundary migration is the energy necessary to fuse n atoms:

$$Q_a = nQ_f \qquad [16]$$

where Q_f is the gram-atomic heat of fusion and may therefore bear no simple relation to Q_L (or Q_a). On this picture the entropy of activation is the entropy gain in melting n atoms:

$$(\Delta S_s)_a = n\Delta S_f \qquad [17]$$

where ΔS_f is the entropy of fusion.‡ n may be a function of strain, temperature and relative grain and boundary orientations. Mott's theory reduces the number of disposable parameters from $(\Delta S_s)_a$ and Q_a to n only and can be tested by comparing $(\Delta S_s)_a$ with n (ΔS_f) where n is calculated from Q_a using eq 16. Mott showed that the theory accounts for the entropy of activation calculated from Anderson's and Mehl's data on aluminum and Smoluchowski[36] has shown that the theory accounts for the grain growth data of Beck, Holzworth, and Hu[36] on pure aluminum and of Burke[31] on α brass of commercial purity.

In order to make a comparison of $n\Delta S_f$ and $(\Delta S_s)_a$ strictly in conformity with Mott's theory, it is necessary to modify the calculation of $(\Delta S_s)_a$ by substituting $n\Delta F$ for ΔF in eq 11, since n atoms are transported in the elementary process. The values of the entropy of activation for boundary migration $(\Delta S_s)_a'$ so calculated from all the available data are compared with $n\Delta S_f$ and $(\Delta S_s)_L$ in Table II.

Though $(\Delta S_s)_a'$ and $n\Delta S_f$ diverge widely in a few instances the comparisons in Table II indicate that Mott's theory in general successfully accounts for the unexpectedly large values of $(\Delta S_s)_a'$. In addition to the divergences noted the main objection to the theory as it now stands is the arbitrariness of the n values. Also in view of the small values of n (<35) it is not correct to ignore surface energy considerations in calculating the free energy of melting. On an energetic basis n should be unity if the surface energy is neglected.

One of the basic assumptions of the theory developed is that the driving energy does not change with temperature. An alternative theory for the large magnitude of the calculated $(\Delta S_s)_a$ values is that they are more apparent than real due to a marked dependence of ΔF upon temperature. ΔF might change markedly with temperature due to matrix processes of recovery, grain growth, or solution of boundary retarding inclusions concurrent with boundary migration. Among these processes only the solution of inclusions is likely to lead to apparent values of $(\Delta S_s)_a$ that are much greater than the actual values.

Following Zener[37] ΔF for boundary migration retarded by inclusions may be expressed as:

$$\Delta F = (\Delta F' - K\sigma\rho V/\gamma_s) = \Delta F' - I \qquad [18]$$

where $\Delta F'$ is the driving free energy in the absence of inclusions, ρ is the volume fraction of inclusions in the matrix, and γ_s is the radius of the inclusion. In general I is likely to be a function that decreases with increasing time or temperature. However, suppose that at constant temperature I reaches a constant value in a time that is short relative to the period of boundary migration. Then with respect to boundary migration, I is a function of temperature only and G is independent of time. In Fig. 4 log G is represented schematically as a function of 1/T for various constant values of I, each characteristic of a different temperature. This family of curves all have the same value of Q_a, but apparently different values of $(\Delta S_s)_a$ that may be quite small. However, since $I = f(T)$ the observed relation for log $G = f(1/T)$ will be schematically as shown by the solid curve through the circles and the apparent values of Q_a and $(\Delta S_s)_a$ will be much larger than those characteristic of $I = 0$.

The inclusion hypothesis predicts that Q_a and $(\Delta S_s)_a$ may decrease as temperature increases due to the progressive solution of inclusions. Ward[6] has found that Q_a and $(\Delta S_s)_a$ do markedly decrease in the secondary recrystallization of cube texture copper as the melting point is approached. Also the results of Burke[31] show that Q_a and $(\Delta S_s)_a$ for grain growth are much smaller for high purity than for commercial purity α brass.

In primary recrystallization $\Delta F'$ probably is very much larger with respect to I than in boundary migration processes driven by surface energy. Suppose that it is known that primary recrystallization occurs at a given temperature, T_1, at a strain of 0.02. Then if Z is proportional to ϵ, as assumed, the inclusions should have a negligible effect in retarding boundary migration at T_1 for a strain of 0.10. Thus, unless the strain energy is greatly reduced by recovery processes, inclusions should be effective in retarding boundary migration in primary recrystallization only when ϵ is very small and $(\Delta S_s)_a$ and Q_a calculated when ϵ is relatively large should approach the real values. In the recrystallization of rock salt single crystals $(\Delta S_s)_a$ and Q_a are very

‡ Mott's formulation has been altered somewhat in order to make it conform to the absolute rate theory.

Table II. Values of Entropy of Activation for Boundary Migration

Substance	Process	Temperature Range	Strain	n	$(\Delta S_i)_L$	$(\Delta S_i)_\alpha$	$n\Delta S_f$
Aluminum[12]	Primary recrystallization	425-540	0.04	13.3		17	36
Aluminum[1]	Primary recrystallization	310-370	0.051	23	9.2	55	63
Aluminum[20]	Grain growth	400-500		34		86	93
Rock salt[20]	Primary recrystallization	650-770	~0.1	8	18.4	36	55
	Primary recrystallization	400-520	~0.3	4.4		20	30
Copper[16]	Primary recrystallization	300-320	0.10	16		39.5	37
	Primary recrystallization	340-360	0.10	10.3	14	13	24
Copper[2]	Secondary recrystallization	900-1000		23.4		41	34
Silicon ferrite[19]	Primary recrystallization	740-800	0.07	20.5	13	31.5	40.5
Silver[3]	Secondary recrystallization	433-533		10.4	9	7	23
α brass[21] (comm. purity)	Grain growth	450-700		21.6*		32	52
α brass[21] (high purity)	Grain growth	450-850		15*		9.6	35

* Entropy and heat of fusion calculated by atomic fraction averaging of corresponding constants for pure metals.

large for small strains (see Table I) and fall sharply as the strain is increased. More direct support for the hypothesis that inclusions often significantly retard boundary migration in primary recrystallization as well as in normal grain growth is furnished by the observations of Muller[20] that the boundaries move in spurts in the primary recrystallization of rock salt.

However, Anderson and Mehl's results on the primary recrystallization of pure aluminum show that at 625°K, for example, Q_o and $(\Delta S_i)_o$ are practically as large for a strain of 0.10 as for a strain of 0.02. These results cannot be reconciled with the inclusion hypothesis, unless it is supposed that recovery reduces the energy of cold working to a value almost independent of strain before boundary migration begins.

Summary

1—The relation between grain boundary migration rates and diffusion coefficients is derived on the basis of the absolute reaction rate theory.

2—It is shown that in lattice self-diffusion the free energy of activation greatly exceeds that in grain boundary migration.

3—A corollary of 2 is that in grain boundary migration the atomic mobility is many orders of magnitude larger than in lattice self-diffusion.

4—In silver the free energy of activation for grain boundary self-diffusion equals that for grain boundary migration, within the experimental uncertainty.

5—The apparent entropy of activation for boundary migration is much larger than for self-diffusion processes.

6—An explanation for the unexpectedly large entropy of activation in boundary migration processes is given based on the concept that inclusions retarding boundary migration become less effective at elevated temperature due to their solution and coalescence.

References

[1] W. A. Anderson and R. F. Mehl: *Trans.* AIME (1945) **161**, p. 140.

[2] R. Ward: General Electric Co. Report (1947).

[3] F. D. Rosi and B. H. Alexander: JOURNAL OF METALS (October 1950) p. 1217.

[4] P. A. Beck, P. R. Sperry, and H. Hu: *Journal of Applied Physics* (1950) **21**, p. 420.

[5] D. Turnbull: Atom Movements Seminar. ASM (1951).

[6] M. Volmer: *Kinetik der Phasenbuldung.* (1939). Dresden. Steinkopf.

[7] D. Turnbull: Thermodynamics in Physical Metallurgy. ASM (1950) p. 282.

[8] G. Borelius, F. Pihlstrand, J. Andersson, K. Gullberg, D. Glansholm, and M. Ekedahl: *Arkiv For Fysik* (Stockholm) (1949) p. 305.

[9] N. F. Mott: *Proc.* Physical Soc. (London) (1948) **60**, p. 391.

[10] R. Smoluchowski: N.R.C. Conference on Imperfections (1950).

[11] S. Glasstone, K. J. Laidler, and H. Eyring: *The Theory of Rate Processes.* (1941) New York. McGraw-Hill Book Co.

[12] P. W. Bridgman: *Reviews of Modern Physics* (1950) **22**, p. 56.

[13] G. I. Taylor and H. Quinney: *Proc.* Royal Soc. (London) (1934) **143A**, p. 307; ibid. (1937) **163A**, p. 157.

[14] W. L. Bragg: *Nature* (1942) **149**, p. 511.

[15] R. D. Heidenreich: *Journal of Applied Physics* (1949) **20**, p. 993.

[16] R. Karnop and G. Sachs: *Ztsch. Physik* (1930) **60**, p. 464.

[17] M. Kornfeld and W. Pavlov: *Physik. Zeit. Sowietunion* (1934) **6**, p. 537; ibid. (1937) **12**, p. 658.

[18] J. K. Stanley and R. F. Mehl: *Trans.* AIME (1942) **150**, p. 260.

[19] J. K. Stanley: *Trans.* AIME (1945) **162**, p. 116.

[20] H. G. Muller: *Ztsch. Physik* (1935) **96**, p. 279.

[21] A. Smekal: *Handbuch der Physik* (1933) **24**, No. 2, p. 883.

[22] J. Steigman, W. Shockley, and F. C. Nix: *Physical Review* (1939) **56**, p. 13.

[23] F. S. Buffington, I. D. Bakalar, and M. Cohen: *The Physics of Powder Metallurgy.* Edited by W. E. Kingston, pp. 92-109. (1951) New York. McGraw-Hill Book Co.

[24] W. A. Johnson: *Trans.* AIME (1941) **143**, p. 107.

[25] G. L. J. Bailey and H. C. Watkins: *Proc.* Physical Soc. (London) (1950) **63B**, p. 350.

[26] G. W. Sears: *Journal of Applied Physics* (1950) **21**, p. 721.

[27] L. H. VanVlack: Thesis, University of Chicago (1950).

[28] J. C. Fisher and C. G. Dunn: N.R.C. Conference on Imperfections (1950).

[29] R. E. Hoffman and D. Turnbull: *Journal of Applied Physics* (1951) **22**, p. 634.

[30] P. A. Beck, M. L. Holzworth, and H. Hu: *Physical Review* (1948) **73**, p. 526.

[31] J. E. Burke: *Trans.* AIME (1949) **180**, p. 73; METALS TECHNOLOGY (October 1948).

[32] C. Zener: Private Communication to C. S. Smith, *Trans.* AIME (1948) **175**, p. 15; METALS TECHNOLOGY (June 1948).

Effects of Manganese and Its Oxide On Desulphurization by Blast-Furnace Type Slags

by Nicholas J. Grant, Ulf Kalling, and John Chipman

THE operation of a blast furnace is dependent to an important extent upon the sulphur content of materials charged and the desired limit of sulphur in the product. It has long been known that the blast furnace is the most efficient tool for desulphurization in common use and that this efficiency is associated with the strongly reducing conditions of the hearth and is enhanced by increased basicity and fluidity of the slag. The chemical reactions of desulphurization may be studied from the viewpoint of the ratio of the process or of the final equilibrium conditions. Both kinds of studies contribute to an understanding of the process and both are included here.

A simple measure of the desulphurization power of a slag is given by the ratio:

$$\frac{\text{Pct sulphur in slag}}{\text{Pct sulphur in metal}} = \frac{(\text{Pct S})}{[\text{Pct S}]}$$

This ratio was used by Holbrook and Joseph[1, 2] to measure relative desulphurizing powers under controlled laboratory conditions. It was also used by Hatch and Chipman[3] as a measure of the equilibrium distribution. For the latter purpose it would be preferable to employ thermodynamic activities rather than percentages, but until very recently this has been impossible for lack of data. Now, thanks to the work of Morris and Williams[4] and Morris and Buehl,[5] the effects of carbon and silicon upon the activity of sulphur in the metal are known. The confirmation of this work and its extension to include the effects of other elements by Sherman and Chipman[6] and by Rosenqvist and Cox[7] make it possible to calculate the activity of sulphur in pig iron of any composition. Hence it is now possible to use data on the equilibrium distribution of sulphur to find its activity in the liquid slag and to approach an ultimate solution of the thermodynamic aspects of the problem.

The rate of transfer of sulphur from metal to slag is the problem of major industrial importance and indeed the principal need for equilibrium data has been as a necessary adjunct to the kinetic studies. The rate of approach to equilibrium under laboratory conditions seems slow compared to the requirements of industrial practice, and it is clear that further laboratory studies of rates are needed.

In the research reported below, the items which were investigated were the following: 1—The role of mechanical stirring on the approach to equilibrium. 2—The role of MgO in desulphurization as compared to CaO. 3—The role of MnO in desulphurization. 4—The limiting reactions which constitute the slow steps in desulphurization.

Experimental Procedure

The experimental set-up and procedure previously described by Hatch and Chipman[3] were essentially followed with several small modifications. The graphite crucible containing the slag and metal charge was altered to provide considerably more

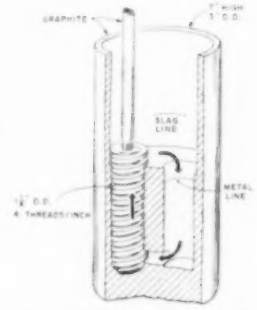

Fig. 1—Modified graphite stirrer and crucible.

active stirring and mixing of the slag and metal in the carbon monoxide atmosphere. For this purpose the crucible was machined to provide two deep cylindrical wells which were interconnected at top and bottom as shown in Fig. 1. A graphite screw with a flat thread and of shallow pitch (4 threads per in.) spinning at 600 to 800 rpm was used to lift the slag and metal over the partition between the two wells and throw them over into the second well, where the metal settled through the slag into the reservoir at the bottom. It was possible to see actual particles of slag and metal being thrown over the partition. In this respect, the stirring was more vigorous than used in the work of Hatch and Chipman.

A charge of 400 g of wash metal was first melted, and 20 g of FeS was then added to yield a bath containing 1.65 pct S. Immediately 400 g of slag (as pure mixed oxides) was added and fused. The slag was generally fused in 1 hr ± 10 min. Within 30 to 45 min after melting, the temperature was adjusted to 1525°C, and the first slag and metal samples were taken. The slag was picked up on the end of a cold Armco iron rod, whereas the metal was sucked into a silica tube.

The wash metal composition was (in percent): 4.29 C; 0.022 S; 0.021 P; 0.38 Si. The slags used were of four fixed starting compositions covering a wide range of acid-base ratios shown in Table I. Deliberate variations in MgO were made in these slags to check the role of MgO in blast-furnace desulphurization. Changes due to additions and reactions were followed by analysis of samples.

Additions of Mn and MnO were made to most of the heats to note the role of Mn and MnO on desulphurization. Three heats (62 through 64) were made in an open pot induction crucible (graphite) using a

N. J. GRANT and J. CHIPMAN, Members AIME, are associated with the Department of Metallurgy, Massachusetts Institute of Technology, Cambridge, Mass. U. KALLING is associated with Avesta Steel Works, Avesta, Sweden.

Discussion on this paper, TP 3108C, may be sent, 2 copies, to AIME by Oct. 1, 1951. Manuscript, Feb. 9, 1951. St. Louis Meeting, February 1951.

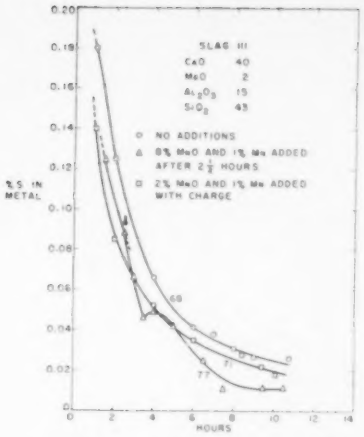

Fig. 2 (left)—Desulphurization of iron by slag III at 1525°C as a function of time.

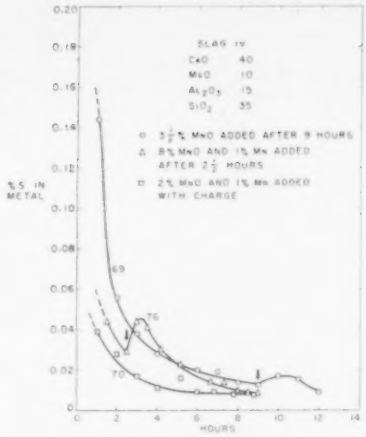

Fig. 3 (right)—Desulphurization of iron by slag IV at 1525°C as a function of time.

slag virtually free of SiO_2 to study the role of Si and SiO_2 on desulphurization. A carbon monoxide atmosphere at an excess pressure of ½ to 1 in. of water was kept constantly over the melt.

Optical temperatures were read frequently throughout the course of a heat by sighting down the graphite tube (stirring shaft) to which the immersed stirrer head was attached. Periodic checks with a platinum thermocouple established the temperature errors to be ±5°C, and deviation from 1525° during a run seldom exceeded this figure.

The stirrer was started as soon as the slag was molten, and this point was taken as zero time.

The compositions of the slag and metal samples are shown in Table II. Table III shows the nature and the time of the additions made to each slag.

The Effect of Slag Basicity: The sulphur content of the metal is plotted against the heat time at 1525°C for each grade of slag in Figs. 2 to 5 with Fig. 2 being slag III, the most acid and Fig. 5 being slag II, the most basic. Zero time is the time when the slag is first judged to be molten. For heats 66 through 80 the time from "start to add cold slag" to "slag molten" ranged from 35 to 65 min except heat 73 which took 120 min.

In each of Figs. 2 to 5 there is a "no addition" heat and these are compared in Fig. 6 from which it is very apparent that the basicity of the slag is an extremely important factor in controlling the speed of the desulphurization reactions and the final sulphur content of the metal. An approximate relationship between basicity, as measured by "Excess CaO" and the time required to read equilibrium is shown in Table IV.

Effect of Stirring: While there is no direct measure of the difference in stirring effectiveness in the present heats compared to those of Hatch and Chipman,[3] it is believed from observations that the present stirring method was much more vigorous. Nevertheless, the time to reach sulphur equilibrium for similar heats of the acid type in both groups of experiments was of the same order, indicating that for these rather fluid slags the added surface content was not too important a factor in the speed of the reactions. The initial desulphurization rate for all slags must be unusually high since the metal contains 1.65 pct S at the start and drops to the levels shown as the first values in Figs. 2 to 5 in 1 to 2 hr.

Role of MnO in Blast-Furnace Slags: Figs. 2 to 5 show the effects of Mn and MnO when added to the initial charge or during the course of a heat. The arrow in each figure shows the time of the addition. When added during the heat, a very interesting and important effect is noted in that immediately after the addition of MnO there is for each slag and in every instance a reversion of sulphur into the metal. These 4 heats are shown in Fig. 7. The full extent of the reversion is not accurately determined because a sufficient number of samples were not taken during this period.

The cause of the sulphur reversion can be ascribed but to one effect and that is the temporary reoxidation of the slag through the reduction of MnO. This is especially interesting when it is considered that MnO is a basic oxide; the expected beneficial effect of the basic addition has been overshadowed by the adverse effect of oxidation. The same or greater effect could have been achieved by the addition of the more easily reducible oxide FeO to the slag which is known to affect adversely the desulphurizing power of slags of this type.[4] It will be noted that recovery of the system from the oxygen addition is more rapid the more basic the slag.

Table II shows that most of the MnO is reduced to Mn in the metal. The maximum MnO remaining in any of the heats (nonequilibrium) is only 1.3 pct in the most acid slag while Mn in the metal runs as high as 5 pct.

Of great current interest is the effect of basicity on the MnO reduction from the slag. Manganese recovery is defined as the ratio of Mn in the metal to total manganese. This ratio is plotted in Fig. 8 against Excess Base. A very similar curve was obtained using Excess CaO with about the same degree of scatter of points. Fig. 8 shows that with the most basic slags a recovery of about 96 pct of the manganese may be achieved, under near-equilibrium conditions. The most acid slag with essentially zero Excess Base shows 82 pct Mn recovery. The curve

Table I. Starting Slag Compositions

Slag No.	CaO	MgO	SiO_2	Al_2O_3
I	50	2	33	15
II	50	10	25	15
III	40	2	43	15
IV	40	10	35	15

Table II—Compositions of Slag and Metal Samples Taken at 1525°C

Heat No., Slag No.	Sample	Time	Metal, Wt Pct C	Mn	Si	S	Slag, Wt Pct S	CaO	MgO	SiO_2	Al_2O_3	MnO	FeO
64	1	0:40	—	—	—	0.006	—	—	—	—	—	—	—
	2	1:40	—	—	—	0.004	—	—	—	—	—	—	—
	3	2:30	—	—	—	0.003	1.15	50.00	—	1.34	48.55	—	0.090
	4	3:00	—	—	—	0.004	—	—	—	—	—	—	—
	5	3:45	—	—	—	0.0044	—	—	—	—	—	—	—
	6	4:20	—	—	—	0.0045	1.24	45.87	—	9.16	44.56	—	0.140
65 II	1	0:25	—	—	0.07	0.012	1.66	48.13	10.24	25.64	16.32	—	—
	2	1:30	—	—	0.15	0.008	1.68	—	—	25.74	—	—	—
	3	3:30	—	—	—	0.008	—	—	—	—	—	—	—
	4	4:30	—	—	0.22	0.005	1.68	—	—	25.52	—	—	—
	5	5:30	—	—	—	0.0084	—	—	—	—	—	—	—
	6	6:30	—	—	0.28	0.004	1.71	48.79	9.90	25.48	15.92	—	0.025
68 III	1	1:00	—	—	0.61	0.18	1.48	36.20	2.33	43.18	17.74	—	—
	2	2:00	—	—	0.96	0.125	1.54	—	—	42.60	—	—	—
	3	4:00	—	—	1.72	0.066	1.59	—	—	41.56	—	—	—
	4	6:00	—	—	—	0.0415	—	—	—	—	—	—	—
	5	7:00	—	—	2.77	0.038	1.64	—	—	40.06	—	—	—
	6	8:00	—	—	—	0.031	—	—	—	—	—	—	—
	7	9:00	—	—	3.28	0.027	1.66	—	—	39.16	—	—	—
	8	10:00	—	—	3.65	0.026	1.68	39.21	2.35	38.56	16.28	—	0.072
69 IV	1	1:00	—	—	0.19	0.144	1.55	34.80	10.38	35.42	17.08	—	—
	2	2:00	—	—	0.32	0.056	1.64	—	—	35.20	—	—	—
	3	3:00	—	—	0.50	0.038	1.65	—	—	35.08	—	—	—
	4	4:15	—	—	0.78	0.028	—	—	—	—	—	—	—
	5	6:15	—	—	1.12	0.020	1.67	—	—	34.20	—	—	—
	6	7:15	—	—	1.23	0.019	—	—	—	—	—	—	—
	7	8:15	—	—	1.32	0.014	—	—	—	—	—	—	—
	8	9:15	—	—	1.45	0.0126	1.72	—	—	33.60	—	—	—
	9	10:15	—	1.39	1.19	0.017	—	—	—	—	—	1.26	0.123
	10	11:15	—	1.79	1.26	0.0155	—	—	—	—	—	0.70	0.073
	11	12:15	—	1.84	1.28	0.009	1.67	38.30	10.07	34.20	14.78	0.51	0.071
70 IV	1	1:00	5.08	1.38	0.22	0.039	—	—	—	—	—	0.87	0.132
	2	2:00	4.88	1.60	0.67	0.028	—	—	—	—	—	0.64	—
	3	3:00	4.82	1.77	1.05	0.017	—	—	—	—	—	0.46	—
	4	4:00	4.75	1.81	1.25	0.011	—	—	—	—	—	0.46	—
	5	5:10	4.50	—	1.50	0.020	—	—	—	—	—	—	—
	6	6:00	4.64	1.81	1.54	0.009	—	—	—	—	—	—	0.086
	7	6:50	—	—	1.67	0.010	—	—	—	—	—	—	0.080
	8	7:50	4.73	1.84	1.74	0.009	—	—	—	—	—	0.37	0.072
	9	8:50	4.64	1.87	1.81	0.009	1.65	39.61	10.16	33.60	17.90	0.31	—
71 III	1	1:00	—	—	0.57	0.14	—	—	—	—	—	—	—
	2	2:00	—	—	1.15	0.085	—	—	—	—	—	—	—
	3	4:00	—	—	1.68	0.052	—	—	—	—	—	—	—
	4	6:05	—	—	2.16	0.035	—	—	—	—	—	—	—
	5	7:00	—	—	2.44	0.041	—	—	—	—	—	—	—
	6	8:30	—	—	3.19	0.028	—	—	—	—	—	—	—
	7	9:30	—	—	3.65	0.022	—	—	—	—	—	—	—
	8	10:15	—	—	—	0.018	—	—	—	—	—	—	—
72 I	1	0:30	5.13	1.35	0.21	0.027	—	—	—	—	—	0.89	—
	2	1:00	—	1.49	—	0.017	—	—	—	—	—	0.57	—
	3	2:00	5.08	1.56	0.48	0.011	—	—	—	—	—	0.57	—
	4	3:00	5.02	1.63	0.63	0.008	—	—	—	—	—	0.38	0.115
	5	4:00	5.00	1.80	0.72	0.010	—	—	—	—	—	0.36	0.071
	6	5:00	—	1.82	—	0.010	—	—	—	—	—	0.34	0.074
	7	6:00	4.95	1.93	1.17	0.008	1.61	—	—	32.60	—	0.33	0.097
	8	7:00	—	2.02	—	0.009	—	—	—	—	—	1.11	0.082
	9	8:00	—	3.15	—	0.0085	—	—	—	—	—	0.64	0.068
	10	10:00	4.93	3.26	1.08	0.007	1.61	47.98	2.06	32.14	15.72	0.52	0.090
73 II	1	0:15	5.12	1.41	0.06	0.016	1.63	47.15	9.39	26.06	15.62	0.64	—
	2	0:40	4.99	1.62	—	0.006	1.70	—	—	26.56	—	0.34	—
	3	1:40	5.15	1.88	0.11	0.006	1.74	—	—	26.14	—	0.14	—
	4	2:40	—	1.85	—	0.005	—	—	—	—	—	0.16	—
	5	3:40	—	1.77	—	0.004	—	—	—	—	—	0.08	—
	6	4:40	5.18	2.96	0.11	0.004	1.68	—	—	26.82	—	0.30	—
	7	5:40	—	—	—	0.004	—	—	—	—	—	—	—
	8	6:40	5.09	3.42	0.22	0.004	1.65	47.21	9.75	26.20	16.50	0.25	0.087
74 I	1	0:30	—	—	0.14	0.037	1.67	47.29	2.33	33.80	17.42	—	0.187
	2	0:65	—	—	0.32	0.022	1.63	—	—	33.88	—	—	—
	3	1:65	—	—	—	0.015	—	—	—	—	—	—	—
	4	2:65	—	—	0.88	0.015	1.64	—	—	33.16	—	—	—
	5	4:10	—	—	1.19	0.0084	1.65	—	—	32.72	—	—	—
	6	5:10	—	—	—	0.009	—	—	—	—	—	—	—
	7	6:10	—	—	—	0.007	—	—	—	—	—	—	—
	8	7:10	—	—	1.47	0.007	1.66	49.41	2.41	32.06	15.58	—	0.058
75 I	1	0:30	—	—	—	0.029	—	—	—	—	—	—	0.109
	2	1:30	—	—	—	0.021	—	—	—	—	—	—	0.160
	3	2:00	—	4.01	—	0.025	—	—	—	—	—	3.00	0.136
	4	2:35	—	4.12	—	0.021	—	—	—	—	—	2.80	0.150
	5	2:65	—	4.41	—	0.014	—	—	—	—	—	2.36	0.125
	6	3:65	—	4.71	—	0.0135	—	—	—	—	—	1.80	0.127
	7	4:65	—	4.87	—	0.011	—	—	—	—	—	1.47	0.122
	8	5:65	—	5.04	—	0.007	—	—	—	—	—	1.23	0.075
	9	6:65	—	5.10	—	0.0054	—	—	—	—	—	0.95	0.089
	10	7:65	—	5.08	—	0.0064	—	—	—	—	—	0.80	0.124
	11	8:50	4.97	5.32	0.96	0.0067	1.50	48.30	2.07	32.52	16.08	0.87	0.105
	12	9:20	—	4.93	—	—	—	—	—	—	—	0.82	0.102
76 IV	1	1:30	—	—	—	0.044	—	—	—	—	—	—	—
	2	2:30	—	—	—	0.029	—	—	—	—	—	—	—
	3	3:00	—	3.65	—	0.044	—	—	—	—	—	2.60	—
	4	3:30	—	4.03	—	0.041	—	—	—	—	—	2.63	—
	5	4:10	—	4.36	—	0.030	—	—	—	—	—	2.22	—
	6	5:10	—	4.38	0.023	0.023	—	—	—	—	—	1.88	0.107
	7	6:40	—	4.51	—	0.014	—	—	—	—	—	1.35	—
	8	7:20	—	4.72	—	0.014	—	—	—	—	—	1.21	0.080
	9	8:00	—	4.84	—	0.010	—	—	—	—	—	1.14	0.055
	10	8:30	—	4.97	—	0.009	—	—	—	—	—	1.29	—
	11	9:00	—	5.07	1.37	0.009	1.61	39.30	9.87	33.38	14.52	0.92	0.065

Table II (Cont.)—Compositions of Slag and Metal Samples Taken at 1525°C

Heat No., Slag No.	Sample	Time	Metal, Wt Pct				Slag, Wt Pct						
			C	Mn	Si	S	S	CaO	MgO	SiO_2	Al_2O_3	MnO	FeO
77 III	1	1:30	—	—	—	0.124	—	—	—	—	—	—	—
	2	2:30	—	—	—	0.088	—	—	—	—	—	—	—
	3	3:05	—	1.14	—	0.066	—	—	—	—	—	3.64	—
	4	3:35	—	3.46	—	0.046	—	—	—	—	—	3.34	—
	5	4:05	—	3.27	—	0.049	—	—	—	—	—	3.06	—
	6	5:05	—	3.89	—	0.042	—	—	—	—	—	2.59	—
	7	6:35	—	4.29	—	0.025	—	—	—	—	—	2.17	—
	8	7:35	—	4.26	—	0.011	—	—	—	—	—	2.01	—
	9	8:35	—	—	—	0.019	—	—	—	—	—	—	—
	10	9:35	—	—	—	0.0115	—	—	—	—	—	—	—
	11	10:35	4.13	4.66	3.46	0.0115	1.50	41.51	2.21	37.90	17.76	1.32	0.094
79 II	1	0:25	—	—	—	0.004	—	—	—	—	—	—	—
	2	0:50	—	—	—	0.004	—	—	—	—	—	—	—
	3	1:15	—	—	0.40	0.004	1.65	48.00	10.03	25.72	15.06	—	0.132
80 II	1	0:05	—	0.015	—	0.028	—	—	—	—	—	0.056	—
	2	0:20	—	0.038	—	0.006	—	—	—	—	—	0.014	—
	3	0:40	—	3.04	—	0.015	—	—	—	—	—	4.86	—
	4	1:00	—	3.93	—	0.010	—	—	—	—	—	2.83	—
	5	1:20	—	4.37	—	0.0065	—	—	—	—	—	1.80	—
	6	1:50	—	4.02	—	0.005	—	—	—	—	—	1.13	—
	7	3:00	—	5.08	—	0.0044	—	—	—	—	—	0.63	—
	8	4:00	—	5.14	—	0.0044	—	—	—	—	—	0.55	—
	9	5:00	5.21	5.24	0.22	0.0046	1.66	46.41	11.56	26.80	13.72	0.44	0.135

shown in Fig. 8 does not represent equilibrium values, since MnO was still in the process of being reduced as shown in Fig. 9.

The effect of manganese on both desulphurization rate and equilibrium is very small and is confined to the two less basic slags. Disregarding the heats in which MnO was added during the experiment and considering only those in which Mn and MnO were included in the charge, the curves of the most acid slags shown in Figs. 2 and 3 indicate that the time required to reach a given sulphur level is slightly shortened by the addition. At the same time the final distribution is slightly improved; this is evident in the most acid slag where the effect is greatest.

If the "manganese recovery ratio" is plotted against time, the curves shown in Fig. 9 for the 4 types of slags are obtained. These curves show the approach to manganese equilibrium with time as a function of basicity. As would be expected, the most basic slag (II) approaches equilibrium most rapidly, but even at 96 pct recovery has not reached equilibrium. The break in the curves for slags II and IV is due to a 2 pct MnO addition to the slag, and shows that the MnO is rapidly reduced. Heat 77 (slag III) did not have Mn and MnO charged initially as did the others and so does not have the same "zero."

The curves of Fig. 9 are almost a mirror image of the curves of Figs. 6 and 7 for desulphurization, the transfer of manganese and sulphur being in opposite directions. This suggests that MnO in the slag or the manganese recovery ratio might be a useful indicator for estimating the basicity of the slag but especially its degree of oxidation.

FeO is too easily reduced, leaving quantities of less than 0.1 pct in the slag. Such a small amount is too difficult to analyze correctly. MnO, on the other hand, is less readily reduced than FeO, is more easily analyzed, and approaches equilibrium in about the same time as sulphur.

Values of "manganese recovery ratio" for the blast furnace strongly suggest that in the blast furnace the slags are not as thoroughly reduced as the slags reported in this research (for a given basicity). This would correspond to a higher degree of oxidation of the slag, causing the lower desulphurization ratios noted in the blast furnace compared to comparable basic slags reported in this work.

Effect of MgO: One of the aims of this research was to establish the effect of MgO on the desulphurizing power of the slag. For this purpose the starting slags were made up with 2 or 10 pct MgO. Since the principal desulphurizing oxide is known to be CaO, the subsidiary effect of MgO can be found by comparing slags with or without this component. The comparison is shown in Fig. 10 where the ratio (pct S)/[pct S] in the final samples is plotted against

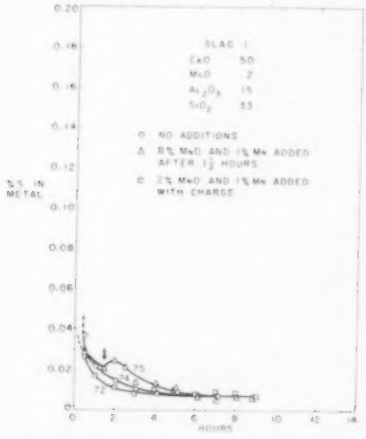

Fig. 4 (left)—Desulphurization of iron by slag I at 1525°C as a function of time.

Fig. 5 (right)—Desulphurization of iron by slag II at 1525°C as a function of time. Inset based on expanded sulphur scale.

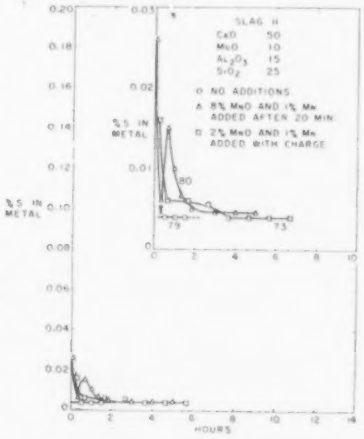

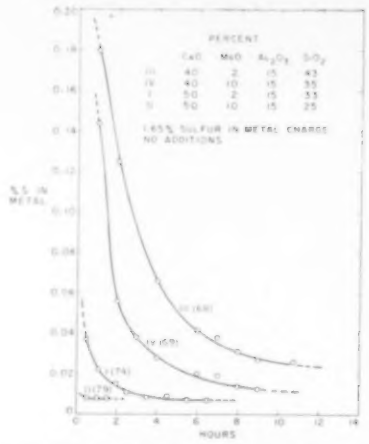

Fig. 6 (left)—Comparison of slags I to IV showing pronounced effect of slag basicity on rate of sulphur removal and final sulphur. All "no addition" heats.

Fig. 7 (right)—Comparison of slags I to IV wherein Mn and MnO are added during the heat.

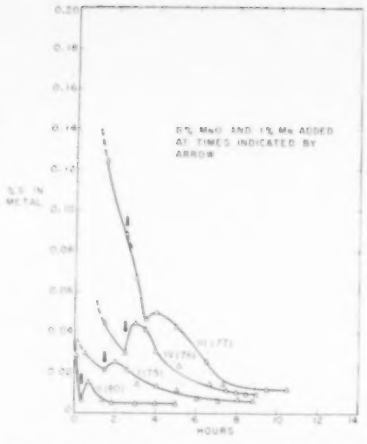

Excess Base. The latter is defined here as the excess number of mols of CaO + MgO, per mol of slag, over and above that required to form compounds of the type $CaSiO_3$ and $CaAl_2O_4$. The straight line is taken from Sherman and Grant's[6] treatment of Hatch and Chipman's[3] data, adjusted slightly for the difference in temperature. The points for 2 pct MgO fall slightly below this line, those for 10 pct considerably below. The one point for a simple lime-alumina slag is on the line.

Fig. 11 is a plot of the same points as in Fig. 10 except that basicity is expressed as "Excess CaO" as defined by Sherman and Grant.[6] The solid line is the same line as the Zero MgO line of Fig. 10; and it is to be noted that the points fall uniformly about this line within the limits of an error of 0.001 pct S in the metal which is represented by the dashed lines. For comparison, the curve at 1500°C based on the work of Hatch and Chipman is also included (dotted line).

There is no preferential grouping of points in Fig. 11 on the basis of MgO content. Thus Figs. 10 and 11 confirm that whereas MgO is equal to CaO on a molar basis in the neutralization of Al_2O_3 and SiO_2, only CaO is truly effective in the desulphurization of iron.[3] It should be added that the term Excess CaO merely serves as an approximate measure of CaO activity in the range of compositions for which it is used.

The simple sulphur ratio in weight percent has been used throughout this work. This was desirable first because a direct comparison was permitted with the results published by Hatch and Chipman,[3] and second because the data on sulphur activity in the metal in the presence of other elements is not yet complete.

Factors Affecting the Rate of Desulphurization: Recently, Derge, Philbrook and Goldman[10] suggested that of three probable reactions applicable to desulphurization occurring in the blast furnace, the limiting reactions were the heterogeneous reactions involving the transfer of Fe and S to the slag and the reduction of FeO from the slag by C.

The present research indicates that this is only true to a limited extent, but that other factors are operative which previously had not been investigated thoroughly enough. It is noted that:

1—Fig. 6 shows the profound effect of basicity on the desulphurization rate which suggests that the C plus FeO reaction is in turn controlled by other reactions.

2—Fig. 7 shows the rapid response of metal sulphur to oxygen and its equally rapid recovery from the effect of oxygen (from MnO) in all slags regardless of basicity.

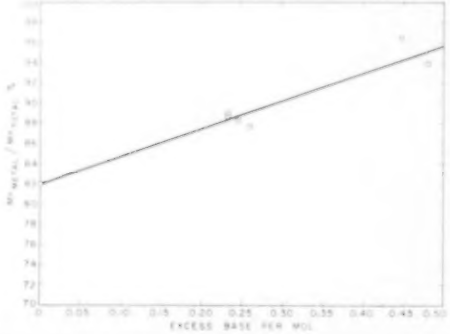

Fig. 8—Manganese recovery as a function of Excess Base at 1525°C.

Table III. Nature of Additions Made to Each Heat

Heat	Slag	Additions to Slag or Metal*
68	III	No additions
77	III	4 g Mn and 32 g MnO added after sample 2
71	III	4 g Mn and 8 g MnO added with initial charge
69	IV	11 g MnO added after sample 8
76	IV	4 g Mn and 32 g MnO added after sample 2
70	IV	4 g Mn and 8 g MnO added with initial charge
74	I	No additions
75	I	4 g Mn and 32 g MnO added after sample 2
72	I	4 g Mn and 8 g MnO added to initial charge 8 g MnO added after sample 7
66	II	No additions
79	II	No additions
80	II	4 g Mn and 30 g MnO added after sample 2
73	II	4 g Mn and 8 g MnO added to initial charge 8 g MnO added after sample 5
64	$CaO-Al_2O_3$	10 g SiO_2 added after sample 3

*Based on 400 g of metal and 400 g of slag

Table IV. Time Required to Reach Sulphur Equilibrium

Slag	Heat	Excess CaO	Approximate Time for S Equilibrium, Hr
III	68	none	12
IV	69	0.185	10-12
I	74	0.253	6
II	79	0.365	1

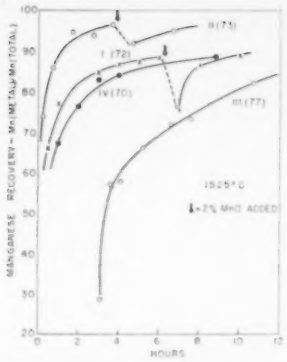

Fig. 9—Manganese recovery as a function of time for slags I to IV at 1525°C.

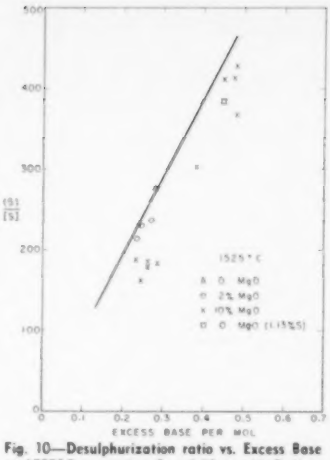

Fig. 10—Desulphurization ratio vs. Excess Base at 1525°C comparing 2 and 10 pct MgO slags relative to the zero MgO line for slags of 1.65 pct S.

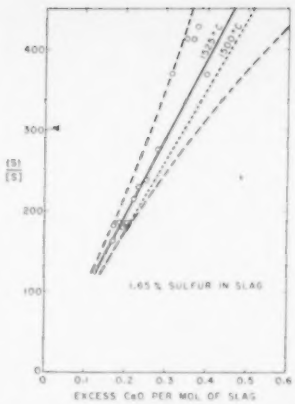

Fig. 11—Desulphurization ratio vs. Excess CaO at 1525°C showing 0.001 pct S limits. Dotted curve for 1500°C.

3—A large increase in stirring efficiency did not materially increase desulphurization rates in the slower more easily observable acid heats.

These observations coupled with an examination of the analytical values in Table II suggested SiO_2 reduction might in fact be the controlling reaction.

Accordingly, a heat was made using a slag composed of 50 pct by weight of both Al_2O_3 and CaO, a slag virtually free of SiO_2 or other reducible oxides. This heat, No. 64, shows that for a slag with Excess CaO of 0.442 the iron was completely desulphurized in less than 40 min from the time of the first, unfused, cold slag addition. The heat was made in a graphite crucible open to the air and therefore was not made under as ideal reducing conditions as the other heats. A very violent gas evolution accompanied the desulphurization reaction the moment the slag and metal were stirred.

From the above it would appear that it is not the C and FeO reaction which makes the desulphurization process slow. Instead it is the slow reduction of SiO_2. This reduction shifts the slag composition to greater basicity which tends to promote the desulphurization reactions but at the same time provides oxygen to the slag which prevents efficient desulphurization. The speed of the desulphurization rereaction is directly related to the degree of oxidation of the slag. Easily reducible oxides such as FeO offer little impediment to desulphurization, whereas oxides such as the more refractory SiO_2 release oxygen slowly, maintaining an oxidized slag over a long period of time. This role of SiO_2 reduction on the desulphurization reactions is to be the subject of a separate research program.

Conclusions

1—Increased vigor of stirring the slag and metal has little effect on increasing the rate of desulphurization of iron for the more acid slags.

2—MnO is readily reduced, reaching a reduction efficiency of 96 pct or more for the most basic slags. MnO remains in such small amounts in the slag that its influence is difficult to measure except in the most acid heats where it appears to increase the rate of desulphurization slightly.

3—Oxygen (from MnO) causes an almost immediate sulphur reversion into the metal. The slag recovers more slowly. The response is more rapid the more basic the slag.

4—Manganese equilibrium is achieved more slowly than sulphur equilibrium but is of comparable time. Manganese recovery may serve as an indication of the degree of slag oxidation.

5—The two most important factors on the speed of desulphurization and on the final sulphur in the metal are the basicity of the slag and the degree of oxidation of the slag.

6—The basicity is best expressed by the value Excess CaO.

7—MgO is a poor desulphurizer but can replace CaO in neutralizing the acid constituents.

8—The limiting reaction in controlling the rate of desulphurization is probably the reduction of SiO_2 and not the heterogeneous reaction between C and FeO.

Acknowledgments

The authors express their thanks to the American Iron and Steel Institute who sponsored this research program. They are grateful to Olaf Troili who participated in making all the experimental heats and especially to Charles W. Sherman for his many calculations and active participation throughout the program.

References

[1] Holbrook and Joseph: *Trans.* AIME (1936) **120**, p. 99.
[2] Holbrook: *Trans.* AIME (1938) **131**, p. 127.
[3] Hatch and Chipman: *Trans.* AIME (1949) **185**, p. 274; JOURNAL OF METALS (April 1949).
[4] Morris and Williams: *Trans.* ASM (1949) **41**, p. 1425.
[5] Morris and Buehl: *Trans.* AIME (1950) **188**, p. 317; JOURNAL OF METALS (February 1950).
[6] Sherman and Chipman: In preparation.
[7] Rosenqvist and Cox: *Trans.* AIME (1950) **188**, p. 1389; JOURNAL OF METALS (November 1950).
[8] Rocca, Grant and Chipman: JOURNAL OF METALS (April 1951) *Trans.* AIME, p. 319.
[9] Sherman and Grant: *Trans.* AIME (1949) **185**, p. 898; JOURNAL OF METALS (November 1949).
[10] Derge, Philbrook and Goldman: *Trans.* AIME (1950) **188**, p. 1111; JOURNAL OF METALS (September 1950).

Effect of Silica Reduction on the Desulphurizing Power Of Blast-Furnace Type Slags

by Nicholas J. Grant, Olaf Troili, and John Chipman

IN recent studies of the factors which affect the rate of desulphurization and its equilibrium, it became apparent that certain concurrent reactions were operative which had a significant effect on desulphurization. This is emphasized in the experiments of Hatch and Chipman[1] and of Grant, Kalling, and Chipman[2] by the slow approach to a final state of equilibrium which is in marked contrast to the initial rapid transfer of sulphur from metal to slag. Since the removal of sulphur is of such profound importance in iron and steelmaking, it appeared necessary to investigate the reactions responsible for this behavior.

It is now known that the presence of iron oxide in the slag interferes seriously with the principal reaction of blast-furnace desulphurization:

$$CaO\ (slag) + \underline{S} + C = CaS\ (slag) + CO \qquad [1]$$

The interfering reaction is most simply expressed as:

$$CaS\ (slag) + \underline{O} = CaO\ (slag) + \underline{S} \qquad [2]$$

and a small concentration of oxygen (or FeO) is sufficient to hold a considerable amount of sulphur in the metal.

It has been shown by Grant, Kalling, and Chipman[2] that the addition of MnO to blast-furnace slag slows the removal of sulphur from the metal. This effect overshadows the contribution of MnO to basicity and is ascribed to its oxidizing power.

It will be shown in this paper that SiO_2 also has sufficient oxidizing power to interfere with blast-furnace desulphurization. This is, of course, only one of its several effects. Primarily it is an acid and therefore reduces the concentration of excess lime. But when silicon is reduced to the metal the oxygen to which it was previously bonded becomes in part available for reaction 2. The proof of this statement is found in the following experiments.

Experimental Procedure and Results

Utilizing the same procedure and apparatus described by Grant, Kalling, and Chipman[2] five additional heats were made using slags IV and II, the starting compositions of which were: slag IV—40 CaO, 10 MgO, 35 SiO_2, 15 Al_2O_3; and slag II—50 CaO, 10 MgO, 25 SiO_2, 15 Al_2O_3.

An important difference between these heats and those previously reported was that silicon to the extent of 1 to 4 pct was added to the present heats whereas the starting silicon content was formerly about 0.2 pct.

Table I shows the slag and metal analyses for heats 82 to 87, and Table II shows the silicon additions made to the charge. These additions are based on 400 g of metal and 400 g of slag. All heats had 1.65 pct S charged before the cold slag additions. The temperature was maintained at 1525°C.

Table I. Slag and Metal Analyses of Samples Taken at 1525°C

Heat, Slag, and Sample Nos.		Time	Metal, Wt Pct C	Si	S	Slag, Wt Pct S	CaO	MgO	SiO_2	Al_2O_3
82 IV	1	0:30	4.61	1.75	0.015	1.64	—	—	33.52	—
	2	1:30	—	—	0.014	—	—	—	—	—
	3	2:30	4.63	2.12	0.0109	1.64	—	—	33.26	—
	4	3:30	—	—	0.0107	—	—	—	—	—
	5	4:30	—	—	0.0100	—	—	—	—	—
	6	5:30	4.40	2.52	0.0090	1.67	38.24	11.11	32.38	15.20
	7	6:30	—	—	0.0094	—	—	—	—	—
83 IV	1	0:30	4.08	2.73	0.0142	1.62	—	—	34.46	—
	2	1:00	—	—	0.0112	—	—	—	—	—
	3	1:30	—	—	0.0110	—	—	—	—	—
	4	2:30	3.98	2.88	0.0106	1.62	—	—	34.24	—
	5	3:30	—	—	0.0101	—	—	—	—	—
	6	4:30	—	—	0.0101	—	—	—	—	—
	7	5:30	4.00	3.05	0.0104	1.63	36.7	12.07	33.94	15.60
84 IV	1	0:30	3.80	3.92	0.013	—	—	—	34.3	—
	2	1:30	—	—	0.010	—	—	—	—	—
	3	2:30	—	—	0.010	—	—	—	—	—
	4	4:30	3.87	4.14	0.009	—	—	—	—	—
	5	6:30	—	—	0.009	—	—	—	—	—
	6	8:30	—	4.27	0.009	—	—	—	—	—
	7	9:30	3.73	4.36	0.009	1.67	36.35	11.51	33.4	16.88
86 II	1	0:20	4.69	1.41	0.0037	1.55	46.6	10.72	25.42	14.82
	2	1:50	—	—	0.0031	—	—	—	—	—
	3	4:50	4.75	1.22	0.0031	1.59	—	—	26.36	—
	4	6:50	—	—	0.0026	—	—	—	—	—
	5	8:50	4.80	1.21	0.0033	1.61	46.7	9.64	26.98	13.16
87 II	1	0:30	4.06	3.50	0.003	1.50	44.8	10.49	27.08	14.56
	2	1:30	—	—	0.003	—	—	—	—	—
	3	3:30	4.21	3.12	0.003	1.64	—	—	27.94	—
	4	6:00	—	—	0.003	—	—	—	—	—
	5	8:30	—	—	0.003	—	—	—	—	—
	6	9:15	4.41	2.59	0.003	1.62	44.4	9.93	28.66	13.50

Rate of SiO_2 Reduction: Fig. 1 shows the silicon content of the metal in contact with slag IV at 1525°C as a function of time. Heat 70 from the work of Grant, Kalling, and Chipman is included as the lowest starting silicon. It will be noted that even with 4 pct Si in the starting metal, there is an increase in silicon content with time. Heat 84 is apparently approaching silicon equilibrium very slowly. Heats 70 and 82 with very much lower starting silicon show a more rapid initial rise in silicon content but do not reach equilibrium during a long holding period.

Fig. 2 shows 3 different initial silicon contents for heats 73 (from Grant, Kalling, and Chipman) 86 and 87, in contact with slag II, the most basic slag. Heat 73 is increasing in silicon with time, whereas heat 87 with an initial silicon content of 3.7 pct shows a decrease with time. Heat 86 shows a very close approach to equilibrium. The rate of transfer of silicon from slag to metal is very slow in all of those heats, even those which are initially far from equilibrium.

N. J. GRANT and J. CHIPMAN, Members AIME, are associated with the Department of Metallurgy, Massachusetts Institute of Technology, Cambridge, Mass. O. TROILI is associated with Avesta Steel Works, Avesta, Sweden.

Discussion on this paper, TP 3107C, may be sent, 2 copies, to AIME by Oct. 1, 1951. Manuscript, Feb. 9, 1951. St. Louis Meeting, February 1951.

[1] G. G. Hatch and J. Chipman: Sulphur Equilibria between Iron Blast-Furnace Slags and Metal. *Trans.* AIME (1949) 185, p. 274; *Journal of Metals* (April 1949).

[2] N. J. Grant, U. Kalling, and J. Chipman: Effects of Manganese and Its Oxide on Desulphurization by Blast-Furnace Type Slags. This volume, p. 666.

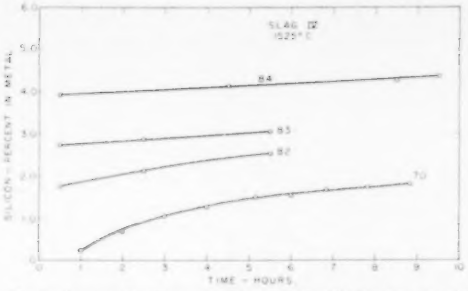

Fig. 1—Increase in silicon content of metal with time for slag IV at 1525°C.

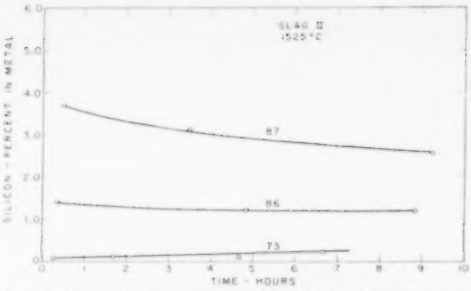

Fig. 2—Change in silicon content of metal with time for slag II at 1525°C.

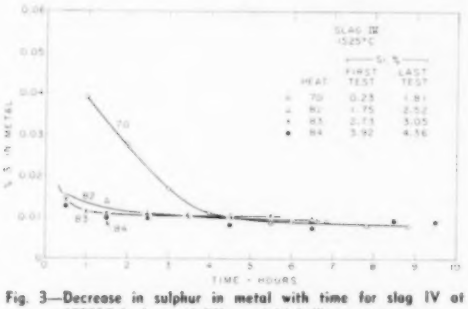

Fig. 3—Decrease in sulphur in metal with time for slag IV at 1525°C for heats of different initial silicon content.

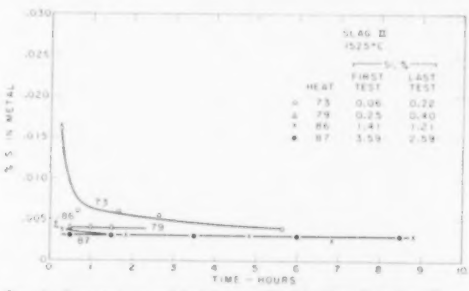

Fig. 4—Decrease in sulphur in metal with time for slag II at 1525°C for heats of different initial silicon content.

Effect of Silicon Content on Rate of Desulphurization and on Sulphur Equilibrium: Figs. 3 and 4 show curves of sulphur in the metal vs. time at 1525°C for the same heats as in Figs. 1 and 2. Fig. 3 is for the more acid slag IV. It is very obvious that the addition of silicon to the charge affects profoundly the rate of sulphur removal. The effect on final sulphur is apparently smaller than the experimental uncertainties. The direct effect of silicon in the charge is to prevent or minimize the reduction of silicon from the slag thus depriving the silica of its oxidizing power.

Fig. 4 is for the very basic slag II, using an expended ordinate of twice that of Fig. 3. For this slag also there is an effect on the desulphurization rate due to an initial high silicon content of the molten iron. Fig. 4 must be viewed with some caution, however. The very high basicity of slag II and the high desulphurization rate imply that some significant desulphurization must have occurred even before the slag was judged to be molten. Accordingly, a better "zero time" might be the time of the initial addition of the mixed cold slag (as oxide components). From "start of cold slag addition" to the first sample for the heats of Fig. 4 the times are: heat 73, 95 min; heat 79, 95 min; heat 86, 140 min; and heat 87, 165 min. Even on this basis there is, however, a significant improvement in desulphurization rate as the silicon in the charge increases. There also appears to be a slight improvement in the final sulphur with increased silicon content of the metal.

Table II. Silicon Additions

Heat	Slag No.	Approximate Addition
82	IV	8 g Si (2.0 pct)
83	IV	14 g Si (3.4 pct)
84	IV	19 g Si (4.5 pct)
86	II	8 g Si (2.0 pct)
87	II	19 g Si (4.5 pct)

Distribution of Silicon Between Slag and Metal: There are no experimental data in the literature on the equilibrium between silicon in pig iron and silica in the slag. This equilibrium is expected to be strongly affected by temperature and by slag basicity. The latter effect is demonstrated in Figs. 1 and 2. Under the more basic slag II the equilibrium silicon content is in the vicinity of 1.2 pct, while with the more acid slag IV it is well above 4 pct. In a qualitative way the data of Hatch and Chipman and of Grant, Kalling, and Chipman show the same effect. Further research is clearly needed before quantitative conclusions regarding this equilibrium can be drawn.

Summary

The rate of removal of sulphur from molten pig iron is affected by the silicon content of the iron. The results are interpreted as showing that silica in the slag is a sufficiently good oxidizing agent to interfere with the principal desulphurizing reactions. When sufficient silicon is present to prevent further reduction of silica the transfer of sulphur from metal to slag is extremely rapid.

The distribution of silicon between slag and metal is an important factor in desulphurization and requires further study.

Acknowledgments

The authors wish to express their appreciation to the American Iron and Steel Institute for support of the research.

Desulphurizing Action of Titanium in Steels

by W. P. Fishel, William P. Roe, and James F. Ellis

This paper reports the distribution of sulphur between iron and titanium in Fe-Ti-S alloys and in Fe-Ti-C-S alloys. The compound TiS was found, which exists as a separate phase at temperatures below 1200°C. Titanium in steels reacts with sulphur in preference to carbon.

THE general relationship between sulphides and oxides suggests that titanium should form a sulphide having properties similar to those of titanium oxide. Specifically, titanium should form a sulphide having a high melting point, indicating a stable compound of low solubility in iron. In order for titanium to function as a desulphurizer or sulphur-fixing agent, it must form a stable sulphide. In order for titanium to be useful in steels as a sulphur-fixing agent, it must react with sulphur in preference to carbon; and to prevent red shortness, the sulphide formed must have solubility characteristics such that grain-boundary precipitation of a low melting phase be prevented. The terms desulphurizer and sulphur-fixing agent when used in this paper mean that titanium effectively ties up the sulphur as a stable sulphide of titanium and prevents the formation of FeS.

The partition of sulphur between iron and titanium was studied first in a series of Fe-Ti-S alloys with carbon absent, and then in similar alloys with carbon present.

It has been established[1,2] that titanium forms in Fe-Ti-S alloys a sulphide of undetermined composition which can be identified microscopically, and that the titanium-sulphur compound does not respond to sulphur printing. It has been suggested[3] that titanium acts as a sulphur-fixing agent, although little proof has been given. A report[4] of The Advisory Committee on Metals and Minerals summarizes the existing knowledge concerning substitutes for manganese in steels.

Distribution of Sulphur Between Iron and Titanium with Carbon Absent

The alloys for this investigation were made by melting Armco iron, metallic titanium, and iron sulphide in alundum crucibles in an induction furnace. The titanium was added after the other ingredients had melted. In these alloys it is recognized that some TiO_2 is present, since the melts were made in the air and since no other deoxidizing agent was used; therefore, some of the titanium was not available for union with sulphur. Thirteen ingots were made. Ingots 2 to 8 were cast in baked-sand molds; ingots 12 and 13 were cast in metal molds; and ingot 9 was allowed to cool in the crucible in which it was melted. All ingots were annealed at 900°C for 3 hr and were cooled slowly in the furnace. Subsequent information indicates that this anneal had no effect upon the titanium sulphide particle size, since the sulphide does not go into solution at this temperature. The ingots as-cast were approximately 8 in. long and ¾ in. diam. The compositions of the eight ingots and the results of the partition of sulphur are recorded in Table I.

Total titanium and total sulphur were determined by standard gravimetric methods. Sulphur, as iron sulphide, was determined by the evolution method. Boiling HCl (1:4) liberates the sulphur from iron sulphide, but leaves the titanium sulphide practically undecomposed. A complete separation of titanium sulphide and iron sulphide cannot be made by digesting these compounds in dilute HCl since titanium sulphide was found to dissolve slowly. The amount of titanium sulphide decomposed will depend upon the time in contact with the acid and upon the particle size of the sulphide. The point

Table I—Partition of Sulphur between Titanium and Iron

Alloy	Total Ti, Pct	Total S, Pct	Ratio Ti:S	S Soluble in HCl, Pct (S as FeS)	S Insoluble in HCl, Pct (S as TiS)	Total S as TiS, Pct
2	0.385	0.504		0.458	0.025	
	0.395	0.504		0.456	0.026	
	0.390	0.504	0.77	0.457	0.026	5.2
4	0.211	0.182		0.158	0.011	
	0.209	0.190		0.162	0.014	
	0.210	0.186	1.13	0.160	0.013	7.0
5	0.468	0.207		0.163	0.031	
	0.458	0.201		0.164	0.029	
	0.463	0.204	2.27	0.164	0.030	15.0
6	0.515	0.189		0.135	0.039	
	0.511	0.187		0.138	0.041	
	0.513	0.188	2.75	0.137	0.040	22.2
8	0.368	0.122		0.012	0.080	
	0.372	0.135		0.013	0.079	
	0.370	0.129	2.86	0.013	0.080	62.0
9	0.700	0.329		0.011	0.313	
	0.699	0.320		0.011	0.307	
	0.700	0.325	2.15	0.011	0.310	95.5
12	0.240	0.234		0.092		
	0.251	0.240		0.114	By difference	
	0.246	0.237	1.04	0.103	0.134	56.7
13	0.154	0.315		0.133		
	0.161	0.295		0.144	By difference	
	0.158	0.305	0.52	0.139	0.166	54.5

W. P. FISHEL, Member AIME, is Professor of Metallurgy, and W. P. ROE is Graduate Student, Vanderbilt University, Nashville, Tenn. J. F. ELLIS, with the American Cast Iron Pipe Co., Birmingham, Ala., was formerly a Graduate Student, Vanderbilt University on a fellowship furnished by the American Cast Iron Pipe Co.

Discussion on this paper, TP 3085C, may be sent, 2 copies, to AIME by Oct. 1, 1951. Manuscript, June 28, 1950; revision, Feb. 14, 1951. St. Louis Meeting, February 1951.

involved is one of reaction or solution rates. Therefore, the figures representing sulphur as FeS in Table I are probably high, and those for sulphur as TiS are correspondingly low. The sulphur not liberated by HCl in the evolution flask was determined gravimetrically. This was considered to be titanium sulphide, which in this paper is represented by the formula TiS.

The percentages of sulphur in these alloys are much higher than would be found in commercial steels. They were made so intentionally in the interest of better separations. The ratio of titanium to sulphur as well as the amounts of titanium and sulphur in these alloys cover wide ranges. In alloys 2, 4, 5, 6, and 8, which were cast in sand molds, there is a gradual increase in the ratio of titanium to sulphur from 0.77 to 2.68. There is also an increase in the amount of total sulphur combined with titanium as the Ti:S ratio increases. The rapid cooling given these alloys produced finely divided particles of titanium sulphide. These small sulphide particles suffered more loss by solution during the evolution analysis with HCl than did the larger particles of alloy 9. The values given for sulphur as TiS could be too low if the samples were digested for a very long time, or too high if not digested long enough so that some FeS was left undecomposed. Considering the methods used in these analyses, it is believed that the values given for sulphur as TiS in most cases are low.

Alloy 9 was cooled slowly from the melt and was found to contain large particles of titanium sulphide. In this alloy 95.5 pct of the total sulphur was present as TiS, although the ratio of Ti:S was only 2.15. In Fig. 1 the micrographs of alloy 9 show large sulphide particles.

Alloys 12 and 13 were cast in metal molds. They had low ratios of Ti:S, yet they showed a rather high percentage of sulphur as TiS. This is probably due to better melting procedures that resulted in less oxidation of the titanium and hence left a higher percentage of titanium to react with sulphur.

From the data presented in Table I, it is evident that titanium reacts with sulphur and that the distribution of sulphur between titanium and iron varies with the amounts of titanium and sulphur present. The ability of titanium to tie up sulphur becomes more pronounced than the above data indicate, when it is remembered that part of the titanium in these alloys has united with oxygen and is not available for union with sulphur.

Composition of Titanium Sulphide

In order to determine the composition of the sulphide formed, residues were prepared from alloy 9. This alloy was carbon-free and contained large sulphide particles. Approximately 300 g of turnings were taken from this alloy and were treated with 1:4 HCl at room temperature in a flask from which air was excluded. After all visible action had ceased, the acid was siphoned off and fresh acid added. This process was continued for six weeks. At this time no noticeable action accompanied the addition of fresh acid. A finely-divided, black residue remained which was washed several times with distilled water and allowed to settle. The same procedure then was carried out with absolute alcohol. The alcohol suspension of the residue was centrifuged; only the heavier portion of the residue was collected. At this point the residue appeared bronze in color. The alcohol was poured off, and the last

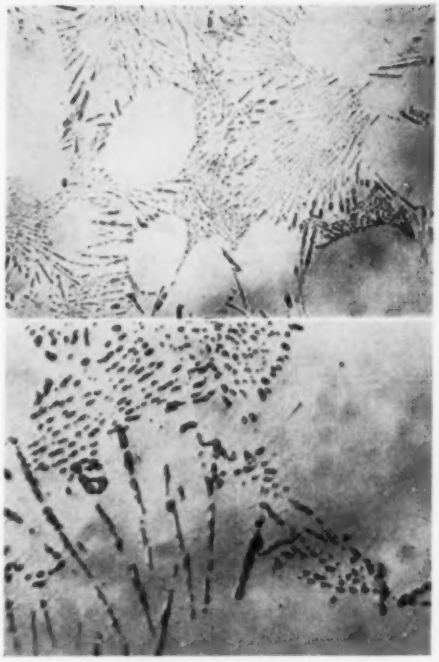

Fig. 1—Micrograph of Alloy 9.
Upper—Fe-Ti-8, unetched. Particles of titanium sulphide and boundary segregation. X160.
Lower—Unetched. Particles of titanium sulphide. X650.

traces were removed by repeated ether treatments. The ether was removed by centrifuging and evaporation; a finely-divided, black powder remained. This residue was nonmagnetic, and appeared stable in air.

This residue was analyzed and gave the following results: Ti, 59.2 pct, 59.2 pct; and S, 18.2 pct, 18.1 pct.

Approximately 20 pct of the total is unaccounted for. The amount missing is about equal to the sulphur present. The most obvious explanation is that the residue is a mixture of about equal parts of TiS and TiO_2. Any mixture of TiS and TiO_2 when ignited to TiO_2 would not change weight, since one sulphur (atomic wt 32.07) is replaced by two oxygens (atomic wt 16.00). This would not be true for any other sulphide of titanium or for a nitride or a carbide.

A sample of the residue was ignited to constant weight. Sulphur dioxide was evolved and a white powder resulted. The weights were as follows: weight of residue, 0.0714 g; weight after ignition, 0.0717 g; and pct Ti in the residue, 60.2 pct. The ignited residue is TiO_2. This is considered proof that the sulphide present in the alloy has the formula TiS. The slight gain in weight which occurred could be attributed to some TiN being converted to TiO_2.

Solubility: In order to determine the temperature at which the sulphide formed or precipitated from solid solution, which should be near the temperature at which it dissolved on heating, several heating and quenching tests were made.

Four pieces of alloy 9 were taken. One sample was held for 2 hr at each temperature listed in

Table II—Temperature and Hardness Tests for Alloy 9

Sample Temperature, °C	Hardness before Quenching, Rockwell E	Hardness after Quenching, Rockwell E
1000	48	50
1100	48	90
1200	48	93
1250	48	93

Table II and then quenched in water. Evidently the TiS did not dissolve at 1000°C, but did dissolve to some extent at 1100°C. This conclusion is confirmed by the microstructure. By a comparison of the structure before and after annealing, it was observed that the large sulphide particles had broken down to some extent at the higher temperatures into smaller ones, and that some grain-boundary precipitation had taken place.

Distribution of Sulphur between Titanium and Iron with Carbon Present

For this study five alloys were made exactly as before with the exception that carbon was added as lump graphite. The carbon was added immediately after the iron was molten and before the addition of titanium. The addition of carbon produced sounder ingots due to the deoxidation of the metal, this in turn allowed for less oxidation of the alloying element so that titanium could exert its full effect as a desulphurizing agent. The melts were poured into metal molds and were annealed at 900°C.

The alloys were analyzed for total titanium, total sulphur, total carbon, sulphur as FeS, sulphur as TiS, and carbon as TiC. Since TiC is insoluble in HCl, a good approximation of the amount of titanium united with carbon may be had by dissolving the steel in dilute HCl, filtering the insoluble residue in a combustion thimble, and igniting to CO_2. The residue from HCl contains all of the TiC present in the steel and some free carbon resulting from the action of the acid upon Fe_3C. The values for carbon as TiC are therefore a little higher than the true values.

Table III—Compounds Present in Iron-Titanium-Sulphur-Carbon Alloys

Alloy	Total Ti (I)	Total S (II)	Ratio Ti:S (III)	Total C (IV)	Ratio Ti:C (V)	C Insoluble in HCl, Pct (C as TiC)* (VI)	S Soluble in HCl, Pct (S as FeS) (VII)	S Insoluble in HCl, Pct (S as TiS by Difference) (VIII)	Total S as TiS, Pct (IX)
A	0.380	0.313		0.272		0.079	0.128		
	0.392	0.357		0.274		0.076	0.148	0.197	
	0.386	0.335	1.15	0.273	1.41	0.078	0.138	0.130	39
B	0.282	0.292		0.109		0.032	0.085		
	0.282	0.279		0.109		0.027	0.085	0.201	
	0.282	0.286	0.99	0.109	2.59	0.030	0.085	0.198†	61
C	0.198	0.246		0.151		0.024	0.089		
	0.221	0.254		0.143		0.033	0.084	0.164	
	0.210	0.250	0.84	0.147	1.43	0.028	0.086	0.182†	74
D	0.281	0.221		0.154		0.027	0.092		
	0.260	0.177		0.152		0.019	0.092	0.102	
	0.270	0.194	1.39	0.153	1.77	0.023	0.092	0.109†	56
E	0.206	0.206		0.358		0.028	0.065		
	0.214	0.185		0.363		0.034	0.071	0.128	
	0.210	0.196	1.07	0.361	0.58	0.031	0.068	0.133†	67

* These values are too high due to free carbon from Fe_3C.
† Results by analysis.

Table III gives the compositions of the five alloys and the compounds found in them. There is more carbon present than is required to react with all the titanium. Despite the presence of excess carbon, the data show that a considerable amount of titanium sulphide is formed. For example, in alloy D over half the sulphur is present as titanium sulphide, even though the Ti:S ratio is only 1.39, and in spite of the presence of twice as much carbon as is needed to react with all the titanium present. Some of the values presented in Table III do not agree very well among themselves. If the amount of titanium as carbide and the amount as sulphide is calculated, the total is greater than the total titanium listed. Part of this discrepancy is due to the known high values of C as TiC, col. VI, part to the inability to make a clean separation between FeS and TiS, and the remainder to analytical errors. In spite of the inexactness of the figures presented, Table III serves to give a qualitative picture of the distribution of sulphur between titanium and iron in alloys containing carbon. In all these alloys, with the exception of alloy A, over half the total sulphur is present as HCl-insoluble titanium sulphide. Very little titanium carbide is present. The values for C as TiC, col. VI, multiplied by 4 gives the titanium as TiC. It will be noted that the Ti:S ratios in these alloys are below 1.5, the ratio for TiS; hence there is insufficient titanium present to react with all the sulphur. At this stage of the research the identity of the titanium sulphide was not known; otherwise, alloys with higher ratios would have been used. Later work by another investigator shows that if the Ti:S ratio is above 2, nearly all the sulphur is present as TiS.[5]

These alloys were examined microscopically. All contained pearlite and particles of titanium sulphide.

From the above it would appear that titanium in steels reacts with sulphur in preference to carbon, and that titanium tends to tie up sulphur as a sulphide, thus inhibiting the formation of iron sulphide.

One ingot containing 0.5 pct C, 0.05 pct S, 0.15 pct Ti, but no manganese was hot rolled to a thin strip. Several ingots of similar compositions were hot forged. The hot working properties were normal.

Conclusions

1—It has been shown that titanium will react with sulphur in steels containing carbon to form TiS, insoluble in γ iron below 1000°C; and that titanium reacts with sulphur in preference to carbon.

2—Titanium can replace manganese as a sulphur-getter in steels.

References

[1] W. P. Fishel and Martha N. Gordon: Sulphur in Iron-Titanium Alloys. Vanderbilt Thesis (1947).

[2] H. Morrogh: *Journal* Iron and Steel Inst. (1941) **143**, p. 207.

[3] Urban and Chipman: Nonmetallic Inclusions in Steel. T.A.S.M. (1935) **23**, p. 645.

[4] Report on Substitution of Manganese by Titanium. The Metals Conservation and Substitution Group to the Office of Production Management. (Aug. 13, 1941).

[5] J. W. Holladay: Unpublished work, Battelle Memorial Institute.

[6] W. P. Fishel and Brison Robertson: Distribution of Carbon Between Titanium and Iron in Steels. *Trans.* AIME (1945) **162**, p. 310.

AIME OFFICERS
Willis McG. Peirce, President
Vice Presidents
A. B. Kinzel Philip Kraft R. W. Thomas
J. L. Gillson M. L. Haider
Vice President and Treasurer
Andrew Fletcher

AIME STAFF
E. H. Robie, Secretary
E. J. Kennedy, Jr., Asst. Secy. Ernest Kirkendall, Asst. Secy.
J. B. Alford, Asst. Secy.
H. N. Appleton, Asst. to Secy. H. A. Maloney, Asst. Treas.
John V. Beall, Eastern Secretary, Mining Branch
R. E. O'Brien, Western Secretary, Mining Branch
808 Newhouse Bldg., Salt Lake City

AIME Board to Vote on Bylaw Changes at Sept. 12 Meeting

The following amendments to the bylaws of the AIME were considered by the Board of Directors at its meeting on June 13, and are published preliminary to a vote thereon at the meeting of the Board on Sept. 12:

1. *To standardize the dues of Student Associates, allowing each a subscription to a monthly journal:*

Amend Art. I, Sec. 8, as follows by deleting the italicized words in the second sentence: "A full-time student in good standing in an approved school, who has been nominated by at least three instructors of the nominee (one of whom must be an Institute member), may affiliate with the Institute as a Student Associate by payment of $4.50 annual fee, for which he shall receive a subscription to one monthly journal and be privileged to attend meetings of the Institute and to use the Engineering Societies Library and the Personnel Service; *provided, however, that for Student Associates who do not elect to receive a monthly journal, the annual fee shall be $2.*"

2. *To provide for a credit of $2 on the initiation fee for each year of enrollment as a Student Associate or Junior Member:*

Amend the first sentence of Art. II, Sec. 1, by adding the italicized words in the following: "Each newly-elected Member or Associate Member, and each Junior Member at the time of his transfer into the class of Member or Associate Member, shall pay, immediately upon notification of such election or such transfer, an initiation fee of $20; provided, however, that said initiation fee may be payable, at the option of the applicant, in four equal annual installments, the first of which shall be due upon notification of election or transfer; *and provided further that, beginning Jan. 1, 1952, a credit of $2 towards the initiation fee be granted for each year up to ten of uninterrupted and continuing membership as a Student Associate or Junior Member, or both. When such credit is allowed, no installment payments of the initiation fee shall be granted.*"

3. *The following changes, to take effect at the annual business meeting, February 1952, are made necessary by the revised procedure of the Nominating Committee in naming a President-Elect instead of a President.* (Currently there is a transition period in which both a President and President-elect are being named for 1952.)

Amend Art. VI, Sec. 1, para. 1 and 2, to read as follows: "The number of Directors of this Corporation is 27, consisting of one President, one President-elect, one Past President, six Vice-Presidents, and 18 other Directors, to be elected as hereinafter provided; and in addition the Chairman of each duly constituted professional Division of the Institute, ex officio, shall serve as a Director, with full voting power, during his term as Chairman.

"At the regular November meeting of the Board of Directors or Executive Committee, the chairman thereof shall declare to be elected, as provided in Article XI of these Bylaws, nine Directors, of whom one shall also be designated as President-elect, and of whom two shall be designated as Vice-President. The nine Directors, including the Directors designated as officers, together with the newly elected Division Chairmen in their capacity as ex-officio Directors, shall take office at the annual business meeting of the Institute next following the meeting at which they were declared elected. The term of all nine elected Directors shall be for a period of three years; provided, however, that the terms of the President-elect and President shall each be for one year, the President thereupon serving one year as Past-President."

Amend Art. VI, Sec. 2, para. 1, sentences 2 and 3), to read as follows: "The President shall be that Director who, in the preceding year, served as President-elect. The President shall be ineligible to hold that office again until two years after the expiration of his term as President."

Amend Art. VI, Sec. 3, to read as follows: "In the event of a vacancy occurring in the Board of Directors by death, resignation, promotion by election as President, President-elect, or Vice-President, or for any other reason than retirement at the end of three years' service, the remaining members of the Board shall elect a successor to fill the vacancy and to serve for the unexpired term. A member of the Board whose term has not expired and who is elected President-elect or Vice-President at an annual election shall be considered to have vacated his former office, and the Board shall fill the vacancy as above provided."

A proposed change in Art. I, Sec. 5, (sentence 2) clarifies the meaning formerly expressed: "He shall not have passed his 30th birthday anniversary at the time his application is received, and shall not remain a Junior Member beyond his 33rd birthday anniversary, except that the Board of Directors shall have the power to waive the age limitation in the case of veterans from military service." Omit: "(This last requirement shall take effect Jan. 1, 1950)" as obsolete.

A proposed change in Art. VI, Sec. 5, (sentence 2) recognizes the new office of Controller, approved by the Board at its meeting on Feb. 12, 1950: "Also, the Board may, upon nomination by the Treasurer, appoint one or more persons to perform the duties of Assistant Treasurer and of Controller."

A proposed change in Art. VIII, Sec. 2, para. 3, (sentence 5) sets a more practical time for the Board to pass on the final annual budget: "The Directors shall pass on this budget at their first open meeting after the annual business meeting of the Institute, modifying it as they consider necessary, and make definite detailed appropriations for the current calendar year."

A proposed change in Art. VIII, Sec. 4, (sentence 1) eliminates the requirement that the Admissions Committee be limited to eight members: "The Committee

on Admissions shall consist of at least eight members of the Institute, the chairman and at least one other member being chosen from the Board of Directors, and shall be appointed by the Board, on recommendation of the President, at the first meeting of the Board after the annual business meeting of the Institute."

A proposed change in Art. IX, Sec. 1, eliminates the second sentence, as no longer applicable. It reads: "In 1951 the Nominating Committee shall also select, as one of the nine Directors, a President to take office in February, 1952."

A proposed change in Art. IX, Sec. 2, para. 2, (sentences 4 and 5) eliminates a provision in the current bylaws that did not prove practical but maintains its intent: "In selecting candidates the Committee shall be guided by such rules of procedure as may from time to time be established by the Board; provided, however, that of the eight Directors in addition to the President-elect, a sufficient number be selected on the basis of geographical districts so that each such district will have at least one representative. The basis of selection of the others shall be at the discretion of the Committee."

A proposed change in Art. XI, Sec. 4, para. 3, 4, and 5, eliminates the requirement that Student Chapter officers, Faculty Sponsors, and Counselors all be required to make annual written reports to the Board:

"Each Student Chapter at its annual election shall choose an AIME member to be its Faculty Sponsor and forward his acceptance to the Secretary of the Institute. It shall be the duty of the Faculty Sponsor to promote the best interests of both the Student Chapter and the Institute and to make written reports of his stewardship to the Directors of the Institute as desired.

"It shall be the duty of the President of the Student Chapter and its Faculty Sponsor to secure, through the Local Section in whose territory it is situated, the appointment of a member of the Institute in the practicing profession to serve as Counselor for the Student Chapter, and to forward his acceptance to the Secretary of the Institute. It shall be the duty of this Counselor to promote cordial relations between the practicing engineers and the Student Chapter and to make written reports of his stewardship to the Directors of the Institute as desired.

"It shall be the duty of each Student Chapter to report promptly to the Secretary of the Institute the results of elections of officers, and to make written reports of activities to the Directors of the Institute as desired."

Opinions of AIME members on these proposed changes are invited and will be submitted to the Board before voting on Sept. 12. A copy of the current bylaws will be sent to any AIME member on request.

Pan-American Engineers Adopt Constitution at Havana Meeting

Pan-American Union of Engineering Societies (UPADI) held a meeting in Havana, Cuba, Apr. 19 to 22, to adopt a constitution for its operation. AIME representatives F. T. Agthe and W. H. Carson were among the Engineers Joint Council delegates representing engineering societies of the United States. The 59 delegates from 19 nations spoke for 165,000 engineers, of which EJC represented 125,000.

A provisional constitution was approved that will be in force until the next UPADI meeting in New Orleans in 1953. The aims of UPADI, as stated in the constitution are to encourage, promote, expand, and guide the work of engineers in the Americas. It will hold periodic Pan-American engineering congresses and expositions that will promote individual and collective visits between member countries and to other places of interest; interchange of teachers, lecturers, engineers, and students between schools and engineering associations; and personal contacts between engineers of different countries.

In addition, UPADI will organize and develop relations between engineering organizations on an administrative level; technical, professional, economic, and social interchange, either individually or collectively, among the members of the constituent organizations; technical competitions among the engineers and engineering students of the Americas; professional rules of practice; and application of professional codes of ethics. It will promote the study of technical problems which jointly affect member countries, and inter-American public works and economic problems.

UPADI aims to contribute to the enhancement of the status of the engineering profession; increased usefulness of the profession to the public; strengthening the cause of peace and the ties between nations; closer technical relations between American countries; and economic development of American countries.

Each country will be represented by only one member. Financing will be through a separate permanent agency that will collect, deposit, and control donations, bequests, subsidies, or grants. Chairmen of each of the four committees organized were representatives of Engineers Joint Council.

Members Offered Technical Booklets

AIME has available for free distribution, 200 copies of the 15-p. booklet *Theoretical Chemical Reactions in the Basic Arc Electric Furnace*, by H. C. Bigge, superintendent, tool steel dept., Bethlehem Steel Co., Bethlehem, Pa. This booklet, which has been sold for $3, contains chapters on oxidizing and reducing reactions, sulphur elimination during the reducing period, desulphurization, and reduction tables for some of the important oxides encountered in the iron and steel industry.

The copies of the booklet were donated to AIME for interested members. Address your request to Order Dept., AIME, 29 W. 39 St., New York 18.

Annual Meeting Paper Deadline

Sept. 15, 1951 is the deadline for all Institute of Metals Division papers for the 1952 New York Annual Meeting and the deadline for all Iron and Steel Division and Extractive Metallurgy Division papers to be prepublished.

OPEN HEARTH SECTIONS:

Pittsburgh Section held their annual golf party at the South Hills Country Club on June 5, attracting 132 golfers. The dinner that followed was attended by 250 persons.

Western Section announced the following officers for the 1951-1952 season: Permanent Chairman, George B. McMeans; Executive Chairman, Barney M. Dagan; Vice-Chairman, John M. Fahey; and Secretary-Treasurer, S. L. Jackson.

Chicago Section held their Fourth Annual golf tournament on June 13, and of the 220 men attending the dinner, 125 played in the tournament.

Southwestern Section will hold its Fall meeting on Oct. 10 and 11 in Pueblo and Colorado Springs, Colo. Colorado Fuel & Iron will be host for breakfast, luncheon, and a plant trip in Pueblo on Oct. 10, and for the Fellowship Dinner following the formal meeting at the Broadmoor Hotel in Colorado Springs on Oct. 11. The Western Section has been invited to participate in this meeting. Reservations should be made as soon as possible to Edward E. Christopher, Secretary-Treasurer, Southwestern Section, NOHC, 912 Buder Bldg., St. Louis, Mo.

AIME Plans Underway For Fall Meeting

In MEXICO CITY!

NO fall meeting of the Institute in years has aroused the interest already shown in that to be held in Mexico City in the week beginning Oct. 29—the 172nd national meeting of the AIME. A substantial contingent even of metals and petroleum members seems likely, even though these groups are not participating in the technical sessions.

The Minerals Beneficiation Div. members will be out in force, attracted by a program of four technical sessions plus a luncheon and the traditional Scotch breakfast, doubtless with Mexican trimmings—such as a few dashes of pulque. Some papers will cover Mexican practice, and a symposium is being planned for the last session on Oct. 31. More program details later. All three groups in the Mining, Geology, and Geophysical Div. are developing programs. The Mining Subdivision will have a session with four or five papers, chiefly on practice in Latin American countries and also a joint session with the Geology Subdivision in which two papers: 1—The organization and policies of the Atomic Energy Commission, and 2—The development of its raw materials supply, will be offered by Jesse C. Johnson, director of raw materials for AEC, and by W. J. Bennett, president and general manager of El Dorado Mining & Refining. The geologists will have one session of their own, with two papers: *Correlation of the Sedimentary Section at Cananea with the Section in Southern Arizona*, by Ruben Velasco and Roland B. Mulchay, and *Geology and Mineral Deposits of Mexico*, by T. P. Clendenin, chief geologist for AS&R.

No details of the Industrial Minerals Div. or the Mineral Industry Education Div. programs are available yet.

The social events and the general arrangements for the meeting were covered in the July issue of MINING ENGINEERING, pp. 620 and 621. A booklet about the meeting is being printed in Mexico City and shortly will be mailed to all who write in expressing an interest in the meeting. Address Mr. William G. Kane, San Juan de Letran 9, Room 805, Mexico D.F., Mexico. Fill in the coupon below if you are fairly certain of going.

For those who plan to drive to Mexico City from Laredo, a geological road log is available, prepared for the field trip of the South Texas Section of the AAPG which went to Mexico City in October 1948. Copies will be supplied on request to the Secretary, AIME, 29 W. 39th St., New York 18, N. Y., and will be mailed about Sept. 1 to those who ask for them.

From El Paso, motorists may take the Central High-

The Palace of Fine Arts, below, can be seen in the center of the aerial view of Mexico City, left.

At Xochimilco, a suburb of Mexico City, natives and tourists drift through the Chinampas, or Floating Gardens.

way, through Chihuahua (227 miles), Ciudad Camargo (332 mi.), Hidalgo del Parral (423 mi.), Durango (680 mi.), Fresnillo (828 mi.), Zacatecas (866 mi.), Aguascalientes (947 mi.), Leon (1021 mi.), [short side trip to Guanajuato if desired, Queretaro (1132 mi.),] Toluca (1247 mi.), to Mexico City (1287 mi.). This is all hard-surfaced highway, and most of it through desert country. It is longer and not as scenic as the road from Laredo, but can be traveled at higher speed.

From Laredo one drives to Monterrey (145 mi.), Ciudad Victoria (320 mi.), Tamazunchale (527 mi.), to Mexico City (750 mi.).

American Airlines issues an interesting little booklet, "In Mexico It's the Custom, Senor!", which any visitor, whether going by air or not, will find informative. Write American Airlines Inc., 100 Park Ave., New York 17, or American Airlines de Mexico, S. A., Avenida Ejido No. 7, Mexico, D.F. Special round-trip excursion fares are available and your family can come with you for half-fare if you travel on Monday, Tuesday, or Wednesday. Tell American when and where you want to go and they will tell you the cost.

Special railroad cars may be provided if there is sufficient demand. A special train is not suggested, for usually inferior equipment is used, whereas modern equipment is available on some of the regular trains, particularly on the Missouri Pacific's streamliner from St. Louis.

Mr. William G. Kane
San Juan de Letran 9, Room 805
Mexico, 1, D.F.

Please make the following reservations for me for the October meeting:
Single Room ____ Double Room with twin ____ double ____ beds, at about $ ____ per day. (Single, $3.50 to $8; double, $4.50 to $8.50.) There will be ____ men and ____ ladies in my party.
Expected date of arrival ____ ; departure ____.
Coming via motor ____ ; air ____ ; rail ____.

Name ____

Title and Company ____

Street ____

City, Zone, State ____ Me8

ASCE to Mark 100th Anniversary With 1952 Centennial of Engineering

In celebration of the 100th anniversary of the American Society of Civil Engineers, a Centennial of Engineering will be held from Sept. 3 to 13, 1952. There will be 1—An international Convocation of engineers in Chicago, 2—An Exposition centering around the Museum of Science and Industry at Chicago, and 3—Carefully prepared literature, moving pictures, radio and television productions. The Convocation should prove to be the greatest gathering of engineers of all time. Many American and foreign engineering societies, including AIME, and international organizations will participate. The greatest single event will be an international banquet meeting on Sept. 10, 1952.

The Exposition will follow the general pattern of permanent exhibits of the Museum of Science and Industry and will not be the general trade show where manufacturers and equipment dealers display their products. The exhibits will be dynamic in character and designed to impress upon the mind the basic principles of science and engineering. The Centennial is planning to install appropriate exhibits in the various major fields of engineering, and will be open to the public in July 1952. In addition, a dramatic pageant built around the accomplishments of engineering will be presented daily during July, August, and September in the 1000-seat auditorium at the Museum. The aim is to awaken the public, particularly young people, to the fundamental reasons why the United States has reached its preeminent position among the nations of the world and to the significant role engineering has played in bringing the country to that position.

Engineering societies participating will hold meetings during the Centennial, and where engineering activities of several societies permit, joint meetings may be held. While there will be a great percentage of papers of a high technical nature on the programs of the societies, it is expected that a substantial number of sessions will be of sufficiently broad interest to attract both engineers and the general public.

To furnish general direction for the $1,000,000 program and to be specifically responsible for all phases of the Exposition and the production of technical and non-technical literature, Centennial of Engineering, 1952, Inc., a non-profit corporation, has been formed. Each society participating in the Convocation will meet the expenses that normally would accrue to its meeting. Formal requests have been made for a postage stamp to commemorate the Centennial of ASCE in 1952.

Oxygen Symposium Papers Requested

The Physical Chemistry of Steelmaking Committee announced that an Oxygen Symposium will be held at the AIME meeting in February 1952. Research groups or persons interested in contributing research papers to the symposium are requested to write Prof. N. J. Grant, Massachusetts Institute of Technology, Cambridge, who is chairman of this symposium.

Journal Articles To Be Microfilmed

A contract has been renewed with University Microfilms, Ann Arbor, Mich. for microfilming complete annual volumes of the three AIME monthly journals, including the Transactions sections. Microfilms of the 1950 volumes are now available from University Microfilms to those who receive the journals. The AIME receives a royalty of 10 pct of the sales price. The microfilm record is valuable to libraries and others who wish to have a complete record stored in a minimum of space.

Easy on the ear

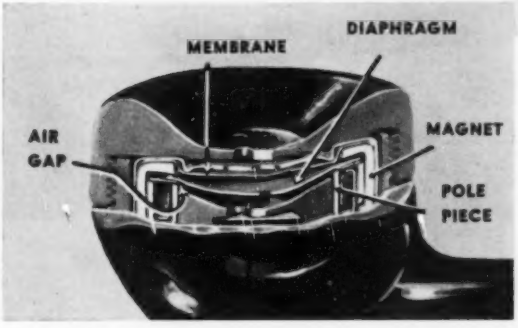

More naturally than ever, your voice comes to the ear that listens through the latest telephone receiver developed at Bell Telephone Laboratories. The reason: a new kind of diaphragm, a stiff but light plastic. Driven from its edge by a magnetic-metal ring, the diaphragm moves like a piston, producing sound over all of its area. Effective as are earlier diaphragms of magnetic-alloy sheet, the new one is better, gives more of the higher tones which add that personal touch to your voice.

To work the new receiver, telephone lines need deliver only one-third as much power. So finer wires can do the job. This is another new and important example of the way scientists at Bell Telephone Laboratories work to keep down the cost of telephone service, while the quality goes up.

BELL TELEPHONE LABORATORIES

WORKING CONTINUALLY TO KEEP YOUR TELEPHONE SERVICE ONE OF TODAY'S GREATEST VALUES

it's a time for pinching ALLOYS

MOLYBDENUM

as an alternative to Tungsten, Nickel, and other scarce, imported elements, is subject now to extraordinary demands beyond its normal uses, and must itself be economized.

TUNGSTEN

in extraordinary demand and in diminished supply, must be used only where nothing else will serve, and very sparingly even in that case.

BORON

which is abundant, serves as an extender of all these essential alloying materials. It is used very advantageously in combination with Molybdenum. In the form of Ferro-Boron, it can be employed with no change of equipment or plant procedure. It improves the quality of rolled steel—cast steel—high-speed tool steel—cast iron—malleable iron—alloyed welding rods—other ferrous products.

The Molybdenum Corporation has been a pioneer in the improvement and a leader in the production of Boron alloys. A most economical and practical form in which Boron can be introduced is a Ferro-Boron (U. S. patents 2,283,299 and 2,509,281) developed by MCA through long research. The company gladly offers its technical and practical experience to aid any user of Molybdenum, Tungsten, or Boron. Full data on request.

AMERICAN Production, American Distribution, American Control, Completely Integrated

Offices: Pittsburgh, New York, Chicago, Cleveland, Detroit, Los Angeles, San Francisco

Sales Representatives: American Steel and Supply Co., Chicago; Edgar L. Fink, Detroit; Brumley-Donaldson Co., Los Angeles, San Francisco

Subsidiaries: Cleveland-Tungsten, Inc., Cleveland, O.; General Tungsten Manufacturing Co., Inc., Union City, N.J.

Works: Washington, Pa.; York, Pa.

Mines: Questa, New Mexico; Urad, Colorado.

MOLYBDENUM CORPORATION OF AMERICA
Grant Building Pittsburgh, Pa.

MCA

Personals

JAMES MAIR

G. O. LOACH

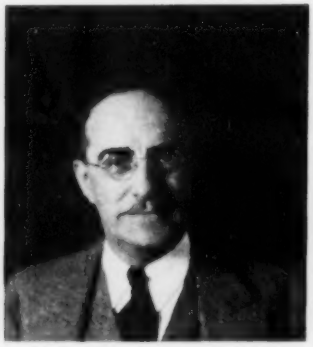

CARL F. DIETZ

James Mair, vice-president of Goslin-Birmingham Mfg. Co., Inc., Birmingham was awarded the degree of chemical engineer by the University of Alabama. Mr. Mair was awarded the degree in recognition of outstanding contributions in the field of evaporator design.

G. O. Loach has been elected director of Electro Metallurgical Co. of Canada, Ltd., Welland, Ont. He was also appointed vice-president of the company.

Carl F. Dietz, president of Lamson Corp., Syracuse, N. Y. was awarded the honorary degree of Doctor of Engineering by the Stevens Institute of Technology, Hoboken, N. J.

Don Bridges is now employed by the Battelle Memorial Institute, Columbus.

John V. Hill is now chief metallurgist and chemist for the U. S. Steel Co., flourspar div., Mexico, Ky.

H. A. Schwartz has been awarded the 1951 Charles H. McCrea medal by National Malleable & Steel Castings Co., Cleveland. Mr. Schwartz was named by the Malleable Founders' Society for his outstanding contribution toward progress and development in the malleable iron industry.

Robert J. Morris has joined General Motors Corp., Allison div., Indianapolis, as metallurgical engineer in the laboratory in the jet engine plant.

J. D. Cooper is presently employed as a graduate metallurgist by Phillips Electrical Works, Ltd., Brockville, Ont.

Gerard H. Boss, formerly with the Oak Ridge National Laboratory, metallurgy div., Oak Ridge, has joined the North American Aviation Corp., Aero Physics div., Downey, Calif.

Clarence Zener has been appointed an associate director of the Westinghouse Research Laboratories, Pittsburgh. He will also serve as acting manager of the solid state physics and magnetics dept. of the research laboratories.

Dexter C. Hatch is with National Lead Co., titanium div., Tahawus, N. Y.

Jose A. Bacigalupo has become chief of industrial dept., Solid Fuels Administration, Florida, Buenos Aires.

R. T. Whitzel, general superintendent, Aluminum Co. of America, has been transferred from the Massena, N. Y. office to Pittsburgh.

Alfred F. Weinberg has been awarded a one-year scholarship at Illinois Institute of Technology by the WAAIME.

Julius M. Simmons has become associated with the Argonne National Laboratory, Chicago. He was formerly with the Joslyn Mfg. & Supply Co., Fort Wayne, Ind.

Alfred A. P. Strasser has resigned from the M. W. Kellog Co., special project dept., Jersey City, N. J., and is now employed as a metallurgist with Wright Patterson Air Force Base, technical analysis div., Dayton, Ohio.

Emanuel Silkiss has joined the Wright Aerorautical Corp., Wood-Ridge, N. J., as metallurgical engineer.

Warren M. Parris is now a research engineer with Battelle Memorial Institute, Columbus.

Heath Steele, vice-president, American Metal Co., recently returned from an inspection tour of the potash properties in New Mexico of the Southwest Potash Corp., a subsidiary of American Metal. The firm is being equipped for production which is estimated to begin during the latter half of 1952.

Dana W. Smith has been named associate director of the div. of metallurgical research for Kaiser Aluminum & Chemical Corp., Spokane, Wash.

I. M. LeBaron has been appointed director of research laboratories, International Minerals & Chemical Corp., Chicago.

John C. Warner, president of Carnegie Institute of Technology, was presented an honorary degree of Doctor of Science by Northeastern University, Boston.

Walter R. Hibbard, Jr. is research associate with General Electric Co., Schenectady, N. Y. Mr. Hibbard was the recipient of the R. W. Raymond Memorial Award for 1950.

John Clifford Mitchell has joined the American Smelting & Refining Co., Leadville, Colo.

Tryggve Angel is now a metallurgical research assistant with the Sandvik Steel Works, Sandviken, Sweden.

NOW - the book you've been waiting for . . .

BASIC OPEN HEARTH STEELMAKING

(A Completely Revised Edition)

Prepared by the Physical Chemistry of Steelmaking Committee, AIME
Sponsored by the Seeley W. Mudd Memorial Fund

Now in 22 chapters, the best in open hearth practice and principles, written and edited by a committee of the foremost steel plant operating and metallurgical authorities. Each chapter considers a specific factor or operation in steel production, and describes methods, practices, and the latest metallurgical knowledge on the subject.

1951 • 960 Pages • $8.00

Part I—Practice

- Basic Open Hearth Furnaces
- Survey of Operations
- Open Hearth Refractories
- Fuels, Combustion, Instrumentation
- Raw Materials
- Slag Control
- Charging and Melting
- Refining
- Finishing and Deoxidizing
- Molds and Pouring
- Ingot Structure, Segregation
- Nonmetallic Inclusions
- Properties of Steel

Part II—Principles

- Chemistry of High Temperature Reactions
- Kinetics of Metallurgical Processes
- Chemistry of Liquid Steel
- Chemistry of Slag-Metal Reactions
- Chemistry of Open Hearth Refractories
- Thermal Changes in Melting and Refining
- Gas Flow and Heat Transfer
- Combustion and Utilization of Fuel
- Rates of Open Hearth Reactions

Brand New . . .

Solidification of Metals and Alloys . . .

A Symposium by the AIME's Institute of Metals Division

NEW—A publication on the subject of major significance to metallurgists, by four of the nation's outstanding authorities. Three papers cover ferrous and nonferrous metals solidification and discuss many of the phenomena of metal freezing.

1951 • 75 Pages • $3.00

Nucleation of Solids, J. H. Hollomon and D. Turnbull

Growth of Metal Crystals, R. F. Mehl

Solidification of Steel Ingots, B. R. Queneau

Preface, Cyril Stanley Smith

OTHER METALS BRANCH BOOKS

Transactions, Vols. 185 ('49), 188 ('50)	$7.00
75 Years of Progress in Iron and Steel, 1948	$1.50
Bergwerk und Probierbuchlein, 1949	$5.00
Stress Corrosion Cracking of Metals, 1944	$5.00
Nonferrous Melting Practice, 1946	$3.00
Brief History of Science of Metals, 1948	$1.50
Nonferrous Rolling Practice, 1948	$4.00
Rod and Wire Production Practice, 1949	$3.00
Proceedings	
Electric Furnace Steel, 1945-1949	$10.00
Blast Furnace, Coke Oven and Raw Materials, 1946-1950	$10.00
Open Hearth, 1944-1948, 1950	$10.00

AIME 29 W. 39th St., New York 18, N. Y.

Please send me the books listed below. Enclosed is Check ☐; Money Order ☐ for $_____. (AIME members may be billed.)

• AIME Members, 30% Discount on All Books.

1. _____ 3. _____

2. _____ 4. _____

Name _____

Address _____

City and Zone _____ State _____

Nonmember Foreign Orders, Add 50c for Mailing.

Obituaries

Harry Hatch Burhans (Member 1937) has died. Mr. Burhans was born at Superior, Wis. in 1884 and attended Michigan College of Mines, Houghton, Mich., graduating in 1906 with the degree of E.M. Following graduation, several years were spent working in Mexico and Arizona. During World War I he was a First Lieutenant. In 1919 he joined the Yukon Mining Co., Yukon Territory as superintendent. He went to Colombia as mill superintendent for the Bar-Principal Mining Co. Mr. Burhans returned to New York in 1921 and was employed by the Dorr Co. Later he became associated with the Consolidated Mining Co., as operating engineer. In 1937 Mr. Smith was manager, Varaguas Mines Ltd., Panama. He remained here for a short time and then joined R. T. Vanderbilt & Co., New York as field engineer. At the time of his death he was residing in Los Angeles.

Frederick Fraley Sharpless (Member 1889), a former Secretary of AIME, died on Apr. 11. Mr. Sharpless, born in West Chester, Pa. in 1866, attended the state normal school in that town, completing his education at the University of Michigan. He graduated in 1888 with the degree of B.S. in chemistry. Following graduation he was an instructor in metallurgical chemistry, assaying and ore dressing at the Michigan School of Mines, Houghton. In 1893 he opened a chemical laboratory in Minneapolis and examined and reported on iron mines and precious metal mines in the Northwest. During this time he was a professor in metallurgical chemistry at the University of Minnesota. In 1899 he was general manager of the mine and smelter of the California Copper Co. He later became a consulting engineer for the Consolidated Mines Selection Co. Ltd. of London. While associated with this firm he traveled through North America, Mexico, Central and South America, West Africa, and Turkey. From 1912 to 1921 he maintained a consulting office in New York. Mr. Sharpless became Secretary of AIME in 1921. He returned to his practice in 1925 and retired in 1938.

Raymond Edgar Tower (Member 1945) has died. Born in Missoula, Mont. on Feb. 24, 1889, he attended Montana School of Mines at Butte. He was manager, Tower & Templeman Leasing Co. from 1915 to 1919. During this same time he was superintendent, St. Louis Mining & Milling Co., Marysville, Mont. He joined the Silver Fissure Mining Co. in 1919 and in 1925 went to Kamloops, B. C. as mill superintendent for the Iron Mask Mining Co. For several years Mr. Tower did general consulting work in Mexico. He built a number of flotation and cyanide plants throughout the West and Mexico. He became manager for the Gold Coin Mining Co., Pittsburgh in 1931 and in 1941 was engaged in private practice and operation of the Hidden Lake, Mont. mine. During World War II he served as chief chemist for the metals reserve plant at Columbus, Mont. At the time of his death he was vice-president and manager of the Sarita Milling Co., Salt Lake City.

NECROLOGY

Date Elected	Name	Date of Death
1899	George H. Ashley	May 28, 1951
1936	Cecil E. Bales	May 26, 1951
1936	Walter M. Charman	June 15, 1951
1904	Herbert B. Cox	Feb. 11, 1951
1917	George C. Crossley	June 8, 1951
1883	F. Lynwood Garrison	June 10, 1951
1944	Kenneth V. Haig	Mar. 27, 1951
1900	Walter Hovey Hill	June 10, 1951
1921	Oscar Mamet	Unknown
1947	William R. Maurer	Mar. 1, 1951
1928	Howard Palmer	Unknown
1928	Eugene P. Shove	Unknown
1928	William R. Tonkin	Unknown

Proposed for Membership

Metals Branch AIME

Total AIME membership on June 30, 1951, was 17,282; in addition 2,498 Student Associates were enrolled.

ADMISSIONS COMMITTEE

Thomas G. Moore, Chairman; Carroll A. Garner, Vice-Chairman; George B. Corless, F. W. Hanson, Albert J. Phillips, Lloyd C. Gibson, R. D. Mollison, John T. Sherman. Alternates: A. C. Brinker, H. W. Hitzrot, Plato Malozemoff, Ivan Given, T. D. Jones, and W. H. Farrand.

Institute members are urged to review this list as soon as the issue is received and immediately to wire the Secretary's office, night message collect, if objection is offered to the admission of any applicant. Details of the objection should follow by mail. The Institute desires to extend its privileges to every person to whom it can be of service but does not desire to admit persons unless they are qualified. Objections must be received before the 30th of the month on Metals and Mining Branches.

In the following list C/S means change of status; R, reinstatement; M, Member; J, Junior Member; A, Associate Member; S, Student Associate.

Arizona
Naco—MacDonald, Fred H. (M)

California
Van Nuys—Johnson, Horace A. (J) (R. C/S—S-J)

Connecticut
Milford—Seeley, Harold O. (M)

Idaho
Kellogg—Ingvoldstad, Donald F. (M) (R. C/S—J-M)
West Preston—Bridges, Donald W. (J) (C/S—S-J)

Illinois
Coal City—Veale, Jack Heagy (M)
Chicago—Lubker, Robert A. (M)
Evanston—Abbott, Mark L. (A)
Oak Park—Over, Ray E. (M)

Indiana
Gary—Kroner, Albert M. (M) (R. C/S—J-M)
Munster—Kraay, Lawrence E. (M)

Maryland
Baltimore—Hoke, John H. (J) (R. C/S—S-J)

Massachusetts
Wilbraham—Rothery, Paul R., Jr. (J) (C/S—S-J)

Michigan
Dearborn—MacNaughton, Fred P. (M)

Minnesota
Minneapolis—Ferman, John W. (J) (C/S—S-J). Koppi, William A. (J)
St. Paul—Joseph, Thomas L. (J). Rink, John R. (J)

Missouri
St. Louis—Deutch, Morton (J) (R. C/S—S-J)

New Hampshire
Portsmouth—Levingston, Howard L. (J) (C/S—S-J)

New Jersey
Dunellen—Couch, George R. (M)
East Orange—Bennett, Winslow W. (J)
Elizabeth—Binns, Frank E. (J) C/S—S-J)
North Plainfield—Axelson, John W. (M) (C/S—A-M)
Westfield—Freeman, Jr., William R. (J) (C/S—S-J)

New York
Chappaqua—Biggs, Thomas K. (J) (C/S—S-J)
New York—Chandler, Henry T. (M). Golding, Donald K. (J) (R. C/S—S-J)
Rego Park—Storchheim, Samuel (J)

Ohio
Middletown—Sant, Robert Thomas (M)
Parma—Yaker, Charles (J)

Oklahoma
Ponca City—Leterle, Jene F. (J)

Oregon
Portland—Waters, Thomas J. (M)

Pennsylvania
Annville—Shroyer, David K. (M)
Butler—Lutz, Richard N. (J) (C/S—S-J)
Midland—Brown, John Carlyle (M)
Monaca—Taylor, Donald J. (M)
Philadelphia—Davidson, Nathan (J) (C/S—S-J)
Pittsburgh—Beckman, Samuel J. (J) (R. C/S—S-J). Turner, William A. (A)

Utah
Salt Lake City—Johnson, Raymond A. (J) (R. C/S—S-J)

Wisconsin
Platteville—Carthew, Douglas J. (J) (C/S—S-J)

Mexico
Coahuila—Foster, M. K. (M)
Sonora—Hay, Harold L. (A)

Buehler . . .

. . . OFFERS A COMPLETE LINE OF EQUIPMENT FOR THE Metallurgical Laboratory

Buehler specimen preparation equipment is designed especially for the metallurgist, and is built with a high degree of precision and accuracy for the fast production of the finest quality of metallurgical specimens.

1. No. 1315 Press for the rapid moulding of specimen mounts, either bakelite or transparent plastic. Heating element can be raised and cooling blocks swung into position without releasing pressure on the mold.

2. No. 1211 Wet power grinder with 3/4" hp. ball bearing motor totally enclosed. Has two 12" wheels mounted on metal plates for coarse and medium grinding.

3. No. 1000 Cut-off machine is a heavy duty cutter for stock up to 3-1/2". Powered with a 3 hp. totally enclosed motor with cut-off wheel, 12" x 3/32" x 1-1/4".

4. 1505-2AB Low Speed Polisher complete with 8" balanced bronze polishing disc. Mounted to 1/4 hp. ball bearing, two speed motor, with right angle gear reduction for 161 and 246 R.P.M. spindle speeds.

5. No. 1700 New Buehler Waisman Electro Polisher produces scratch-free specimens in a fraction of the time usually required for polishing. Speed with dependable results is obtained with both ferrous and non-ferrous samples. Simple to operate—does not require an expert technician to produce good specimens.

6. No. 1410 Hand Grinder conveniently arranged for two stage grinding with medium and fine emery paper on twin grinding surfaces. A reserve supply of 150 ft. of abrasive paper is contained in rolls and can be quickly drawn into position for use.

7. No. 1400 Emery paper disc grinder. Four grades of abrasive paper are provided for grinding on the four sides of discs, 8" in diameter. Motor 1/3 hp. with two speeds, 575 and 1150 R.P.M.

8. No. 1015 Cut-off machine for table mounting with separate unit recirculating cooling system No. 1016. Motor 1 hp. with capacity for cutting 1" stock.

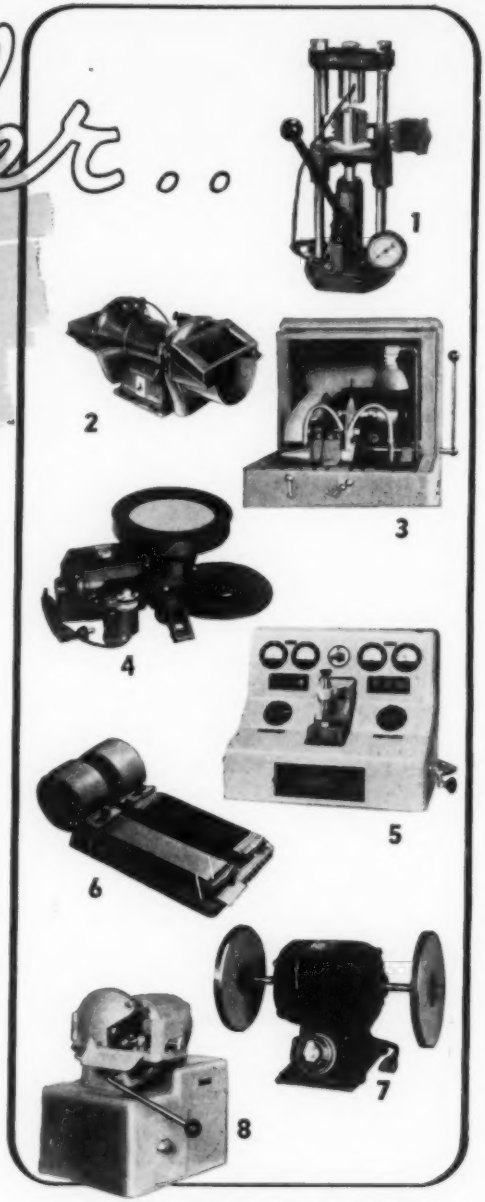

THE BUEHLER LINE OF SPECIMEN PREPARATION EQUIPMENT INCLUDES . . . CUT-OFF MACHINES • SPECIMEN MOUNT PRESSES • POWER GRINDERS • EMERY PAPER GRINDERS • HAND GRINDERS • BELT SURFACERS • MECHANICAL AND ELECTRO POLISHERS • POLISHING CLOTHS • POLISHING ABRASIVES

Buehler Ltd.
A PARTNERSHIP

METALLURGICAL APPARATUS
165 WEST WACKER DRIVE, CHICAGO 1, ILL.

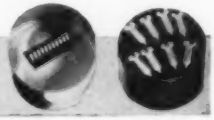

Advertisement

ELECTROMET Data Sheet

A Digest of the Production, Properties, and Uses of Steels and Other Metals

Published by Electro Metallurgical Company, a Division of Union Carbide and Carbon Corporation, 30 East 42nd Street, New York 17, N. Y. • In Canada: Electro Metallurgical Company of Canada, Limited, Welland, Ontario

How SILICOMANGANESE Saves Furnace Time . . . Produces Better, Cleaner Steel

Silicomanganese is used by the steel industry as a furnace block* and deoxidizer, and also for manganese additions.

The cleanness and quality of steel depend largely on how well it has been deoxidized. Deoxidation also greatly influences the physical properties of steel for rolling and subsequent fabrication. Silicomanganese combines two active deoxidizers in a single alloy and it has proved to be a more effective deoxidizer than silicon or manganese alloys added separately. This combination alloy contains silicon and manganese in the correct proportion (approximately 1 to 3.5) to be most effective in reducing the oxygen content of the bath to a low level. The use of silicomanganese produces cleaner steel, saves furnace time, and gives high alloy recovery for manganese additions.

Gets More Oxygen Out of Bath

When silicomanganese is used for blocking and deoxidation, the combined effect of silicon and manganese lowers the oxygen content to a greater degree than silicon alone. This is due to the fact that the amount of oxygen in equilibrium with a given amount of silicon is lower in iron-silicon-manganese alloys than it is in plain iron-silicon alloys, as shown in Fig. 1.

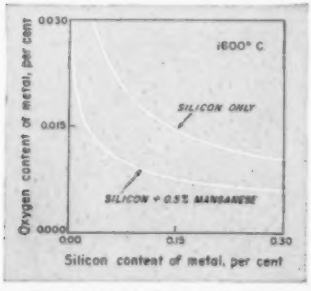

Fig. 1. Limit of solubility of oxygen in iron-silicon alloys, plain and with 0.50 per cent manganese at 1600°C.

*The initial deoxidation of steel, frequently referred to as the furnace block, stops the carbon-oxygen reaction in the furnace. This arrests the carbon drop immediately and makes it possible to secure close control of analysis. If the oxygen content of the metal is reduced well below the level established by the carbon-oxygen reaction, initial deoxidation is accomplished.

Less Inclusions, Cleaner Steel

In addition to lowering the oxygen content, silicomanganese has a specifically beneficial effect on inclusions. The inclusions in a steel depend in large part on how low the carbon content (or how high the oxygen content) is before blocking. The lower the carbon, the dirtier the final steel, almost regardless of the subsequent deoxidation treatment. Since silicomanganese has a low carbon content, it is not necessary to drive the carbon as low (or make the oxygen as high), as when high-carbon or standard ferromanganese is used, so that the final steel is cleaner and has better working properties. The improved cleanliness resulting from silicomanganese is usually noticeable in higher carbon steels, but is outstanding in steels below 0.25 per cent carbon where inclusions and surface defects are a vital problem and where the time saved by blocking at a higher carbon level is significant.

Fast Solubility In Bath

Because of the high concentration of active elements in silicomanganese, less time is required to effect solution of this alloy than when equivalent amounts of silicon and manganese are used separately in the form of ferrosilicon and ferromanganese.

For example, compare these typical analyses of silicomanganese, standard ferromanganese, and 50 per cent ferrosilicon:

	Silicomanganese, %	Standard Ferromanganese, %	50% Ferrosilicon, %
Manganese	66.5	80	—
Silicon	19	—	50
Carbon	1.5	7	—
Iron, approx.	13	13	50

From this it can be seen that 1,000 lb. of silicomanganese would contain 190 lb. of silicon and 665 lb. of manganese. These amounts of silicon and manganese would require 380 lb. of 50 per cent ferrosilicon and 830 lb. of standard ferromanganese, or a total of 1,210 lb. Obviously it is easier and faster to dissolve 1,000 lb. of the combination alloy silicomanganese than 1,210 lb. of these separate silicon and manganese alloys.

Lower Carbon Content

Silicomanganese contains less carbon than any combination of ferrosilicon and standard ferromanganese. Therefore, the carbon-oxygen reaction in the bath can be stopped earlier when silicomanganese is used for blocking. Heats can be blocked at higher carbon levels and hence lower oxygen contents, and the amount of deoxidation required is less.

Fig. 2. Charging silicomanganese into an open-hearth furnace.

Saves Furnace Time

Because of the advantages outlined, silicomanganese can save as much as 20 minutes per melt in the production of open-hearth steel. For low-carbon steel, an even greater saving in time can be realized.

For Producing Engineering Steels

Silicomanganese is also used for alloy additions of manganese, particularly in the production of engineering steels containing 0.10 to 0.50 per cent carbon.

When manganese or other oxidizable additions, such as chromium, must be made to the bath, the use of a block provides a higher alloy recovery. Silicomanganese introduces manganese with the silicon and the usual recovery of this manganese will range from 70 to 85 per cent.

Metallurgical Service Available

Ask to have one of our metallurgists call and explain more fully the advantages of silicomanganese as a furnace block and deoxidizer. He will be glad to help you with the use of ELECTROMET silicomanganese. This alloy contains 65 to 68 per cent manganese and is produced in maximum 1.50, 2.00, and 3.00 per cent carbon grades. All grades are furnished in a lump size of 75 lb. x 2 in. and in a crushed size of 2 in. x down. Write, wire, or phone the nearest ELECTROMET office.

The word "Electromet" is a registered trademark of Union Carbide and Carbon Corporation.

A BIG HIT EVERYWHERE IT IS SHOWN

. . . the Outstanding New

DESK-TYPE

Metallograph

. . . and no wonder, for it introduces to metallographers so *much* that is completely new—new simplicity of operation, new convenience, new speed and accuracy. Everyone who sees the AO Metallograph takes the time to study it thoroughly, operate it, and become *convinced* that here is a radical advancement in the field of metals microscopy.

SIT DOWN AND STAY SEATED. From start to finish every control, every operation, is at your fingertips.

FOCUS QUICKLY, AUTOMATICALLY, ACCURATELY. Final focusing for photography is accomplished through the parfocal visual system.

UNBELIEVABLE SPEED AND PRECISION in changing magnification, adjusting lamp, making exposure, taking notes.

OTHER FEATURES: monocular or binocular bodies, revolving objective turret, 2 lamps—visual and photographic, perfect arc lamp performance with *both* AC and DC current, "autofocus" coarse adjustment stop.

Every user of metallographic equipment should *know* this AO instrument. For your copy of our descriptive 12 page catalog, write Dept. V 182.

American Optical

INSTRUMENT DIVISION • BUFFALO 15, NEW YORK

for

80Bxx, 81Bxx and 94Bxx Steels

with maximum properties

USE *Grainal* ALLOYS

Maximum hardenability in very low alloy steels, with dependable uniformity of results, is assured by the addition of Grainal alloys.

The use of Grainal alloys promotes maximum hardenability with minimum amount of boron. The possibility of obtaining undesirable effects resulting from over-treatment by boron is avoided by the action of other elements of Grainal alloys in combining with oxygen and nitrogen and permitting full utilization of the low boron content.

More than a million and a half tons of steels made with Grainal have proved the superiority of these alloys in producing maximum hardenability.

VANADIUM CORPORATION OF AMERICA

420 LEXINGTON AVENUE NEW YORK 17 N.Y. • DETROIT • CHICAGO • CLEVELAND • PITTSBURGH

MAKERS OF ALLOYS

VANCORAM

CHEMICALS AND METALS

flexible*
accurate*

*Two good words to aptly describe the operation of a *Salem Rotary Hearth Heating Furnace* at work in your plant. Whether your hot-metal operations include piercing, forging, or rolling ferrous or non-ferrous metals, your automatically controlled Salem Rotary will flexibly and accurately adapt itself to large variations in heating and tonnage rates —thus maintaining economy despite downtime for changeover in your metal forming operations. Moreover, you'll reduce scale loss, simplify handling, and save money on labor and maintenance. For greater yield at lower cost, you should be using a Salem Rotary. Write to us.

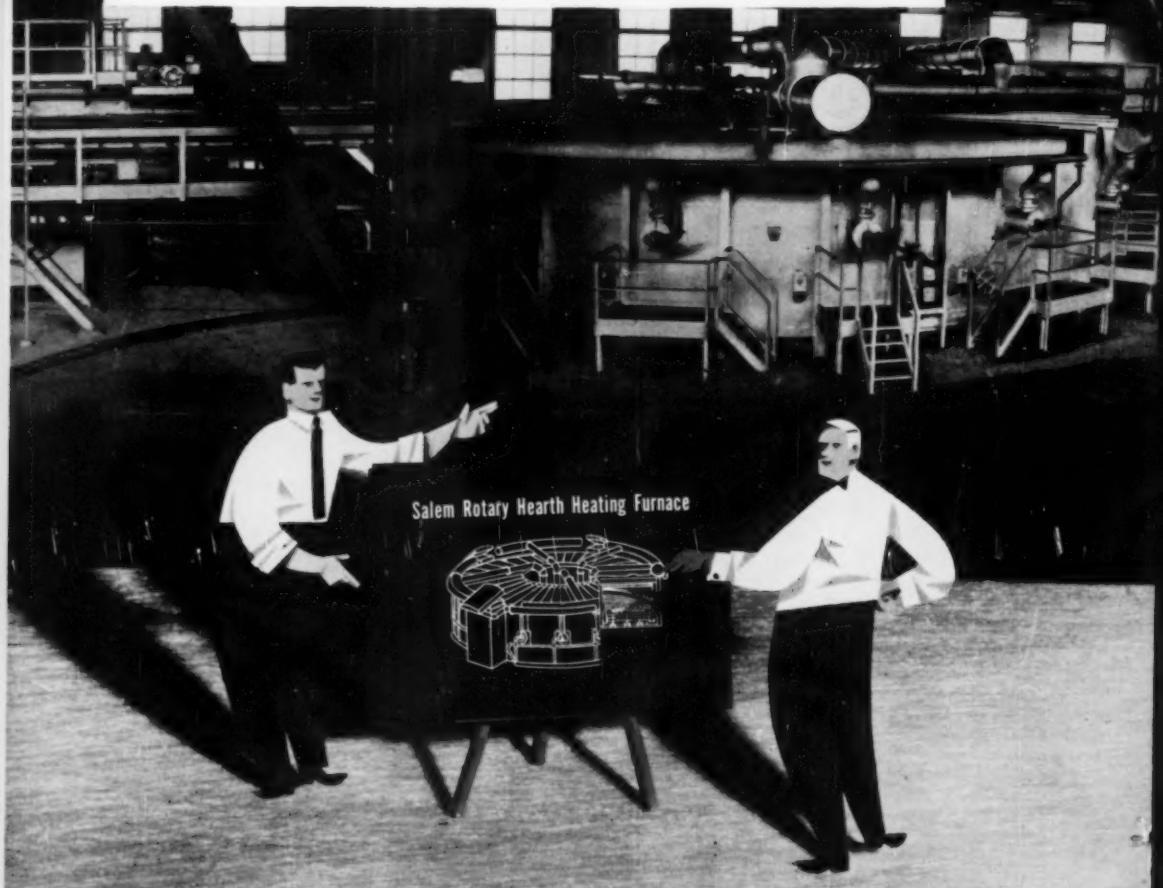

SALEM ENGINEERING DIVISION,

Salem-Brosius, Inc. Salem, Ohio

Affiliates: Brosius Division, Pittsburgh 15, Pa.
Salem Engineering Co., Ltd., Milford nr. Derby, England. Salem Engineering (Canada) Ltd., Toronto, Canada